A quoi peut être attribué le bruit de fond ?

Tout d'abord, aux conditions dans lesquelles sont faites les lectures par les pilotes :

- cadrans petits et peu précis ; la lecture peut être faite indifféremment par le pilote ou le co-pilote sur l'instrumentation commune ;

- conditions de vol difficiles à stabiliser pendant la période de 5 minutes recommandées par le constructeur ;

- charges électriques, hydrauliques et prélèvements d'air mal identifiés ; en théorie les pilotes doivent faire les relevés dans des conditions toujours identiques, mais les impératifs de vol ne le permettent pas toujours et parfois même il n'y a aucune consigne donnée au pilote de ce côté ;

- les résultats sont très sensibles à la température extérieure de l'air ;

- ensuite, les erreurs de transcription et de saisie des opérateurs au sol.

Il est à noter qu'un bruit de fond important correspond, pour les PRATT & WHITNEY, à une défectuosité du moteur, du type encrassement du compresseur.

Il semble qu'une bonne coopération pilotes - responsables techniques aide à améliorer le bruit de fond.

Autres difficultés :

- Le constructeur recommande de marquer en parallèle avec la courbe tous les évènements de maintenance susceptibles d'intéresser la vie du moteur (lavages compresseur / turbine, changement d'équipements, réglages, etc...), pour que l'opérateur chargé de l'interprétation des courbes ait tous les éléments de jugement à sa disposition ; on constate fréquemment en pratique des oublis ou des retards importants.

- L'exploitation au sol des relevés du pilote ou de l'enregistreur est faite périodiquement, généralement une ou deux fois par semaine, et le constructeur est fréquemment consulté pour lever les doutes ; l'ensemble des délais peut demander jusqu'à 100 heures de vol entre la lecture et l'exploitation définitive ; ceci suppose un matériel suffisamment robuste pour supporter une dégradation rapide. C'est le cas pour le PT 6 qui est un moteur sûr et bien connu ; c'est moins évident pour le CT 7 et surtout le PW 120.

- Pour que les seuils d'alerte préconisés par le constructeur aient une signification, il faut que la surveillance ait été mise en place dès la sortie d'une révision générale ou d'une visite de section chaude ; aujourd'hui, ce réflexe de faire systématiquement au moins une visite section chaude avant mise en place du Trend Monitoring n'est pas entré dans les moeurs ; de plus, la facilité avec laquelle les PT 6 sont vendus ou transférés entre compagnies ne facilite pas la rigueur d'application des consignes du constructeur.

5 - RESULTATS

D'une manière générale, le Trend Monitoring fait ressortir très rapidement les problèmes affectant les équipements périphériques du moteur (vannes, harnais, transmetteurs de vitesse et de couple, les thermocouples) ; mais la recherche de panne qui permet d'identifier le composant responsable est souvent assez laborieuse ; les spécialistes qui dépouillent les courbes identifient plus facilement les pilotes de l'avion que le composant.

La première conséquence de l'introduction du Trend Monitoring dans une petite compagnie est l'achat d'un lot très complet de bancs d'essais, appareillages, boroscopes, etc... permettant la vérification précise des instruments de base, des injecteurs et du moteur. Ceci améliore considérablement le suivi général des machines et c'est en soi un premier bon résultat.

L'utilisation des cahiers de signatures de pannes données par le constructeur est très difficile : l'interprétation des courbes par la plupart des exploitants leur permet tout au plus de dire qu'il y a "quelque chose". La lecture des courbes établies à la main (figure 2) est particulièrement délicate ; les pentes sont faibles.

Deux exemples caractéristiques :

Le moteur, objet de la figure 2, surveillé à titre expérimental par Trend Monitoring, a été déposé normalement à l'issue de son potentiel déclaré ; il présentait un état mécanique très bon avec le compresseur encrassé. Le constructeur, consulté pour avis sur la manière de mettre en oeuvre le Trend Monitoring, a estimé que le moteur était en mauvais état.

Dans la figure 7 ci-dessous, qui représente la totalité de la vie d'un PW 120 (environ 2 200 heures depuis neuf), les paramètres de base semblent typiques d'une détérioration de section chaude et ont atteint les seuils d'alerte ; cependant, pour des raisons non connues, le moteur a été laissé en service et a eu du pompage avec surchauffe violente au décollage et destructions importantes. Une autre compagnie a eu exactement la même allure de courbe mais a su déposer le moteur à temps : celui-ci présentait des brûlures importantes en bout de pales de turbines.

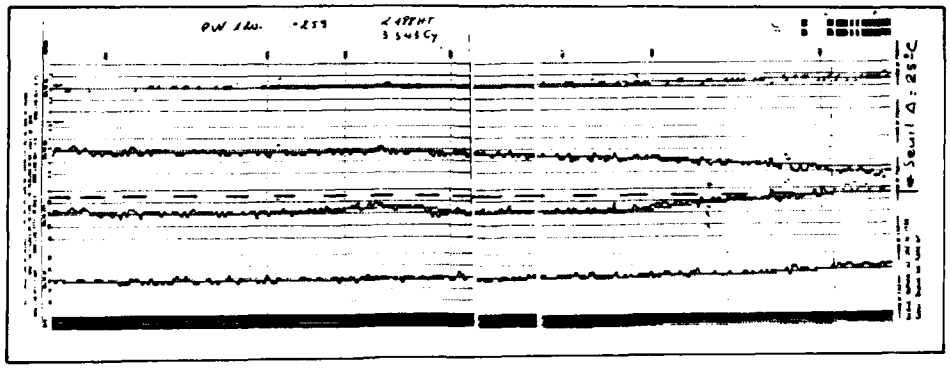

Figure 7

Comparer avec la figure 6 qui représente un exemple récent de détérioration importante de chambres de combustion.

PT 6

Sur cette machine, les dérives semblent provoquées essentiellement par le jeu en bout de pales de turbine du générateur de gaz ; dans l'expérience que nous en avons et avec les limites actuelles, ce jeu provoque l'application des consignes de dépose avant qu'il y ait eu réellement des dégradations importantes. Nous n'avons pas vu de contre exemple caractéristique.

PW 120

Sur 12 cas d'incidents survenus à des compagnies françaises, 3 ont été détectés par Trend Monitoring ; mais sur les 4 incidents analysés comme susceptibles d'être détectés au Trend Monitoring, 3 l'ont été effectivement ; le 4ème cas est celui cité ci-dessus.

Dans 2 cas de moteurs déposés suite au Trend Monitoring, un présentait des dommages réels mais mineurs (injecteur défectueux et légère brûlure sur 1 pale distributeur HP), l'autre des brûlures importantes en bout de pales sur les 2 premiers étages de turbine.

La sensibilité semble très faible en regard de l'importance des dégâts constatés sur plusieurs moteurs ; il y a, d'autre part, dans l'interprétation des courbes une notion qui est l'évolution du rapport des vitesses NH par rapport aux vitesses NL. Cette notion n'est pas appréhendée de la même manière par tous les utilisateurs et n'est pas facile à exploiter.

CT 7

Nous avons vu un cas où un impact de corps étrangers ayant déformé 1 seule pale a été détecté au Trend Monitoring (voir figure 5) et un cas de dépose suite à indications Trend Monitoring ayant effectivement une détérioration importante de la section chaude.

La sensibilité semble suffisante.

6 - CONCLUSIONS

Le "Trend Monitoring" existe, il est utilisable mais il nécessite une attention très soutenue et une connaissance fine, non seulement de la mécanique du moteur mais des principes de son fonctionnement thermodynamique, si l'on veut interpréter correctement les courbes en l'absence de consignes type "tout ou rien" sur l'ensemble des paramètres ; en fait, il faut un petit bureau d'études. Dans une petite compagnie, ce n'est pas évident et le changement d'une seule personne peut amener la perte quasi complète d'une longue expérience.

Du fait de ses possibilités limitées, le Trend Monitoring doit être impérativement complété et recoupé par d'autres méthodes de contrôles non basées sur les performances en vol, telles que mesures de performances au sol par mécaniciens, inspections endoscopiques systématiques et fréquentes, visites diverses, etc... Ceci existe déjà pour le PW 120 et le CT 7 et les inspections endoscopiques, en particulier, sont assez bien maîtrisées par la plupart des compagnies. La périodicité de ces inspections est moins bien maîtrisée en raison de la faible expérience générale de ces machines et la tendance est au resserrement.

Dans ces conditions, l'élimination de la butée périodique de visite de la section chaude est admissible, sauf pour le PT6. En effet, de par la conception et l'installation du moteur qui présente très peu de points d'accès et qui sont masqués par de nombreux équipements, la section chaude de ce moteur se prête mal à l'inspection endoscopique ; de ce fait, nous avons été amenés à maintenir pour le PT6 une butée en heures pour la révision de la section chaude, à titre de précaution, avec l'espoir que l'expérience future de chaque exploitant permettra de la rendre inutile.

L'emploi d'un ordinateur et d'une imprimante pour les tracés est indispensable, à notre avis, dans tous les cas.

DISCUSSION

C. SPRUNG

Quelles sont les différences, du point de vue performances, puissances et consommations, entre les tolérances du matériel neuf et celles acceptées en maintenance? Vous avez précisé que cette tolérance est de $\pm$ 2% par rapport à la valeur nominale pour du matériel neuf.

Author's Reply:

Les tolérances indiquées sont celles appliquées par rapport aux relevés fait en vol par la méthode du "trend monitoring". Elles sont complètement indépendantes de celles utilisées en maintenance, même si elles s'en rapprochent.

GAS PATH ANALYSIS AND ENGINE PERFORMANCE MONITORING IN A CHINOOK HELICOPTER

by
D.E. Glenny
Aeronautical Research Laboratory
Defence Science and Technology Organisation
GPO BOX 4331
Melbourne Victoria 3001
Australia

SUMMARY

Periodic and consistent assessment of engine performance in military helicopters is essential if in-service operating margins are not be be eroded by harsh environmental conditions. Manually initiated GO-NO-GO pre-flight checks (HIT etc) or ad-hoc in-flight performance checks rarely provide sufficiently reliable data for maintenance or diagnostic purposes. In contrast, performance assessment methods based on gas path analysis principles and engine/aircraft data, automatically recorded during flight, offer a potentially attractive alternative. ARL has investigated a number of these alternatives, and has carried out an in-service trial on a Boeing CH47C Chinook helicopter operated by the RAAF. In the trial existing aircraft/engine instrumentation was complemented by specially designed probes located at module interfaces whilst the data were recorded on an ARL designed acquisition system. The performance-fault algorithms used in the analyses were configured for a range of engine operating speeds. Results for the trial are presented in terms of deviations, from pre-established base-line conditions. Statistical analyses using linear regression fits and Kalman Filtering techniques have been investigated to minimise the effects of data uncertainty. The applicability of the procedures, including thermodynamic analyses and equipment, are discussed in terms of fleetwide adoption for the Chinook.

Nomenclature

A	Area
BB	Bleed Band
C	Corrected
CVA	Coefficient of Variation ($\sigma/\bar{x}$%)
FF,WF	Fuel Flow
HIT	Health Indicator Test
IAS	Indicated Air Speed
IGV	Inlet Guide Vanes
IFM	In Flight Monitoring
$K_{a\ b}$	Influence Coefficient
$K_{A\ B}$	Fault Matrix Coefficient
N_1	Gas Generator Speed
N_2	Power Turbine Speed
p	Static Pressure
P	Total Pressure
PPI	Power Performance Indicator
T	Temperature
TEAC	Turbine Engine Analysis Check
TOR	Torque
WA	Mass Flow
$\bar{x}$	Mean
δ	Pressure Ratio
θ	Temperature Ratio
η	Efficiency
σ	Standard Deviation (STD)
1--5	Station Numbers
	Subscripts
c	Compressor
ct	Compressor Turbine
pt	Power Turbine

1. INTRODUCTION

The arduous operating environment of the military helicopter requires that effective power assurance checks are carried out routinely prior to, or during flight. Procedures currently used are configured around well established methods such as HIT, TEAC (topping) and PPI : the procedure used by an operator has usually been a function of the country of origin, or major user of the helicopter. The results of these checks are invariably treated as GO-NO-GO indicators and are rarely retained from one flight to the next for trending or prognostic purposes. In contrast to these methods the RAAF has, on its Iroquois helicopters, used an in flight performance assessment/monitoring method (IFM), Reference 1, which compares actual engine performance with prespecified baseline values. Deviations in torque and exhaust gas temperature are monitored routinely to give an indication of engine condition or performance deterioration. This procedure was implemented because of a long history of severe blade erosion and stability - surge problems experienced by the T53 engine, and the fact that the HIT method was carried out at relatively low power levels whilst daily use of topping checks was counter productive in terms of engine life. Notwithstanding the potential gains available by the adoption of an IFM procedure the viability of the method is limited by scatter due to visual observations of aircraft instrumentation and the difficulty in maintaining a steady state power setting during the monitoring period. Because only a limited number of gas path parameters were recorded during the IFM test it was also difficult to isolate performance decrements to given engine components or modules.

Recognising these problems a combined RAAF/ARL programme was initiated to investigate the effectiveness of using automatically recorded engine/aircraft data, combined with gas path analyses techniques to assess performance deterioration and component degradation in a military helicopter. At the request of the RAAF the investigation was centred on the Lycoming T55-L11 engine in the Chinook helicopter. This paper describes the Chinook engine performance monitoring programme, it covers development of fault algorithms, specification of instrumentation and data recorder, and finally data analysis of an in service trial.

2. PERFORMANCE ANALYSIS

Currently fault diagnosis and module assessment methods available to helicopter maintenance personnel are simple fault tree logics, ie:

If A + B then C, or if A - B then D.

More complex star charts have been proposed but have rarely been incorporated into maintenance manuals. Comprehensive fault tree libraries can be derived from engine thermodynamic models in which component faults can be implanted. This capability was not fully developed at ARL at the time this investigation was commenced, and therefore could not be used. Gas path analyses such as those proposed by Staples and Saravanamutto, Reference 2, were investigated but were rejected in favour of the more "apparently" definitive/analytic differential gas path analyses suggested by Urban, Reference 3. This latter method offered a potential to trend data measurands and predict component efficiencies, and hence to diagnose faults to a model or component level using analytical methods. The Urban technique of differential gas path analysis is based on relating changes in independent component performance parameters (WA, η , Areas etc) to changes in dependent engine measurands (P,T) via a series of analytically derived influence coefficients. The technique has been used by both Shapiro, Reference 4, and Cockshutt, Reference 5, in the analysis of compressible flow and gas turbine cycle studies. Urban has further developed the method by formulating diagnostic equations or fault matrices for given operating conditions. In its most simplistic form it just relates changes in gas path components to changes in measured engine parameters whilst in its more developed algorithms attempts have been made to compensate for instrumentation errors and multiple faults by use of modern estimation theory (References 6 and 7). Similar diagnostic procedure are now commerically available from most major engine manufacturers TEMPER/GEM(GE), COMPASS (RR) and GTEVA (P & W). These recent additions to the engine diagnostic library utilize similar basic principles but incorporate varying enhancement techniques such as weighted least squares, Kalman Filtering or proprietary routines to derive the most likely faulty component.

This particular investigation only used a simple version of differential gas path analysis so limiting its complexity and compulational requirements. The procedure is justifiable in the case of a simple single spool gas turbine and has the added advantage of allowing faults or deficiencies in the analysis itself to be more readily identified. The use of the simplified procedures does not preclude, at a later stage, the adoption of a more complex analysis. The task was basically aimed at investigating methods for acquiring, analysing and interpreting data obtained in flight from an operational military helicopter and so establishing a technology base in engine monitoring procedures.

2.1 Module Assessment

RAAF operational experience with the Lycoming T53 engine in the Iroquois helicopter indicated that major deteriorations in performance occurred due to erosion in the compressor rotor blades and erosion or deposition in the turbine nozzles. As it was expected that similar problems would occur in the Lycoming T55-L11 engine the investigation was based on the Chinook helicopter. The T55-L11 engine has a single spool gas generator driving an essentially constant speed power turbine, it consists of 4 gas path modules, Figure 1 shows its configuration and the engine station numbering. The condition of gas path modules may be deduced from changes in their respective flow areas and efficiencies, however to assess the level of degradation of an individual component or discriminate between modules then many more measurands may be required for analysis than are practically available in a particular installation. A study of the T55 thermodynamic cycle shows that at least 13 aircraft/engine measurands are required to define a "corrected or normalized" operating point from which basic component performances can be assessed. The particular types of measurands determine the level and accuracy of the fault isolation capability.

In the Chinook/T55- 7 parameters (N_1, N_2, TOR, T5, P_1, T_1, and IAS) are readily available from the existing wiring harness. For this investigation an additional 6 parameters (P_2, p_3, T_3, FF, IGV and BB position) were incorporated into the aircraft-engines.

Using these measurands the following basic performance parameters could be derived.

$N_1/\sqrt{\theta}$		Corrected Engine Speed	N_{1C}
p_3/P_1		Compressor Pressure Ratio	CPR
T_3/T_1		Compressor Temperature Ratio	CTR
T_5/T_1		Power Turbine Temperature Ratio	TTR
$FF/\ \delta\sqrt{\theta}$		Corrected Fuel Flow	WFC
TORC		Corrected Torque	TORC
Where	θ	$T1/_{288.15}$ Temperature Ratio, and	
	δ	$P1/_{14.7}$ Pressure Ratio	

Of these parameters at least one, either N_{1C} or p_3/P_1, is required to specify a reference point. Using basic performance parameters and the gas turbine cycle equations a series of influence coefficients relating changes in efficiencies and areas, etc to changes in pressures and temperatures can be determined. Typically

$$\Delta T_3 = K_{a1}\ \Delta N_1 + K_{a2}\ \Delta T_4 + K_{a3}\ \Delta WA + K_{a4}\ \Delta \eta_c + K_{a5}\ \Delta \eta ct + K_{a6}\ \Delta A_4 \ . \ . \ .$$

$$\Delta p_3 = K_{b1}\ \Delta N_1 + K_{b2}\ \Delta T_4 \ . \ . \ .$$

The infuence coefficients K_{a1---n}, K_{b1---n}, etc. are evaluated from engine design parameters and are presented in matrix form for each operating point.

$$\begin{vmatrix} \Delta T_3 \\ \Delta p_3 \\ \Delta TORC \\ \Delta FFC \\ \Delta T_5 \\ \Delta A_5 \end{vmatrix} = \begin{vmatrix} K_{a1} & K_{a2} & K_{a3} & K_{a4} \\ K_{b1} & K_{b2} & & \\ K_{c1} & & & \\ & & & \\ & & & \\ & & & \end{vmatrix} \begin{vmatrix} \Delta N_1 \\ \Delta T_4 \\ \Delta WA \\ \Delta \eta_c \\ \Delta \eta_{ct} \\ \Delta A_4 \\ \Delta \eta_{pt} \end{vmatrix}$$

where for this paper

$$\Delta T_3 = \left(\frac{T_3}{T_1} - \frac{T_3}{T_1}\right)_{\text{baseline}} \qquad \Delta TOR_C = (TOR_C - TOR_C)_{\text{baseline}} \text{ etc,}$$

can be evaluated at a reference operating point of either p_3/P_1 or N_{1C}. Inversion of the matrix generates a fault matrix for the engine at the given reference operating point. The fault matrix represents a set of linear equations relating faults in the component or module to changes in corrected variables at given prespecified operating points. For example using N_{1C} as a reference.

$$\Delta T4 = K_{A1}\,\Delta T_3 + K_{A2}\ \Delta p_3 + K_{A3}\,\Delta TOR + K_{A4}\ \Delta FF + K_{A5}\ \Delta T_5$$

A typical numeric fault matrix is given in Figure 2 for N_{1C} = 95%. Calculation of trends in the independent variables W_A, T_4, etc, require fault matrices at each operating point for N_{1C} or p_3/P_1 if a fixed analysis point, as in the HIT method, is not to be prespecified. In this investigation it was found to be sufficient to generate fault matrices at 5 engine speeds 80, 85, 90, 95 and 100% N_{1C} and to interpolate linearly, for intermediate points.

ie : $K_{A1}/_{95.6} = M\ N_{95.6} + C$

Figure 3 shows typical fault coefficient for K_{A2}, K_{A1} etc, for the ΔT_4 and delta compressor efficiency, algorithms where M and C are the slope and constant of the linear equation.

For this analysis N_{1C} was taken as the reference baseline as it was an existing paramter, displayed in the cockpit and used by operators for driving and setting purposes. More importantly compressor erosion is directly related to changes in compressor pressure ratio p_3/p_1, and this parameter could be readily trended, and treated independently of any fault matrix.

To determine the respective deltas for each measurand, the individual variables were compared with engine data from both computer model predictions and actual engine tests. It was found that, as the model predictions were derived from engine specification data, large deltas or deviations in measured and calculated variables were generated, consequently to give more representative trend lines only actual engine test data were used in the subsequent analysis. Furthermore, to avoid the effects of bleed band on the trend lines and the diagnostics, all data for $N_{1C} < 83.5\%$ were ignored.

3. MONITORING UNIT

A schematic of the Data Monitoring Unit is given in Figure 4. It consists of 3 separate parts :

- Data Acquisition System
- Instrumentation and Wiring
- Data Transcription and Reduction.

3.1 Data Acquisition System

A 16 channel analogue and digital data recorder (16 CAD) was designed and manufactured at ARL in the late 70's for Engine Performance Monitoring work in the RAAF Macchi Jet Trainer, Reference 8 gives details of the basic system. The original 16 CAD systems used an 8 bit, tri-tone, recording mode, however the resolution was too small for engine performance trending. For this investigation two 16 CAD recorders were combined and converted to allow the recording of 16 channels at 10 bits and 14 channels at 8 bits. The system was based on small, rugged, low cost consumer available cassette tape recorders, and had performed more than adequately in the low vibration environment of the Macchi jet trainer. However problems arose with the low frequencies emanating from the helicopter rotor blades, the vibration predominantly affecting the data tape and its transport mechanism. Data were recorded on commercial C-90 compact cassettes in 30 second blocks at scan rates of 15 channels/sec : each block was therefore made up of 15 sets of measurands. The data recording was initiated by the pilot and activated by a crew man using a control box located in the galley way leading to the cockpit. Recording was carried out at least once per flight, once steady state operating conditions had been achieved. The data recorder control box imprinted a date-time-group and event number on the tape, however engine numbers had to be recorded by hand. Data tapes were removed once per week and forwarded to ARL for analysis.

3.2 Instrumentation and Wiring

17 analogue and 5 digital channels, comprising pressures, temperatures, engine speeds, fuel flows and discretes were recorded for both engines and the aircraft : a list of the instrumentation is given in Figure 4. Four of the instrumentation channels were non aircraft standard, they were :

- Compressor inlet pressure - Total
- Compressor outlet pressure - Static
- Compressor outlet temperature, and
- Fuel Flow

Special probes for P_1, p_3 and T_3, Figure 5, were manufactured by Hawker de Havilland Australia, whilst the fuel flow metering system, based on Faure Herman Turbine Flow meters, was detailed by the RAAF. Figure 6 shows a fuel flow meter installed in the Chinook No. 1 engine fuel line, whilst a typical pressure transducer installation is given in Figure 7. The installation of probes, wiring looms, data recorder and break in points to existing instrumentation lines were carried out by RAAF personnel at No. 3 Aircraft Depot Amberley. All instrumentation wiring looms were terminated in the aircraft cabin heater bay where the data recorder was located. The complete installation was covered by a RAAF Draft Modification Order - DMO 178.

Instrumentation calibration was carried out initially at ARL and then following installation in the aircraft. Calibrations were updated at approximately six month intervals and coincided with pressure transducer changes and investigations into torque meter system irregularities. The only problems experienced with the instrumentation were with incorrect positioning of the P_1 probes (180° out of phase), fatigue failures in the T_3 thermocouple, and repeatability problems in the torque meter system. Throughout the trial most of the equipment was found to be reliable : the only component affected by the helicopter vibration was the tape recording unit. The instrumentation transducers used in this trial were selected primarily for their repeatability as against overall accuracy; Table 1 gives a summary of the instrumentation and their basic specifications.

TABLE 1

MEASUREMENT	TRANSMITTER	ACCURACY	REPEATABILITY	No. of BITS
IAS	SETRA 239	± .1% FS	± .02 FS	10
PRESSURES	ROSEMOUNT 1332A	± .1% FS	± .1% FS	10
TEMPERATURES	ANALOG DEVICES 2B 52 TYPE K	± .1% FS	± .1% FS	10
TORQUE	MAGNETIC RELUCTANCE	± 2.5%	NOT KNOWN	10
FUEL FLOW	FAURE HERMAN	± .25%	± .25%	10
N_1 - N_2		± .1%	± .1%	10
BLEED BAND	PRESSURE SWITCH IN IN FCU LINE			8
IGV	POTENTIOMETER			8

3.3 Data Transcription and Reduction

The engine/aircraft data were transcribed from the tri-tone format on the cassette tape to octal using an ARL designed transcription unit, Reference 8. Transcription of data proved most difficult due to apparent variations in tape speed, caused (it is thought) by helicopter vibration. On many occasions data strings appeared to be corrupted and were automatically deleted by the error code algorithms. A manual scan of data during conversion using a data "break out box" indicated that most of the data had in fact been correctly recorded. Because of the simple design of the system it was not possible to syncronize helicopter data record speed with transcription play back speed even though a time pulse had been imprinted on the tape. Repeated transcriptions at modified play back speeds, ± 10% of nominal, would generate different data sets : a collation of these transcriptions could on occasions be used to form a complete data block. Throughout the trial the transcription unit and the data tape play speed proved to be the most unsatisfactory component of the monitoring investigation.

Data reduction was undertaken on a DEC LSI-11/23 computer using instrumentation calibrations to convert to engineering units. Data correction, analysis, trending and plotting were carried out using standard routines written in FORTRAN.

4. RESULTS AND DATA ANALYSIS

The data acquisition system was installed in Chinook helicopter A15-009 for 2 years when it was removed prior to the helicopter under going a major servicing : the instrumentation, wiring looms were however left in the aircraft. In the course of the trial 18 engines changes occurred, 7 on the starboard and 11 on the port side. A post analysis of the engine records showed that only 7 removals were indicative of faults which could have been diagnosed by performance trending, ie FCU, air leaks from compressor gallery etc. Examinations of all monitored data revealed that only 7 engines had data trends with more than 60 points, and of these only two were associated with the 7 engines removed for gas path related problems. One of these was due to an FCU change whilst the other was a high HIT reading which had occurred at the begining of a trend record and was corrected by a change in the T_5 harness without a permanent engine removal.

4.1 Data Reduction and Screening

Initial data analysis was carried out by plotting performance curves for CPR, CTR, TORC etc against N_{1C}. The value of CPR etc was determined from an arithmetic mean of the individual values of p_3, and P_1 from the data block. The means were therefore an average of 15 nominally steady state points. Typical plots for CPR and CTR against an N_{1C} baseline are given in Figure 8, while Figure 9 gives a cross plot of CTR versus CPR for the data of Figure 8. In both sets of plots the data scatter is small. The only measurement to exhibit large scatter bands was Torque ; these plots were much more inconsistent. Analysis of the raw data from a typical record block indicated large differences in the magnitude of the torque measurement. Variations of individual readings for p_3, T_5, Torque from a data block with time (0-15 secs) are given in Figure 10, together with respective values of standard deviation and coefficient of variation. The high value of CVA for torque appears to be a result of aperiodic "drop outs" in the indicating system which were not picked up by the analogue cockpit gauge. Applications of standard statistical rejection criteria ($\pm 2\sigma$) for example were not totally successfull in eliminating the erroneous, and obvious, torque variations and an alternative data rejection algorithm was developed. This algorithm used a combination of engineering judgement and statistical principles and incorporated a selective use of data means, standard deviations and coefficients of variations. Figure 11 illustrates

the process on some sample torque data in rejecting an obvious data "outlier" which if left in would have degraded the data mean. The rejection algorithm was used in the initial data reduction program and applied to all recorded data. It is interesting to note that it had only a significant effect on the torque values, Table 2 shows typical result for P_3, T_5 and Torque.

TABLE 2

DATA	INITIAL			FINAL		
MEASURAND	$\bar{x}$	σ	CVA	$\bar{x}$	σ	CVA
P_3	86.0	1.2	1.4	86.4	.95	1.1
T_5	938	6	.6	939	3.8	.4
TOR	48	4	8.3	50.2	.65	1.3

Not withstanding the above selection procedure the torque data were still marred by much higher scatter than the other variables, and throughout the trial it posed a significant obstacle to generating representative trends in many of the independent, or design variables. A further problem in the data analysis was the large distance between ARL and RAAF Amberley, and the consequent time delay in checking consistency of data. On many occasions at least a month elapsed between data recording and data analysis. Considerable data would be lost if a probe were broken or incorrectly installed. A further problem in the analysis was the lack of engine numbers inscribed on to the tape: at least twice an engine change had taken place and had not been correctly identified. However step changes in data trends readily indicated this fault. Notwithstanding the above comments the basic quality of the data was good, and considered adequate for diagnostic purposes provided a comprehensive check of the records was carried out.

4.2 **Case Studies**

As mentioned above little of the data recorded had immediate application to performance trending and gas path diagnostics, however a number of cases warranted further investigation, and provided good examples of problems occuring in service, three of these are presented as case studies :

- Data Consistency - CASE I
- Deterioration in Performance - CASE II
- Component Change - CASE III

It should be noted that the analysis of these cases was carried out retrospectively; analysis in real time may not have provided such definitive conclusions.

CASE 1 - Data Consistency

This particular case emphasises the need to monitor closely the changes in engine - instrumentation - calibration - configuration. In the course of the trial, the electrical connections for both engines N_1 recording systems were reversed as part of a trouble shooting exercise. Failure to include this fact in the initial trend analysis resulted in a step change in all measured and calculated variables. It should be noted that N_{1C} was the baseline parameter. Although the perturbations in trends were eliminated by application of a statistical outlier algorithm developed by Frith, Reference 9, it did raise doubts about the quality and consistency of the data. Cross correlations of both sets of engine data, in this case for corrected fuel flow, Figure 12, immediately showed that the outlier data points were in fact from different families and not true faulty data points. Reprocessing trends, with these points reversed, eliminated the perturbations without resort to an outlier algorithm. This data "mix-up" should not have occurred if the data had been processed at unit level in real time : flags would have been set showing the change in electrical configuration.

CASE II - Performance Deterioration

Analysis of measured data trends for this engine indicated a clear downward slope, or fall off, in fuel flow and torque, there was also a minor yet perceptible reduction in power turbine inlet temperature T5. Figure 13 details the results for fuel flow with a single piece-wise linear least square fit showing the downward slope. Application of the gas path algorithms or fault matrix, not suprisingly, diagnosed a reduction in gas generator turbine nozzle area A_4, Figure 14, and a reduction in engine mass flow WA, Figure 15. However because of the assumptions used in developing the fault matrix, Figure 2, an increase in power turbine efficiency was also predicted, Figure 16. Conversely, because of the assumption that $\Delta\eta_{pt} = -\Delta A_5$, a decrease in power turbine nozzle area would also have been predicted. In this case it is not possible to discriminate accurately as to which turbine was at fault. Further data in terms of either turbine inlet or exhaust gas temperatures are required. This uncertainty is a major fault of the assumptions required in simple URBAN analysis. Application of uncertainty techniques as proposed by Frith & Frith Reference 10 could perhaps help in the discrimination process if sufficient data were available.

Cross correlation of this fault in the actual engine was not possible as the diagnostic analysis was carried out some time after the monitoring programme had been terminated and the engine allocated to another aircraft.

CASE III - Component Change

In this last example a double piece-wise linear least squares fit was applied to the trend data. The results indicated small but distinct changes in the measured parameters p_3 and T_5, Figure 17 and 18. A single least squares fit could have easily masked the change in T_5, and the p_3 change would have been interpreted incorrectly. When both p_3 and T_5 changes are considered together it is suggestive that the engine operating or running line has been modified : this is consistent with a change in the fuel control unit (FCU) However as this fault or component modification was not "programmed" into the fault matrix an alternative raison d'etre must be generated. In this case an increase in compressor efficiency was predicted see Figure 19. This result is unlikely as there has been no commensurate change in Turbine Inlet Temperature T_4, Figure 20. Examination of engine/aircraft maintenance records for Chinook 009 indicated that an FCU change had occurred at precisely the indicated trend point. Prior to the FCU change Torque levels on the reported engine were observed to be erratic and at high levels. Whilst this was consistent with the trend records for torque the latter were judged inconclusive due to the large inherent scatter in that measurand. The reason for the in service FCU change was a attributed to a slow time for the engine - N_1 - to unwind as the throttle was retarded. This fault would not have been recorded or analysed in the trial as only steady state data records were used. A transient diagnostic procedure, as being developed by Merrington, Reference 11, could possibly have indicated the FCU fault by assessing changes in the engine spool dynamics, provided transient data records were available.

CONCLUSIONS

A helicopter engine performance monitoring programme, covering the installation of an automatic data recorder and its instrumentation, the development of fault algorithms, and the analysis of data has been described. The in service trial on a RAAF Chinook helicopter was most ambitious, and suffered due to the large distance between the helicopter operating base and the laboratory at which the programme was managed and data analysis carried out. On occasions this resulted in many weeks delay before data reduction could be undertaken or equipment faults remedied. Notwithstanding this, and the limited resources deployed on the total programme, the results were most promising. Major problems occurred due to torque sensor "drop-out" and variability of data cassette recording speed due to helicopter vibration. These faults reduced the range and quantity of the data available. Further problems also occurred due to the relatively large number of engine changes, and the lack of an engine number - identifier - on the tape.

Analysis of the results showed that there was little scatter in the data (with the exception of torque) and that data trends for both measured and calculated gas path parameters were clearly visible. The trends indicated that overall performance deterioration could be inferred from long term trending whilst diagnosis of individual or component faults could be identified and diagnosed from step changes in both measured and calculated variables. Precise interpretation of the trend, especially the step changes, was difficult due to the simple fault matrix used. The form of the matrix was directly related to the small number of measurands available and the assumptions used in the analysis. A developed or operational system should incorporate at least measurements of inter-turbine pressure (P_5) and exhaust gas temperature (T_6) in order that faults can be related to either the high or low pressure turbines. More consistent torque records/data would also be required.

Overall the trial has demonstrated that an automatic performance monitoring programme on a military helicopter is a viable proposition, and that the monitoring system can be retrofitted. It has also shown that data can be acquired which are much superior in quality and prognostic capabilities to that available from either a HIT or IFM check. However before such a system is adopted for fleetwide use, the basic ground hardware and developed software should be available at an early stage of the installation.

REFERENCES

1. GLENNY D.E. — An Evaluation of Engine Performance Assessment Procedures for the Lycoming T53 Engine as Installed in the Iroquois Helicopter, DSTO ARL ME Note 387, April 1981.

2. STAPLES, L.J.; SARAVANAMUTTO, H.I.H. — An Engine Analyser Program for Helicopter Turbo shaft Powerplants, AGARD CP 165, April 1974.

3. URBAN, L.A. — Parameter Selection for Multiple Fault Diagnostics of Gas Turbine Engines, ASME Paper No. 74-GT-62.

4. SHAPIRO, A.H. — The Dynamics and Thermodynamics of Compressible Fluid Flow, J. Wiley 1953.

5. COCKSHUTT, E.P. — Gas Turbine Cycle Calculations. Differential Methods in the Analysis of Equilibrium Operation, NRC Aeronautical Report LR.481, March 1967.

6. BRYSON, A.E. HO, Y-C — Applied Optimal Control, J. Wiley 1975.

7. VOLPONI, A.J. — Gas Path Analysis - An Approach to Engine Diagnostics, 35th Symposium - Mechanical Failures Prevention Group. Gaithersburg M.D. April 1982.

8. ADAMS M.T. — Digital Data Acquisition System for Use in Aircraft Engine Condition Monitoring DSTO ARL ME Report 151, August 1978.

9. FRITH, P.C.F. — Implications of Performance Shifts for Trending Procedures, TTCP HAG 8 Gas Turbine Engine Performance Monitoring - Proceedings of 2nd Meeting (Vol 2) April-May 1986.

10. FRITH, D.A. FRITH, P.C.F. — Procedures for Trending Aircraft Gas Turbine Engine Performance, 7th ISABE Conference BEIJING China, September 1985.

11. MERRINGTON, G.L. — Identification of Dynamic Characteristics for Fault Isolation Purposes in a Gas Turbine Using Closed Loop Measurements, AGARD 71st Symposium of the Propulsion and Energetics Panel (Paper 36) Quebec City Canada, May-June 1988.

ACKNOWLEDGEMENTS

The author would like to acknowledge the considerable assistance received from other members of staff at ARL and in the RAAF. In particular the efforts of:

- The members of the Engine Control and Data Systems Group at ARL,
- RAAF personnel at No. 3AD and No. 12 Squadron at RAAF Base Amberley, and
- A.S. Vivian of the Engine Performance Group at ARL.

FIGURE 1

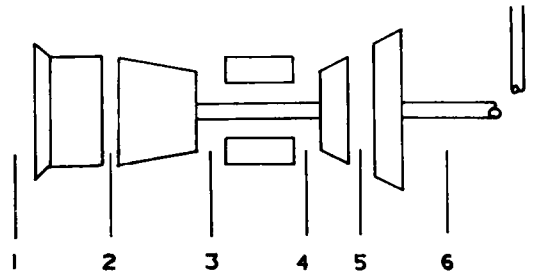

TURBOSHAFT ENGINE STATION NUMBERS

$$\begin{vmatrix} \Delta T_q \\ \Delta WA \\ \Delta \eta_C \\ \Delta \eta_{CT} \\ \Delta A4 \\ \Delta \eta_{PT} \end{vmatrix} = \begin{vmatrix} .43 & 0 & 0 & 0 & .78 & 0 \\ .07 & 0 & 0 & 1.0 & -1.47 & 0 \\ -1.96 & .66 & 0 & 0 & 0 & 0 \\ 1.43 & -.88 & .43 & 0 & -1.17 & -.43 \\ .29 & -1.0 & 0 & 1.0 & -1.08 & 0 \\ -.18 & 0 & .49 & -1.0 & .53 & .51 \end{vmatrix} \begin{vmatrix} \Delta T_3 \\ \Delta P_3 \\ \Delta TORC \\ \Delta FFC \\ \Delta T_5 \\ \Delta N_1 \end{vmatrix}$$

FIGURE 2 T55-11 FAULT MATRIX N_{1C} = 95.0%

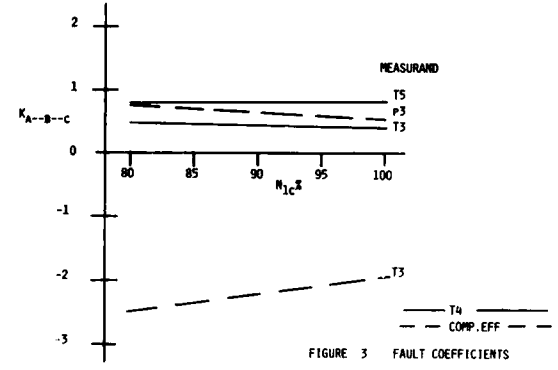

FIGURE 3 FAULT COEFFICIENTS

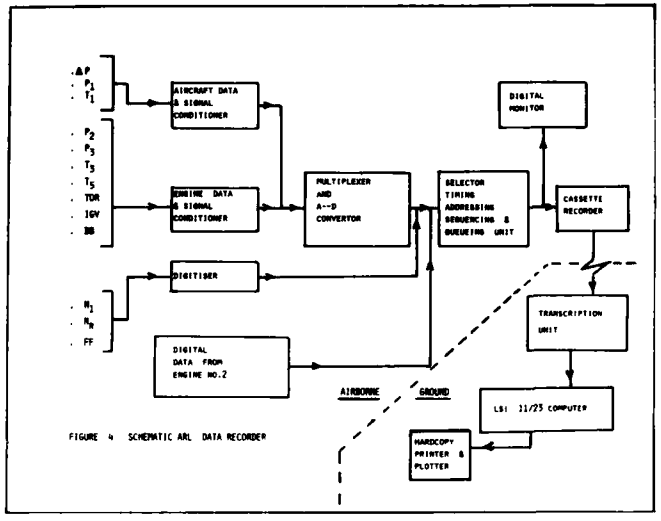

FIGURE 4 SCHEMATIC ARL DATA RECORDER

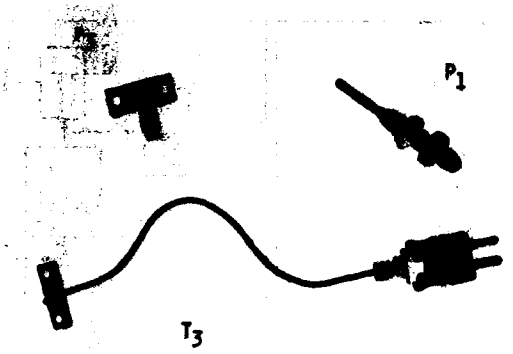

FIGURE 5 CHINOOK PROBES

FIGURE 6 FUEL FLOW METER

FIGURE 7 PRESSURE TRANSDUCER

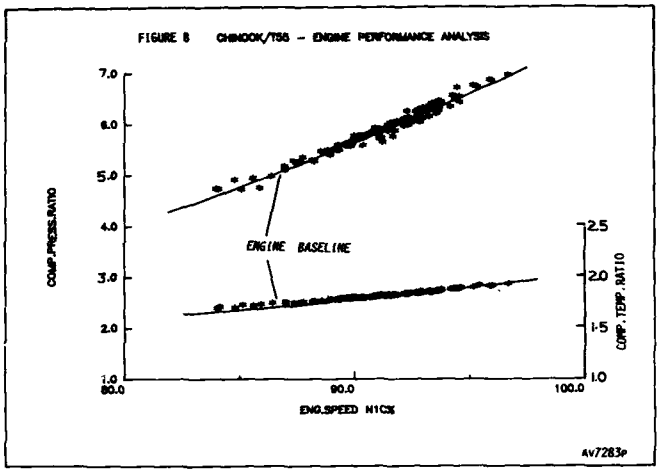

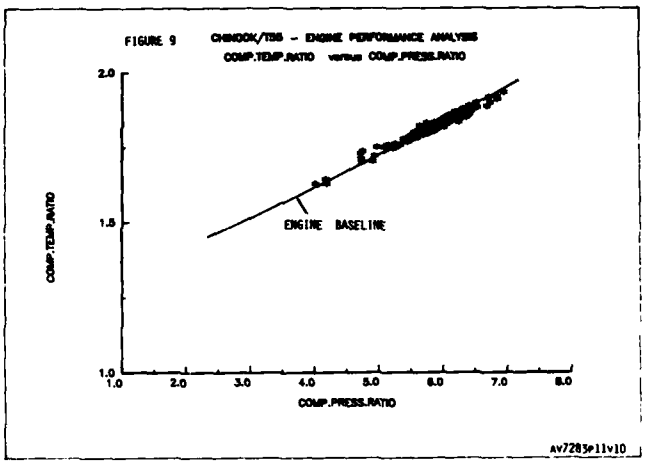

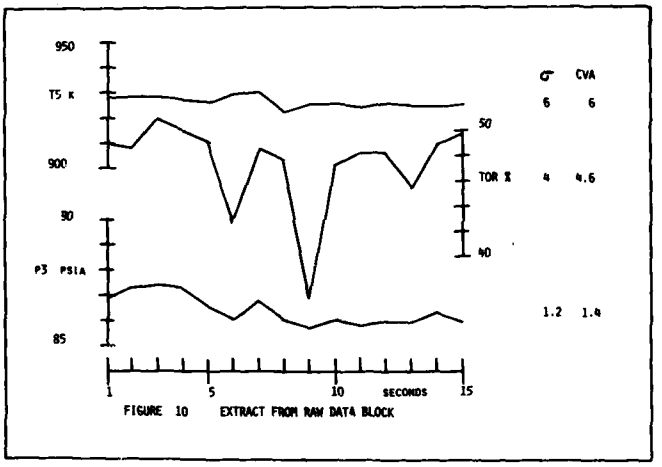

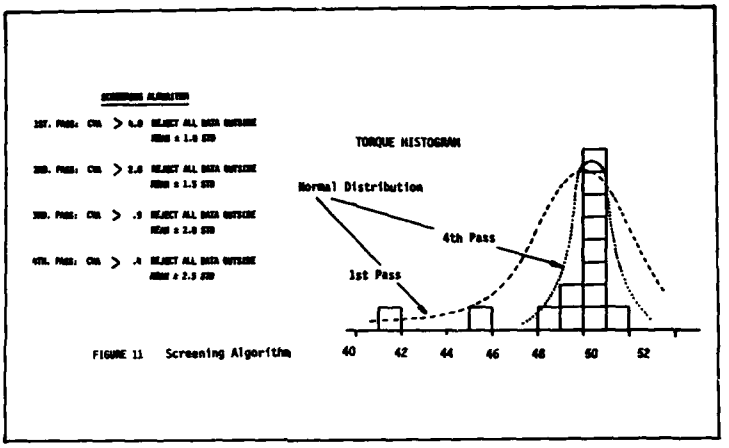

FIGURE 11 Screening Algorithm

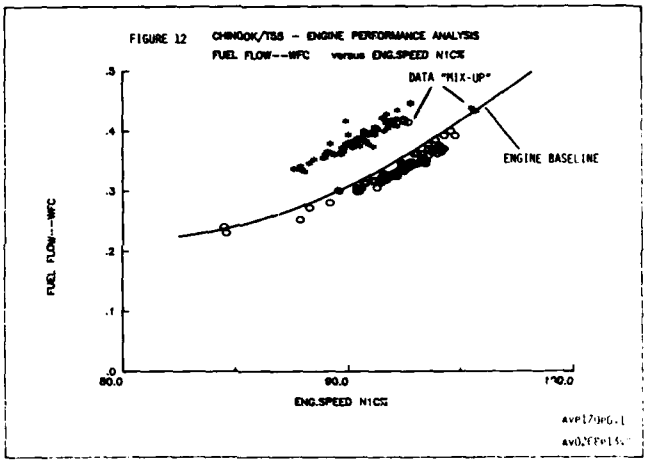

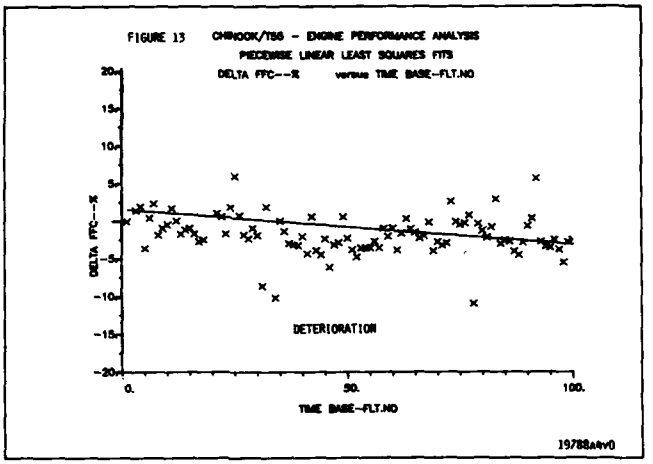

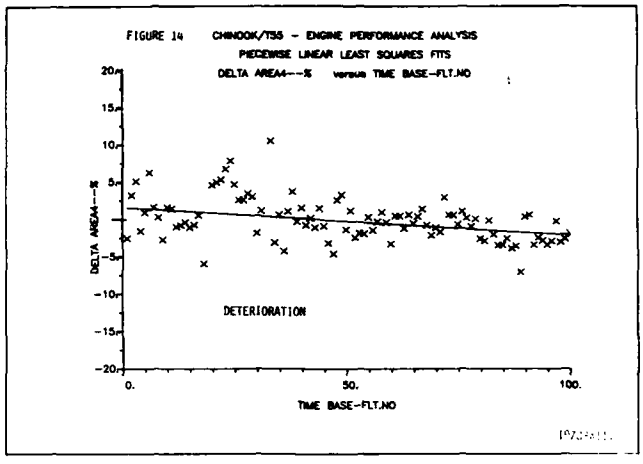

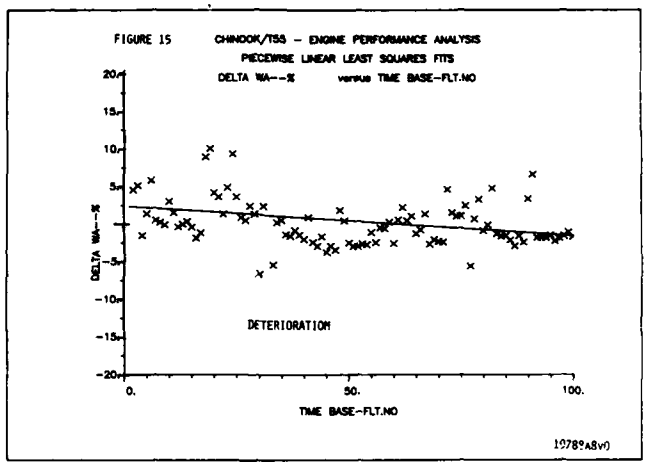

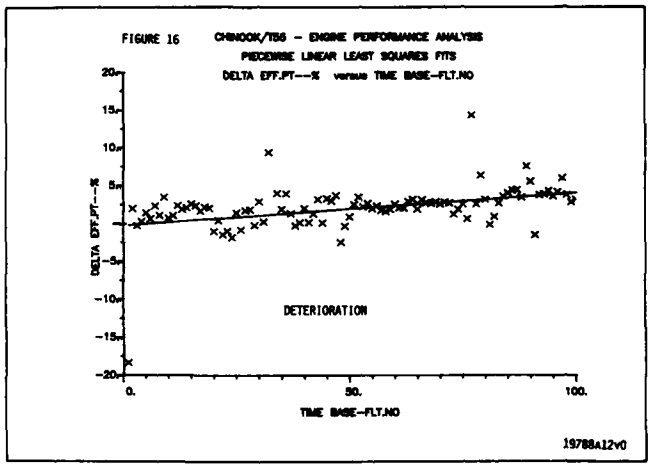

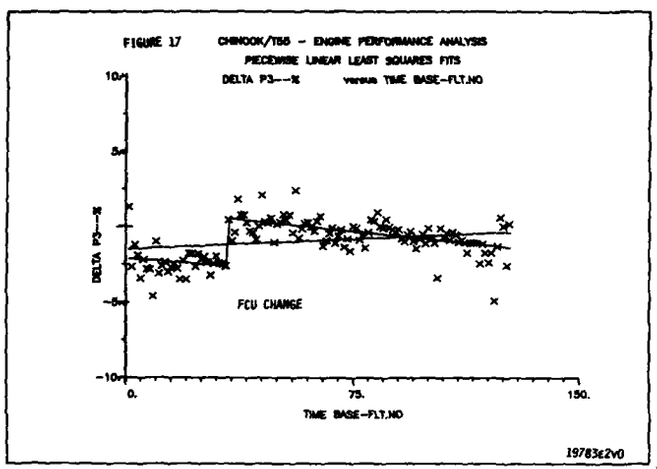

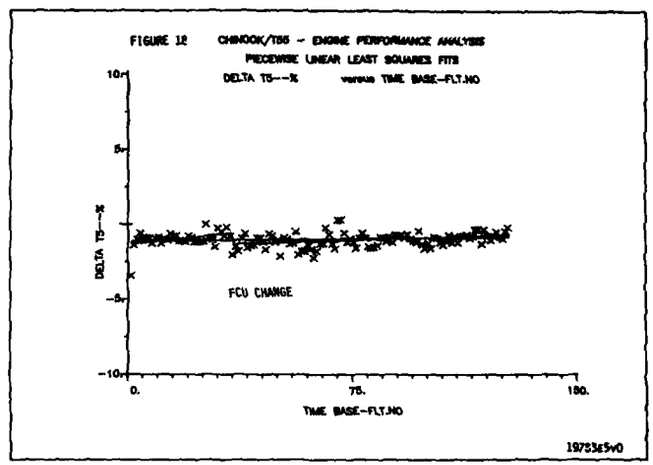

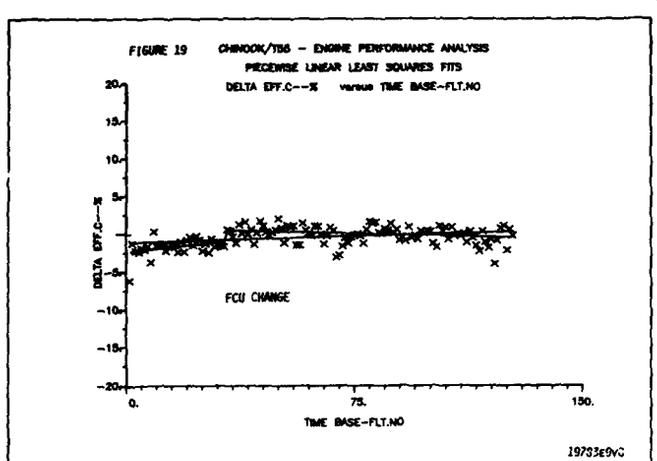

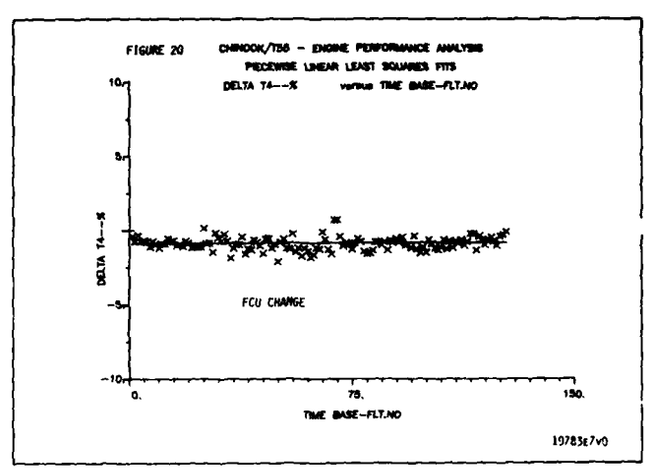

THE EFFECTS OF A COMPRESSOR REBUILD ON GAS TURBINE ENGINE PERFORMANCE

J.D. MacLeod
Research Officer
National Research Council
Montreal Rd, Building M-7
Ottawa, Canada, K1A 0R6

Capt. J.C.G. Laflamme
Air Maintenance Squadron
Canadian Forces Base
Baden-Soellingen
Federal Republic Germany

SUMMARY

The Canadian Department of National Defence, in conjunction with the Engine Laboratory of the National Research Council Canada, initiated a project for the evaluation of gas path coatings on the Allison T56 engine. The objective of this work was to evaluate blade coatings in terms of engine performance effects and material durability. The project included a study of the influence of rebuilding the compressor on performance, since dismantling and rebuilding was required for the coating process.

This paper describes the compressor rebuild study, including the overall objectives, the test set-up, the performance effects, and the uncertainty of the measured results. The impact of this work on the coatings project is also documented.

1.0 BACKGROUND

In 1983, the Canadian Department of National Defence expressed serious concerns over the rapidly escalating cost of operation and maintenance of aircraft gas turbine engines. The components of major concern were compressor and turbine blades and vanes. The increasing rate of rejection of these items during overhaul prompted a reassessment of the time between overhaul for certain engine types.

The blades and vanes of gas turbine engines are susceptible to deterioration as a result of erosion and corrosion. The deterioration (increased surface roughness, loss of material, and alteration of aerodynamic profile) manifests itself in terms of reduced stall margin and lower performance, characterized by poorer fuel economy and increased operating temperatures. The T56 engines used in the C130 Hercules and the CP140 Aurora aircraft have proven susceptible to this type of deterioration.

Recently, advances have been made in the state of the art in blade coating technologies. In addition to offering erosion and corrosion protection, these new "super smooth" coatings are claimed, by their manufacturers, to offer significant aerodynamic performance improvements. Modern blade coatings have not previously been qualified on T56 engines. Since smoothness effects are a function of blade Reynolds number, which is dependent on engine size and speed, claims based on evaluations on other engines were not satisfactory. Thus, there was a requirement to undertake an analytical and experimental engine testing program to identify and quantify the effects of coating a compressor.

As the program involved considerable, high-accuracy engine testing, the Canadian Forces requested the support of the National Research Council of Canada to undertake this evaluation and qualification. While the engineering documentation (blade frequency response, durability testing, surface finish, etc.) and the material characteristics study were assigned to the Materials Laboratory, the Engine Laboratory was requested to perform a performance evaluation on a coated engine. The Engine Laboratory has actively supported the development of military aero engine performance monitoring and fault isolation procedures. Current projects are aimed at correlating changes in gas turbine component and overall engine performance to physical degradation in the engine.

The Engine Laboratory was tasked to evaluate the effect of coatings on engine performance and efficiency, and make recommendations for subsequent widespread use of coatings for operational application on the T56 and other gas turbine engines.

Since the compressor must be disassembled in order to be coated, it was deemed necessary to isolate the effect on performance of the rebuild from that of the coating. To achieve this, a program comprising three consecutive rebuilds was established which would quantify the portion of any performance shift which was not attributable to the coating itself. The assessment of the results from this rebuild program forms the basis of this paper. The specific objective of this paper is to establish the magnitude of the change in compressor and overall engine performance which was caused by the disassembly/reassembly of the compressor during overhaul.

2.0 EXPERIMENTAL INSTALLATION

To properly assess the various effects of a compressor rebuild on the performance of a gas turbine engine, a sophisticated test set-up, with specialized instrumentation was required. A description of the engine, instrumentation and test facility used for this assessment is included to illustrate the complexity of this project.

2.1 ENGINE DESCRIPTION

The test vehicle being used for this rebuild study is the Allison T56-A14LFE single-spool turboprop engine from a CP-140 Aurora patrol aircraft. This engine is an excellent candidate for this study because it has no variable geometry or transient bleed valve operation that might vary the back-to-back performance of the engine. The particular engine used in these tests had no flying hours since it was originally built. The T56 engine has a fourteen stage compressor, with bleed valves which are only open below the idle speed, a six can combustor, and a four stage turbine. The single shaft is coupled to a reduction gearbox mounted forward of the compressor. For the NRCC tests, power was transmitted through the gearbox to a flywheel and a Froude waterbrake dynamometer, which replaced the propeller used on the aircraft. A schematic diagram of the engine test set-up is shown in Figure 1. The figure illustrates how the engine, gearbox, dynamometer, and inlet duct were arranged in the test stand.

The engine control is one of a constant speed design using a governor to maintain a constant rotor speed of 13820 RPM. Power is controlled by setting the turbine inlet temperature with the power lever angle. In the experimental program, the engine was run at a fixed aerodynamically corrected rotational speed to provide a common basis for comparison. This required that the mechanical speed of the engine be adjusted using the dynamometer, as a function of the ambient temperature. The procedure used for each test run consisted of establishing a series of increasing power settings, for a given corrected rotor speed. At each power setting, the engine was allowed to stabilize for five minutes, then two sets of data were recorded. Typically, up to six power settings (12 data points) were recorded for each test.

2.2 INSTRUMENTATION

Instrumentation used on the T56 was divided into two categories, external, and internal. The external instrumentation included a high Mach number airmeter in front of the engine, compressor inlet pressure and temperature rakes, a tailpipe airmeter mounted after the turbine, vibration sensors on the engine carcass, and turbine-type fuel flowmeters. The high velocity airmeter facilitated accurate flow measurement because of the large local difference between the total and static pressure. A diffuser mounted behind the airmeter reduced the airspeed down to a normal entrance velocity. The internal instrumentation consisted of total temperature and pressure probes in every stage of the compressor, as well as, compressor discharge and turbine inlet pressure/temperature rakes. With this degree of instrumentation, it was possible to monitor not only the condition of the overall engine, but also the performance of its major components, and the individual compressor stages. This report is limited in scope to an assessment of the data collected for the overall engine and its major components.

The data were recorded using a NEFF 620 data acquisition system controlled by a DEC PDP 11/34 computer. For each test, the engine was operated at a constant speed over its full power range. At various established power settings, a five minute stabilization period was observed before two three minute steady-state data scans were initiated.

2.3 TEST FACILITY

The test cell used for the rebuild testing at the Engine Laboratory NRCC, at Ottawa, Canada, was Cell No. 2. Ambient air enters vertically from the roof through a retractable door. The planar dimension of the cell is a constant 4.6 x 4.6 metres throughout the test section. Engine exhaust and the entrained secondary airflow egress from the cell through a collector/augmentor tube to a vertical stack that discharges to the atmosphere. There is no acoustic attenuation in the inlet or outlet of the test cell. The entire cell is constructed of heavy reinforced concrete. The walls are covered with a 100 mm thick acoustic barrier to minimize noise propagation. The control, observation, and data acquisition room is located on the starboard side of the cell. An operator's window and a closed circuit television camera permit visual monitoring of the engine.

Since humidity affects the thermodynamic properties of the engine cycle, the following atmospheric limitations were observed to avoid condensation in the inlet air stream and minimize performance corrections:

maximum relative humidity: 75%

maximum absolute humidity: 14 g water per kg of air.

Humidity corrections for specific heat ratios used in the calculation of airflow were obtained from Reference 9.

3.0 SUMMARY OF TESTING AND REBUILD PROCEDURES

In an attempt to isolate the effects of a compressor rebuild by monitoring small thermodynamic performance changes, a highly structured test plan was required. To achieve this goal, a test sequence was established which would best suit the requirements of the rebuild study, based on the knowledge of how the rebuilds were to be performed.

3.1 TEST SEQUENCE

To establish the effects of rebuilding the compressor on overall engine performance, a comparison of the results of three rebuilds was chosen. A larger sample would have been preferred, however, there were significant cost and time constraints on the project. The T56-A-14LFE engine chosen for the testing had no flight hours, in order to develop a legitimate "as-new" baseline. Baseline testing of the engine was performed to establish the "as-received" condition of the engine. Performance signatures of the overall engine and all its individual components were then quantified. During the test runs, data were recorded while the engine was operating at a constant corrected rotor speed. Several different corrected speeds, ranging from 13,000 to 14,500 RPM were run to assess the effects of corrected speed on any performance changes.

After the baseline testing was completed, the engine was sent to the overhaul contractor to be disassembled and rebuilt following normal procedures. Upon return to NRCC, the engine was retested using the same procedures utilized in the baseline tests. Following this testing, the engine was sent for the second rebuild, returned, and retested. Currently, the engine is undergoing its third and final rebuild.

3.2 REBUILD PROCEDURE

The rebuild procedure used for this project consisted of a disassembly, inspection, and reassembly of the compressor section only. For each rebuild, the engine was removed from the NRCC test cell, and shipped to the overhaul contractor, Standard Aero Ltd. in Winnipeg, Manitoba.

The disassembly procedure entailed the removal of the turbine and combustor modules, leaving only the compressor. The compressor casing was then removed from the rotor, and the stator vanes were then detached from the casing. The rotor was unstacked and all the individual blades were removed. During removal, each blade was numbered, so that it could be returned to its original position upon reassembly. After disassembly, each piece underwent a petroleum solvent wash followed by an inspection to insure that no parts are damaged. Corrugated seals for stator vane segments were not replaced, nor were labyrinth seals reworked. Measurements of critical dimensions such as blade tip clearances, vane axial clearances, and rotor balance condition were recorded before disassembly and after reassembly. During the first rebuild, these measurements revealed that the axial clearance between the rotor and stator of several stages was out of tolerance. This may have occurred because of shifting during operation or improper assembly of the original build by the manufacturer. During reassembly, the clearances were set within the specified tolerances.

Upon reassembly of the compressor case, the stator vane axial clearances were set. The rotor blades were replaced in the same numbered order, and their balance checked. The entire compressor was then mated with the combustor and turbine modules, and a functional test was performed. The engine was then returned to NRCC for testing.

4.0 DATA PRESENTATION

Data recorded during a test were stored in basic engineering units so that observers could visually check the data quality as the test progressed. After a test was completed, the data were reduced to absolute values, and used to calculate performance parameters such as, pressure and temperature ratios, corrected air and fuel flow, etc. These performance parameters were then curvefitted to quadratic equations, using a least squares method. The dependent variable for curvefitting engine data was corrected turbine inlet temperature. Comparisons between various test runs were then made using the curvefitted values of each parameter. All data presented in this study were taken at 100 percent corrected rotor speed, or 13,820 RPM. For curvefit comparisons, the reference value used for the corrected turbine inlet temperature was 2200 degrees Rankine.

Engine station designations used for the T56 are numbered as shown in Figure 2, in accordance with the SAE-755A recommendations (Reference 5). To facilitate comparisons with manufacturer's data, the performance parameters are presented in the U.S. Inconsistent system of units (Reference 12).

4.1 EFFECTS OF AMBIENT CONDITIONS

The NRCC test cell has no provision for controlling the ambient inlet air temperature. The engine was therefore operated over a wide range of temperatures experienced over the Canadian seasons. All performance data were corrected to standard day reference conditions for comparison. Previous experience at NRCC (Reference 1) and other test facilities (Reference 2), suggests that the normal standard day corrections do not ensure that the data will collapse to a single curve. Since temperature lapse rate data were not available for all of the parameters being considered in this study, test data presented here were all recorded at similar ambient temperature conditions.

The use of the long inlet duct on the T56 (Figure 1) causes a significant pressure loss and distortion at the compressor face. This pressure loss simulates an altitude of nearly 500 metres and a ram pressure ratio of approximately 0.97. The ram pressure ratio is defined as the ratio of the compressor inlet total pressure divided by the static pressure at the exhaust exit plane. The effect of ram pressure ratio on output

power is accounted for using the manufacturer's procedures (References 6 and 7). However, there are no guidelines for any other parameters which may be affected by the ram conditions.

5.0 TEST RESULTS

For this study, fourteen performance parameters were chosen to describe the condition of the engine for each power setting. The selection of appropriate parameters was made to analyze the performance of the overall engine and of its individual components, namely the compressor, combustor and turbine. To assess the compressor behavior, isentropic efficiency, corrected airflow, corrected speed, and compressor pressure and temperature ratios were examined. For combustor performance, combustor pressure and temperature ratios were analyzed. Isentropic efficiency was picked as a suitable parameter to describe the performance of the turbine. Corrected fuel flow, corrected output power, and specific fuel consumption were chosen for overall engine behavior, as were engine temperature and pressure ratios. Corrected torque was added as a redundancy check on corrected output power.

Most of the performance parameters chosen for this study are commonly used in the existing literature (Reference 13). However, on the T56 engine, the presence of both turbine inlet temperature and pressure provided several additional parameters which are normally excluded from many engine test results. Combustor pressure and temperature ratios and turbine efficiency are notable examples of such additional parameters.

Since only the compressor was disassembled during the rebuild sequence, the strongest emphasis was in monitoring changes in the compressor performance and in turn, the effects on the overall engine performance. Combustor and turbine performance are included to see if a change in compressor operation affects any of the downstream components.

5.1 DATA QUALITY

There are many indicators of the data quality in any given set of engine test results. Influences of the test facility on engine operation are best typified by plotting the inlet and exhaust pressures, and temperatures as a function of power setting. Indications of engine thermal stability may be detected by observing the repeatability of the readings of engine spool speed and temperature and pressure ratios throughout the engine.

For this study, the quality of the data for each test was determined by the back-to-back repeatability of each of the performance parameters. This was done by comparing the deviations of the individual data points from the curvefitted quadratic equations derived from the data. A mean value of the deviation of the data from its curve was used to establish the repeatability of each parameter within each test.

To establish the quality of the data recorded within each rebuild-test sequence, an analysis of the run-to-run repeatability was performed. This analysis consisted of comparing curvefitted test data recorded under the same ambient conditions during the same rebuild sequence. A mean deviation between the curvefits of each of the performance parameters was then used to define the repeatability within each rebuild.

An estimate of the overall repeatability of each of the parameters was accomplished by combining the back-to-back and run-to-run repeatabilities. With these estimated uncertainty values, a true comparison of the build-to-build effects would be carried out.

5.1.1 BACK-TO-BACK REPEATABILITY

For each power setting during a test, two complete scans were recorded by the data acquisition system. To assess the back-to-back repeatability, the values of these recorded points were compared to the values of the curvefit generated points at a specified corrected turbine inlet temperature. This procedure gave an indication of how close the repeated data points were to each other, and the "goodness" of the curvefit to the actual data points. These deviations are shown in Table 1 for the baseline tests and the first and second rebuilds. A representative sample of the back-to-back repeatability of compressor efficiency and corrected output power are shown in Figures 3 and 4, respectively.

The compressor efficiency (Figure 3), corrected air and fuel flows (see Table 1) all show very tight repeatability (±0.02% to ±0.11%) for all three cases. The compressor pressure and temperature ratios also indicate very small deviations from the curve (±0.01% to ±0.09%), as do the combustor pressure and temperature ratios (±0.01% to ±0.07%), and the engine temperature ratio (±0.06% to ±0.08%). The corrected output power (Figure 4) and specific fuel consumption reveal a larger scatter (±0.28% to ±0.38%), especially during the second rebuild (±0.49% for SFC). The turbine efficiency, engine pressure ratio and the corrected torque also display some noticeable data scatter (±0.14% to ±0.39%).

The deviation in the corrected output power and specific fuel consumption are to be expected because each of these parameters were calculated from two or three measured quantities. The scatter in the turbine efficiency is also expected because it is calculated using an approximate value for the specific heat ratio within the turbine.

In addition, the turbine efficiency is an inverse parabolic function, which may not be conducive to a least squares quadratic curvefit.

5.1.2 RUN-TO-RUN REPEATABILITY

Within each rebuild test sequence, at least three complete runs were recorded for each corrected rotor speed condition. Having established how well the test data agree with the generated curvefits, the next step was to determine how well these curves collapsed within each rebuild. To evaluate the run-to-run repeatability of the data within each rebuild, the values of curvefitted data were compared from at least two runs taken at similar ambient conditions. These deviations within the rebuilds are shown in Table 2 for the baseline, the first, and second rebuild. Unfortunately, during baseline testing, no two tests were performed at or near the same inlet temperature, so the repeatability figures for the baseline, quoted in Table 2, represent the average of the repeatabilities of the first and second rebuilds. For compressor efficiency and corrected output power, the repeatabilities from the second rebuild can also be seen in Figures 3 and 4.

Close examination of the run-to-run repeatability results (see Table 2) showed that compressor efficiency (Figure 3) and corrected airflow were reasonably close (±0.15% to ±0.24%). Corrected fuel flow displayed a slight aberration during the second rebuild (±0.41%), as did specific fuel consumption during the first rebuild (±0.36%). The corrected output power (±0.39%) and the corrected torque (±0.41% to ±0.52%) revealed significant scatter within each rebuild (see Figure 4). Compressor pressure and temperature ratios were extremely repeatable (±0.05% to ±0.07%), as were the combustor (±0.02% to ±0.07), and engine pressure and temperature ratios (±0.07% to ±0.08%). The corrected speed (±0.02% to ±0.18%) and the turbine efficiency (±0.05% to ±0.06%) were in close agreement.

Certain parameters, such as turbine efficiency and engine pressure ratio had better run-to-run repeatability than back-to-back repeatability. In the case of turbine efficiency, this anomaly presumably results from difficulties in representing the uniquely shaped efficiency function with a quadratic equation.

5.1.3 COMBINED REPEATABILITY

Before a comparison of the rebuild data could be made, it was necessary to establish the overall or combined repeatability of the data from each rebuild. Since the same equipment, instrumentation suite, data system, and facility were used for each test, it is unlikely that the measurement bias errors would have changed. Thus the population of observed measurements taken at the same environmental conditions for a given engine build would be combined to form an overall datum with a defined data scatter. If when compared to the data taken under similar environmental conditions for an engine rebuild, there is a shift outside the scatter band, then a performance shift would be deemed to have occured. Normally a statistical approach (Reference 4) would be used to calculate expected measurement uncertainty, but for this experiment it has not yet been completed. Lacking this information, a more basic method was used. To accomplish this, a worst case scenario was assumed. In other words, it was assumed that both the back-to-back and run-to-run repeatabilities were acting in the same direction within each rebuild, and opposing each other across each rebuild. Therefore, the overall measured repeatability for each parameter would be the sum of all four observed repeatability figures (from Tables 1 and 2), between the baseline and its corresponding rebuild. For example, from Tables 1 and 2, the overall repeatability for compressor efficiency during the first rebuild would be,

$$(\pm 0.02\%) + (\pm 0.06\%) + (\pm 0.21\%) + (\pm 0.24\%) = \pm 0.53\%.$$

More probable, the data scatter would be calculated using the root-sum-square, which in this case, the observed repeatability in compressor efficiency would be only ±0.33%. Thus, the method chosen to define the overall repeatabilities for this rebuild study always over-estimates the more appropriate statistical value.

Since the first rebuild becomes the new baseline for the second rebuild, the overall repeatabilities will be slightly different for each cross-examination of rebuild data. A complete list of the overall repeatabilities for each of the parameters, for the first and second rebuild are given in Table 3.

For the first rebuild, several parameters such as, compressor efficiency, corrected airflow and fuel flow, turbine efficiency, and engine pressure ratio, all exhibited overall repeatabilities of approximately ±0.50%. Other parameters such as, corrected speed, compressor and combustor pressure and temperature ratios, and engine temperature ratio, had overall repeatabilities ranging from ±0.16 percent to ±0.32 percent. By far the largest overall data scatter appeared in the corrected output power (±1.44%), specific fuel consumption (±1.25%), and the corrected torque (±1.67%). The majority of the scatter in specific fuel consumption was attributed to the output power term. The corrected torque indicated some speed dependence which was accounted for in the output power measurements. The overall repeatabilities for the second rebuild were very similar to those of the first rebuild.

In general, the quality of the test data for the baseline, and first and second rebuilds appeared to be very good, with the possible exception of output power.

Overall, the test data recorded for the rebuild study were considered to be of sufficiently good quality to be used for an accurate comparison.

5.2 COMPARISON OF REBUILD DATA

Having established the overall repeatabilities of the performance parameters selected for the rebuild evaluation, one representative test run from each rebuild was compared to its corresponding baseline. The observed shifts in the various performance parameters are given in Table 3. Several of these shifts are shown graphically in Figures 5 through 9. The results of each rebuild are discussed separately.

5.2.1 FIRST REBUILD RESULTS

To assess the various effects of the rebuild, the engine and its individual components were handled separately. The effects on compressor performance were noticed in the compressor efficiency (Figure 5), which showed an increase of 1.2% from the baseline value. This increase was double the pessimistic repeatability of the measured parameter. Corrected airflow (Figure 6) showed an increase of 0.77% from baseline to the first rebuild, which was also larger than the repeatability. The compressor pressure ratio increased by 1.3%, which was nearly five times the estimated repeatability. The shift in the compressor temperature ratio was of the same magnitude as its uncertainty.

It was interesting to note that the performance of the combustor was also affected by the compressor rebuild. The combustor pressure ratio decreased by 1.0%, which is significantly larger than its repeatability. This phenomenon is not entirely unexpected because earlier work (Reference 8) had suggested a direct relationship between the combustor pressure loss and the flow function at the compressor exit. In this case, the compressor exit pressure increased more than the airflow, thereby decreasing the flow function at the compressor exit. The effect on the combustor temperature ratio (+0.20%) was negligible, as was the effect on the turbine efficiency.

As far as overall engine performance was concerned, an increase of 0.73% was observed in the corrected fuel flow (Figure 7). Shifts in the corrected torque (+1.5%) and corrected output power (+0.79%), shown in Figure 8, were measured, but they were within the overall repeatability band. The specific fuel consumption (Figure 9), showed no shift because both fuel flow and output power shifted about the same amount and in the same direction.

5.2.2 SECOND REBUILD RESULTS

For the second rebuild, the first rebuild was used as the new baseline for comparison. The observed shifts in the performance of the engine and its components were very similar to the first rebuild. The compressor efficiency (Figure 5), showed a decrease of 0.84%, which was larger than the estimated repeatability. The corrected airflow (Figure 6) only decreased by 0.23%, which was less than the repeatability. The compressor pressure ratio also decreased, this time by 1.3%, definitely beyond the measurement repeatability limits. The compressor temperature ratio remained unchanged.

As in the first rebuild, the combustor pressure ratio was affected by the changes in compressor performance. An increase of 0.52% was observed in the combustor pressure ratio, which is well above its repeatability estimate. An increase in the compressor exit flow function, resulting from the compressor exit pressure decreasing more than the airflow, could be the cause of this behavior. The combustor temperature ratio was again unaffected by the rebuild, as was the turbine efficiency.

Concerning the overall engine performance, the corrected fuel flow (Figure 7), decreased by 1.4%, which is more than twice the established repeatability. Decreases in corrected output power (Figure 8), specific fuel consumption (Figure 9), and corrected torque (-0.76%) were observed, but these shifts were all below the projected repeatabilities for these parameters.

5.3 DISCUSSION OF THE REBUILD RESULTS

The results of the two rebuilds were compared assuming the overall repeatability was the worst combination of all of the back-to-back and run-to-run repeatabilities. In actual fact, statistically speaking, the real precision would be less than this, and in some cases, much less. At present a complete uncertainty analysis, using the methods described in Reference 4, is underway to more accurately determine the bias and precision errors. A comparison of these errors with the results in Table 3 may prove that the overall repeatabilities estimated in this study were too large, in which case, several other parameters, such as corrected output power and specific fuel consumption may be included as significant performance shifts.

The actual cause for the observed shifts in the performance parameters is open for speculation. During the first rebuild, axial clearances were slightly altered between the rotor and stator of several of the compressor stages. In addition, inspections of critical internal gas path dimensions made before and after each rebuild (References 10 and 11) suggest that the compressor internal geometry changed slightly, albeit within the manufacturers specified tolerances. These minor geometry changes include seal clearances, blade tip clearances, and stator position. Although these changes are very

small, the random combination of them may cause the compressor performance to shift sufficiently for laboratory instrumentation to detect it.

6.0 CONCLUSIONS

In setting up a project to quantify the effects rebuilding the compressor has on the performance of a gas turbine engine, there is always some difficulty in defining statistically measurable performance shift. The data presented here for the Allison T56 engine, illustrates that while some parameters have reasonably large repeatabilities associated with them, others have quite small limits, which makes them ideal for measuring important but small changes in performance.

The results of the rebuild study to date have indicated that performance shifts from simply disassembling and reassembling a compressor are measurable. The most significant shifts appear in parameters such as compressor efficiency, corrected airflow, compressor pressure ratio, corrected fuel flow, and combustor pressure ratio. The latter parameter is affected because of a change in the exit conditions of the compressor.

The effects of a compressor rebuild are, of course, statistically random. After the first rebuild, the compressor performance improved, while following the second rebuild, the compressor performance deteriorated. Whether or not these two rebuilds have shown the full extent to which the performance may change is unknown. The third and final rebuild will add to this knowledge.

The impact of the rebuild study on the compressor blade coating is important. To the users of coated engine parts, the performance parameters of most concern are output power and specific fuel consumption. The repeatabilities associated with these parameters are larger than most other parameters and thus only gross shifts could be detected. The same may be said for engine health monitoring (EHM) testing, where faults are implanted in engine components to detect performance changes.

7.0 RECOMMENDATIONS

It is recommended that more attention should be paid to the effects of temperature variation on the T56 engine. This would allow a larger supply of data from which a more confident set of repeatability estimates may be obtained. Until such time, data should only be compared when it has been recorded at the same ambient temperature conditions.

When analyzing data taken from the blade coating project and/or implanted fault studies, the effects of the rebuilding of the compressor should be considered. This implies increasing the uncertainty interval on certain parameters when comparing data taken across a compressor rebuild.

8.0 REFERENCES

1) MacLeod, J.D., Effect of Inlet Temperature Variation on Gas Turbine Engine Performance, National Research Council of Canada, LM-ENG-007, 1987.

2) Greco, L., Gordon, S., Allison T56-A-14 Engine - Official Sea Level Low and High Temperature, and Altitude Performance Tests, NAEC-AEL-1836, 1966.

3) Imray, M.D., Analysis of T56 Experimental Data, GasTOPS Report, GTL-19-28.5-TR.1, 1988.

4) Abernathy, R.B., Thompson, J.W., Handbook of Uncertainty in Gas Turbine Measurements, AEDC-TR-73-5, 1973.

5) Gas Turbine Engine Performance Station Identification and Nomenclature, SAE ARP 755A, Revised April, 1974.

6) T56-A-14LFE Overhaul Manual, Volume I, C-14-33-000/MP-001, 1983.

7) Military Turboprop Engine Specification 670-D for Model T56-A-14, 1976.

8) Kirkhope, K.J., Computer Model of the T56 Turboprop Engine: Thermodynamic Analysis and System Design, GasTOPS Report GTL-TR-19-22.1.1, 1984.

9) Samuels, J., Gale, B., Effect of Humidity on Performance of Turbojet Engines, NACA TN 2119, 1950.

10) Dyke, L., NRC T56-A-14LFE Test Bed Engine: SAL Detailed Inspection Report, Standard Aero Report 54947, 1986.

11) Dyke, L., NRC T56-A-14LFE Test Bed Engine: SAL Compressor Inspection Data, Standard Aero Report J76796, 1987.

12) Streeter, V.L, Wylie, E.B., Fluid Mechanics 7th Edition, 1979.

13) Saravanamuttoo, H.I.H., et al, Gas Turbine Theory 3rd Edition, 1987.

TABLE 1: BACK-TO-BACK REPEATABILITY

PARAMETER	DEVIATION FROM CURVE (%)		
	BASELINE	FIRST REBUILD	SECOND REBUILD
Compressor efficiency	±0.02	±0.06	±0.08
Corrected airflow	±0.06	±0.06	±0.11
Corrected fuel flow	±0.07	±0.10	±0.09
Corrected output power	±0.28	±0.38	±0.35
Specific fuel consumption	±0.28	±0.29	±0.49
Corrected speed	±0.01	±0.03	±0.04
Compressor pressure ratio	±0.05	±0.09	±0.08
Compressor temperature ratio	±0.01	±0.04	±0.05
Turbine efficiency	±0.20	±0.23	±0.23
Combustor temperature ratio	±0.01	±0.03	±0.04
Combustor pressure ratio	±0.07	±0.04	±0.05
Engine temperature ratio	±0.06	±0.07	±0.08
Engine pressure ratio	±0.15	±0.14	±0.15
Corrected torque	±0.30	±0.39	±0.35

Reference: Corrected speed = 13820 RPM
Corrected Turbine Inlet Temperature = 2200 °R

TABLE 2: RUN-TO-RUN REPEATABILITY

PARAMETER	OEVIATION WITHIN REBUILD (%)		
	BASELINE	FIRST REBUILD	SECOND REBUILD
Compressor efficiency	±0.21	±0.24	±0.18
Corrected airflow	±0.15	±0.16	±0.13
Corrected fuel flow	±0.28	±0.16	±0.41
Corrected output power	±0.39	±0.39	±0.39
Specific fuel consumption	±0.32	±0.36	±0.27
Corrected speed	±0.10	±0.18	±0.02
Compressor pressure ratio	±0.06	±0.07	±0.05
Compressor temperature ratio	±0.07	±0.07	±0.07
Turbine efficiency	±0.06	±0.05	±0.06
Combustor temperature ratio	±0.07	±0.07	±0.06
Combustor pressure ratio	±0.03	±0.02	±0.04
Engine temperature ratio	±0.08	±0.07	±0.08
Engine pressure ratio	±0.07	±0.08	±0.07
Corrected torque	±0.46	±0.52	±0.41

Reference: Corrected speed = 13820 RPM
Corrected Turbine Inlet Temperature = 2200 °R

TABLE 3: REBUILD EFFECTS

PARAMETER	OVERALL REPEATABILITY (%)		DEVIATION BETWEEN REBUILD (%)	
	FIRST	SECOND	FIRST	SECOND
Compressor efficiency	±0.52	±0.56	+1.16	-0.84
Corrected airflow	±0.43	±0.46	+0.77	-0.23
Corrected fuel flow	±0.61	±0.76	+0.73	-1.44
Corrected output power	±1.44	±1.51	+0.79	-0.70
Specific fuel consumption	±1.25	±1.41	-0.07	-0.80
Corrected speed	±0.32	±0.27	-0.11	-0.06
Compressor pressure ratio	±0.27	±0.29	+1.26	-1.31
Compressor temperature ratio	±0.19	±0.23	-0.20	+0.02
Turbine efficiency	±0.54	±0.57	+0.09	+0.18
Combustor temperature ratio	±0.18	±0.20	+0.20	-0.05
Combustor pressure ratio	±0.16	±0.15	-1.00	+0.52
Engine temperature ratio	±0.28	±0.30	+0.01	+0.01
Engine pressure ratio	±0.44	±0.44	-0.07	+0.23
Corrected torque	±1.67	±1.67	+1.50	-0.76

Reference: Corrected speed = 13820 RPM
Corrected Turbine Inlet Temperature = 2200 °R

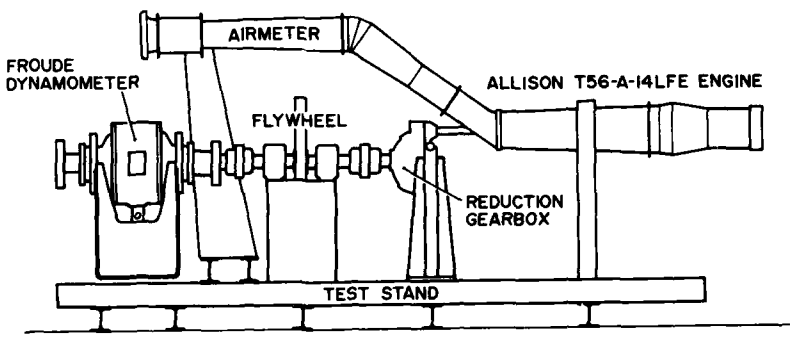

FIGURE 1: SCHEMATIC OF T56 TURBOPROP ENGINE ON TEST STAND

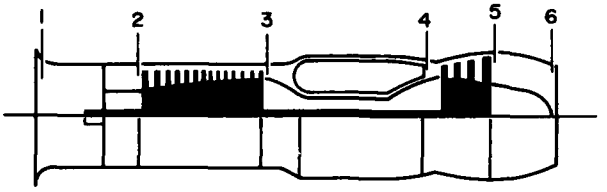

STATION	DESCRIPTION
1	ENGINE INLET
2	COMPRESSOR INLET
3	COMPRESSOR DELIVERY
4	TURBINE INLET
5	TURBINE DELIVERY
6	TAILPIPE EXHAUST

FIGURE 2: T56 STATION NUMBERING

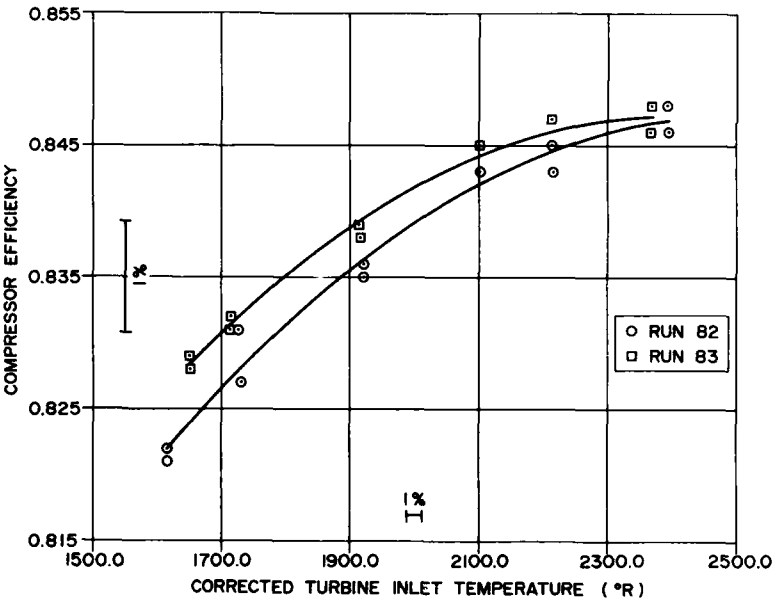

FIGURE 3: DATA QUALITY - COMPRESSOR EFFICIENCY

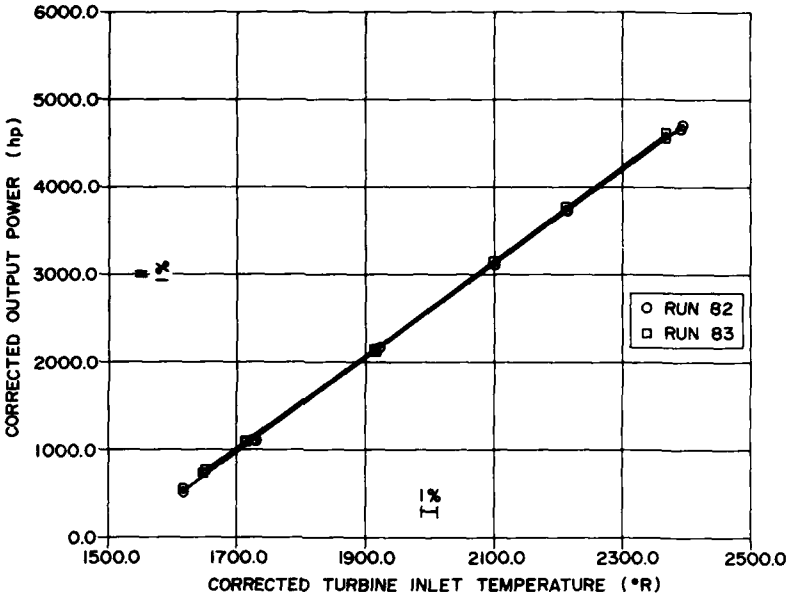

FIGURE 4: DATA QUALITY - CORRECTED OUTPUT POWER

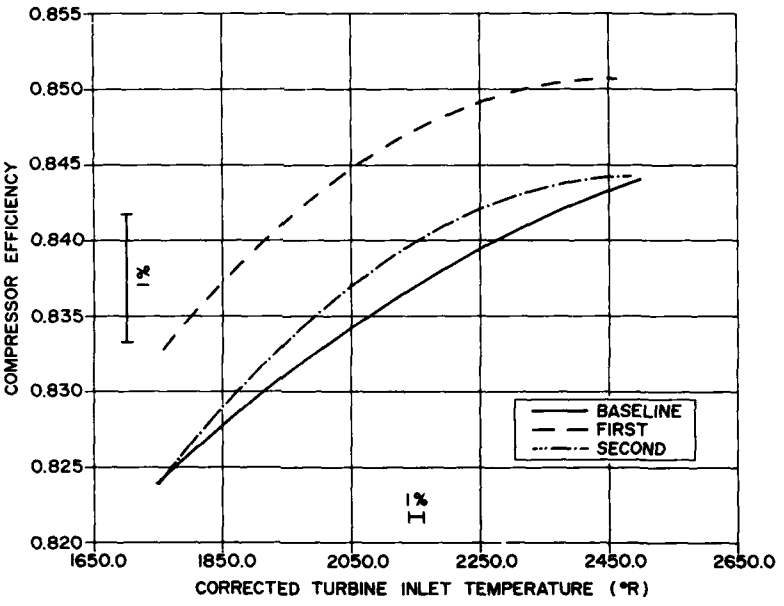

FIGURE 5: ENGINE PERFORMANCE - COMPRESSOR EFFICIENCY VS CORRECTED TURBINE INLET TEMPERATURE

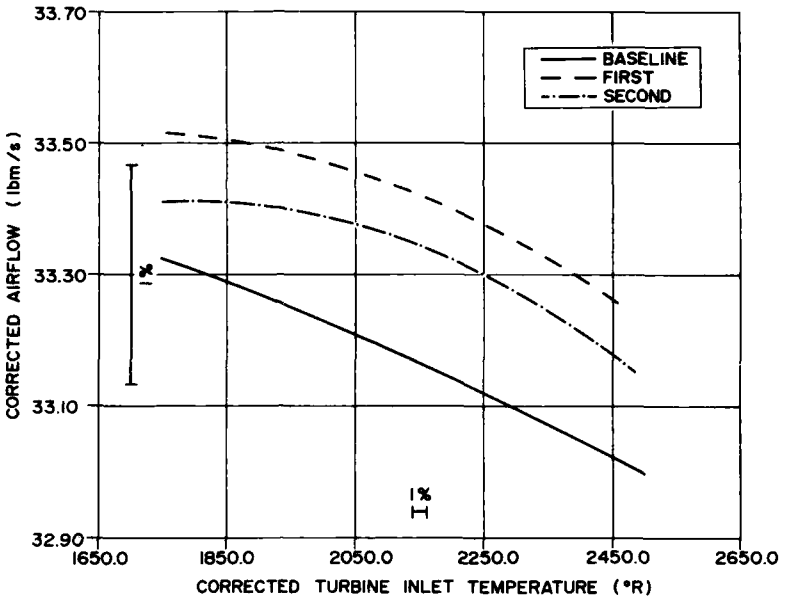

FIGURE 6: ENGINE PERFORMANCE - CORRECTED AIRFLOW VS CORRECTED TURBINE INLET TEMPERATURE

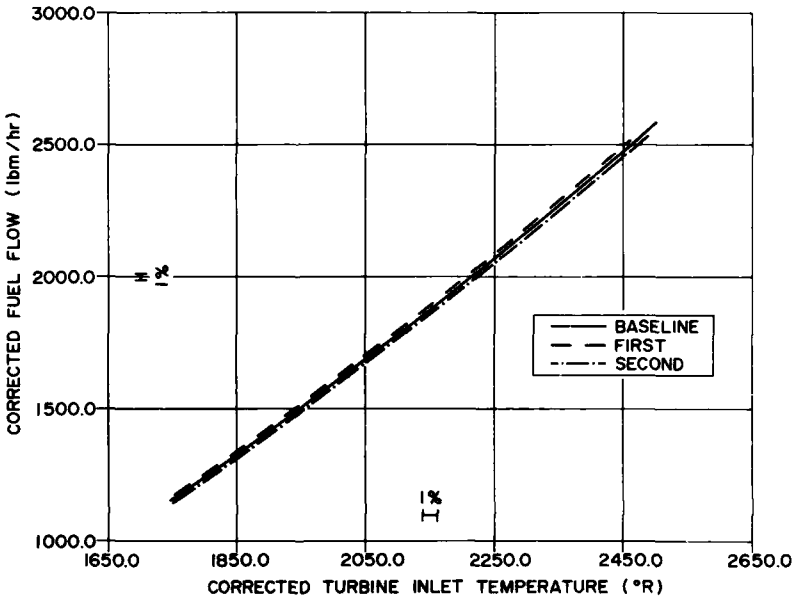

FIGURE 7: ENGINE PERFORMANCE - CORRECTED FUEL FLOW VS CORRECTED TURBINE INLET TEMPERATURE

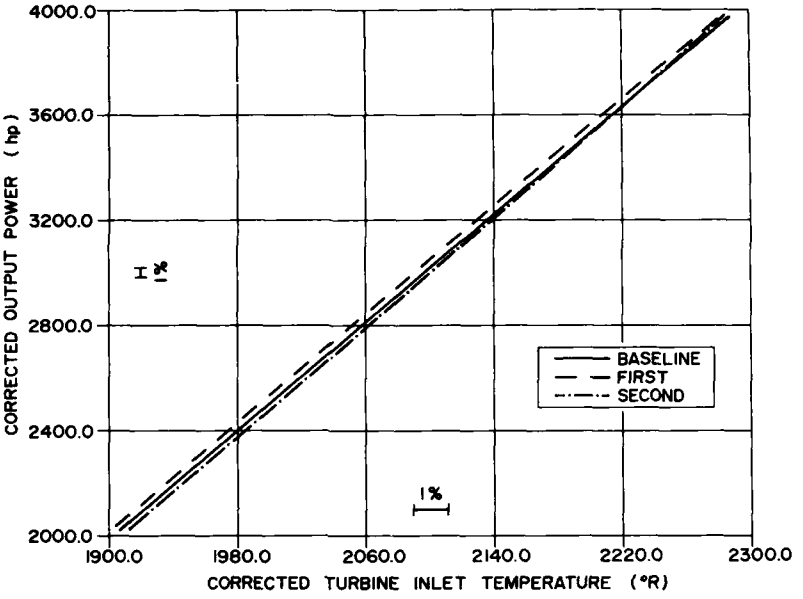

FIGURE 8: ENGINE PERFORMANCE - CORRECTED OUTPUT POWER VS CORRECTED TURBINE INLET TEMPERATURE

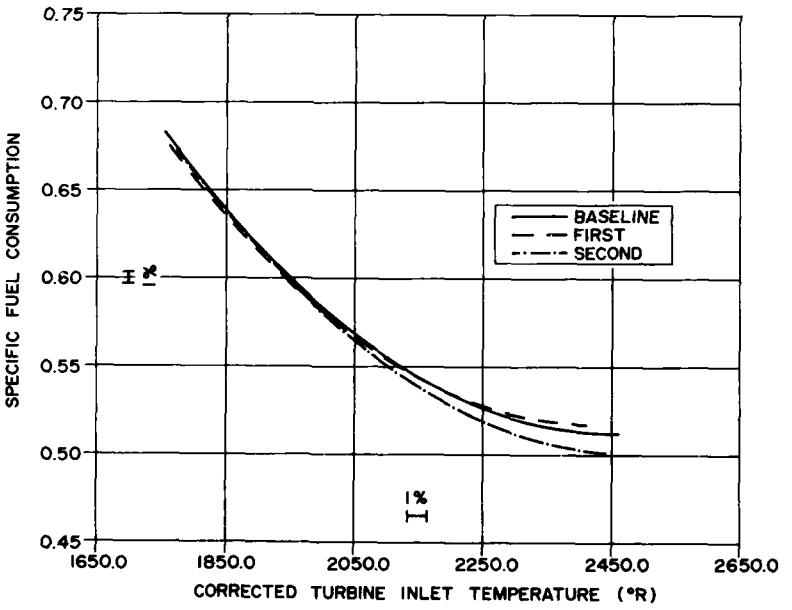

FIGURE 9: ENGINE PERFORMANCE - SPECIFIC FUEL CONSUMPTION VS CORRECTED TURBINE INLET TEMPERATURE

DISCUSSION

D.E. GLENNY

What is the acquisition rate for steady state analysis points and what average is taken over the 2½ min sample period? What is the acquisition rate per channel/second? What are rates for pressures,temperatures and speeds?

Author's Reply:

The NEFF data acquisition system used for this test-program, has a variable scanning frequency. The scanning rate for steady-state testing was 100 Hz for all channels. This includes all pressures, temperatures frequencies etc. Unfortunately we don't have individual pressure transducers for each pressure probe on the engine, thus mechanical multiplexers are used. The scanning time for each port on these multiplexers was approximately 3 seconds.

SYSTEM CONSIDERATIONS FOR INTEGRATED MACHINERY HEALTH MONITORING

by
R.M. Tester
Manager - Future Systems Group
Powerplant Systems Division
GEC Avionics Limited
Airport Works
Rochester
Kent ME1 2XX
England

SUMMARY

Aircraft engine health monitoring, and other related machinery condition monitoring, has been gaining in credibility and implementation over recent years. It is destined to become 'standard fit' on all new major aircraft programs in the near future. To date the monitoring systems have mainly been stand alone in form, and have been treated as separate functions. This paper discusses the considerations for integrating health monitoring into other aircraft systems, and reviews the potential benefits to be gained by such integration. In conclusion the paper will present two products from both ends of the spectrum, which represent a simple single unit integration, and a full aircraft wide implementation.

INTRODUCTION

Aircraft health monitoring, linked with on-condition maintenance philosophies, has been the topic of much increased interest in recent years. A considerable number of development programs have been undertaken across the industry, and these have sometimes been extended to evaluate their benefits in limited operational trials. The results of these programs have led to establishing the credibility of condition monitoring, to the extent that the concept of condition monitoring systems is being designed in from the start on major new aircraft programs - and also some major retrofit programs.

Central to the debate on the implementation of any condition monitoring system is ensuring that the user gains a benefit from the investment that he has made. The benefits are gained by reduced operating costs from on-condition maintenance, together with added safety margins that can be obtained by more absolute knowledge of component condition. Traded against them are the recurring and non-recurring costs of incorporating sensors, acquisition and processing to the aircraft. The additional ground support facilities and overall information infra-structure add to this investment, but are needed to efficiently realize the benefits.

Balancing these two sides of the equation, in what is essentially a Cost Benefit Analysis, will demonstrate whether any particular system (configuration) is worth implementing or not. Where there is scope to reduce the investment side of the equation, then either more cost benefit can be realized for a particular implementation, or other configurations that were previously uneconomical can become attractive propositions. It is this scope for reduction in investment that is explored in this paper. This is accomplished by considering the the integration of health monitoring into other aircraft systems, rather than treating it as a separate, stand-alone entity.

HEALTH MONITORING FUNCTIONS

It is worth very briefly reviewing the general types of health monitoring. This will ensure a common information baseline from which the rest of the paper can be considered.

* Life Usage Monitoring - this is a means of better estimating a component's life by considering how much work it has actually done, rather than by defining a maintenance action after a safe, predefined number of hours. Usage algorithms can be as complex as required - basically a balance is struck between simplicity and accuracy.

* Direct Analysis - this is where component health is directly measured, normally based on actuals above or below defined boundaries. For example vibration monitoring and quantitive debris monitoring (QDM) immediately relate actual data to transmission components.

* Trend Monitoring - this is a method for evaluating deterioration of a component(s) condition, by analysing changes over a period of time of directly measureable parameters. Features of this type of monitoring are repeatable, accurate measurements and historical data, coupled with statistical computation to remove erroneous data trends. Data from long term/fleet wide trend monitoring is used to update on-board direct analysis boundaries and algorithms, in support of continually improving the effectiveness of the health monitoring system.

Ideally, all of the above techniques could be variously applied to the different components of an aircraft, in order to provide comprehensive health status reporting of any particular system. Whilst effective this would represent a very costly investment, in financial, operational and organisational terms.

It is essential, therefore, that a strategic approach to health monitoring be taken. Figure 1 shows a typical plot of benefit vs investment for a health monitoring system. Whilst the plot has no scales, it is the shape that is relevant, and illustrates that whilst zero investment obviously produces zero benefit, relatively small investments can produce significant benefits. After this the Law of Diminishing Returns applies as increasing investment produces progressively less increase in benefit.

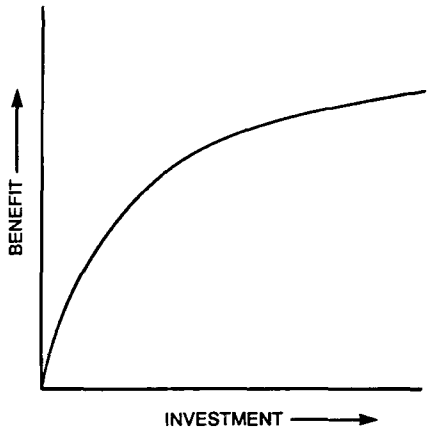

Figure 1 - Health Monitoring, Benefit vs Investment

The type and mix of health monitoring techniques applied to a given situation relates totally to the aircraft and its operation. Different techniques may be applicable to the same aircraft type used in different roles; for instance, training, ground attack and interception. When trying to balance the Cost Benefit Equation, all these points on type, mix and level of health monitoring have to be taken into account.

INFORMATION FLOWS

In order to determine the level of integration that can be economically obtained in a health monitoring system, it is vital to first analyse the flow of information and the data distribution in the operating environment of the system. This is best considered in a diagramatic form. Figure 2 shows the information flows when the aircraft is in flight and the monitored components are 'accruing life', and figure 3 shows the information flows when the aircraft is in 'post operational' mode on the ground.

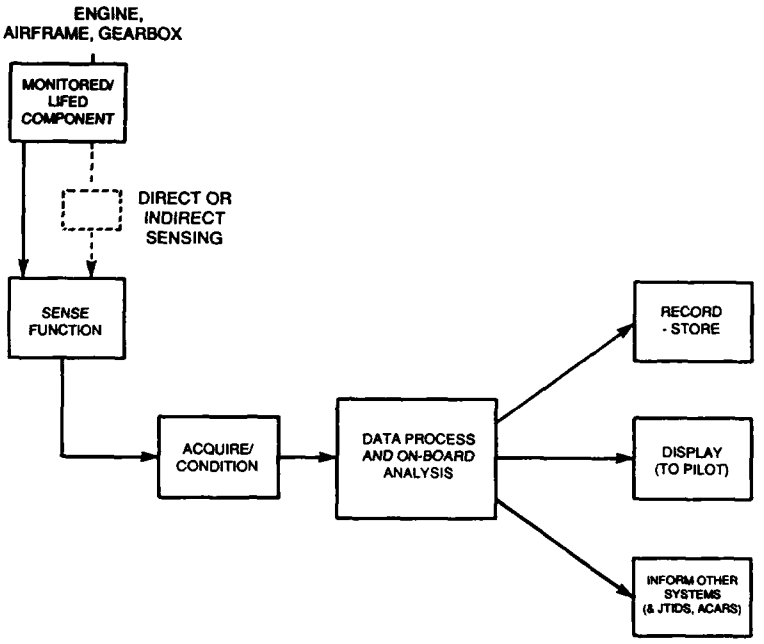

Figure 2 - In Flight Information Flows

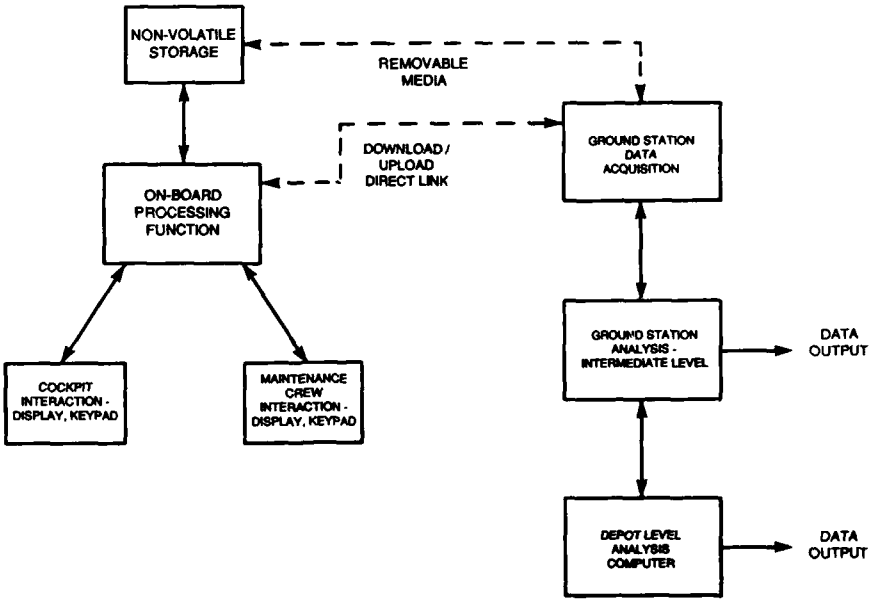

Figure 3 - Ground/Recovery Information Flows

Considering first the in flight case, the aircraft/engine monitored components must have some indication of their current state, normally via a direct transducer on that component or indirectly via another component(s). The transducer signal then has to be acquired (or conditioned) to get it into a useable form - normally digital. The acquisition process may involve noise filtering, bandwidth reduction, vibration tracking filters etc. The conditioned signal then requires on-board data processing and analysis, the extent of which is determined by the health monitoring strategy that is adopted. Finally, the processed data is then handled in one or more of the following ways:

* It is recorded on non-volatile storage media, for subsequent retrieval. This applies to non-flight critical data, that is relevant to post sortie maintenance functions.

* It is displayed to the pilot. This only applies when either the safety of the aircraft, or the ability to complete the mission, is compromised.

* It is distributed to other aircraft systems. This applies to maintenance management systems, JTIDS/ACARS downlinks etc.

Therefore in flight a data acquisition and processing function is implemented, very similar in many ways to other aircraft system functions.

Now consider the second case, the information flows for ground recovery and action upon the data. This can be split into two areas; actions associated with operational level (1st line) maintenance, and actions associated with intermediate and depot level (2nd and 3rd line) maintenance:

* Operational level: Access to the information is via a cockpit display device, and/or a maintenance data display panel. For the ground crew this gives the facility for failure indication and immediate actions required for any operational level fault rectification. It also gives them the opportunity for interactive diagnostics by using the on-board processing power. Effectively utilizing on-board processing reduces the required ground processing, logistics support, and their corresponding costs.

* Intermediate and Depot Level: Information is transfered to the ground stations via data transfer devices, or direct serial data downlink line. ACARS and JTIDS links could also accomplish this function. Ground analysis then initiates intermediate and long term maintenance actions, both in terms of that individual aircrafts' service future, and in terms of fleet wide maintenance policies.

The ground recovery functions for the turnaround of the health monitoring information can be summarized as:

* Interrogate

* Diagnose

* Action

* Update

Note that updates to the health monitoring system are equally as important as extraction of data. Effective health monitoring is only maintained by continual refinement of the processes, algorithms and procedures, and in turn this can only be accomplished by continual acquisition and analysis of data from the field. Thus the aircraft to ground station interface is definately a two-way communication link.

AIRCRAFT SYSTEMS

It is worth briefly considering a generalized case of a typical modern aircraft system (see Figure 4), to enable integration to be considered from a common viewpoint. Whilst oversimplified in some respects, it shows how modern avionic structures ensure the wide availability and distribution of data via data buses. The figure shows a few systems pertinent to maintenance of lifed items on the aircraft. Considering the functions of these illustrated equipments:

* The engine and its controller. There are a number of sensors/transducers on the engine, which are used for the control function. The controller contains all necessary circuitry to acquire and signal process the incoming signals, and possesses processing power to perform the control function.

* The maintenance management system. This is responsible for monitoring all aircraft systems during flight, reporting history and current status on the ground, and to aid ground diagnostics and other maintenance functions. In these systems exists the ability to acquire data from any other system, reduce it, analyse it, and store it. There is the ability to load a data transfer device, to link the aircraft systems to AGE, and to link to a man/machine interface for organisational level maintenance.

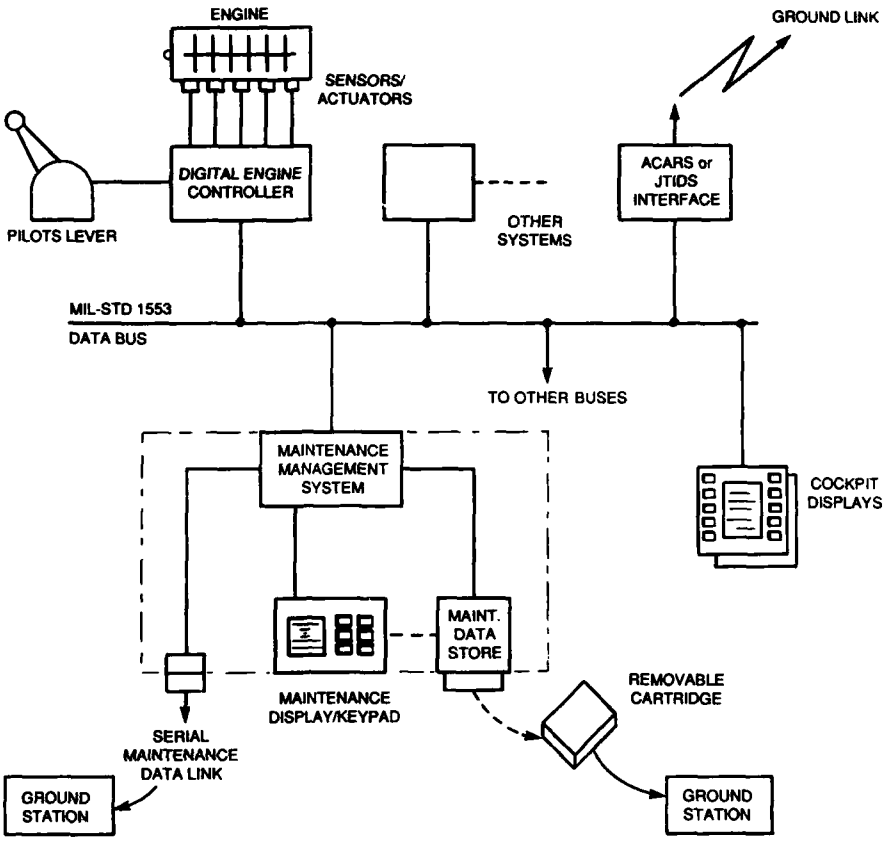

Figure 4 - 'Typical' Aircraft System

* *Cockpit Displays.* Used to provide information to the pilot in flight, and for maintenance work from the cockpit on the ground.

* Other systems, data buses, ACARS/JTIDS. Using the data buses, information flows are possible between virtually any aircraft systems. Thus a very flexible and powerful facility is available to the system designer. However, care should be taken over where the large amounts of data are processed or reduced, to avoid overloading the bus system.

* Ground Maintenance Systems. Operators normally have large integrated computer networks to support maintenance activities - these also support automated, fast data transfers between facilites. Automated transfers from the aircraft are desirable to eluminate human errors and reduce workloads. Linking into these systems, for ground analysis of health monitoring data, would reduce overall maintenance costs.

Referring back to figures 2 and 3, the above functions are analogous to those required for health monitoring. The aircraft systems also have the necessary data distribution infra-structure. Extensions of, or additions to, the data collection, signal conditioning and data reduction functions on the aircraft are what is needed to implement a fully integrated health monitoring regime.

INTEGRATION, STEP-BY-STEP

From the discussions on information flows and current aircraft system configurations, there is obviously a case for integration, but to what level? There is no clear cut answer, as each case must be examined on its own merits. Consideration must start at the beginning of any project/program to gain maximum benefit/integration, and must begin with overall aims and policies. This section of the paper will consider each of the functions of a health monitoring system, and in line with the title of the paper, present considerations for integration.

(i) Sensors. Each of the lifed components requires either direct or indirect measurement of its current condition. If the component has any other kind of electronics associated with it, these will also require sensors or transducers. Normally for health monitoring the required accuracies and repeatabilities of the sensors has to be better than for other purposes. Considerations are therefore:

* If the same measurement is required for health monitoring and other functions, by fitting the better transducer could not both functions be achieved by one transducer?

* If no sensor currently exists for the health monitoring function, could that function be determined in a different manner using existing sensors?

* Could addition of a health monitoring sensor in one position on the component/item, eliminate the need for another functions' sensor in another location?

* Does any control system require separate monitoring, and independant/redundant data for health monitoring (separate sensors?)?

As sensors and transducers are relatively expensive to purchase and locate, there must be an obvious drive to minimize the net increase in their quantity for the incorporation of health monitoring.

(ii) Acquisition. Acquisition and signal processing of the sensors output to a digital form is a fairly routine task. Normally the closer to the sensor the better, for reduced wiring runs in terms of weight/cost, and better signal treatment. The first place to look for integration is any existing unit that is already connected in that area - for instance on our previous example the engine controller on the engine. This is further enhanced if the sensors have been integrated in some manner. Thus a totally integrated sensing and acquisition package looks very attractive, and readily implementable in new systems. However EHM data sampling rates, and their compatibility with the other systems' units' iteration rates, must be ensured to be compatable with both functions; both the required accuracy and the required resolution are significant in this respect.

Another configuration would be to have one (or several) aircraft data acquisition units, to acquire health monitoring signals from all lifed components in one geographical area or from one aircraft system. This means the addition of specific health monitoring unit(s), with all their associated operational and logistic additional costs. This option is most useful in development type projects, or in retrofit applications.

(iii) Data Processing and Analysis. For data processing and analysis there is another dimension to the considerations. There is a balance to be obtained between how much processing is carried out on-board, and how much is carried out on the ground. For the purposes of the integration arguments, I have merely assumed that some processing and analysis will be required on-board and some off-board.

This task could theoretically be carried out anywhere that has the requisite processing capability, and assuming a multiplexed data bus structure, could actually be split up if necessary. Referring back to the figure 4 example, there are two obvious places that could handle the task - the engine controller and the maintenance management system. The more logical choice is the maintenance management system - health monitoring is a part of maintenance management, and the MMS is already set up to acquire data from all aircraft systems. Locating here will also have advantages in other areas (see storage and ground link discussions). It could be located in the engine controller, but this poses potential integrity problems as the controller is a flight critical system. Health monitoring software is continually changing by its nature, in the light of acquired field experience, and so continual updates to critical certified software would be expensive in revalidation. Another possibility is carrying out data processing in any specific health monitoring unit.

(iv) Data Storage/Transfer Media. Data can be stored on-board in the local media to the analysis function, but there is an explicit requirement to retrieve data post-flight. It is considered impractical to bring any major ground station to the aircraft, and so three candidate solutions exist:

* Download via an ACARS/JTIDS type link during flight.

* Connection of some portable intermediary device to an AGE serial port on the aircraft.

* Use of a removable data transfer device containing non-volatile memory devices.

Considering the operating scenario or maintenance information flows, any one or all of the above three data transfer media are currently employed. Organisational and operational environments support the establishment of maintenance activities as separate from mission activities, in terms of upload/download of information to the operational aircraft. The addition of health monitoring to the maintenance information flow can only enhance its effectiveness, and strengthen the argument for maintenance activities standing in their own right. The alternative is to have separate health data transfer media, which implies additional I/O devices, logistics and information management systems - in an operational environment this can be costly.

(v) Display Systems - Pilot/Cockpit. The scope for integration here is large, as there is always a premium on cockpit space. Current MFD's are connected to the aircraft's data buses, and so are readily able to gather data if so scheduled. With the multifunction nature of their operation, they can be effectively used to highlight safety/mission critical situations as they occur during flight. In ground maintenance mode the cockpit displays can also be used in an essentially interrogative mode to extract data from the system (via the data bus from any unit), and to initiate further interactive analysis if desired. Separate cockpit displays for health monitoring use can be employed, if cost-effective.

(vi) Display Systems - Maintenance Crew. Integration with any maintenace display is an obvious step, especially if other functions are integrated into the maintenance management system. For use at operational support level, these displays are preferable to cockpit displays, as cockpit access may be restricted. Limited use is made of on-board displays for health monitoring on the ground - only data associated with immediate maintenance actions is required to be displayed. Therefore with all health monitoring displays critical evaluation of their actual operational use is required.

(vii) Ground Stations. Currently systems exist on the ground to manage and analyse maintenance information, and also to analyse health monitoring information. These are tending to become more generic in nature to aid their transportability onto numerous machine types, to suit most operator's existing working environments. Procurement of health monitoring generic software and integration of specific component algorithms is an increasing possibility. Further integration into a total maintenance information and management package is also desirable. Referring back to (iv), overall major support cost savings can be achieved by integrating all of:

* Aircraft Data Transfer Interface.

* Data Transfer Media.

* Ground Based Data Transfer Interface.

From the discussion presented in these sections, given a clean sheet of paper for an aircraft system design, then significant advantages can be obtained by integrating health monitoring into other aircraft/ground maintenance functions. It is also recognised that such a clean sheet is not always possible and so compromises may be necessary; however in the these cases partial levels of integration may still reap benefits, provided they are assessed in the context in which they are to be implemented.

The problems of integration of health monitoring into other aircraft systems have been discussed. The remainder of this paper will be devoted to two examples currently being manufactured by GEC Avionics, that represent opposite ends of the spectrum. A totally integrated maintenance system, and an application where one specific unit has been modified to integrate health monitoring into it.

HEALTH MONITORING IN INTEGRATED AIRCRAFT MAINTENANCE SYSTEMS

Integrated maintenance systems, in their overall context of operating in the aircraft, require significantly more consideration at aircraft system level in order to produce effective results. This tends to make them more relevant to new aircraft designs or major refit/update exercises. In their favour there is greater time available to profit from the investment. Health monitoring can be incorporated into such systems for relatively little extra cost, but can yield significant benefits.

Figure 5 shows the conceptual functions of an integrated system. Sub-systems within the aircraft will have self test capability and will be able to transfer maintenance data to the maintenance system via digital highways. This data will be analysed by the system in order to present any flight critical information to the pilot, and to reduce the data storage requirements. Basic flight history, events, trend data and incipient failures are recorded so that the aircraft permanentely maintains its current health status. This information is transmitted to maintenance management,

either in-flight or via ground data transfer, in order to facilitate maintenance action planning. Information display is the key to effective integrated system design; only relevant and appropriate data should be presented to the right person, in the right place at the right time. Single point access to the maintenance system should be provided such that all information required to turn-round an aircraft can be quickly and effectively accessed.

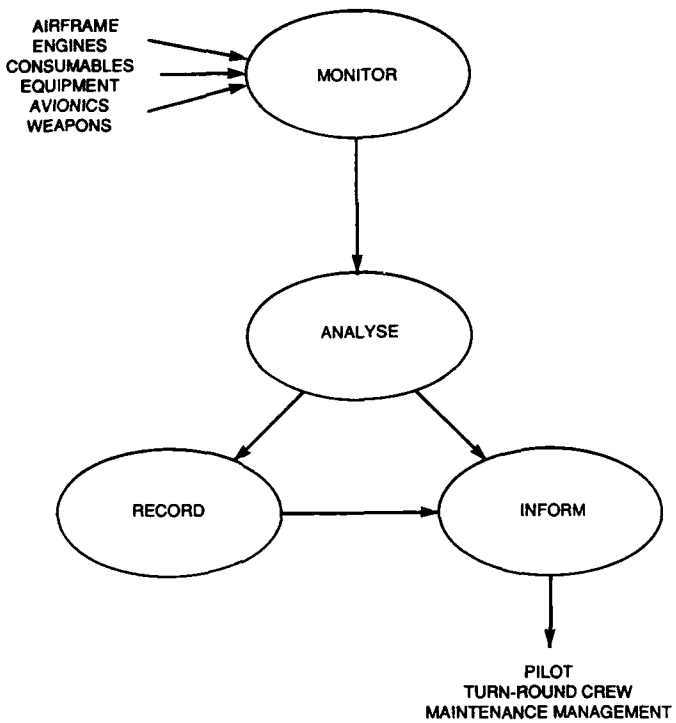

Figure 5 - A Basic Integrated Maintenance System

Whilst the inherent technologies used in aircraft design today imply a need for integrated maintenance systems, it can also be seen that substantial cost savings will be achieved over the life of the airframe. These savings will basically arise from reduced maintenance costs, less support equipment, faster aircraft turn-round, lower spares holdings and higher aircraft availability.

This philosophy was employed in the design of GEC Avionics Maintenance Data Panel, which was manufactured in support of the British Aerospace Experimental Aircraft Program (EAP). It has proved itself an extremely useful tool in both ground checks and recording in-flight maintenance occurances. This unit featured a single point access to all aircraft turn-round information. Information is ergonomically displayed using low power LCD's, and a touch keyboard designed for gloved operation is provided for ground crew interface. It interfaces with other systems via a 1553 data bus, and provides the following functions:

* Real time recording of aircraft faults to below LRU level in solid state store.
* Display of aircraft consumable quantities with fill requests and target levels.
* Control of aircraft refuelling and defuelling to tank level.
* Initiation of BIT in other aircraft systems with monitoring of results and recording of faults.
* Recording of expired life of aircraft lifed items, and display of expired and total life in hours.
* Serial download data link for direct connection to AGE.

Subsequent development of the MDP has led to a much more integrated maintenance tool. Technological advancements and the operational experience on the EAP has led to a second generation Maintenance Management Unit, which particularly encompasses health monitoring. Figure 6 shows the block diagram for the MMU. It is a generic design, in that flexibility for adaption to various applications is a key feature. From the original MDP functions list, a number of additional functions are now considered as standard fit. These include maintenance data transfer to the ground via removeable data transfer unit, additional dedicated sensor/data acquisition capability, and additional processing and internal storage.

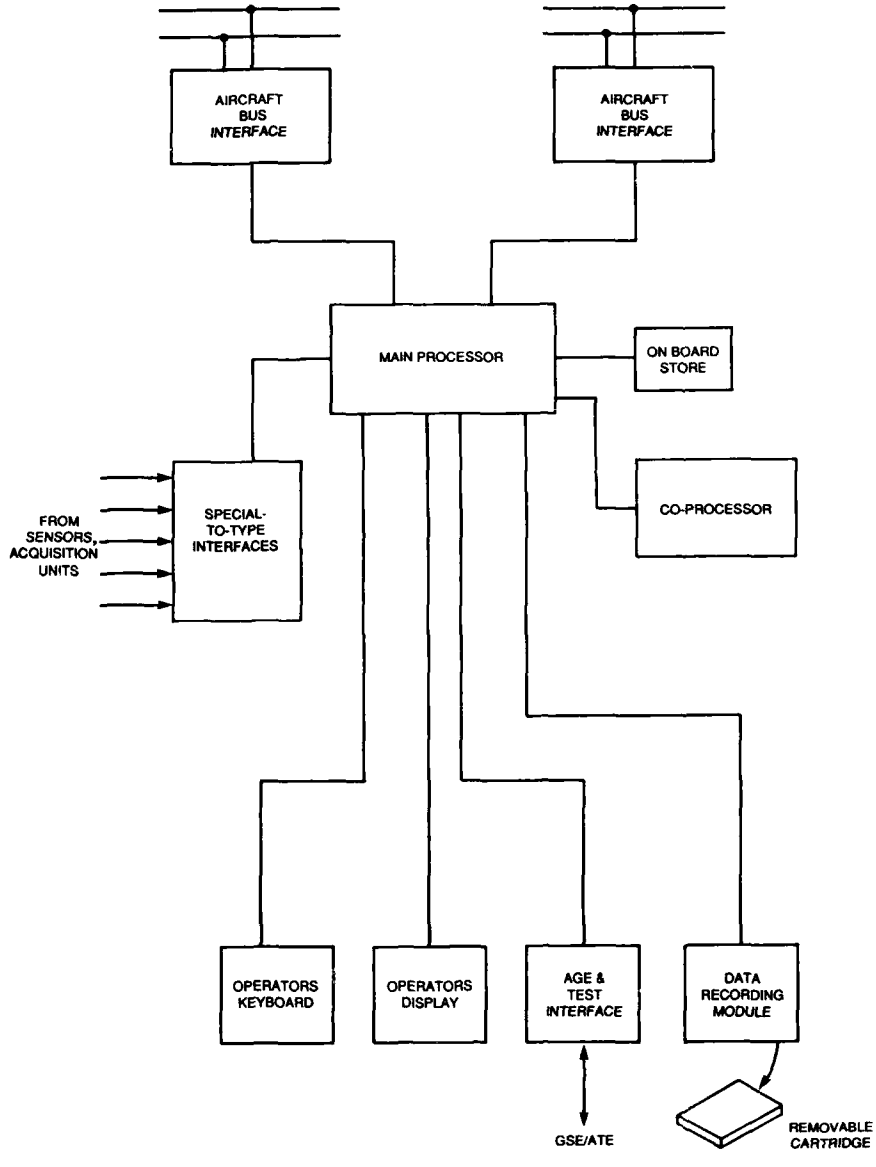

Figure 6 - Maintenance Management Unit

The unit offers all the functions required to implement health monitoring, in terms of integrating it into maintenance management. Going back to the list of required functions:

* Acquisition - Data is acquired via dedicated circuits or from other aircraft systems via the data bus.

* Processing - Some data will arrive pre-processed - for instance data reduction will have been applied to avoid bus overload. The MMU can perform all further on-board calculations, and has an optional co-processor to carry out complex calculations. However it is important to remember that certain processing functions require raw data, possibly in real time (eg vibration analysis).

* Storage - Both on-board and removable cartridge methods of storage are available.

* Display - In flight the MMU can transfer safety and mission critical health monitoring data to the pilots displays via the data bus. On the ground it has integral LCD displays, and keypad for interrogation.

* Data Transfer - The MMU can send processed data to the ground stations using the cartridge, using the AGE link, or using ACARS/JTIDS via the data bus and the ACARS/JTIDS interface units. The latter method has obvious advantages in improving turn-around times, by delivery of data ahead of the actual turn-around itself.

The MMU represents the realization of a complete health monitoring system, in an integrated fashion. However the true cost benefits are only realized on new or major retrofit aircraft programs.

HEALTH MONITORING IN AN "INTELLIGENT INSTRUMENT"

Work in the cost benefit analysis area identified a need for a low cost, low initial investment level of health monitoring. Considering the graph of Figure 1, then significant benefit can be realized. The retrofit market, and also the smaller aircraft/operator market, are particularly suited to gain maximum advantage from such an implementation.

The retrofit application is characterized by consideration of the costs and the difficulty of adding a new system both to the airframe and to the support organization. Against an already known support cost structure, cost benefits can be objectively calculated; against already known machinery weak points, health monitoring can be applied in a specific direction to have maximum effect. Thus an easily fitted, directed retrofit health monitoring system looks very attractive, and GEC has adopted the concept of intelligent instruments to fulfil this need.

GEC Avionics has a background in powerplant LCD displays, and it was recognised that such instruments have both available processing power, and the necessary parameters, to perform basic engine health monitoring. Therefore the concept of an integrated display and EHM unit was realized, which as a retrofit item offered the following advantages:

* Low retrofit costs. The unit simply replaces existing instruments; no aircraft wiring modifications are required.

* No separate EHM unit. Again no aircraft modifications are required and there is no addition to the spares holding.

* Weight, power and reliability. LCD displays are generally low weight, lower power and more reliable than their mechanical equivalents. This is shown by Table 1.

* Integrity. In this implementation the EHM function does not compromise the integrity of the existing display. Furthermore, since the display is flight critical, the EHM function is effectively promoted to this status.

* Display capability. If desired, direct post-flight readout of information can be provided on the display itself.

The first development of such a system is COSHIHUM, Combined Speed Indicator and Health Usage Monitor. It is designed to replace two standard 2 ATI engine speed instruments with comparable displays, while carrying out usage montoring in the background. Usage data such as starts, hours, maxima, minima and exceedances, is recorded together with real-time calculations of fatigue cycles accured. Low Cycle Fatigue is calculated using a unique algorithm patented by GEC Avioncs in 1979.

Table 1 Comparison between LCD and Standard Instruments

Parameter	Conventional Instrument	LCD Instrument
Weight	1300 g	750 g
Power	20 W	3 W
Reliability (MTBF)	7200 hours	>10000 hours
Accuracy	2.5%	0.5%
Flexibility	None	Multiple symbols/ characters

Figure 7 shows a block diagram of the COSIHUM. Data is acquired through isolated signal conditioning and then formated for the display by the microprocessor. A non-volatile store is used to retain life usage data during and between flights. Comprehensive self calibration and self test features combine with a reliable, maintainable design to provide a high operational availability. Where "firewall" independance of display channels is required, a second electronic channel is added. The serial interface is provided for production test but may also be used for transfer of engine health monitoring data when operational.

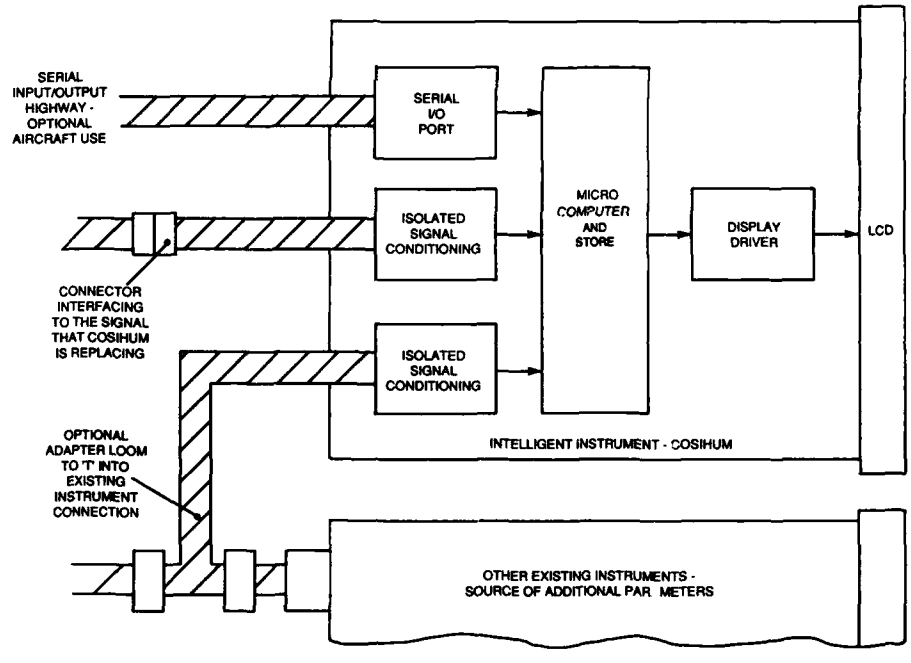

Figure 7 - Display Block Diagram

An important feature of the unit is that it is able to acquire other data which is available in the cockpit with only simple wiring modifications. This is achieved by "T-ing" into connections to other instruments. Access to other engine speeds, temperatures and air-data considerably enhances the health monitoring capability that is available. However the integrity of these other display systems must not be compromised. With these intelligent, integrated instruments, the following health monitoring functions can be performed.

* Basic Usage Data. The system can monitor engine operating hours, number of starts, maxima, minima, exceedances and time at certain power levels.

* Calculations of fatigue cycles. Major and minor cycle usage can be calculated directly from speed. However, given temperature and air data information, actual stress within blades may be estimated to give a more accurate datum for cyclic life calculation.

* Trend Monitoring. The unit has continuous access to engine and air data parameters. Trend monitoring may be implemented as snapshots of data at pre-defined conditions - eg placard checks for ground trending analysis.

* Direct Analysis. If an intelligent display is used to show the output of a vibration transducer then other HUM functions, including exceedance monitoring and data storage, become available. Similar techniques may be applied to other engine and airframe transducers. However an important criteria is that the instrument receives prime sensor data and not pre-processed signals - the latter restricts the "directness" of analysis than can be achieved.

Efficient post flight retrieval of the data is essential, and here the flexibility of the LCD instruments can be exploited. Currently two methods are available for data extraction, but more are being investigated where other on-board equipment can be linked in. The two methods are:

* Direct Display. The programmable liquid crystal display provides a readily available media for post-flight readout of HUM data. This can be either automatically or manually stimulated and would step through annotated HUM parameters. Such a system, whilst cost effective, is generally applicable to basic usage monitors where only a few parameters are being transferred. Transfer of large amounts of data would involve considerable maintenance crew time, and potential injection of human error.

* Serial Output. The intelligent instrument has an EIA-RS422 standard serial highway. Data is formatted by the unit in ASCII style, facilitating file transfer and handling. A commercially available "data bucket" is then used to extract and display data and to provide transfer storage to any further ground processing stations. The unit may also be used to reset counters after maintenance actions, providing that the appropriate security code is used. This highway could also link to other on-board data collection systems.

The intelligent instrument/COSIHUM approach facilitates a progressive EHM strategy, where functions can be simply modified and added as operator experience grows. Generally this is accomplished through board replacement or additional software packages.

CONCLUSION

In conclusion, the requirements and methodologies for health monitoring in aircraft machinery have been reviewed, and their integration into other aircraft systems has been discussed. It is acknowledged that there is no single answer to the question of integration. However various levels of integration, to suit various configurations and operational environments, are undoubtedly going to show significant benefits if implemented correctly. Two examples of GEC Avionics products have illustrated what can be achieved by strategic thinking on integration to provide maximum benefit for a minimum investment. As new aircraft systems are developed in the future, it is anticipated that health monitoring concepts will become an integral part of the design process, and will be a natural part of any consolidated maintenance system - both on-board and on the ground.

ACKNOWLEDGEMENTS

The author would like to thank colleages from Powerplant Systems Division, GEC Avionics, for their assistance in the preparation of this paper.

DISCUSSION

G.TANNER

1. Is the unit fitted on EAP carrying out any engine health monitoring of the RB 199?

2. Is there spare capacity if so required?

Author's Reply:

1. For the British Aerospace EAP standard engines RB 199 engines were fitted, complete with standard control systems. The engine data was available via the 1553 bus, so no RB 199 health monitoring was possible. To demonstrate the maintenance data panel's capacity in this area, life used on the APU's was tracked and highlighted when near its limit.

2. Yes, there is spare capacity to do health monitoring of varying types as described in the paper. It was an area identified as having a lot of potential in the future for this type of unit.

I.C. CHEESEMAN

You described your latest instruments as intelligent. These instruments appeared to me have a versatility in their display forms in terms of the variables indicated. To me "intelligent" implies that the display is automatically changed to provide the most relevant aid to the enquirerwithout external intervention. Have I missed something?

Author's Reply:

The concept is some what simpler than the question infers. The term "intelligent" as applied in this context means that the instrument is capable of carrying out a function that is in addition to its main job of displaying raw information. The intelligent instrument in the presentation is capable of calculating basic useage cycles, at the same time as displaying engine speed (real-time) in the cockpit. On the ground the display can be used to directly extract the useage information.

M. BEAUREGARD

How is data acquired by the generic Basic Integrated Maintenance System? Is the data multiplexed in some way?

Author's Reply:

Sensor data is primarily acquired via the data bus, relying on other units where possible to condition the sensor signals. Where this is not possible the unit has an installation specific card slot that can be adapted to engine data directly from the sensor in whatever manner is dictated by the installation (raw, partially pre-conditioned, multiplexed, etc). This latter method may also be used where direct processing on real-time raw data is required, for instance vibration analysis.

CHETAIL

Even if your presentation refers obviously only to military applications I feel this would also apply to civil applications. Don't you believe that the curve on fig 1 would go through a maximum value of benefits, above which additional investment will not pay off?

Author's Reply:

The presentation is not only applicable to the military environment, although most examples given were from military aircraft. I introduced fig 1 without scales on the axes as there would always be cases that did not conform. There is also an argument for the slope of the line, and for some cases your assertion may well be true. However the underlying argument is still true, for some investment there will be some benefit, but for a lot more investment you don't necessary get a lot more benefit.

C. SCURA

During the persentation you showed extensive use of instrumentation with L.C.D. What kind of problem did you encounter during cold weather and night operations? What solutions did you adopted?

Author's Reply:

For cold weather operation we use an integral heater to maintain the L.C.D. at a t° that ensures a good crystal response. For night operations a variable intensity backlight is employed.

MAINTENANCE AID SYSTEM FOR WIDE BODY AIRCRAFT

by
Albert LEVIONNOIS
Measurement & Flight Test Department
SOCIETE DE FABRICATION D'INSTRUMENTS DE MESURE
13, Av. Marcel Ramolfo-Garnier
F91344 MASSY CEDEX - France

SUMMARY
Aircraft engines belong to the essential part the maintenance people need to get a great deal of information of, in order to define conditions under which incidents happened for failure troubleshooting purposes. Modern aircraft with numerical equipment provide all necessary parameters with a good precision. Aircraft condition monitoring systems (ACMS) centralize all information mainly from data buses, compute flight phases, determine the reports to be made per flight phase and function and carry out automatic parameter picking. Should an incident occur, then parameters' history is stored before and after the incident, together with their evolution. All those information are stored into static memory inside the equipment for being transmitted by data link or printed during or after flight or down loaded to a transfer tool,when the aircraft is back to its base. Today between 35 and 40 types of reports are currently operating on wide body aircraft. This technology is easily adaptable to combat aircraft.

List of Abbreviations

AC	Air Conditioning
A/C	Aircraft
ACARS	ARINC Communication Addressing & Reporting System
AIDS	Aircraft Integrated Data System
ACMS	Airplane Condition Monitoring System
APU	Auxiliary Power Unit
ARINC	Aeronautical Radio Incorporated
ATS	Autothrottle
CAS	Computer Air Speed
CDU	Control & Display Unit
DAR	Digital Aids Recorder
DFDAMU	Digital Flight Data Acquisition & Management Unit
DFDR	Digital Flight Data Recorder
DIV	Divergence
DMU	Data Management Unit
DMT	Display and Mass Memory Terminal
EGT	Exhaust Gas Temperature
ETA	Elapsed Time to Arrival
FDAU	Flight Data Acquisition Unit
FDEP	Flight Data Entry Panel
FLT	Flight
ft	Foot, feet
FM	Flight Mode
FWC	Flight Warning Computer
GW	Gross Weight
ITT	Internal Turbine Temperature
LA	Linear Accelerometer
LRU	Line Replaceable Unit
MCDU	Multipurpose Control and Display Unit
MCU	Modular Common Unit
MN	Mach Number
mn	Minute
N1	Fan Speed
N2	Core Speed
NH	Generator Speed
NL	Generator Speed
NP	Propeller Speed
OATL	Outside Air Temperature Limit
OIP	Oil Pressure
OIT	Oil Temperature
O/R	On Request
PCM	Pulse Code Modulation
PEH	Pre Event History
PLA	Power Lever Angle
PRT	Printer
QAR	Quick Access Recorder

R/U	Run Up
SAR	Smart Airborne Recorder
TAT	Total Air Temperature
TBD	To be defined
TGOC	Touch and Go Counter
TLA	Thrust Lever Angle
TTP	Time to Peak
UTC	Universal Time Coordinated
VC	Vibration Compressor
VF	Vibration Fan
VH	Vibration High Turbine
VL	Vibration Low Turbine
VRTG	Vertical Acceleration

1. Introduction

Health monitoring on airplane engines leads to appropriate maintenance actions which are consequently made from ground inspection, but also thanks to the record of engine reports which are processed in real time during the flight. The above data are available from the ACMS (Airplane Condition Monitoring System, previously AIDS Aircraft Integrated Data System), which maintains a record of engine performance, so that mechanical malfunctions and gas path deterioration may be recognized adequately.

SFIM's large experience in Flight Data Acquisition Systems for military and commercial aircraft led to develop and manufacture ACMS systems. Those products are now fitted on various aircraft such as :

- Twin turboprop aircraft : ATR 42, ATR 72,
- Twin-engined jet : A 310, A 300-600, B 737-300,
- Four-engined jet : KC 135.

On all those aircraft, SFIM's ACMS concept was based on developing a FDAU-DMU integrated in one box :

- 1/2 ATR short for ATR 42, ATR 72, KC 135,
- 6 MCU for A 310, A 300-600, B 737-300.

This paper will examine the various tasks achieved by ACMS.

2. Four-Engined Jet : KC 135

2.1. - FDEP

The FDEP is installed in the cockpit and is used for :

- Manual introduction by means of 4 thumbwheels of time setting and identification numbers on request by the crew,
- GMT display,
- "Event" push button,
- FDAU and system status lamp display,
- Maintenance use : control and display of each parameter of the PCM data frame.

2.2. - FDAU + DMU

The FDAU + DMU in one box is installed in the electronic bay and is used for the FDAU :

- To acquire all mandatory parameters,
- To generate the PCM data frame for the DFDR,
- To dialogue with the FDEP.

For the DMU :

- To acquire additional ACMS parameters,
- To recognize flight phases,
- To achieve ACMS processing,
- To store reports in the DMU mass memory,
- To dialogue with the DMT for data outputting on the ground before laboratory processing.

2.3. -DMU Reports Processing

Flight phases are recognized and DMU creates 5 different reports which are :

- Report 1 : Automatic cruise recording,
- Report 2 : Manual recording,
- Report 3 : Take-off recording,
- Report 4 : Recording on threshold overshoot,
- Report 5 : Recording on landing.

In addition, the mass memory of the DMU can be milked out by the DMT.

2.4. - Automatic Cruise Recording

Report 1.
This record is made once per flight in stabilized conditions :

- Altitude variation lower than +/- 100 ft for 2 mn (if parameters acquired),
- N2 variation lower than +/- 1 % for 5 mn on the 4 engines,
- PLA variation lower than +/- 1 % for 5 mn on the 4 engines,
- MN variation lower than +/- 1 % for 5 mn.

The variation ranges together with the stabilization period are programmable and can be revised. At the end of a 4 mn stabilization period on N2 and MN, the computer takes the average over 1 mn of the engine parameters : PLA, N1, N2, EGT, Fuel flow. If no stabilization is obtained during a flight, the recording is not made.

List of parameters used for manual or automatic recording :
- Engine parameters : PLA, N1, N2, EGT, Fuel flow, Oil pressure, Oil temperature,
- General parameters : ALT, MN, TAT, Flight counter, TGOC,
- and documentary parameters.

2.5. - Manual Recording

Report 02.
This report is triggered by depressing the MAN RECORD button located on the instrument panel. The AUTO/MAN RCORD indicator lamp lights up when the report is recorded.
N.B. - Thee manual record button action is filtered on the ground (switch train or ground).

2.6. - Take-off Report

Report 03.
This recording of the take-off report is triggered when the radioaltimeter reading reaches 600 ft. The recording consists of a direct sampling snapshot of the engine parameters. After recording , the processing of this report is no longer authorized for the rest of the flight. Processing is authorized again at the end of a flight, after a landing.

Touch and go : The system detects "touch and go" events and does not trigger the recording of the take-off report on transition to 600 ft.

Definition of "touch and go" : A take-off is considered as a "touch and go", if the transition to 600 ft takes place after 60 seconds or less following a landing.

"Touch and go" counter (TGOC) : A counter (TGOC) is incremented each time a "touch and go" is detected. The counter is recorded in the take-off report.

Counter reset to zero : The "touch and go" counter (TGOC) and the flight counter (FLCT) are reset to zero each time a transfer of reports takes place on the DMT unit.

2.7. - Exceedance Report

Report 04.
When engines are running on ground during the flight, engine exceedance monitoring is permanently performed under the following conditions :

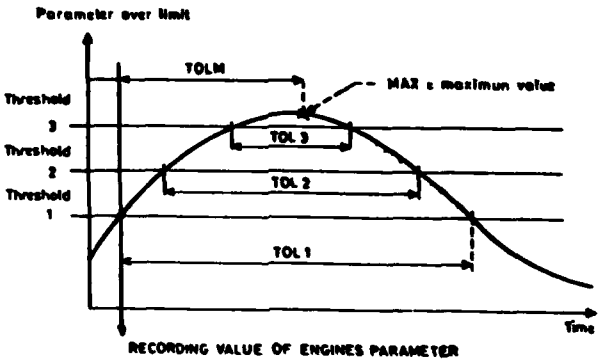

For each parameter, 3 thresholds are resident into the software and times over limit are computed as follows :
- TOL 1 : Time over limit threshold 1 = t1,
- TOL 2 : Time over limit threshold 2 = t2
- TOL 3 : Time over limit threshold 3 = t3,
- TOLM : Time over limit between the first threshold and the maximum value of the parameter = t4.

Acquisition of engine parameters : When the first threshold is exceeded, a recording is made of all the engine parameters. The system then monitors the evolution of the exceeded parameter, and measures the maximum value reached by the parameter together with this exceeded times (t1 - t2 - t3 - t4).

Threshold exceedence recording : The parameters PLA, N1, N2 and EGT are under continuous surveillance, and a recording sequence is executed, if any of the threshold values is reached. The programme is capable of processing 3 thresholds. The exceedence times (t1 - t2 - t3) of each threshold are measured and recorded, together with the time (t4) elapsed between the exceedence of the first threshold and the maximum value reached by the parameter.

Filtering and transient conditions : A threshold exceedence must be confirmed for 3 seconds to trigger the recording of the report. The acquisition and recording of engine parameters is the same as for the ATR 42 aircraft.

2.8. - Landing Recording

Report 05.
This report is recorded at the moment of landing ("on ground" train switch), if there was no automatic recording (Report 01) or manual recording (Report 02) during the flight. The format of report 05 is identical to that of Reports 01 and 02.

Recording of Report 05 : Report 05 is recorded automatically when the FLIGHT/GROUND transition takes place, if no cruise report has been recorded during the flight in manual or automatic mode. The AUTO RECORD indicator lamp goes out at the instant of FLIGHT/GROUND transition.

3. Twin-Engined Jet : A 310, A 300-600 and B 737-300

On the above aircraft, SFIM's ACMS consists in fitting on-board a CDU and a DFDAMU. Those LRUs are normally linked to a DFDR, PRT, QAR or DAR and ACARS. The reports processed by the DMU part can be achieved automatically or on request by using the remote print button of the cockpit and/or the print button on the CDU. As an example, you will find listed below the reports which are available in one configuration of BOEING B 737-300 aircraft.

3.1. - B. 737-300 ACMS Reports

Ten reports are available in this configuration and they are listed below with their appearance as far as flight modes are concerned.

The flight modes are : 1 Preflight
2 Engine start
3 Taxi
4 Take-off
5 Climb
6 Cruise
7 Descent
8 Approach
9 Roll

and reports appearance with related flight mode is as below :

B 737 - 300 AIMS REPORTS	FLIGHT MODE								
	1	2	3	4	5	6	7	8	9
01 ENGINE CRUISE REPORT						X			
02 ENGINE CRUISE REPORT (NO STABLE DATA ATS = OFF)						X			
04 ENGINE T/O REPORT				X	X				
05 ENGINE REPORT O/R	X	X	X	X	X	X	X	X	X
06 ENGINE GAS PATY ADV REPORT		X	X	X	X	X	X	X	X
07 ENGINE MECH ADV REPORT (MECHANICAL)		X	X	X	X	X	X	X	X
09 ENGINE EGT DIV REPORT					X	X			
11 ENGINE R/U REPORT	X	X	X						
15 FLT LOAD REPORT				X	X	X	X	X	X
16 REAL TIME REPORT	X	X	X	X	X	X	X	X	X

3.2. - Report 01 : Engine Cruise Report

Relevant flight modes : Cruise only.
Trigger conditions : 5 consecutive cruise reports, if selected via CDU input, i.e. on request mode.
Stability criteria : Stable frame conditions met.
Data type : The following data to be average values : TAT, Mach Number, Altitude, N1, N2, EGT, Fuel Flow, TLA, Oil Temperature, Oil Pressure, Vibration Magnitudes, Phase Angles, Flight Path Acceleration, Inertial Vertical Velocity, Angle of Attack. The following data to be raw values at the end of the stability search : Gross Weight, True Heading, Latitude, Longitude.

3.3. - Report 02 : Engine Cruise Report

Relevant flight modes : Cruise only.
Trigger conditions : If no Report 01 is generated, no stable data were found.
Stability criteria : No stable frame found.
Data type : The same data to be average values as for Report 01.

3.4. - Report 04 : Engine T/O Report

Relevant flight modes : Take-off only.
Trigger conditions : To be generated 30 seconds (time reprogr.) after entering flight mode take-off under additional conditions as follows :
- Every 30th flight, or
- Five consecutive T/O's if selected via CDU, i.e. on request mode, or
- Five consecutive T/O's after engine change.

Data type : The following data to be average values taken from the 12 seconds PEH-buffer (status 5 seconds after trigger time, see figure below) : Oil Temperature, Oil Pressure, Vibration Magnitudes, Phase Angles. The following data to be snapshot (raw) values taken from PEH at trigger time : TAT, Mach Number, Altitude, N1, N2, EGT, Fuel Flow, TLA.

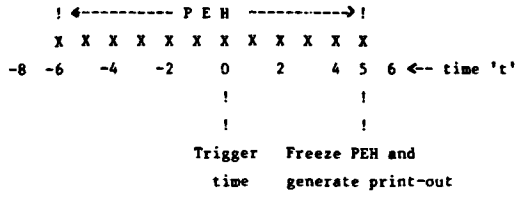

3.5. - Report 05 : Engine Report O/R

Relevant flight modes : All.
Trigger conditions : Via push button, see figure below for details.
Data type : All data to be shapshot (raw) values taken from the 12 seconds PEH-buffer. Data to include the t = + 5 data set stored in the PEH-BUFFER.

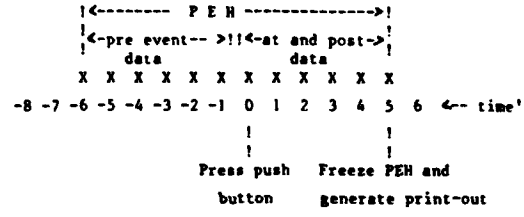

3.6. - Report 06 : Engine GAS PATH ADV Report

Relevant flight modes : All.
Trigger conditions : Report to be generated when limit exceedence conditions met. Exceedence parameters N1, N2 and EGT are continuously smoothed by exponential smoothing (both engines) :
New value (smoothed) = Old value (smoothed) + Alpha x (New value (raw) - Old value (smoothed))
Alpha to be reprogrammable. Check exceedence versus smoothed parameters.
Limit type : Fixed limits for N1 and N2 are independent of flight mode. N1-limit : 102 %, N2-limit : 105 %. Fixed limits as a function of flight mode to be defined for EGT.
Limit 1 : 905° C, valid for FM 2,3
Limit 2 : 905° C, valid for FM 4
Limit 3 : 870° C, valid for FM 5, 6, 7, 8, 9.
Data type : Pre event data to be snapshot (raw) values taken from the 12 seconds. PEH-buffer freezes PEH, when limit exceedence is detected. Data at and post event to snapshot (raw) values taken from the 60 seconds exceedence buffer.

3.7. - Report 07 : Engine Mechanical ADV Report

Relevant flight modes : All.
Trigger conditions : Report to be generated when limit exceedence met. Exceedence parameters VF, VC, VH, VL, OIP AND OIT (for both engines) are continuously smoothed by exponential smoothing :

New value (smoothed) = Old value (smoothed) + Alpha x (New Value (raw) - Old Value (smoothed)

Alpha to be progammable.
Limit type : Limits as a function Y = f(X) defined via a set of linear equations. Polygone to be defined for the following parameter functions : VF = f (N1), VC = f (N2), VH = f(N2), VL = f(N1), OIP = f (N2). All functions per engine. Limit curves are defined through 5 linear segments per function. Monitoring of OIT has to be performed with a fixed limit valid for all flight modes like N1, N2 and EGT monitoring in Report 06. OIT-LIMIT 1 : 165° C. In addition, it has to be alerted, if a second (lower) limit has been exceeded for more than 15 minutes. OIT-limit 2 : 160° C.
Data type : Pre event data to be snapshot (raw) values taken from the 12 seconds. PEH-buffer freezes PEH when limit exceedence is detected. Data at and post event to be snapshot (raw) values taken from the 60 seconds exceedence buffer.

3.8. - Report 09 : Engine EGT DIV Report

Relevant flight modes : Climb and/or cruise.
Trigger conditions : Report to be generated when divergence conditions met. Only one report per leg and threshold.
Data type : Pre event data to be snapshot (raw) values taken from the 12 seconds PEH-buffer. Data at and post event to be snapshot (raw) values taken from the 60 seconds exceedence buffer.
Interactivity : After generating the Report 09, the software has to initialize the search logic for stable data determination to generate a Report 01, as soon as possible for divergence verification purposes.

3.9. - Report 11 : Engine R/U Report

Relevant flight modes : On ground only.
Trigger conditions : Via remote push button.
Data type : The following data to be average values : TAT, Mach Number, Altitude, N1, N2, EGT, Fuel Flow, TLA, Oil Temperature, Oil Pressure, Vibration Magnitudes, Phase Angles.

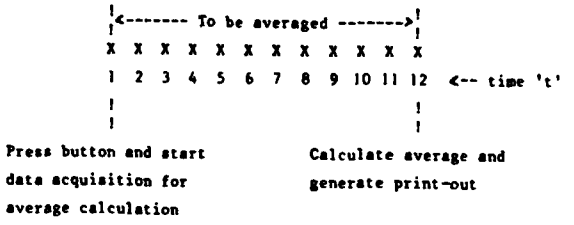

3.10. - Report 16 : Real Time Report

Relevant flight modes : Any.
Trigger conditions : 1. CDU menu selection.
2. Depression of remote print button.
3. Start/Stop logic.
Data type : If the report is generated by trigger condition 1 and 2, a maximum of 20 seconds (40 data lines) shall be printed at an update rate of 1 second. The print report shall be terminated normally either when 20 seconds of data have been printed or the print button is twice depressed within short time. If a continuation of Report 16 is desired after the first 20 seconds of data, the print button on CDU or the remote print button must be pressed again prior termination of the first print-out, to receive consecutive data between the reports. If the report is generated by trigger condition 3, then the report shall be generated until the print stop logic is true (normally 20 seconds, if no further stop input entered or max up to 80 seconds).

4. Evolutions on ACMS Systems

At the very beginning of ACMS, mainly the system was dealing with engine monitoring, but the current and next generation will process also reports such as :

- Crew proficiency
- Aircraft performance monitoring
- Incident investigation
- Flight path report
- Windshear report
- Fuel consumption

etc...

In addition to these new processing capabilities, the system will extend its peripheral communication with MCDU, multipurpose printer, ACARS and multipurpose Disk Drive Unit. The disk drive capability will bring a very high flexibility in the system in such a way that the user will have the possibility to program new reports from a ground personal computer. The ACMS linked to the ACARS will dramatically decrease the critical maintenance action leadtime, assuming that reports can be transmitted on the ground station before landing.

4. Conclusion

The numerous advantages of the ACMS system utilisation such as maintenance cost saving, enhanced safety, performance analysis, incident investigation, show the ever increasing role they can play in the overall operation and maintenance plan of current and future airplanes. In other words, ACMS is one key to a healthy on-going avionics activity.

INSTALLED THRUST AS A PREDICTOR OF ENGINE HEALTH FOR JET ENGINES

by
G.B.Mackintosh
Senior Engineer
and
M.J.Hamer
Principal Engineer
COMPUTING DEVICES COMPANY
P.O.Box 8508
Ottawa, Ontario
Canada
K1G 3M9

SUMMARY

Extensive installed and uninstalled gross thrust measurements were made over one complete maintenance cycle on nineteen afterburning turbojet engines. Installed measurements utilized a sensor which can compute the thrust in real time from engine tailpipe pressure measurements. Correlation of installed thrust with maintenance history indicated a maximum degradation below which engines were removed from service.

The engines were trimmed uninstalled, using lapse rate charts to produce a specific value of uninstalled thrust, corrected to standard conditions. Significant variations in installed corrected thrust resulted. Higher initial values of installed corrected thrust resulted in more rapid engine degradation and a shorter time before maintenance was required.

Conclusions are:

i) rapid installed thrust degradation indicates probable early engine failure
ii) a high initial installed thrust results in more rapid thrust degradation.

Periodic monitoring of installed thrust will detect both of these conditions and thus aid significantly in engine health analysis.

DATA DESCRIPTION

Engine ground performance data were available from a group of nineteen afterburning turbojet engines installed in a twin engined supersonic military aircraft. Sixteen of these engines were monitored over a complete maintenance cycle of six hundred hours. Installed performance checks were obtained at intervals of approximately 50 flying hours and additionally whenever engine retrimming occurred. Each engine remained in the same aircraft and engine bay for the duration of the data collection exercise to enable longer term trends to be discerned.

The engines were trimmed in an engine test cell to produce a military power thrust which was a function of the ambient temperature and pressure. The trim procedure sets the uninstalled thrust level to a constant using an engine test stand. The definition of this function was intended to correct for ambient conditions so that the engines would produce a specific standard day uninstalled military power thrust. Maximum afterburning power was checked against a second thrust function to ensure that it was adequate. Uninstalled data defining the operation of the engine after trimming was obtained from the thrust stand and related test cell instrumentation.

Fuel flow, exhaust gas temperature (EGT) and rotor speed (RPM) were obtained using standard military test equipment. The installed thrust, ambient pressure and intake air temperature were measured using a proprietary system developed by Computing Devices Company. This equipment will be further described below as it provides the facility to easily measure installed thrust which makes practical its use as an engine health parameter.

THRUST MEASUREMENT SYSTEM

Description

The Thrust Measurement System calculates the gross thrust from pressure measurements made in the engine tailpipe plus ambient static pressure. The method has been used by NASA on the F-15, HiMAT and X-29 programs. The results (references 1, 2, 3 and 4) show advantages over the traditional methods, such as the manufacturer's inflight thrust program, in that much less instrumentation is required and accurate thrust can be computed in real time. All engine pressure measurements are made downstream of the rotating machinery using special probes and taps installed in the diffuser and tailpipe. As a result measurement accuracy is not affected by engine degradation or intake distortion.

The pressure inputs are combined to determine the thrust produced by the engine using equations developed by Computing Devices Company and constants determined by testing an engine in a thrust stand. This testing does not have to be done for each individual engine. Once the calibration constants are determined for the engine model, good accuracy is obtained for all engines of this model without further testing.

Pressures are sensed at three locations in the engine tailpipe. Figure 1 is an engine schematic which shows the locations of the required pressure measurements.

Turbine exit total pressure is measured by a set of rakes which extend into the flow in the diffuser section. Each rake carries several total pressure probes which are manifolded together. The outputs from the rakes are further manifolded to obtain a single pressure signal. Design of the rakes and manifolding is such that the pressure signal represents the average value of the total pressure at the measurement location. These rakes are the only immersed probes required.

Static pressures are measured at two downstream locations. These measurements are made using taps mounted flush with the wall of the tailpipe liner. Several taps were used at each axial location, manifolded together to obtain a single representative pressure signal. The locations of these taps, one set at the flameholder and the other at the entrance to the exhaust nozzle, enables the effect of afterburning combustion to be included in the thrust calculation, while the use of only wall taps at the nozzle entrance enables the sensors to withstand the reheated exhaust gas without damage.

In addition to these engine pressures, the computation of gross thrust requires measurement of the ambient static air pressure. During the tests described in this paper, ambient pressure was obtained from a static pressure probe located adjacent to the aircraft. No other measurements such as temperature or mass flows are required for gross thrust computation.

The pressure transducers and computing hardware necessary to compute the thrust are housed in the Sensor, Thrust Computing which may be mounted on or adjacent to the engine or, for ground use mounted in a separate package external to the aircraft.

The equipment may also be configured for measurement of net thrust, which corrects for the ram drag experienced in flight as a result of ingestion of moving air by the engine. The calculation of ram drag requires additional inputs of true air speed and exhaust gas temperature. These parameters are already measured for use by aircraft instrumentation, so that suitable input signals can be obtained.

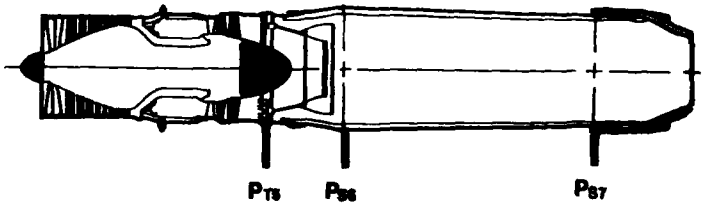

Figure 1. Pressure Measurement Locations in the Engine Tailpipe.

Accuracy

The thrust measuring accuracy was evaluated on an aircraft thrust stand and found to be within ±2.5 percent at military power, at the 95% confidence level.

The thrust algorithm has also been used by NASA on the F-15, HiMAT and X-29 programs. On the X-29 the thrust was computed and displayed in real time. Inflight gross thrust measurement total uncertainty is ±1.5 percent at intermediate power at the aircraft design point (0.9 Mach at 30,000 ft). Owing to the higher thrust levels produced, the percentage accuracy at maximum afterburning power was somewhat greater (±1.1 percent).

The X-29 program included testing of the thrust computing algorithm in the altitude cells at NASA/Lewis Research Center. Using pressure transducers associated with the altitude cell to collect data, the thrust algorithm calculated thrusts which agreed with the cell thrust within ±1.8 percent for 131 data points at 11 simulated flight conditions over the Mach/altitude envelope.

ENGINE PERFORMANCE DATA

Installed Thrust Range

The installed thrusts display a considerable range of variation due to installation effects, engine degradation and temperature lapse rate variations. Figure 2 shows the installed military power gross thrust corrected to sea level standard pressure as a function of the ambient temperature. These data are from sixteen engines tested over the full 600 hour maintenance cycle. The data are presented as a function of the nominal sea level thrust. The spread about the mean is ±5.35 percent at the 2 sigma level (over 200 points). Correcting for installed thrust measurement accuracy results in an observed thrust spread of ±4.62 percent.

Thrust Degradation and Temperature Lapse Rates

A better understanding of the mechanisms causing performance variations can be obtained by considering the performance of individual engines.

Intake air temperature significantly affects the thrust produced by a turbojet engine. As the temperature increases, the air mass flow is reduced and thrust decreases. For the engines tested, the rate of thrust reduction, known as the temperature lapse rate, proved to vary considerably between engines and to be affected by engine maintenance. Because the test data were collected at the prevailing ambient conditions, this variation must be accounted for in analyzing the data. The procedure used was to

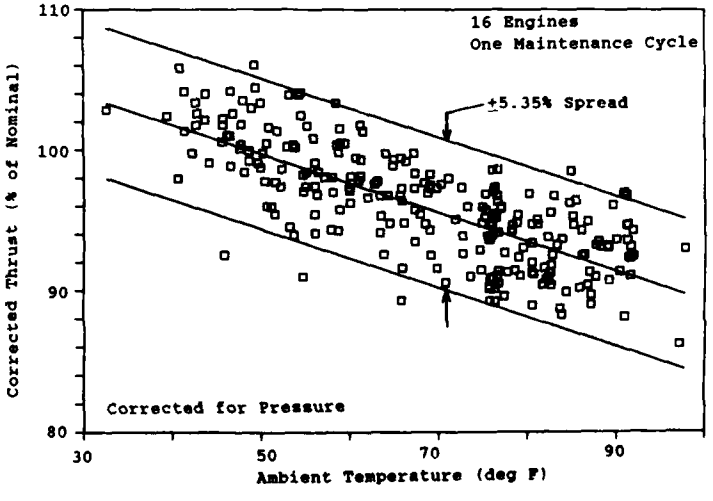

Figure 2. Military Power Thrust Distribution from Test Data.

first correct the thrust data to sea level pressure and then to perform a regression against both ambient temperature and accumulated engine time. In cases where an engine was retrimmed, the data accumulated for each trim were analyzed separately. This accounted both for the differing trim conditions resulting from restoring the uninstalled engine thrust to the initial level and for changes introduced by the engine maintenance which had resulted in the requirement for retrimming.

Figures 3 and 4 show the performance of an engine at a single trim condition. In each figure, the line derives from the regression analysis and shows in one case the variation of thrust with changing ambient temperature at zero hours since trim and in the other the variation of thrust with accumulated hours of service at an ambient temperature of 59 degrees Fahrenheit. The engine data points are also shown on the figures. The data were corrected to 59 degrees Fahrenheit or 0 hours since trim as appropriate by using the slope parameters from the regression analysis. This means simply that the deviation between the point and the line shown in the figure is equal to the deviation of the data point from the regression plane. The average thrust degradation rate for the engines tested was 1.0 percent of nominal thrust per hundred hours.

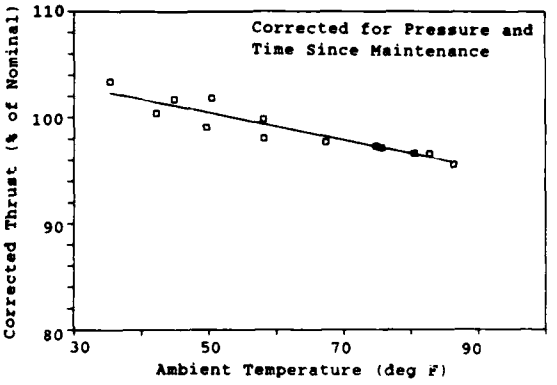

Figure 3. Thrust Variation with Temperature (Lapse Rate).

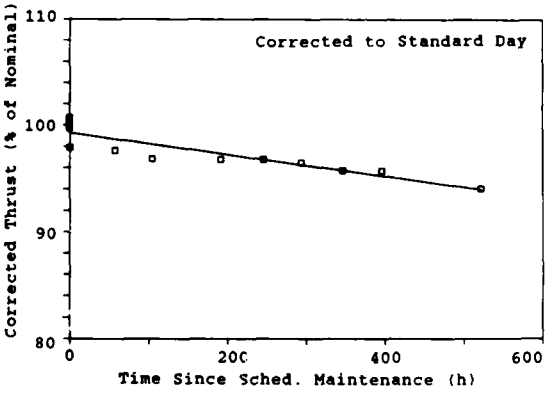

Figure 4. Thrust Degradation with Time.

During the course of data collection, the engines were removed for maintenance and retrimming a considerable number of times. As a result, much of the trim data was from engines which had accumulated a number of operating hours since the time of scheduled maintenance. Despite the performance of unscheduled maintenance, these engines exhibited a measure of performance deterioration and it was necessary to trim them to a higher EGT to restore the thrust to the trim level. Figure 5 shows that the EGT to which engines were trimmed tended to increase as the accumulated service hours at the time of trim increased. This figure shows considerable scatter because the measured EGT is based on the readings of a limited number of thermocouples mounted in the engine tailpipe. Even small amounts of mechanical variation in engine assembly can significantly alter the temperature profiles in the tailpipe so that the thermocouple reading is not a good absolute indication of the variations in aerodynamic temperature between engines. However, on the average, the EGT which was set when the engine was trimmed increased at the rate of 3.2 deg C per 100 hours since scheduled maintenance. Note that this increase applies only to the temperature which was set at the time of trimming. After the engine was trimmed and returned to service, the EGT was held constant by the engine control system and the thrust decreased as service hours were accumulated.

As the performance level of the engines was increased the internal operating temperature of the engines increased and more rapid degradation would be expected. This is clearly illustrated in figure 6 which shows the degradation rate as a function of the initial installed military power thrust. A linear fit results in the anomalous conclusion that engine performance would improve with time if the initial thrust were low

enough. The exponential curve shown avoids this problem by becoming asymptotic to the zero degradation line at low thrust levels.

The overall result of these effects was that engines which entered service with a relatively high installed thrust degraded at a faster rate than engines which started at a lower thrust level.

A significant point about figure 6 is that the initial installed thrust levels vary by about 8 percent. These are the thrusts produced by engines which have just been installed after uninstalled trimming. The trim procedure sets the uninstalled thrust level to a constant using an engine test stand. The only variation is that introduced by the test stand accuracy. Much of the variation in thrust level shown in figure 6 is a result of the engine installation. The probable mechanism is that relatively small changes in flow distribution change the temperature profiles in the engine and thus result in a different average exhaust gas temperature. The control system operates to maintain a constant temperature at the single radius where the thermocouples are located. These variations, which can be detected only by monitoring engine performance after installation are sufficient to influence the rate at which the engine deteriorates in service.

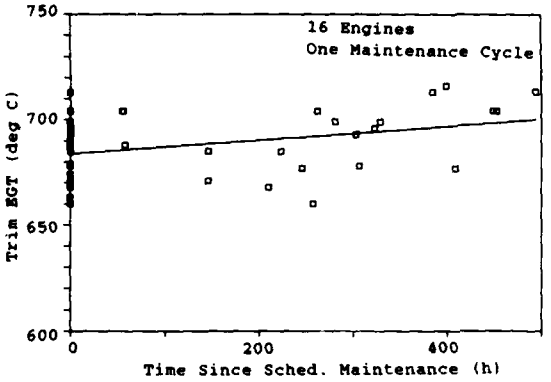

Figure 5. EGT Increase after Unscheduled Retrim.

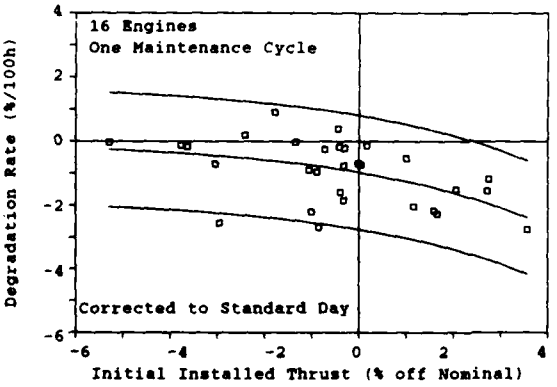

Figure 6. Effect of Initial Installed Thrust on Degradation Rate.

Afterburning Performance

Afterburning performance of the engines was studied by calculating the augmentation ratio. In addition to the three military power measurements, each data point included two maximum afterburning measurements. These were averaged and the ratio of averaged maximum afterburning to average military power was calculated. This proved to be very close to constant for each engine. Low augmentation ratio did not appear to be a significant problem. Adequate afterburning thrust was found when the military power thrust was satisfactory. Further analysis was not performed. This conclusion applies only to ground static conditions, performance in flight could prove to be considerably more complex.

Historical Data -- Individual Engines

Figure 7 shows the installed performance data for an engine which ran without retrimming for the full 600 hour period. This figure shows four data points taken immediately after installation and additional points taken at intervals of approximately 50 engine hours. The engine was removed once, at 261 hours, to facilitate maintenance unrelated to the engine. Analysis showed a temperature lapse rate of -14.6 percent of nominal thrust per 100 degrees and a thrust degradation rate of -0.4 percent per 100 engine hours. There are sixteen data points and the standard deviation about the regression is 1.211 percent of nominal thrust. The 95 percent band for the thrust is therefore $\pm$ 2.61 percent. In view of the measurement errors quoted above this represents a relatively good set of data.

It appears from the figure, that the engine removal and reinstallation at 261 hours had some effect on the thrust level of the installed engine. As shown in figure 8, the

data before and after the engine removal and replacement fit very well into two different families showing a distinct change in installed thrust level. The individual fits also show a small change in the thrust degradation rate (the slope of the lines) however this is not significant in view of the limited amount of data in each group.

Since no engine maintenance was reported, it may be that this results from a change in intake/engine alignment resulting from the removal and replacement. Alternatively, some maintenance may have been done that was not determined from the maintenance records.

Plotting thrust against ambient temperature for this engine (figure 9) reveals that the temperature lapse rate for the engine is similar for both data subsets. This is what would be expected for a thrust level variation caused by a change in engine intake alignment. A further notable point is that the lapse rate revealed by the four zero time points also agrees with the other data. The significance of this is that the determination of degradation rate could be simplified if the temperature effects were separated by determining the lapse rate from a series of zero time data points. In practice however, this requires that the engine remains under test for a prolonged period in order to obtain a sufficiently large ambient temperature spread to define the lapse rate with reasonable accuracy.

A second engine is shown in figure 10. This engine was tested installed at a number of ambient temperatures over a period of several days before the aircraft started flying. Shortly thereafter, the engine was removed and replaced two, possibly three, times for repairs to the EGT measurement system. It was not retrimmed. The figure shows a clearly defined degradation trend for the data taken after the EGT repairs were completed. The initial tests performed before these repairs do not lie on the same line. At the end of the cycle, the engine was removed for repair of a stuck exhaust nozzle and low thrust. The final group of data points, collected after this repair, show correction of the low thrust problem.

This figure shows a feature which recurs with fair regularity. When an engine has been retrimmed after maintenance, the installed thrust often changes quite rapidly over the first few hours of engine operation. In both the first and last groups of data the thrust

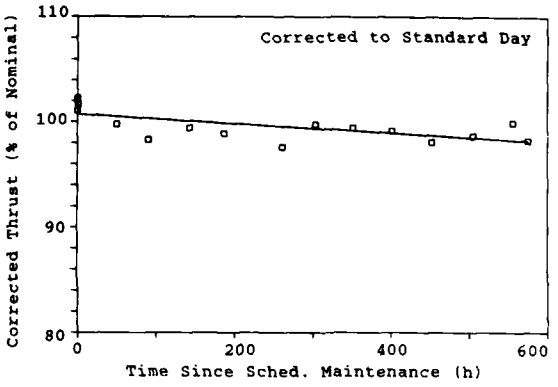

Figure 7. Thrust Degradation over 600 Hours.

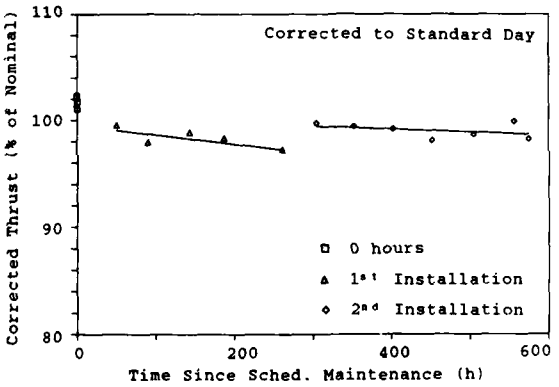

Figure 8. Thrust Degradation, Effect of Engine Removal.

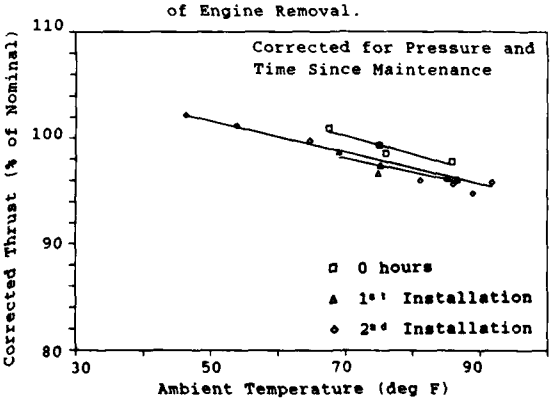

Figure 9. Thrust Level, Effect of Engine Removal.

starts at a high level and decreases as repeated data points are taken. This behavior appears to correlate with maintenance to the turbine section of the engine. The turbine rotors were replaced before the first trim shown and the turbine nozzles (stators) were replaced before the final trim.

Figures 11 and 12 show the performance of an engine which underwent frequent removals and replacements for a variety of reasons. In contrast to figures 3 and 4, the data scatter is greater although both lapse rate and engine degradation are clearly defined. The various removals were identified as follows:

1 for other maintenance
2 hot start -- MFC replaced
3 compressor rotor and bearing, oil cooler and pressure transducer, gearbox, combustor liner
4 for other maintenance
5 EGT amplifier
6 AB no light -- AB case repaired
7 cocked nozzle

The engine was retrimmed after removal number 3 and the repeated data points taken at this time show that the thrust level has been restored. However separating the two sets of data does not appreciably reduce the scatter in the data. Typically those engines which undergo a large number of removals exhibit a fairly wide scatter in the recorded data.

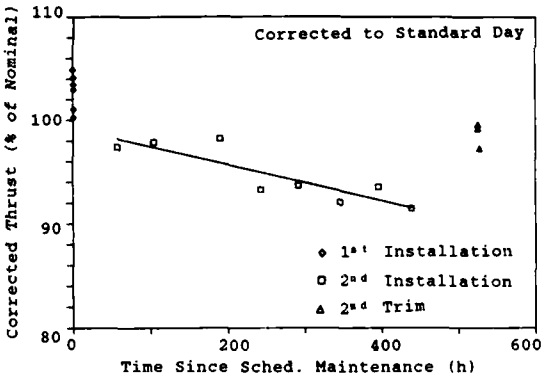

Figure 10. Thrust Degradation, Effect of Maintenance.

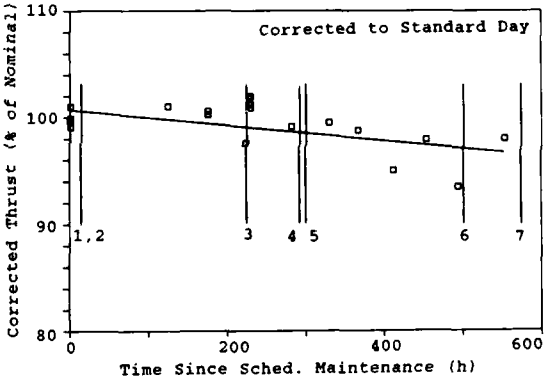

Figure 11. Thrust Degradation, Frequent Engine Removals.

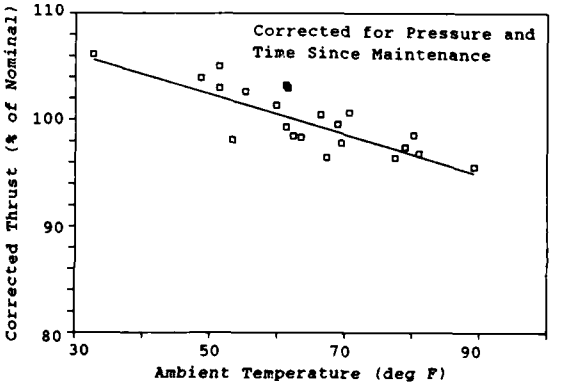

Figure 12. Thrust Lapse Rate, Frequent Engine Removals.

DISCUSSION

Installed Thrust Degradation Rate

There is an installed thrust level below which engines tend to be removed from service. The data show that engines which have a rapid rate of thrust degradation are generally removed at an early time whereas those having lower rates may remain in service for a prolonged period. Installed thrust monitoring on a regular basis can enable the rate of thrust degradation of individual engines to be established. This will permit estimation of the remaining service life before the performance of the engines degrades to an unacceptable level. It will also enable detection of an increase in degradation rate which would indicate incipient failure of some of the internal gas path components of the engine.

It is clear from the data that monitoring of the degradation rate requires that the lapse rate of thrust versus ambient temperature

is also determined. To a great extent, the ambient temperature of measurements cannot be selected, the prevailing value must be accepted. Two possible methods of dealing with this exist. Individually, they both appear to present some problems.

The first method is to establish the lapse rate initially by making a series of measurements over a range of ambient temperatures. This approach has the appeal of simplicity, since the lapse rate can be defined immediately and without consideration of the degradation rate. Unfortunately, it can result in tying up the equipment for a prolonged period as it is necessary to wait for the ambient temperature to change over a sufficient range and it may be necessary to extrapolate from this range in order to correct degradation data recorded at a later time. Neither of these is desirable.

The second method is to obtain data without regard to ambient temperature and then to perform a regression on two variables to separate the effects of lapse rate and thrust degradation. This has the virtue of eliminating any wait for desired ambient conditions to occur, but presents problems of its own. The first problem is that no conclusion can be drawn from the data until a sufficient number of points have been collected for a reliable regression to be performed. Since it appears that a number engine failures develop early in the life cycle, an infant mortality effect, this is a very undesirable restriction. The second problem is that if no attention is paid to ambient temperature in accumulating data there may be occasions on which a very narrow spread of ambient temperatures is obtained or on which a linear correspondence exists between ambient temperature and accumulated service hours. In the latter case, separation of the effects of the two variables is not possible although a nominal lapse rate may be assumed. In the former case, either a nominal lapse rate may be used, or the ambient temperature correction may be neglected altogether, however both of these approaches leave the fit liable to a complete breakdown if the next data point does not occur at the required ambient temperature.

The most desirable approach is probably a combination of both of these two. On initial engine installation an attempt can be made to obtain a range of ambient data which can then be used to correct subsequent data for a regression against time in service only. Simultaneously a multivariable regression can be performed against both variables which will be adopted when statistical analysis indicates that its accuracy is superior to the initial approach. This two tiered approach seems to combine the advantages of both methods of analysis at a small increase in mathematical complexity, which is well within the capacity of available computing equipment.

Installed Thrust Monitoring

The data presented show that a significant potental exists for using the regular monitoring of installed static engine thrust to identify deviations from normal time trends which can indicate either approaching component failure or an inadequate level of performance. Utilization of this capability will require regular, routine recording of the static thrust by engine health diagnostic equipment, for example during a static engine runup prior to takeoff, to build up the required data base. Such an application will also provide an opportunity for cross correlation of the thrust data with other available engine health indicators, thus enhancing the efficiency of the total health monitoring effort.

The discussion herein has been focussed on the use of static engine thrust because of the availability of static data. It seems very likely that additional information would be available from in flight data which could be recorded by an onboard engine health monitor which was equipped to measure thrust. The capability of the Thrust Measurement System to measure both gross and net thrusts would be significant in such an application. Experience with the X-29 thrust measurement has shown that accurate inflight thrust can be obtained, but so far no data is available to indicate what type of data correlations could be obtained to aid in engine health monitoring. This data would be relatively easy to obtain as an additional function of the onboard thrust measurement system which would be used to monitor engine health based on static measurements.

CONCLUSIONS

There are several benefits to be obtained from the use of installed thrust as an engine health parameter.

Significant installation variations exist so that although uninstalled thrust may be

controlled to a close tolerance, the installed thrust spread is considerably greater. Since engine degradation rate is linked to the initial installed thrust level, higher thrust levels result in more rapid engine degradation and should therefore be avoided where possible. In addition, some maintenance actions appear to result in a rapid variation of installed thrust over the first few hours of operation. This could result in the uninstalled trim setting engine performance which was not typical of that obtained after a short period in service. Installed trim monitoring would detect these occurences for possible corrective action.

There is an installed thrust level below which engines tend to be removed from service. The data show that engines which have a rapid rate of thrust degradation are generally removed at an early time whereas those having lower rates may remain in service for a prolonged period. Installed thrust monitoring is capable of determining the rate of thrust degradation of installed engines so that remaining time in service can be predicted.

Installed measurement of thrust is available with the technology described in this report. This capability can be utilized either as a ground based system for static use or as part of an onboard engine health monitoring system. Further work is required to assess the ways in which thrust monitoring, particularly on an inflight basis, can be combined with the other engine health parameters which are available in order to make the most efficient use of this capability.

REFERENCES

1. Kurtenbach, Frank J., NASA, "Evaluation of a Simplified Gross Thrust Calculation Technique Using Two Prototype F100 Turbofan Engines in an Altitude Facility" 1979, TP 1482.

2. Kurtenbach, Frank J., Burcham, Frank W., Jr., NASA, "Flight Evaluation of a Simplified Gross Thrust Calculation Technique Using An F100 Turbofan Engine in an F15 Airplane" 1981, TP 1782.

3. Baer-Riedhart, Jennifer I., NASA, "Evaluation of a Simplified Gross Thrust Calculation Method for a J85-21 Afterburning Turbojet Engine in an Altitude Facility" 1982, AIAA Paper 82-1044.

4. Ray, Ronald J., Hicks, John W., Alexander, Russell I., NASA/Computing Devices Co., "Development of a Real Time Aero-Performance Analysis Technique for the X-29A Advanced Technology Demonstrator" 1988, AIAA 4th Flight Test Conference.

DISCUSSION

D.DAVIDSON

Your system is very sensitive to small changes in engine performance. You have talked exclusively about the time-dependant degradation without mentioning the very important incident related degradation. Looking at your history plots, at least one of them could be interpreted as indicating a step change in performance that might be related to a single incident. Have you explored this at all?

Author's Reply:

I agree that the system should be able to detect incident related data. In fact we found a number of data records which suggested that incidents occurred. Unfortunately the available data was too limited to show with a high confidence level that incidents had occurred.

D.DOEL

For most engines the thrust lapse rate with temperature is constant from one engine to another. This lapse rate could be obtained from the engine manufacturer. Why not use this rather than the lapse rate derived from the data?

Author's Reply:

In the case that the lapse rate is available and the same for every engine this would a good approach.

For the engine data which we analysed, there were significant variations in lapse rates between engines.

M.J. SASPARD

You applied linear regression to EGT, I detected an initial decrease in EGT, perhaps due to running in, before a gradual rise occurred. Have you tried piecewise continuous techniques or higher order polynomial curve fitting techniques, so that such characteristics of running in are more readily detected?

Did you detect the effects of compressor washing?

Author's Reply:

Some of our data show an "initial running in" type change in engine performance. Because this engine is controlled to constant EGT at military power, this appears as a thrust change rather than an EGT change. We did try a piecewise regression approach but found that for short elapsed time period the inherent measured errors gave results with prohibitive large confidence bands. This is a good idea but would need more data than we had available. We did not try higher order curve fitting, this would require more data.

We did not have any data to examine the effects of compression washing.

GETTING MORE FROM VIBRATION ANALYSIS

R M Stewart, I C Cheeseman and K Librowski
Stewart Hughes Limited
Chilworth Manor, Southampton, Hampshire, United Kingdom

SUMMARY

Traditional vibration monitoring of gas turbines has been restricted to activation of alarms from overall levels and shaft orders. Use of more of the information contained in the signal could improve fault coverage and diagnostics. The practical problem is one of being able to model the vibration of an engine in sufficient detail. Furthermore, some problems experienced in the field have origins that no designer could be expected to predict, eg module mismatch.

How therefore are we to proceed? Any practical system must incorporate an evolutionary mechanism that feeds skilled field operators experience to a computer based monitoring system. This is based on the machine designers knowledge and improves its performance by this feedback.

Fortunately, there is a growing body of technology on the vibration produced by gas turbine engines, both to do with its interpretation and signal processing which make such a system feasible. Two areas of application are dealt with, the first connected with engine module roughness diagnostics and the second with fault identification of individual components such as main line bearings and accessory drive gears. For both, much of the hardware required to gather the necessary data is being specified and constructed, so overcoming a major objection to furtherance of this technology.

1.0 INTRODUCTION

Aeroengine and helicopter transmission monitoring systems in general, and the vibration aspects of those in particular, have long been a cause of much frustration to engineers in terms of false alarm performance and failure to detect faults that ought to have been 'obvious'.

Many reasons for this can be given, including in the authors' view the following. First, effective analysis of an aeroengine or transmission system's vibration signal requires a fairly detailed understanding of the signal's character- istics in terms of what dominates its energy, in what part of the spectrum are signs of the important faults likely to appear etc; systems in the past have included very little, if any, of this type of knowledge. Secondly, though we may understand how the signal is constituted, and in general what may change under fault conditions, we have often had no accurate knowledge at the design or development stage of either the magnitudes or inter-relationships of these changes, which has made data management in the field very difficult.

The objectives of writing this paper have therefore been to address these two key elements of the problem, in simple terms, (a) the selection of vibration features or discriminants able to maximise fault detection efficiency, and (b) the techniques of ground station data processing required to turn speculative design choices of discriminants into valuable maintenance and safety monitoring tools.

The concern for such systems is neither academic nor long term. At this moment flight systems are being constructed around the principles outlined in this paper for aircraft trials around the 4th quarter of 1988. Furthermore, many civil helicopter operators anticipate fitting these systems in the 1990-92 time frame to counter what many see as the unacceptable high accident rate of helicopters (Reference [1]). Such systems have architectures of the type shown in Figure 1, with an aircraft borne computer for the production of carefully discriminated results and a ground station for the integrated processing of these that runs the most modern databasing and expert system technology available.

2.0 THE OVERALL DATA PROCESSING SCHEME

As the problem being addressed is primarily one of data logistics it makes sense to look first at the the data flow diagram, Figure 2.

2.1 The link with design

The starting point is information on signal discriminants to be monitored, based largely on the recommendations of design and support engineers (Reference [2]). For example, should the engine incorporate a squeeze film bearing, vibration discriminants indicative of loss of oil from that component might be deemed important (see for instance Section 3). Equally well, should the gearbox incorporate a critical gear it might well be considered important to monitor the vibration discriminants associated with cracked teeth (see Section 4).

A key feature of any discriminant is the separation it effects between faulty and normal states, see Figure 3, and it is useful if it accomplishes this in a generic fashion, so enabling experience from one aircraft or aircraft type to be read across to another. The discriminant must be related to some definable method or algorithm which operates on the raw signal to make the fault more apparent. This could mean anything from simple filtering (eg to extract once-per-rev vibration) to sophisticated

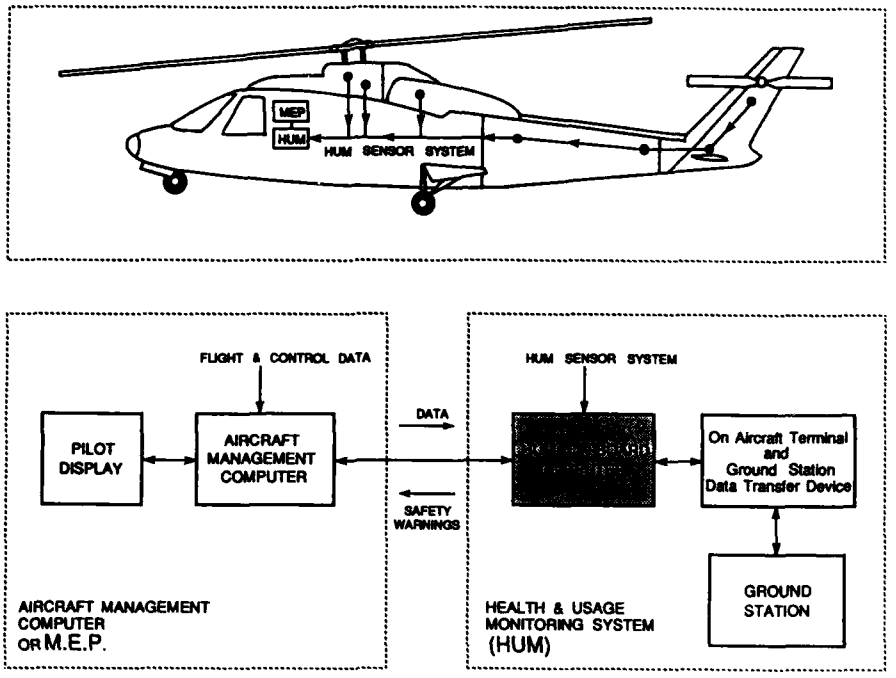

Figure.1. Avionics and Ground Station Configuration of a HUM System.

stripping away of high rotor and gear components to reveal low level bearing spall signals. Figure 3 illustrates this by showing what happens in the case of gear tooth damage detection. The lower left hand diagram (pre discriminant analysis) plots the rms value of vibration acceleration against vibration velocity (two of the commonest parameters used by the aviation industry for vibration analysis), whereas the lower right hand diagram plots vibration acceleration against a special purpose tooth damage discriminator called FM4A (see Section 4). The 'o' points indicate 'no fault found after strip' whereas the '+' points indicate 'fault found'. Prior to discriminant analysis they have no spatial separation, whereas after they have. Also the 'no fault' points have clustered along a fairly narrow vertical line the level of which can be predicted.

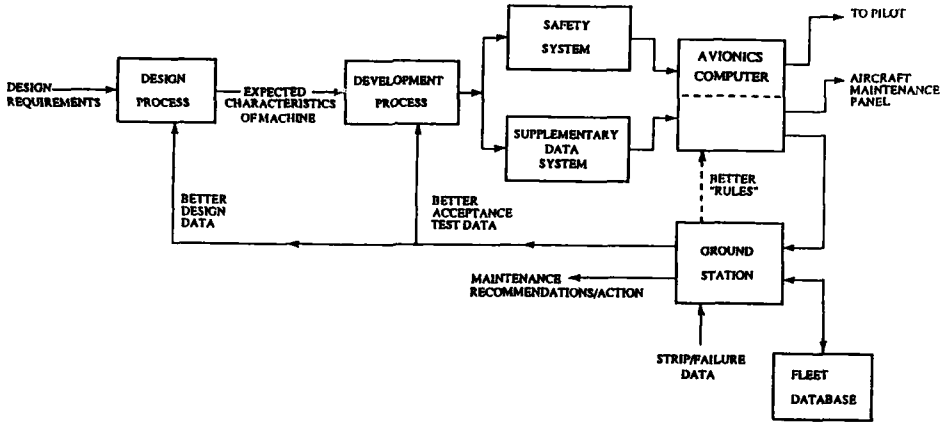

Figure.2. Data Flow Diagram for an Advanced HUM System.

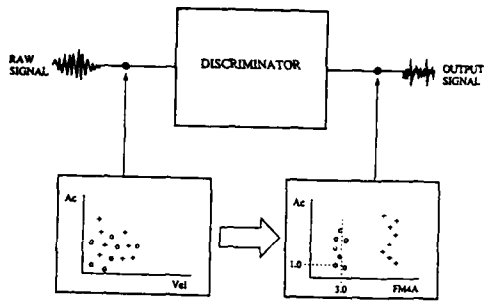

Figure.3. Discriminator Action that separates "Fault" from "No Fault" Data.

of signalling failures that could cause the aircraft to crash. Supplementary results can therefore be defined as those that do not satisfy these criteria.

2.2 On board the aircraft

The second step is generation of results on board the aircraft. It is assumed that the aircraft will have fitted to it a reasonably powerful signal processor, possibly as part of an integrated avionics or mission equipment package. This would produce results of basically two kinds:

1 Data critical to aircraft safety in the short term, called **Safety Data**.

2 Data relevant to safety in the long term, or maintenance planning, called **Supplementary Data**.

There is no rigid rule that places a result into one group or another. Generally speaking, Safety results are those that are readily computed, statistically stable under a wide range of operating conditions and capable

Figure 4 illustrates some of the differences in terms of parameter value ranges under both 'No fault' and 'Fault' conditions. For a parameter to be used in the detection of unsafe conditions (and perhaps therefore be displayed in the cockpit) it is essential *that it has (a) a low variance under 'no* fault' conditions, and (b) a very significant change in level from 'no fault' to 'fault' or 'safe' to 'unsafe'. When the fault occurs the indication is therefore quite clear, preferably totally unambiguous and the alarm 'computable' in the aircraft management computer using simple, testable logic.

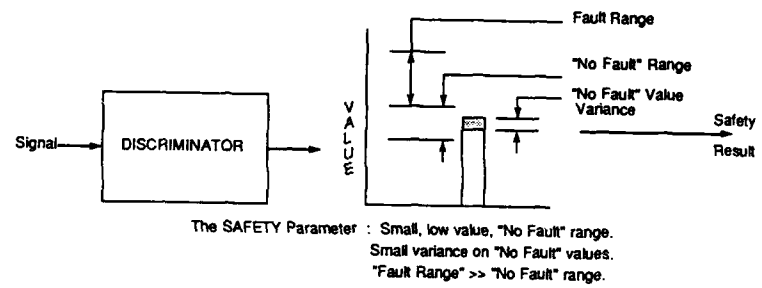

The SAFETY Parameter : Small, low value, "No Fault" range.
Small variance on "No Fault" values.
"Fault Range" >> "No Fault" range.

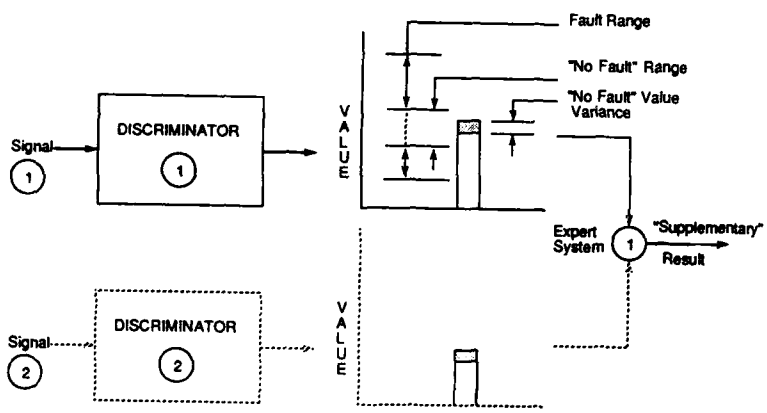

The SUPPLEMENTARY Parameter : "No Fault" range indeterminate until machine is built and tested.
"Fault Range" indeterminate until failures observed.
Variance of "No Fault" values << Fault Range.
Results from several discriminators combinable via an Expert System.

Figure.4. Safety versus Supplementary Parameters.

The supplementary parameter can however be much different. It does not matter fundamentally whether or not the level under fault conditions is above or below the 'no fault' one - the ground station can sort out such trends based on the analysis of actual 'fault' and 'no fault' data, see Section 5. Supplementary results may therefore take on almost any level so long as the statistical spread (eg four standard deviations from the mean) of 'no fault' data covers a reasonably small fraction of the possible measurement range and is significantly different from the spread under 'fault' conditions. Furthermore, supplementary results may be combined logically through an expert system to produce derived results, eg:

```
If Result 1 is high
 & result 2 is low
 & result 3 is high   then  Result 4 is high.

If Result 4 is high   then  create an alarm.
```

which is something that we might not be quite so willing to allow for the more critical safety results.

Obviously it is important that the Safety Data be totally free of false alarms and amenable to simple thresholding. Supplementary Data on the other hand would almost by definition never be used in the air, and so could therefore be used to generate complex, derivative alarms on the ground to do with long terms trends of engine performance, as described later in Section 5.

2.3 The ground station

The third step is ground station processing primarily of the Supplementary Data. The important feature here is the making of connections between machinery strip reports and the supplementary data. Bear in mind that decisions to include measurement of a certain characteristic in the supplementary group may have been taken on relatively flimsy grounds, for example, because on previous generations of aircraft it had proved useful. A main purpose of ground station processing is therefore to gather enough evidence to substantiate the speculative selection of the parameter and set its alarms to the most efficient level. This third step therefore involves significant database and rule generating activities.

It is vitally important that the system be seen as a whole rather than as a collection of parts. Nowhere is this more important than in the ground station and the processing of supplementary data, which depends on being able to consider long term trends of data in relation to accurate strip information. Herein however lies a major problem with systems of this type, namely the importance of skilled engineering analysis of engines or transmissions returning for maintenance.

It is the authors' experience that accurate strip data in service is difficult to acquire. For whatever reason this may have been true in the past, remedying this loss of knowledge must have high priority for the future.

3.0 AEROENGINE MONITORING TECHNOLOGY

The interpretation of faults in gas turbines using vibration sensors has had a chequered history. In the period 1960-75 vibration monitoring got a bad name because much was claimed but what was achieved was blighted by a large number of false alarms. Part of the problem lay with sensor and system unreliability. It goes without saying that the need to check sensor and system integrity must have an important place in any system. More to the point for this paper was the lack of knowledge of suitable diagnostic tests to be applied to the sensor data produced. Since that time considerable progress has been made and vibration has an important part to play in aeroengine monitoring technology, albeit in parallel with other techniques like the "Electrostatic Gas Path Monitoring Technology" described by C Fisher of Stewart Hughes Limited in Reference [4].

Knowledge of what and where to monitor is obtained from a variety of sources. The designer in his work to ensure that the engine will not fail within the operational envelope considers the various failures that could occur. In most cases mathematical modelling is utilised, the output from which could be interpreted to provide diagnostic techniques. Engine tests are another fruitful source of information. For example, the data which shows an engine operating correctly provides the datum from which faulty engines depart. For human identification of faults the method of presentation is very important. The wealth of information contained in a ZMOD, Campbell or waterfall plot enables a skilled observer to identify a wide range of faults by comparing the actual with the ideal. A plot for an engine is shown in Figure 5. The facility of the human observer to make a rapid visual scan and identify differences allows unusual features to be detected even though at that time it is not possible to associate these features with a particular engine condition. The ability to translate this feature or 'picture' information to a database for field use is under development. The correlation with faults requires fault data. The problems of acquiring accurate strip data mentioned in 2.3 apply.

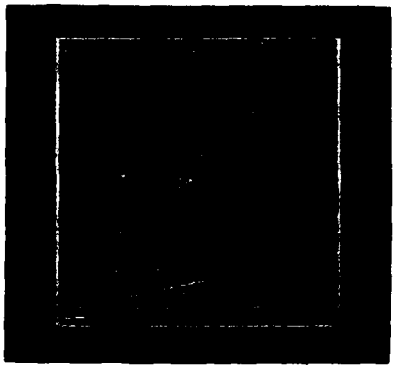

Figure.5. A Typical Gas Turbine "Z-Modulus" Plot.

While association of signature change with fault is a useful step, behind all good diagnostics there must be a body of scientific knowledge which relates the diagnostic to the fault through the laws of physics. It would be nice to think that this relationship could always be

expressed in quantitative terms. However, often the mechanism is clear but the modelling is far too complex to justify the effort involved. In this case a qualitative connection between the two must suffice. However, such a qualitative understanding is one which is of enormous value in confidence building in the diagnostics. One way to build this confidence is to establish techniques using scaled rig tests which simulate parts of the gas turbine. To illustrate the value of this approach an example where a rig illustrated clearly how confusion might arise between two well known faults is given. A further example illustrates a fault which gave what at first sight was a surprising result. The relation between the rig and full scale engine is relatively easy to establish in these cases.

3.1 The application of simple modelling to fault determination

In modular engines the problem of determining which module may have a fault is of crucial importance if the full economic benefit of this type of design is to be realised. Two of the most common faults are out of balance and misalignment between modules.

For the vibration analyst, one problem with the modern gas turbine is that its rotor system incorporates non linear elements, in particular squeeze film dampers. However, it is clearly an advantage if a linear model could be used as this simplifies computational requirements. As part of a large scale programme to develop second generation vibration diagnostics for turbine engines, Stewart Hughes Ltd were funded by the Ministry of Defence and Rolls Royce Limited to build and run the experimental rig shown in **Figure 6**. The rig was run in the various configurations shown. An important purpose of the rig was to test certain design hypotheses about faulty squeeze films and misaligned rotors. Dynamic scaling of important parameters for the rig was maintained.

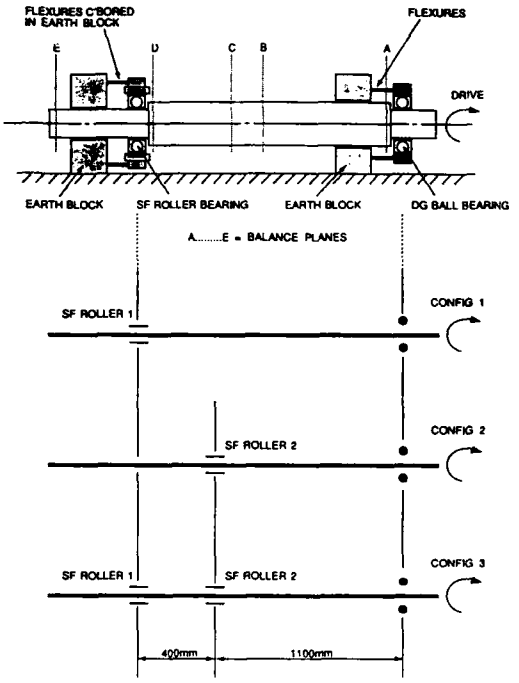

Figure.6. Layout of Scaled Simplified Gas Turbine Demonstrator.

How far can linear system techniques be applied? To assess the linearity of the rig the influence coefficient response technique was used. Out of balance weights were seeded at various planes in the rotor and the influence coefficients for the accelerometers at the positions indicated determined. It will be noted that the rig in **Figure 6** (configuration 2) contained a squeeze film bearing and this was exercised by the magnitudes of the out of balance fitted. As an indication of the value of the linear model the results for two out of balance weights of 20g and 28.3g respectively were obtained. The relative response levels for these two out of balance figures should be 1.41 and this is approximately the case in **Figure 7** over the run up speed range. To ensure that the squeeze film bearing was fully exercised the out of balance was increased to 48.3g, a ratio of 2.41 relative to the 20g. Again **Figure 7** shows that the response was acceptably good. One may therefore use the assumption of linearity with care.

The application of this technology to simultaneous determination of out of balance mass in more than one plane has been demonstrated on the rig. Detection of a mass out of balance in plane A and another one in plane D simultaneously is shown in **Figure 8**. It will be noted that the discrimination is not uniformly good through the whole of the rig acceleration. This is associated with the modes of the rig. It is necessary to choose the speed range where the response is assessed relative to the modes which are being exercised during the acceleration. In the case of this rig it was a relatively simple situation, but for the more complex gas turbine the choice may not be as obvious. In that case further expertise must be added, for example from the designers calculations, in order to get the most accurate estimate of the out of balance and its location.

Out of balance is a well understood phenomenon although the technology used here is not currently in widespread use. Shaft misalignment can also be modelled when squeeze film bearings are used. Combination of the two models leads to an interesting conclusion. Consider the case where the misalignment of the shafts causes the squeeze film bearing to act as a cam and therefore to produce a force of constant amplitude that rotates with the rotor. The amplitude of this force is related to the misalignment and the effective stiffness of the system which is resisting the motion. The resulting vibration frequency is equal to the shaft rotational frequency. For misalignment and out of balance together the result is the addition of an out of balance vector which increases as shaft speed squared and a speed independent vector for the misalignment. The response generated during an acceleration will depend on the phase between the out of balance and the misalignment. To illustrate this consider the response when the out of balance is diametrically opposite to the cam effect. At very low speeds the cam effect will dominate because the Ω^2 term of the out of balance will be extremely small. However, as shaft speed increases the magnitude of the out of balance force increases rapidly and at some shaft speed the two will become equal but opposite. Above this shaft speed the out of balance will be the dominant

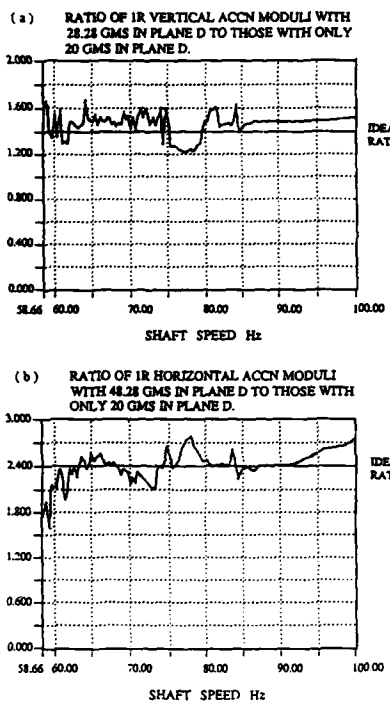

Figure.7. Results from Linear Modelling of Out of Balance Effect with Squeeze Film Damper operating.

On the rig shown in **Figure 6** (which simulates as accurstely as possible the main shaft of an aeroengine) the oil supply to the damper can be varied from 0-60 lbs/sq ins. In order to test the behaviour of the squeeze film dampers under various applied pressures a single level of out of balance was seeded in the rig and a particular axial clearance in the bearing chosen. The rig was then accelerated from rest to running speed and the acceleration on the squeeze film housing measured in both the horizontal and vertical directions. The test was then repeated at a variety of supply pressures.

Excluding the case where the oil is switched off the response found was effectively independent of the supply pressure. This shows that the squeeze film damper is a genuine hydrodynamic device, the forces generated by the damper being independent of the static oil pressure. When the oil is switched off it will be noticed in **Figure 11** (which is a ZMOD not plotted in the conventional way against engine speed, but simply against time) that there is a change in the overall pattern. The first is that the 1R response decreases, which was an unexpected result. The second is that the half order components on the rig start to appear, $\frac{1}{2}$R, 1$\frac{1}{2}$R etc can be seen. The appearance of $\frac{1}{2}$ orders was also noted when very low viscosity oil was used in a separate experiment, indicating that the origin of the $\frac{1}{2}$ orders is insufficient damping.

The definitive characteristic in this case is therefore the half-R components in the signal from either the casing mounted accelerometer or pressure transducer in the feed or drain lines to the damper. The ZMOD plot itself does not of course have to be used - it is merely a powerful laboratory tool. What probably does have to be measured however is the vibration of the engine under run-up conditions, which is relatively easy given digital signal processing hardware within the avionics kit.

effect and therefore the force will appear to have changed in phase through 180°. This cancellation effect can occur at any shaft speed being a function of the cam effect and the mass out of balance only. In this respect it is different to an anti-resonance which can only occur between two natural frequencies. The phase change due to a change in net force is extremely abrupt. Illustrations of this effect are shown in **Figures 9** and **10**. From the plots of phase, **Figure 9(a)** shows the cancellation with 20 grms OOB to occur at 51 Hz, whereas **Figure 9(b)** with an equivalent 48 grms OOB the cancellation speed has reduced to 40 Hz. This effect can also be seen clearly if Log amplitude is plotted - **Figure 10**. The algorithm which was developed and illustrated for determining location of out of balance has been extended to include the effect of misalignment and to detect the magnitude and position of the misalignment in a very similar way.

In the cases given above, the intelligent use of a linear model coupled with selective interpretation of the results based on a good understanding of the design of the system has enabled valuable diagnosis to be made.

3.2 Oil starvation of a squeeze film

The majority of aeroengines employ squeeze film dampers placed between the outer race of the bearing and the casing to limit the vibration caused by out-of-balance, especially in blade-off situations. These devices are intricate mechanisms that depend on careful control of axial and diametral clearance as well as a supply of new oil to replenish that lost through clearances. A badly set up squeeze film can have dramatic effects on engine vibration. We are therefore acutely interested in the vibration characteristics of good versus faulty squeeze films. One fault is oil starvation either through excessive clearance or low supply pressure.

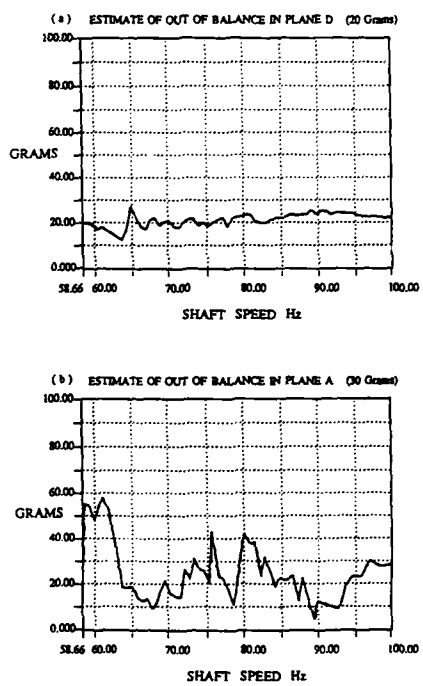

Figure.8. Use of Linear Model to predict Two Out of Balance Masses.

3.3 Other techniques

As far as the aeroengine is concerned, vibration analysis is probably of lesser importance than either performance or debris analysis. Nevertheless, the principles expounded here about selecting the most appropriate characteristic to measure apply equally well to those. The latest techniques of oil supply debris analysis, gas path debris analysis (**Reference** [4]) and performance analysis reflect this well.

4.0 MECHANICAL TRANSMISSION SYSTEM MONITORING

The use of transmissions in aeroengines is associated with turbo-props and with auxiliary drives in aircraft. In the case of helicopters the engine and transmission are seen as an overall package. Due to the high integrity of helicopter transmission systems they have been the subject of intensive study in the UK. Currently, two major competing monitoring systems are under development and about to enter trials with North Sea operators, sponsored by the Civil Aviation Authority (CAA).

The key elements of a transmission system are generally the gears, bearings and shafts. Stewart Hughes Limited has played an important role in the development of monitoring technologies for these, both from technique and avionic hardware points of view.

Taking the gear as an example, the 'characterisation' technology about to implemented in North Sea targeted systems has as its foundation something called the FM number vector. This is a group of closely inter-related parameters derived from analysis of the gear's signal or synchronous average (**Reference** [5]). The elements of the 'vector' are as shown in **Figure 12**.

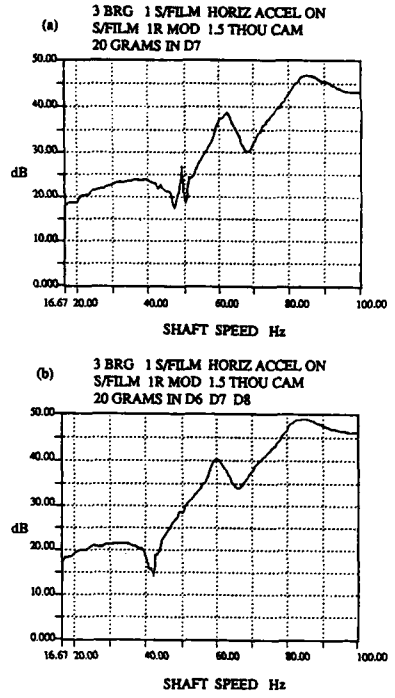

Figure.10. Shaft Speed for cancellation of Out of Balance and Squeeze Film Bearing Cam Misalignment, indicated by Amplitude.

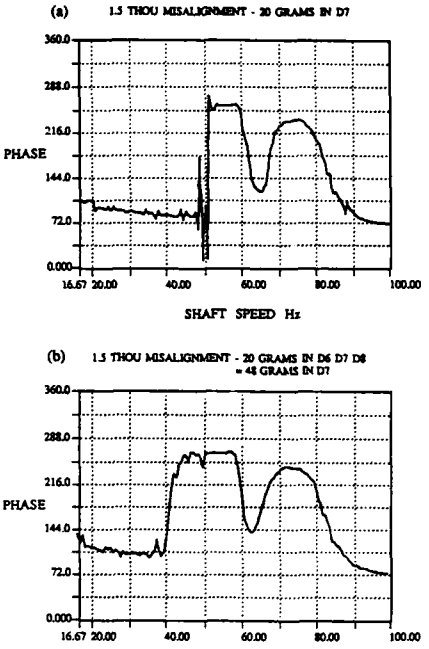

Figure.9. Shaft Speed for Cancellation of Out of Balance and Squeeze Film Bearing Cam Misalignment, indicated by Phase Change.

The system was designed with two important criteria in mind. First, vibration monitoring of gearing is greatly complicated by the fact that the components of the vibration signal that indicate faults are not those that dominate its energy - the simple measurement of energy (eg in the way that the aeroengine industry currently does it for engines) is therefore almost certainly doomed to failure. Secondly, the vibration sensor can almost never be optimally positioned on the gearcase for all gears, so that there is generally a high degree of uncertainty in the early stages of monitoring as to which numbers will be most effective. This is particularly true of epicyclic systems. The situation is somewhat analogous to FM radio reception where reception techniques able to handle a diversity of possible reception paths are in common use. The equivalent 'diversity' of the FM system comes, for example, from having a variety of detectors able to sense localised tooth damage (FM2A, FM4A, FM5A, FM6A etc) and gear or gearcase structural failure (probably the commonest cause of catastrophic failure).

An important discriminant for the FM number system is the so-called 'surface noise' of the gear. This may be derived either from the amplitude or phase part of the signal average in an attempt to remove from the signal average all components related to 'normal meshing action'. The normal component most often seen in the spectrum of gear vibration is that of the meshing frequency and its harmonics. It is not uncommon for this to be 100 times greater than components due to localised tooth damage (eg spalling, root bending fatigue), and seldom is it less than

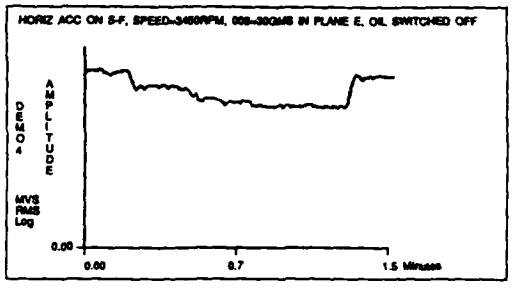

Figure.11 (a). Variation of 1/Rev Amplitude following Oil Starvation of Squeeze Film Bearing.

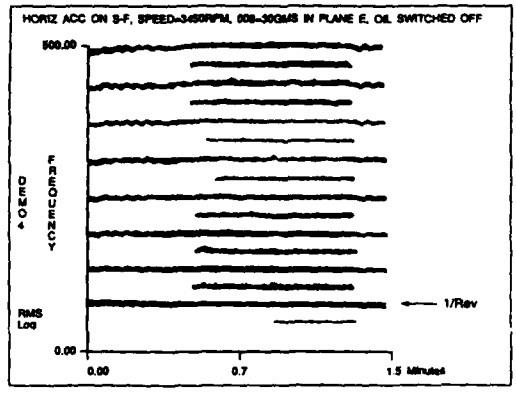

Figure.11 (b). Principal Changes in Frequency Components following Oil Starvation of Squeeze Film Bearing.

10 times greater. The characterisation algorithm in this case is known as a 'de-correlator' which effectively removes from the signal average all components that are correlated over more than three teeth. This always includes the meshing frequency components.

An actual example of what good characterisation can do for the monitoring system was shown in Figure 3. This actually presented a comparison of vibration velocity against FM4A for a the main rotor drive gear tooth bending fatigue failure, with the purpose of demonstrating the much wider separation of 'fault' from 'no fault' values made possible by good choice of discriminators. Because of its impressive discriminating properties FM4A has been selected by several helicopter manufacturers as a Safety parameter.

A good example of a supplementary result is MF1 in the table above. This is in fact the ratio of energy at two frequencies in the spectrum of the average and is thus susceptible to casing transmission effects. It therefore has a very large range of possible values, and for this and other reasons its measurement variance may be high, so dictating the imposition of strict test conditions (ie flight regime, gearbox rotational speed). When sensibly applied, however, it can be very useful as a measurement of gear profile wear and other assembly faults that can afflict the mesh.

In spite of the sophisticstion of the analysis which has greatly simplified the signal interpretation, there is still the need for expert guidance in relating the output of the parameters of Figure 12 to the faults.

5.0 THE GROUND STATION

As far as the technician operator is concerned the key component of the system is likely to be the ground station, for it is here that any economic advantage, exclusive of improved safety, is likely to be generated.

Ground station technology has a fairly long history of development. Among the first was a system developed for the US Airforce call MIMMS (Reference [5]) which was based on a DEC 11/70 mini computer and a relatively simple hierarchical database. Between that time and now at least one generation of equipment has passed and the system currently being developed by the authors' company uses a -386 based PC along with a relational database and a variety of AI tools, including a powerful data classifier.

5.1 The application of classifier technology

Much has been written on classifier technology but the application to real engineering problems is still in its infancy. Stewart Hughes are actively using classifier technology for the following reasons.

The power of this approach lies in the exploitation of the complementary capabilities of the engineer and computer. The relevant skills are described in Figure 13.

Rather than dealing with the complex problem of representing background engineering knowledge, or leaving the burden of consistency checking with the engineer, our approach aims to integrate the good capabilities of both actors to yield a system whose performance is superior to either individual capability. The human-computer interaction places a heavy responsibility on the quality of the interface between them.

The problem of constructing a fault diagnosis system can be split up into three phases:

ELEMENT	PURPOSE	DATA TYPE (Sup = Supplementary)	
SDA	Gear vibration	Safety	
MF1	Profile wear		Sup
	Advanced structural failure		Sup
FM1A	Gear Misalignment		Sup
	Gear structural failure	Safety	
	Gear case failure	Safety	
FM2A	Localised tooth damage	Safety	
FM3	Parametric excitation		Sup
FM4A	Localised tooth damage	Safety	
	Advanced structural failure	Safety	
FM4B	Distributed tooth wear		Sup
FM5A	Localised tooth damage		Sup
FM6A	Tooth manufacturing defects		Sup
	Early localised damage		Sup

Figure.12 The FM Analysis System

(i) Transforming the incoming data into a representation appropriate to the problem. This is done by devising discriminators and applying them to the data;

(ii) Associating the transformed data with the faults which need to be detected, and constructing a mapping between the two;

(iii) Analysing the devised mapping by comparing its performance with previous known cases, and considering its 'physical reasonableness'.

From a knowledge engineering point of view, the characteristics of the problem are as follows:

(i) A large part of the knowledge is encapsulated in the choice of discriminators (eg the FM discriminator for gear work)

(ii) Knowledge of the relationship between discriminators and faults is very scarce;

(iii) Large (>100K) quantities of data can be involved. This data can be noisy and incomplete. Much knowledge lies buried in this data.

These characteristics have a direct impact on the type of fault detection system that would be useful for the monitoring problem.

-	ENGINEER	COMPUTER
Engineering background	Good	Poor
Qualitative assessment	Good	Poor
Qualitative evaluation	Poor	Good
Data processing capacity	Poor	Good
Intuition	Good	Poor
Accuracy and consistency	Poor	Good

Figure.13. Skills in fault diagnosis tasks and their distribution

Devising a set of useful discriminators is the key to success in the construction of a fault detection system. Different problems require different discriminators. This has been illustrated in the early part of this paper. Currently, knowledge of which techniques to apply where is the province of the (signal processing) engineer. In constructing a set of discriminators, the engineer may engage in three tasks:

(i) Devising a new discriminator. This may be termed a research activity and would need to be performed if no existing discriminators were suitable;

(ii) Selecting a discriminator from a 'library' of available techniques. This would be done on the basis of the perceived usefulness of the discriminator to the task in hand;

(iii) Assessing the actual usefulness of a discriminator when applied to the current problem. The criteria of usefulness would be defined by the nature of the problem and might include such factors as computational speed, accuracy, reliability, etc. It is important to note that the usefulness of each discriminator is dependent on which others are used. If, for instance, two discriminators performed an equivalent task, one of them would be redundant.

The first two of these tasks are exceptionally difficult from a computational point of view, as they involve a substantial amount of engineering background and intuition. The third task, that of assessing the selected discriminators, is to some extent a purely algorithmic procedure, and can therefore be performed by the classifier system. In this respect, the classifier acts as a 'hypothesis tester'. The engineer proposes that the discriminators chosen are useful for the fault diagnosis task, and the classifier is used to determine whether, and to what extent, this is true.

One of the simplest representations that can be used is that of the fault tree. Fault trees provide an efficient means of mapping between discriminator values and faults by using the equivalence and conjunction operators. More sophisticated representations include propositional logic, first order predicate logic and extensions thereof. Ideally, the representation chosen should be the simplest one which is adequate for the problem. The classifier can be constrained to use simpler representation when required.

The classifier performs a search of the chosen mapping space, driven by specific examples, hints, problems specific constraints and general heuristics, and produces a mapping consistent with what it has been told. This mapping then needs to be tested to assess its usefulness.

As an example of how all these ideas are implemented in practice, consider the problem of reducing the incidence of false alarms in a multi-sensor monitoring system. The diagnosis problem is that of deciding whether an alarm (or set of alarms) is false or genuine. A database is available of cases when the alarms were justified, and cases where they were not.

In this case, the engineer may start by choosing a simple representation formation, such as attribute-value pairs. (Similar to Michalski's VL_1 logic). An obvious set of discriminators to start with would be the individual alarms themselves. Each discriminator needs a domain to be defined for it. In the case of the alarms, this may be a simple boolean (alarm-on, alarm-off) or an extended one (alarm-off, alarm-warning, alarm-serious). There may be constraints on the discriminators, eg some may be mutually exclusive, and some relationships may already be known.

For this simple representation formation, the general heuristic of minimising entropy, as used in the ID3 algorithm (Quinlan) is particularly appropriate. Applying this technique to the specified discriminators, whose values are extracted from the database, results in a fault tree. This fault tree is then applied to examples not used in its creation, to assess its predictive reliability. Other quality

criteria which may be of relevance are number of leaves, number of discriminators used and the size of the tree relative to the size of the training set.

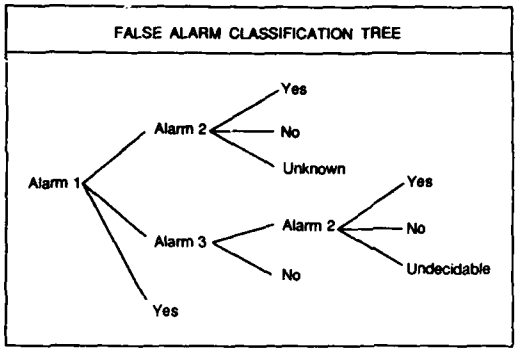

Figure.14. A typical fault tree

Such trees are represented graphically in a window based environment, so large trees can be viewed by scrolling about, Figure 14. The benefit of this explicit representation is that it focuses the engineer's attention. For example, the tree can represent, and allow the engineer to 'home in on' inconsistencies in the data, rules or constraints, and incompleteness in the mapping. Further inspection of the tree may bring to the engineers attention the fact that some discriminators are being combined to produce a result. This may be noted as interesting or unreasonable. In the latter case, the engineer is forced to consider why this is so, and hence knowledge, which might have been missed, is brought to attention. Consideration of the numerical quality of the tree gives the engineer a clue as to the usefulness of the discriminator set chosen, and additionally, an assessment of the usefulness of each individual discriminator is provided.

'Unknown' signifies an incompleteness in the mapping, 'undecidable' signifies an inconsistency. Note that both apply only to restricted parts of the tree, and not the tree as a whole. The association of Alarm 1 with Alarm 2 may be significant.

This classifier can be thought of as a sophisticated database analysis tool, which helps the engineer choose useful discriminators for the problem, and then produces an efficient mapping between these discriminators and the faults which have to be detected, together with an analysis of the quality of this mapping. Assuming that the quality is acceptable, the mapping can then be embedded in either an off-line data analyser or an on-line fault monitoring system.

The task of the classifier can be made clearer by considering the situation depicted in Figure 15. This shows the time trends of a gear monitoring 'vector' composed of the FM numbers described in Section 4, and some additional ones to do with calculated gear usage (UF = structural failure related usage, UW = gear tooth wear related usage) and debris production (DL, DS).

The time trend data has been broken up into three phases, namely (i) the burn in phase (from acceptance testing to 20 hrs flying time), (ii) the threshold setting phase (next 10 hrs flying time) and the monitored phase (from 30 hrs to time of failure at 510 hrs). The trends shown are hypothetical but based on long experience of how such analysis techniques function.

At the end of the threshold setting phase all alarms are set based on the mean and standard deviation of all measurements made during that phase, or absolute level if knowledge about how to set that exists.

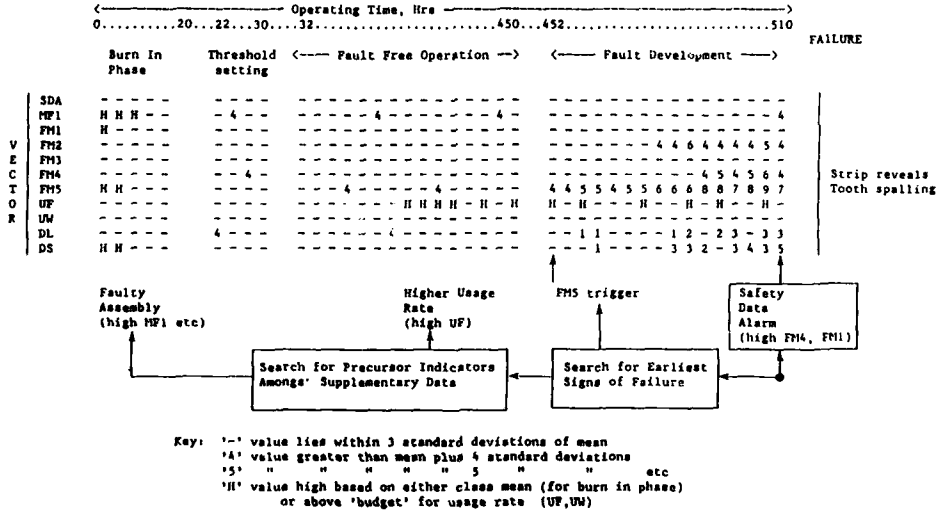

Key: '-' value lies within 3 standard deviations of mean
'4' value greater than mean plus 4 standard deviations
'5' " " " " " 5 " " etc
'H' value high based on either class mean (for burn in phase) or above 'budget' for usage rate (UF,UW)

Figure.15. Time Trend of Gear Monitoring Vector

For the next 420 hrs the gearbox operates without any safety alarms being triggered. However at 452 hrs the FM5A parameter exceeds its threshold, followed soon after by the debris and FM4A numbers. At 510 hrs the unit is pulled for examination and spalls are found on two teeth of one of the gears. (Along with miscellaneous amounts of fretting, corrosion, initial pitting etc.)

The classifier is then set two tasks:

1 Determine the best complex of rules for detection of this fault on all other units at the earliest possible stage.

2 Determine any precursors of the failure in terms of build quality or operational usage.

The first problem it would treat by analysis of something called 'fan out'. Remembering that the vector is made up of discriminants that look for the fault in several different ways, some discriminants will undoubtedly be more sensitive than others. The technique employed therefore involves marching backwards through the database looking for the first signs of parameters exceeding a threshold lower than the safety level (which is set very high in order to limit false alarms).

Fan-out then describes the process whereby as time marches forward more and more alarms are seen, either by results breaking through higher and higher threshold levels or completely new ones arising. The fan-out shown in **Figure** 15 starts with FM5, propagates to debris then FM4A and ends up with SDA and MF1 just beginning to exceed their lowest threshold level.

The second problem is more difficult to treat. What the classifier would be looking for are connections and anomalies between the reported fault, the usage of the aircraft and the data gathered during acceptance testing and burn-in. For example, the system designer could have given it the rule:

If the failure is 'wear' and the aircraft usage related to wear is high, then the fault is anticipated.

the implication being not to bother searching for an assembly or manufacturing cause.

An important issue at this juncture is the significance of 'class' versus 'particular aircraft' data. If the number of aircraft in the fleet is low (say less than 20 aircraft) the use of fleet (or 'class') statistics is problematical, largely on account of measurement noise. However, if the fleet happens to be large (> 50 aircraft), the usage of each aircraft is being monitored accurately and the discriminators have been carefully selected, experience has shown class data to be extremely valuable.

6.0 AVIONIC HARDWARE

The goal is systems that fly with aircraft and produce both safety data in the air and highly effective maintenance data on the ground.

The part that flies must be both light in weight and cost effective with respect to whatever else is on the same aircraft. In practice this usually means that it must make maximum use of whatever sensors and computers are fitted to the aircraft as standard.

The system currently being developed by the authors' company for application to both helicopters and fixed wing aircraft has already been shown in overall system terms, see **Figure** 1, and the intention is ultimately to produce a system that can interface to any existing or new avionics package, regardless of whether the latter is 'integrated' or 'discrete'. The main design problem is the front end signal processor needed to operate on the multitude of sensors, some of which require only infrequent interrogation, others constant interrogation; some of which require only minimal processing to produce a result, others massive amounts of processing. The key therefore is the main processing unit and for this difficult task the super flexible device known as the Transputer was selected (**Reference** [6]).

7.0 CONCLUDING REMARKS

The authors have presented an approach towards vibration monitoring that gives a great deal more than has hitherto been possible. This new approach relies on integrating three critical technologies, namely:

1 The availability of discriminants able to detect the important faults in a safe and false alarm free manner.

2 The ground station technology able to process large volumes of safety and supplementary data. In particular this means database and classifier software.

3 The availability of avionic computers flexible and powerful enough to generate the safety and supplementary data.

All three are needed, and to be developed the system probably has to fly on a significant number of aircraft. Any attempt to develop the Supplementary Data aspect of the system via tape recorded data would almost inevitably fail due to logistical problems of data collection.

8.0 REFERENCES

[1] 'Review of Helicopter Airworthiness', Report CAP491
Civil Aviation Authority, London 1984

[2] Stewart R M, Cheeseman I C, Bonfield D G
'How to Get The Designer Into The Box'
Mechanical Failures Prevention Group, Patuxent River, 1986

[3] Ehrich F F
'Sum and Difference Frequencies in Vibration of High Speed Rotating Machinery'
ASME Trans, J Eng. Ind., Feb 1972, pp 181-184

[4] Fisher C E
'Gas Path Condition Monitoring Using Electrostatic Techniques'
AGARD 71st Symposium of Propulsion and Energetics Panel
30 May - 3 June 1988, Quebec Canada

[5] Dolny L J, DeHoff R L
'Maintenance Information Management System (MIMS) - Strategic Maintenance Decision Support'
Condition Monitoring 84, pp17-31
Published by: Pineridge Press, Swansea, UK

[6] Stewart R M, Sulley C
'Compact Diagnostic Co-Processors for Avionic Use'
Mechanical Failures Prevention Group, Patuxent River, 1986

DISCUSSION

R.FEATHERSTONE

Could you give an example of a discriminator?

Author's Reply:

The computer program must be "open". This allows designers or other authorised users to insert their knowledge without having to expose that information to a third party.

It is possible, and sometimes desirable, to demonstrate a technique for monitoring design knowledge using an "idealised" machine. The designer can then insert the particular information pertinent to his machine at a later date.

J. DAWSON

If design information is so important to diagnostic work,how do you deal with the proprietary position of the machine designer?

Author's Reply:

FM4A applied to gear fault detection utilises the kurtosis of the signal appropriate to the shaft on which the gear under examination is running. The isolation of the signature for the shaft is achieved by synchronous averaging. The value of FM4A is related directly to known values of the kurtosis of various signals, eg a sine wave has the value 3 which enables the "no fault" condition to be specified with confidence.

A JOINT STUDY ON THE COMPUTERISATION OF IN-FIELD AERO ENGINE VIBRATION DIAGNOSIS

H.R. CARR GROUP LEADER
MECHANICAL TECHNOLOGY (MILITARY)
ROLLS-ROYCE plc
PO BOX 3
FILTON
BRISTOL
BS12 7QE

G.J. IVES GROUP LEADER
MECHANICAL TECHNOLOGY (MILTARY)
ROLLS-ROYCE plc
PO BOX 3
FILTON
BRISTOL
BS12 7QE

SQUADRON LEADER P. JENKINS
UK MoD (PE)
ST GILES COURT
ST GILES HIGH STREET
LONDON

ABSTRACT

Test House methods used by the RAF for diagnosing causes of excessive vibration in Military Engines are based on a visual comparison of the test 'signatures' with those from built in fault tests. Interpretation depends largely on operator experience. A joint programme was launched in 1984 to develop a software based analyser to diagnose a range of mechanical abnormalities including unbalance, malalignment of bearings and shafts, and squeeze film bearing malfunctions. The analyser would handle a variety of engine types and would be suitable for inexperienced operators.

The ensuing programme between MOD and RR plc developed data acquisition and interpretive routines, and provided recorded engine signatures from both the RAF and Rolls-Royce plc test beds. Important aspects were the essential combination of intuitive operator experience, detailed strip and inspection of problem engines, and an engineering understanding from Rolls-Royce plc. The current intention is to install an Automatic Data Processing system by 1990/91.

This paper reviews the successes achieved and problems encountered.

1.0 INTRODUCTION

Current stress analysis techniques enable modern gas turbine engines to withstand steady state loads with a high degree of certainty and so in service problems due to this cause are rare. In contrast, engine vibration behaviour is less predictable and it is generally accepted by engine manufacturers and operators, both civil and military, that in a practical engine design a degree of vibration will always be present.

Acceptable vibration levels are specified by the manufacturer and adopted for ground acceptance testing and during flight. Such limits reduce possible fatigue failures of external dressings, particularly important oil or fuel pipes, and reduce discomfort to passengers and aircrew from noise. Other problems from vibration can include loosening of electrical and mechanical connections as well as a number of clipping, fretting and wear difficulties. Despite rigorous control of manufacture and assembly techniques, vibration problems can occasionally arise after first or subsequent builds prior to installation. Foreign object damage (FOD) to compressor rotor blades and other faults will also cause unwanted vibration in flight.

Limitation of the consequences of engine vibration is achieved by monitoring the vibration levels from suitably positioned external transducers. On RR plc test beds and the RAF's uninstalled engine test houses (UETH) a fixed vibration limit is displayed in velocity or displacement units and used to assess acceptability. On board systems also detect levels above the fixed limit, but in addition identifies sudden or gradual changes in vibration indicating potential problems.

When the limit is exceeded, the complex signal is analysed to display vibration characteristics at various engine rpm's from which a degree of visual diagnosis is possible. Vibration diagnostic methods in RAF UETH's examine out-of-balance (OOB) but current guidelines require considerable interpretive skills. Other more subtle causes of engine vibration currently receive limited attention and are not part of a formal diagnostic procedure.

By using modern signal analysis procedures the vibration transducer signal can now be examined in much greater detail than before. There follows the exciting capability to characterise an engines 'signature' more fully by identifying symptoms not previously detectable but which can greatly enhance diagnosis of rejected engines. It is this aspect that prompted the UK MOD(PE) and Rolls-Royce plc to investigate ways of using modern Automatic Data Processors (ADP) to improve their existing diagnostic techniques. The joint investigation would, at its conclusion, provide the basis for specifying a new generation of vibration analysis (VA) equipment for current and future aero engine vibration diagnosis in UK bases. Benefits are anticipated to be

An improvement in diagnostic efficiency

A reduction in unnecessary strip and rebuilds, and related uninstalled engine test house (UETH) acceptance testing time.

A consistent and uniform method of diagnosis which does not totally rely on operator expertise in the long term.

The study was one of a number of UK MoD funded development programmes aimed at improving aero engine health monitoring techniques see ref.1. It was seen in the context of a developing field in rotor

diagnostic technology within Rolls-Royce plc, current UK University research, and a number of sub-contract companies. This paper describes aspects studied relating to improvements in vibration health monitoring. It is appropriate to first outline the causes of vibration, the RAF's current maintenance policy and practice, in sections 2 and 3.

2.0 USING VIBRATION TO ASSESS MECHANICAL ACCEPTABILITY

For complete and effective engine vibration analysis, two problems must be addressed. The first and immediate concern is undoubtedly to find the cause of excessive vibration. The second problem is to find how to interpret the engine signature to detect mechanical faults which don't necessarily cause excessive vibration, but which cause distress and the risk of subsequent failures, eg in gearboxes, bearings, or oil restriction to bearings etc. These separate aspects are examined below. The reader should first refer to Fig.1 to become familiar with the modular type of construction in a typical two shaft aero engine.

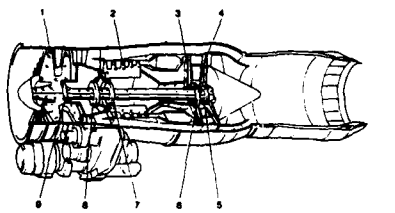

1. LP COMPRESSOR
2. HP COMPRESSOR
3. HP TURBINE
4. LP TURBINE
5. LP TURBINE BEARING
6. HP TURBINE BEARING
7. HP LOCATION BEARING
8. LP BEARING
9. LP LOCATION BEARING

FIG 1 TYPICAL TWO SHAFT AERO-ENGINE

2.1 Excessive Engine Vibration

The vibration signal is complex and contains energy components relating to structural natural frequencies, to forcing 'once per rev' signals from rotational forces at each rpm of the spools, LP or HP as appropriate and to forces at other frequencies. Fig.2 shows typical features extracted from the transducer signal and used for diagnosing the particular type of problem. Generally, the responses of 1st order NH or NL for example are related to the out of balance in the relevant rotor assembly and are the cause of most engine rejections. Such causes are from adverse tolerance build up at couplings, splines etc. during engine build or from FOD damage to blading during flight.

Typical vibration amplitude responses within the rpm range idle to maximum result from excessive OOB and are strongly influenced by the engine dynamic characteristics and as a result are engine type dependent.

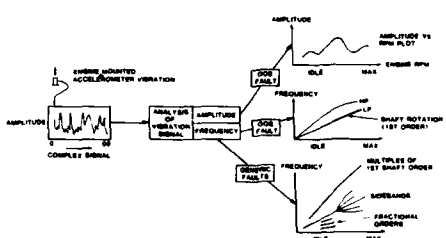

FIG 2 DIAGRAMMATIC ILLUSTRATION OF 'GENERIC' SYMPTOMS OUT OF BALANCE

2.2 Examples of using Vibration to detect faults

Symptoms of non linear vibration, eg harmonics and sidebands, can be detected from faults occasionally found in engines relating to malalignment of bearings and/or housings, eccentricities of bearing inner track locations, swash at thrust bearing location faces for example. Subsequent in service non linear faults include rotor to stator rubs, trapped oil in a rotor or squeeze film bearing malfunction (which could also be categorised as a 'build' cause). Most of these faults are not currently the cause of rejection since high amplitudes are not observed at the externally mounted vibration transducers. They are usually identified by frequency analysis alone and are 'generic' ie independent of engine type - see Fig 2. They give corroborative evidence to improve the range and confidence level when diagnosing high or unusual vibration characteristics. Such symptoms may also provide early warning of vibration problems after a period of operational use.

Gear meshing and accessory faults, are of course not related directly to engine vibration, but can be identified by examination of frequencies usually much higher than engine main shaft frequencies.

3.0 CURRENT RAF MAINTENANCE PRACTICE AND METHODS OF DIAGNOSIS

3.1 RAF Maintenance Policy

The RAF have adopted a policy of maintaining their engines themselves, rebuilding and testing at 2nd line bases, and having a deep strip facility of 3rd line bases. By so doing, turn round times are reduced to a minimum avoiding transportation to and from the contractors for overhaul. To make their task easier a modular engine construction was adopted to facilitate the replacement of life expired rotating components under a planned maintenance programme.

Fig.3 shows the maintenance cycle, identifying the requirement for vibration diagnosis and for deciding which module should be replaced to reduce vibration. Every engine is tested for vibration analysis (VA) and performance after each strip and rebuild. The limits of vibration, specified by Rolls-Royce plc for UETH and aircraft pass off, are included in a procedure written by the RAF's Central Servicing Development Establishment (CSDE) who are very active in areas of improving diagnostics.

3.2 Current RAF Vibration Analysis Techniques

Once an engine is confirmed as a reject in the UETH, a diagnostic check is carried out appropriate to engine type. Adour engines are tested at 12 set speeds for approx 2 mins at each speed. A manually adjusted frequency filter/analyser identifies the amplitudes at 1st LP and 1st HP shaft order. A 'broadband' level is also observed covering the ranges 30-400Hz approx. Each amplitude point is first tabulated and then plotted by hand to produce amplitude vs rpm plots between idle and max rpm's. The frequency analyser is the analogue 'Vibrometer' VM3C and typical results are shown together with the analyser in fig.4a. If any vibration level exceeds the relevant limit, the response characteristic is compared with those derived from tests having OOB deliberately applied to each of the main modules. A 'best fit' by eye gives guidance on identifying the offending module. There is no test bed display other than from the VM3C itself.

This system is under review and is expected to be changed with the introduction of a new ADP software driven system described later.

RB199 engines also require testing at set rpm's but analysis equipment is different, comprising digital analyser, the Spectral Dynamics SD340 to provide Fast Fourier Transforms of the broad band signal from the accelerometers. See fig.4b The engine is run at 5 set rpm's and at each rpm the frequency spectrum is plotted covering 0-500Hz. When the front transducer plots are completed, the whole process is repeated for the rear transducer.

The plotted spectra are examined to identify the source of vibration - whether it is from engine spool OOB or from an accessory, such as a fuel or hydraulic pump. Amplitudes are trended from previous test results where appropriate.

In general the RB199 engines do not have many vibration problems and those which do occasionally occur are easy to identify and in most cases, examination over 0-500Hz is confined to:-

checking LP order from the front transducer for LP compressor OOB, or

HP order from the rear for HP compressor or turbine OOB,

IP order is checked from either transducer for IP turbine OOB and

a constant frequency signal which on rare occasions has shown a bearing alignment or oil supply fault

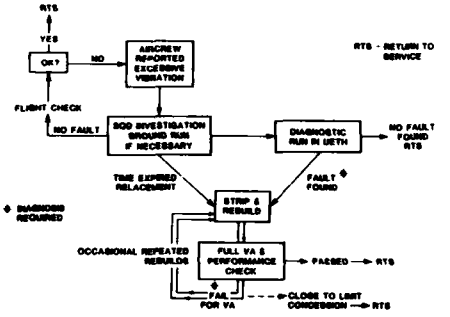

FIG 3 RAF MAINTENANCE CYCLE

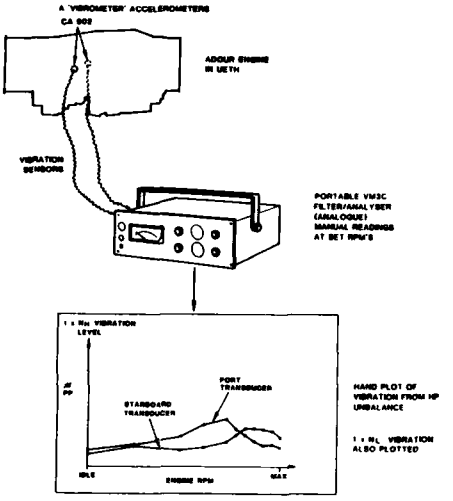

FIG 4a ADOUR UETH VIBRATION TESTING

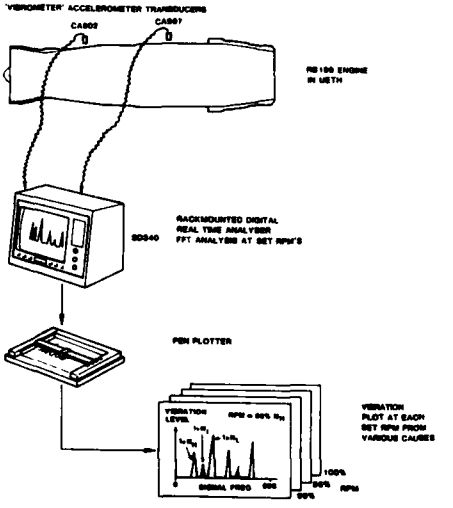

FIG 4b RB199 UETH VIBTATION TESTING

In addition spectral plots over 0-5000Hz are used to detect the margin for onset of unusual forms of compressor blade vibration at extreme operating conditions. Data for this is derived from an installed pressure transducer.

The RAF do not as yet have dedicated engine test houses for the vertical lift Pegasus engines but intend to acquire them in the future. All acceptance testing is done at RR plc for new and rebuilt engines. However the Pegasus is fitted with a comprehensive Engine Monitoring System (EMS) primarily for life usage counting, but includes vibration measurement and analysis and will be entering squadron service in the near future. The vibration signal is received by the EMS unit and analysed by 15 fixed band filters between 30 and 5000Hz to identify 1st engine order OOB and other causes of vibration.

By using fixed band frequencies the total spectrum is examined as the engine accelerates and decelerates. The amplitude in each band is plotted in a ground base station from down-loaded data from which visual diagnosis can be made by using a diagnostic chart relating frequency band, speed and fault.

This system combines a degree of frequency and amplitude analysis with a trending capability in flight. It is designed to identify airborne characteristics such as engine/aircraft touch points in high 'g' load conditions as well as engine related faults mentioned above. There is also a built in potential for detecting gear and bearing faults but an additional vibration transducer(s) may be required for this specialised analysis. Suitable VA procedures have yet to be defined for future RAF test beds.

3.3 Some Problems and Concerns of Current RAF Diagnostic Methods

The success of current methods relies largely on the experience and enthusiasm of key personnel, particularly for Adour engines. The mobility of service personnel requires that they are posted from time to time, when their knowledge is lost to the base. Although previous records are available, there will inevitably be a reduction is diagnostic efficiency for a while. There is also concern that Technician time is needed for manual plotting of test data which could be done automatically using more modern equipment.

Current methods are generally effective for single OOB faults but discrimination to modular level becomes increasingly difficult when more than one source is present eg at HP compressor and HP turbine. Some Adour engines can be almost impossible to diagnose correctly using existing practices even after several repeated strip and rebuilds. There is also concern that some engine faults, or accessory and gear damage symptoms remain undetected by current methods or by the use of standard fit transducers.

It is recognised that for a number of reasons, particularly that of maintaining equipment which is no longer supported by the suppliers, there is a need to replace some or all of the analysis and display equipment. There is concern here that future equipment should be common to all UETH's and engine types, and should have considerable development stretch potential and capable of obtaining signatures in flight as well as during *ground testing*.

There is clearly a need for a knowledge based ADP system which stores the collective experience and automatically fully processes data vibration characteristics.

4.0 SPECIFIC OBJECTIVES TO IMPROVE DIAGNOSTIC EFFICIENCY

To overcome these concerns, certain technical objectives were defined. Firstly, there needed to be an extension of the data base of the recorded engine signatures from installed (ground runs) and UETH acceptance tests. Secondly, the fault/symptom correlation was to be extended using in service experience from the RAF and RR plc, who would underpin their validity by analytical studies and rig testing. Thirdly, the development of common hardware and software techniques for a new ADP system should incorporate a 'knowledge based' system. The software should be very easy to use and capable of accepting new fault/symptoms as they become available from a number of sources. Easy transfer of data between operational stations was also a requirement.

Organisational objectives were to set up a direct line of communication between Rolls-Royce plc specialists and the RAF's front line. This involved the manufacturer more directly in diagnosing and inspecting suspect components at 3rd line maintenance bases to relate build abnormalities to unusual signatures - a very important aspect.

Finally a dialogue between Rolls-Royce and RAF advisors from the Central Servicing Development Establishment group was required on a number of important VA aspects including training and dealing with station queries on prototype software systems undergoing in service trials.

5.0 IMPROVEMENTS IN DIAGNOSTIC EFFICIENCY

This section briefly describes the various related areas to widen the knowledge base and the development of signal processing and software techniques for an ADP system.

5.1 Widening the Symptom Data Base

The RAF agreed to tape record signals from engines during a continuous acceleration and deceleration in UETH's and installed in aircraft to widen the existing data base. A special purpose kit was prepared at Rolls-Royce plc for Adour's in Hawk and Jaguar aircraft and RB199's in Tornado. Details of the recorded signatures are given in fig.5 which were returned to Rolls-Royce for full analysis and inclusion in the data bank. Rejected engine response characteristics were filed manually until subsequent rebuild and

test had confirmed or changed the original diagnosis. After a sufficient number of datum signatures had been obtained, recordings were made only from rejected engines. Examples of additions and improvements to the existing knowledge base included better discrimination of Adour HP compressor and turbine OOB by identifying differences in the 1st EO HP response between each of the two standard fit accelerometers (transducers) mounted either side of the intermediate casing.

Vibration related to the LP rotor was identified as looseness of a rotating anti-icing tube location band which increased LP order vibration rapidly at 100%NL rpm in engines having location wear at very high in-service lives. An example of a more complex fault was of particular benefit to the RAF after attempted diagnosis using their current 'compressor' OOB diagnostic graphs were repeatedly unsuccessful (over some 5 builds). By a close inspection of the signal characteristic at Rolls-Royce the suspect module - No 3 the intermediate casing - was identified and stripped out for detailed checks for OOB and geometric tolerance build up. The symptom was found to relate to a considerable couple imbalance. The characteristic included non linear vibration, notable the 1/2 orders indicating perhaps an overload of the HP shaft squeeze film - see fig.6.

ENGINE TYPE	NO OF ENGINE SIGNATURES	ADDITIONS TO KNOWLEDGE BASE	NUMBER OF REJECTED ENGINES	NUMBER OF REBUILDS
ADOUR FOR HAWK	17 UETH 10 INSTALLED	- HP COMPRESSOR - HP TURBINE	3	3
ADOUR FOR JAGUAR	36 UETH	- ANTI ICING TUBE LOOSENESS - HP STUBSHAFT OOB (MODULE 3)	4 FOR HP VIBN 1 FOR LP VIBN	6 2
RB199 TORNADO	13 UETH	HP TURBINE	1	1

UETH - UNINSTALLED ENGINE TEST HOUSE

FIG 5 RECORDINGS OF ENGINE VIBRATION SIGNATURES FROM RAF BASES

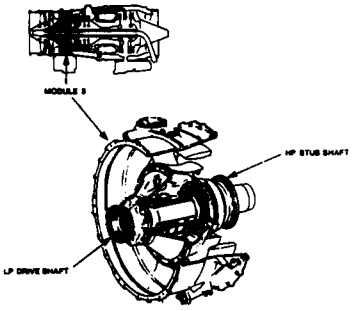

ADOUR MODULE 3 - INTERMEDIATE CASING

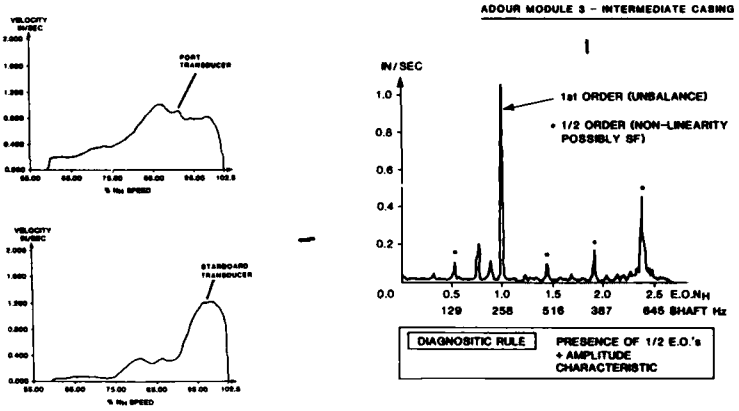

FIG 6 EXAMPLE OF IMPROVED FAULT CHARACTERISATION

The only RB199 engine 'fault' found during the period of signature recording was related to HP turbine OOB. This was shown as a vibration peak near 88%NH.

Engine testing at Rolls-Royce plc included built-in faults on Adour development engines to validate whole engine model predictions and to provide diagnostic symptoms. Testing included 'faults' within the HP compressor and turbine, LP compressor and turbine (singly and together, in and out of phase) and swash at a curvic coupling. It was completed in late 1987 and much analysis has yet to be done. An example of the use from the validation of an Adour finite element model is given later.

In the absence of specific LP compressor and turbine faults during recording at RAF bases the characteristics from Rolls-Royce's LP compressor and turbine OOB results have been used to update the set of standard fault characteristics used for vibration diagnosis.

To complement the OOB symptoms, a special purpose rig was built to identify symptoms of a 'generic' nature from misalignment and OOB combinations. Rolls-Royce defined the test programme, applying OOB, axial loads and misalignment conditions appropriate to military engines. Rig testing was carried out by Stewart Hughes Ltd on two and three bearing arrangements of a single shaft system having squeeze filmed roller and thrust bearings. Axial loading was applied for some tests. Characteristics seen from the initial results indicated that the use of a squeeze film bearing reduced resonant vibration amplitudes by a factor of 4 indicating satisfactory operation of the squeeze film and that small vertical misalignments within the squeeze film bearing clearance reduced the damping efficiency sufficiently to give symptoms of 1/2 order frequencies. Dynamic (eccentric) misalignment of the bearing inner track showed an amplitude reduction and phase change when the OOB and eccentric displacement forces were equal and out of phase.

This amplitude reduction has been noted in engines when assembled rotors are difficult to balance to the very low levels normally achieved.

An investigation into gear meshing faults began by analysing Rolls-Royce recordings for Pegasus accessory gearbox mounted transducers. Using a Stewart Hughes Ltd - analyser (described later) and their diagnostic software on recordings from several development engine gearboxes, a deep mesh characteristic was identified from a bevel gear as shown in fig.7a From this encouraging result, a special gearbox rig was commissioned to investigate the following potential build faults including:-

mesh depth of bevel drive gears,

swash of drive shaft.

Faults likely to occur in operation use were:-

half chipped tooth and surface damage to a single tooth,

damage to contact face of a single tooth,

oil starvation to the gearbox for 10 minutes

Methods of diagnosing gear faults are very different from those used for engine vibration. The identification of unacceptable levels of gear faults relies on trending either energy or pattern analysis and the user must use trending parameters which are related to specific known faults. Pattern analysis can also give 'one-shot' diagnosis for some faults and this was used by RR during these tests. Data from a particular gear shaft is derived from the accelerometer signal mounted on the outside of the gearbox by synchronous time averaging related to one rotation of that shaft.

Once a stable time averaged waveform has been derived, then the waveform characteristics are presented as figures of merit. These parameters can be related to specific faults and were used successfully to identify most of the 'built in' abnormalities in the rig tests. Gear analysis techniques and parameter definition are now well defined and a number of companies - see Fig.7b have this capability. This work related diagnostic parameters to known faults for Rolls-Royce gearboxes which can be used in a more comprehensive engine health diagnostic package, linked with engine vibration, in the future.

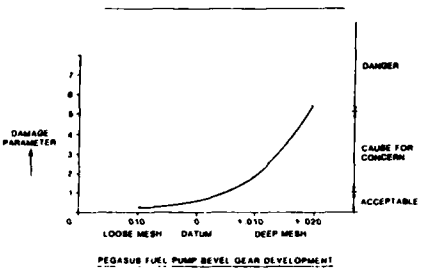

FIG 7a

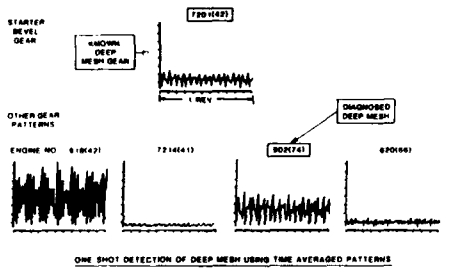

FIG 7b GEAR VIBRATION WITH VARYING MESH DEPTH

5.2 Exploratory Use Of Analytical Models For Understanding Vibration Symptoms

Work in this area has progressed at RR plc and UK Universities at Aberdeen and Southampton in recent years. Much more remains to be done before a rigorous physical understanding of non linear vibration characteristics can be claimed. It is the long term intention to provide a theoretical data base for rotor OOB for each engine type as well as non linear generic effects. Refer to reference 2 for related reading.

RR plc has finite element whole engine models for new and current in service engines, though their use is essentially for structural load analysis, particularly of newer engines. Dynamic analysis from OOB forces has been done to underpin the understanding of measured fault symptoms likely to cause engine rejections. Linear analysis can predict resonant frequencies of 2 or 3 spool engines with reasonable accuracy and good correlation is achieved with measurements. Predicted amplitudes are however strongly dependant upon damping within the (complex) structure. Application of OOB forces to the Adour low pressure rotor, identified mode shapes and corresponding resonant amplitudes peaks and rpm's - see fig.8. Mode B is found

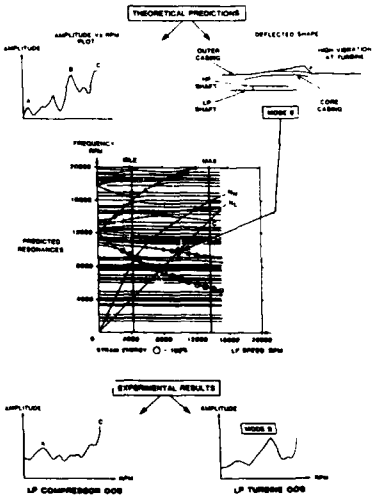

FIG 8 USE OF A FINITE ELEMENT WHOLE ENGINE MODEL TO ASSESS ADOUR VIBRATION SYMPTOMS

experimentally to be prominent when LP turbine imbalance is present, rather than compressor imbalance. This is more easily understood by reference to the mode shape in which the turbine casing exhibits significant movement in this mode.

Step changes in amplitude during an acceleration or deceleration which are attributed to the 'stiffening spring' effect of squeeze film under increasing deflection can also cause rejections. This bi-stable symptom has been observed on rigs and engines and is typical of non-linear systems. Such effects have been modelled with good agreement for a 2 shaft engine and an example is given in fig.9. The diagnostic value of the step characteristics is that they indicate a stiffening support characteristic implying that a squeeze film efficiency is less than adequate, especially if measured vibration levels are low. Occasionally a gradual change of amplitude at a fixed rpm is observed, the level reducing to a perhaps 1/4 of its original value over a few mins. Possible causes for such symptoms include:

changes in squeeze film clearance ($\propto$ to $1/\text{clearance}^3$).

changes in axial load on the bearing as a result of seal clearance changes, or

in rotor bend with temperature stabilisation.

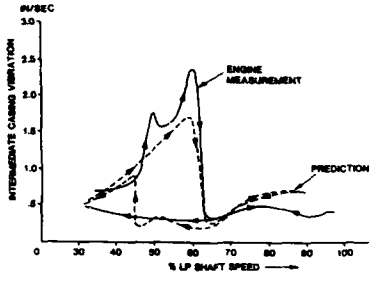

FIG 9 PREDICTED & MEASURED RESPONSES

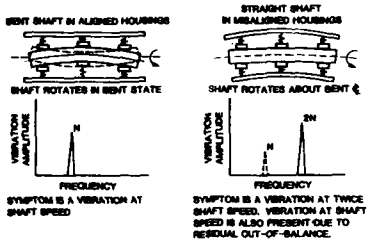

FIG 10 MISALIGNED SHAFTS AND HOUSINGS

Typical malalignments and associated 'generic' symptoms are shown in fig.10. The essential difference is between those which rotate about a 'bent' axis and those shafts which have a 'dog leg'. Measurements frequently show 2nd order and higher harmonics for malaligned systems. A possible mechanism for this symptom is the variation of rotational reactions at the bearing supports causing very small changes in amplitude of shaft orbits from which harmonics of shaft rotation will result. Lack of thrust bearing squareness has a similar effect.

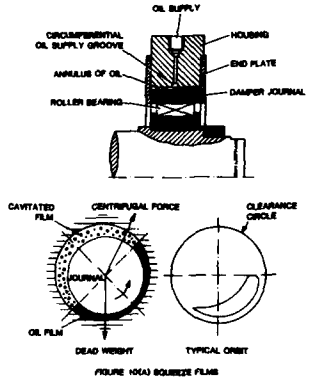

FIG 11a FEATURES OF A SQUEEZE FILM

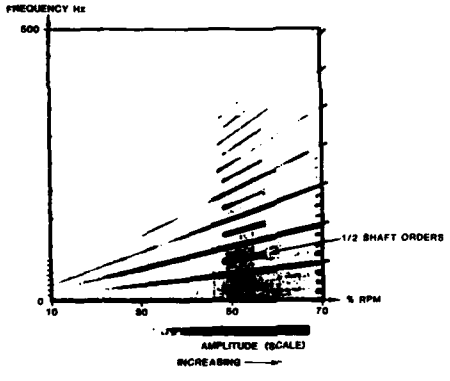

FIG 11b OIL FILM OVERLOADED IN BEARING

A typical squeeze film damper design for aero engine main bearings is shown in fig.11a. Its ability to reduce perceived vibration comes from hydrodynamic damping of shaft orbits but also by accommodating malalignment errors in 3 bearing assemblies. The benefit is well established after some 20 years experience in RR plc engines. However, vibration symptoms from incorrect operation have been observed when the oil feed or clearances are not as designed or have deteriorated. Once metal to metal contact occurs, frequency symptoms are noted at fractional orders or at fixed frequencies - as shown in Fig 11b.

Recent work at Aberdeen University has modelled the effect of a discontinuous bearing support housing and have predicted and verified *sidebands from 1st engine order starting at a resonant frequency*. These are shown in fig.12 with a similar result shown in a Pegasus engine. For further details refer to reference 3. Various simple mechanisms of partial and continuous rubs have been modelled by Rolls-Royce which identify complex orbit shapes. FFT transforms readily show various fractional orders, 1/3, 1/5 etc which are measured during rig or engine tests.

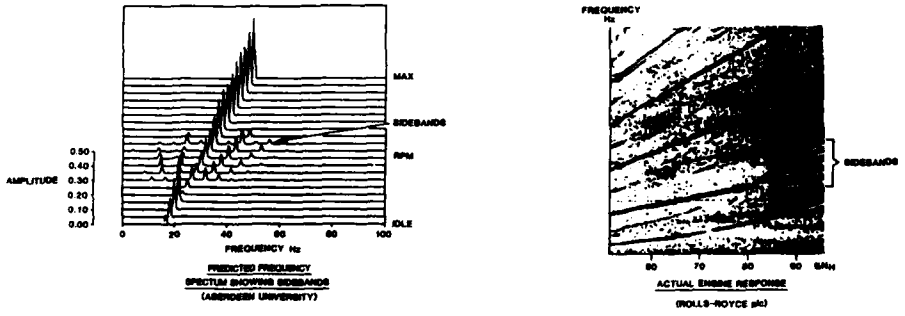

FIG 12 SYMPTON OF A NONLINEAR BEARING SUPPORT

5.3 Improvements to Signal Analysis and Diagnosis Using Pattern Matching Statistics

An off the shelf analyser, the 'Mechanical System Diagnostic Analyser' (MSDA), marketed by Stewart Hughes Ltd was supplied to Rolls-Royce by MOD PE for evaluation for engine vibration analysis. It is normally programmed for a choice of several vibration diagnostic applications eg gear and bearing problems in helicopter transmissions, rotor tracking errors, and monitoring cracking in power generating shafts, but had not previously been applied to aero gas turbine engine vibration diagnosis. It is illustrated in fig.13a. See also reference 4 for further reading. The engine input signals required are the standard fitment vibration transducer(s) - 2 in most cases - and the LP and HP shaft rpm's.

The executive programme was written by Rolls-Royce plc personnel for the specific exercise described in this paper. It started data collection at ground idle rpm, and instructed data sampling from a variable frequency range covering 4 x shaft rpm. A slow acceleration to max rpm and deceleration back to idle was adopted, being the traditional Rolls-Royce test method for a vibration survey. The MSDA was programmed to continuously measure rpm and automatically plot a 100 point graph of 1st order amplitude variation against (vs) rpm. Originally the MSDA's computer controlled band-pass filters tracked the spool frequencies but this method required more than one slow acceleration to acquire data and only displayed amplitude information at once per rev frequencies. There were also problems in discriminating between close once per rev frequencies such as the Adour which has 1st order NH and NL separated by only 30Hz at max engine rpm. This early system, though, gave a much improved definition of amplitude vs rpm variation *compared with* the RAF's 12 point hand plot.

It was decided to abandon the tracking filter approach and instead to acquire and store Fast Fourier Transform Data for the following reasons:-

to provide better frequency determination,

to shorten data acquisition time to one slow accel (1.5 mins) and decel, and to

to enable examination of a wider frequency spectrum, for a fuller diagnosis of the signature.

The framework of the programme remained the same, but now the sampled measurement points were Fourier transformed and stored on disc - each transform being tagged with the shaft rpm.

After data collection the spool frequencies were tracked through the stored data and amplitude vs rpm responses at INL or NH, or broadband 30-300Hz is plotted on the MSDA's printer plotter. The diagnostic

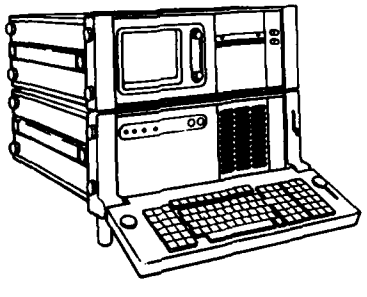

FIG 13a

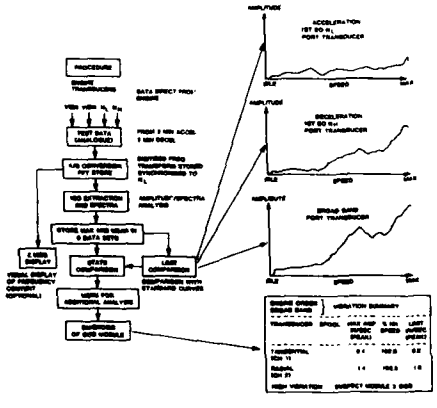

FIG 13b MSDA DIAGNOSIS

stages for checking limit exceedence and fault finding together with an example of the output is shown in Fig 13b. Detection of the unbalanced module was by 'Pattern Matching' the test engine characteristics with pre determined amplitude vs rpm plots from RAF and Rolls-Royce experience. A statistical technique using one way analysis of variance of the sum of squares difference gave degrees of certainty from which the most probable fault was defined.

There are various ways of presenting amplitude, frequency and engine rpm (on time) information in two dimensions. The reader may be familiar with 'waterfall' plots which superimpose individual frequency spectra (amplitude vs frequency) to give a perspective view of time. In this way amplitude and frequency variation can be seen together as engine rpm changes, an example is shown in fig 12. The method favoured by Rolls-Royce plc is to plot the spectra sequentially on frequency and rpm axis, modulating the amplitude with colour in the third or Z axis. This type of presentation is known as the Z Modulation or (Z Mod) plot and is a very valuable tool for engineering interpretation of unusual symptoms see also fig 12. Amplitudes are plotted on a log scale to improve detection of relatively low levels which are not otherwise easily observed.

At this stage of the study, the MSDA provided essentially an automatic analysis and diagnostic system which emulated the current procedures used by the RAF. Two major benefits were shown, firstly that of having an automatic system to analyse, diagnose, and display data in a matter of minutes. Secondly there was potential for a large reduction in the vibration test, say by a factor of 7. The next major step was to increase the flexibility and ease of improving and updating the range of diagnostic symptoms particularly those of showing 'generic' faults. This is discussed in the next section.

5.4 Development of a Systematic Knowledged Based Diagnostic Method

Symptoms for non linearity offered additional diagnostic information to the existing knowledge base of OOB resonant responses. (The capability to extract the information automatically is currently being developed under a separate ALVEY funded programme). A revised diagnostic tree to include these symptoms is shown in fig.14 based on 'if/then' rules widely used by engineers in fault diagnosis. Like all diagnostic systems, the prototype ADP system addressed the following points:

1) was the acquired data valid, and was there a limit exceedence?

2) was OOB easily diagnosed (by response pattern recognition)?

3) was non linear vibration characteristic evident eg squeeze film malfunction?

4) what diagnostic statement can be given for maintenance action?

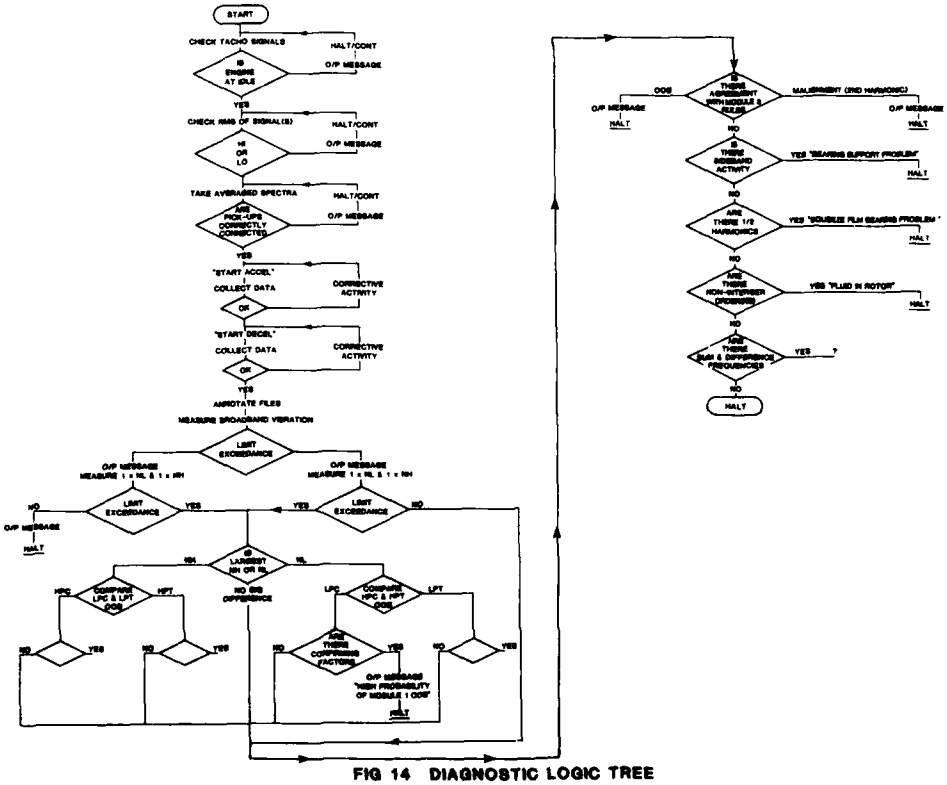

FIG 14 DIAGNOSTIC LOGIC TREE

Initial use of the MSDA described in the previous section gave good results for simple OOB faults and was generally as successful as the diagnosis of OOB by RAF technicians. Non linear responses were first investigated at Rolls-Royce by visual examination of the Z mod plots and applying Engineering judgement. However, addition of new symptoms to the MSDA Fortran menu proved to be labour intensive, and the initial software was not sufficiently user friendly for use in the field. To improve the ability to input new interpretive data and to reduce time spent in changing software it was decided to take away the decision process from the MSDA. A separate knowledge base was achieved by adding an IBM Personal Computer with LISP software to communicate with the MSDA Fortran menu, leaving the MSDA as a data base and analyser.

Diagnosis started by instructing the MSDA to extract 1st order NH or NL amplitudes from FFT files of an engine acceleration/deceleration and to plot the 1st engine order amplitudes vs rpm as before. A series of rules were then invoked by the control programme , the extent and order depending on results of the previous operation. By using a separate knowledge base, it was relatively easy to add a new characterised fault after only a half hours programming time.

6.0 PROBLEMS REVEALED DURING THE STUDY

6.1 Engineering Technical Problems

The importance of engine mounting support flexibility was demonstrated by looking at differences between uninstalled and aircraft installed characteristics. This underpinned the need to have a knowledge base appropriate to the engine and support structure combination. For future diagnosis in installed situations a different rule base would be required from that normally used in UETH's.

Amplitude vs rpm response plots published by the RAF's CSDE in 1982 were generated from the Jaguar version of the Adour and applied to both Jaguar and Hawk versions. The main differences are in the addition of a reheat system and an axial spring to preload the LP thrust bearing. Differences in engine responses have subsequently been identified by finite element models and measurement. Separate definition of response plots for each engine could improve diagnosis of some OOB characteristics.

The diagnosis of vibration above the acceptance limit using pattern matching techniques was not adequate for engines having more than one unbalanced module, or where severe non linear vibration was present.

Current RAF guidelines were based on the best fault/symptom data available when published, but new symptoms have recently become available which should expand their interpretive skills.

6.2 Hardware and Software Problems

First hand experience of RAF technicians using prototype ADP systems at the front line emphasised the importance of adequate training and having extremely friendly software. Difficulty was found in using the prototype ADP system despite having extensive descriptive and operational manuals - this is further discussed in section 6.3.

The combination of the MSDA and IBM PC was adopted to enable the use of "expert" software which could not be implemented in the MSDA. An anticipated by product of using LISP is that it has 'garbage collections' which are outside the programmers control. The occurrence of one of these collections during an MSDA/PC data transfer caused the program to abort. Future alternatives would be either not to use LISP or have only one data transfer.

The type of transducer and the signal indicating shaft rpm is different on each engine in service. Some give low frequency (70Hz maximum) and others have high frequency (60 pulses/rev). Whilst suitable for normal engine control for which they are intended, there was often sufficient 'jitter' in the signal to make synchronous processing of the accelerometer signal difficult and extensive speed signal conditioning was required. The use of a once/rev pulse from new engines is essential to avoid the need for such equipment on future software based systems.

6.3 THE HUMAN FACTORS

Initial ideas for an ADP centred around a closed system to which the operator fed in rpm and vibration signals, and from which a diagnosis appeared after comprehensive examination of all possible solutions. However, given the incomplete data base of characterised defects, and the need for involvement of the RAF UETH personnel, it was decided to give much more visibility of the reasoning behind the diagnosis to improve confidence in the outcome.

It is vitally important that the engineering philosophy of the user is fully understood and that the system is introduced in a sympathetic manner. Typically, the Chief Technician in charge of a UETH will have over 15 years service. He will not necessarily be familiar in detail with computers especially as in his basic trade, ie propulsion, he will have had relatively little exposure to microprocessor driven equipment. The scene is set, therefore, for a potential rejection when for the first time the computer based analysis is seen, or perceived, to fail. It is often at this point that a technician, who feels threatened by the equipment, or jealous that his position as the best diagnostician is being undermined, will begin the process of denigration of the equipment. Once such a process starts, it is very difficult to halt and reverse it. The lesson, therefore, must be to present the strengths and weaknesses of the new technology and to give users a practical way in which their considerable diagnostics skills can be used to improve the automatic system. It is important to be frank about the weaknesses of the system and to educate the user in the reason for the shortcomings so that when a failure occurs it is greeted with constructive comments to improve it. How then does one go about this task?

Firstly, one must explain in simple terms the philosophy being employed in the software analysis. Here good 'user friendly' software is a must, but the extent of a prior specification of the software was underestimated. As a result we tried and failed, to use fairly unfriendly software with a comprehensive user guide. The problem with this approach is the expense both in terms of preparing the explanation and in terms of stopping work to release technicians to assimilate it. However, unless this phase is covered, subsequent feedback will be disappointing.

Secondly, one should point out how the user can help in overcoming the weaknesses. New users will always see far more variety in degrees of defect as well as, inevitably, finding all the 'new' ones. They should be encouraged to examine data, insofar as they are able to, and to give the manufacturer as much background information as possible. Allied to this is the essential requirement to store the data on analysis failures so that it can be passed back for more detailed analysis and the introduction of new diagnostic rules.

Thirdly, good staff work at all levels is particularly important during the period of establishing a new knowledge base or improving an existing one. Once a problem is identified it is essential to provide feedback quickly so that the originator can see the fruits of his labour. It was of tremendous assistance to have direct link between the front line and Rolls-Royce, this reduced the time taken to process enquiries and enabled supplementary information to be speedily elicited. It is intended to continue this dialogue on current in service engines to encourage technicians to participate in widening existing knowledge bases in ADP systems as a forerunner to widening the limited knowledge base necessarily supplied with new engines.

Fourthly, it should be made quite plain that there is currently no computer learning (normally called artificial intelligence) involved in the analysis and that the diagnostic rules are based on the detailed *analysis of vibration signatures from engines with particular defects.* To that extent, it is no different from a technician. Most importantly, however, unlike the (human) technician who can be prone to 'jumping to the wrong conclusion', the automatic system is immune to pressure and always follows a thorough and logical fault diagnosis. Equally, though the automatic system cannot exhibit 'flashes of brilliance'.

Finally, and of equal importance to the prime task, the automatic system can be used to teach or pass on diagnostic techniques to counter the effects of personnel movements. In the past, diagnostic success decreased on the posting of the 'ace of the base' until his replacement became equally experienced when the whole cycle repeated itself! This aspect should be virtually a thing of the past with this new concept.

Military systems should provide a degree of redundancy to cater for system damage or denial during operations. By always describing the diagnostic route followed, this system will train users in its methods so that when faced with a temporary loss of the automatic analysis facility the human technician could still diagnose the majority of defects on an engine, albeit that it could take longer.

In summary then, it is not sufficient to just develop an improved, more reliable analysis system. One must also consider how to present it to the user without antagonising him. One should aim to present the system as a facility which will assist the user in discharging his task but one which does require his input in order to maximise its potential.

7.0 FOR THE FUTURE

By demonstrating the advantages of ADP systems using prototype technology described earlier and by involving Air Force technicians in evaluation of this new approach, an understanding and acceptance of software based VA equipment has emerged. The philosophy of diagnosis will of course continue to be based on established engineering principles and improved as new understanding evolves. New software based systems have the potential for cutting out tedious routine tasks, providing a means of communicating diagnostic experience to other RAF stations by simple means of transferring software data. It will encourage a new emphasis on increasing the knowledge base of engine vibration symptoms using Service experience and knowledge, with assistance from Rolls-Royce engineers where appropriate when better diagnosis is required.

MOD (PE) intend to place contracts in 1988 for manufacture of new equipment and for Rolls-Royce to develop the diagnostic software for Air Force use.

Towards the conclusion of the study a total processing philosophy for aero engine vibration emerged for use by the RAF or any other Air Force see fig 15. It used a systematic approach by having a common

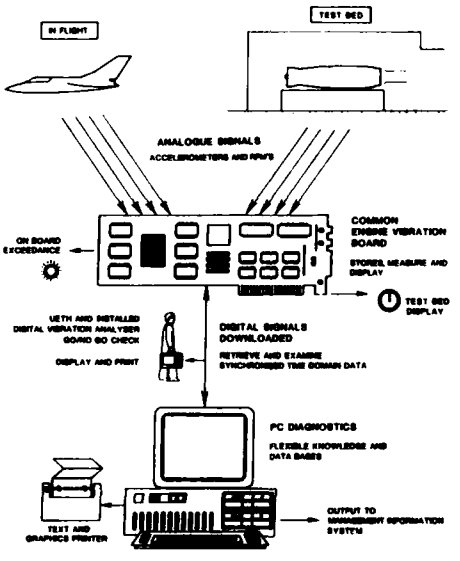

FIG 15 VIBRATION MEASUREMENT AND DIAGNOSTICS FUTURE BASIS OF ADP SYSTEMS

diagnostic logic with separate and updatable knowledge bases and had the ability to acquire and store synchronised time histories and to process and display data simultaneously to meet 1st and 2nd line need for initial acceptance/rejection of engines. A separate diagnostic 'off the shelf' Personal Computer, using RR software, would diagnose the faults and to recommend action for the rejected engines. Its main benefit is the potential to provide continuity of diagnostic efficiency when key personnel are posted elsewhere, will enable individual specialised training packages, to be run on the diagnostic PC.

The ADP system conceived will offer the new opportunity to adapt a standardised software system for acquisition, storage and display facilities which can function equally well in test beds or as part of an on board health monitoring computer. As a manufacturer Rolls-Royce in the long term intends to take advantage of this new technology and prepare diagnostic software during the development phases of new or improved engines. By so doing, engines will be made available to customers for the first time with a diagnostic capability at entry into service. As far as the RAF is concerned, they will have a system in place to use it.

8.0 INTEGRATION OF ENGINE VIBRATION DIAGNOSIS INTO INFORMATION MANAGEMENT SYSTEMS

The RAF use a Rolls-Royce engine performance diagnostic 'package' and is developing suitable methods of diagnosing gear faults in helicopter transmission systems as well as for main rotor tracking errors. Sub-contractors involved are Stewart Hughes Ltd and Smiths Industries. There are also well established trim balancing systems for high bypass ratio fan engines.

It is intended that in the future Engine Information Management Systems will combine performance with more detailed mechanical condition information for acceptance testing or a combined gear, rotor tracking and engine vibration for helicopter maintenance. On board vibration monitoring systems for Rolls-Royce military engines are increasing the ability to detect and diagnose in-flight vibration problems which can be very different from those found from acceptance testing. Pegasus/GR5 in flight vibration data retrieved from the EMS system in digital form (section 3.2.3) will be processed by the Harrier Information Management System (HIMS) for which a display facility is being developed. Rolls-Royce has identified a diagnostic rule base in the form of a chart based on accumulated engine development experience. As in-flight vibration problems arise, this will be updated.

One can see then a gradual progression in VA from basic test bed diagnostic aids, to an on board digital processing system with diagnosis for the Pegasus/GR5, through to a totally software based ADP system, providing complex diagnostics within a full Information Management system towards the late 1990's.

CONCLUSIONS

The considerable advances made in vibration analysis and diagnosis of engines used by the RAF has, without doubt, been achieved only because of the close liaison and involvement of the manufacturers with the users at the front line. Both the understanding of complex modern aero engine dynamics and the acceptance of automatic data processors by experienced diagnosticians demands this approach for a successful conclusion. It must be said that current engines operated by the RAF do not have major vibration concerns, but in the human world we live problems do arise from time to time. Future use of the ADP system will assist the RAF in containing new in-service vibration problems with even greater efficiency.

REFERENCES

1) C M O'Connor
Rolls-Royce plc
Military Engine
Condition Monitoring - the UK Experience
AGARD PEP 71st SYMPOSIUM

2) J B Wynne
Advances in Aero Engine Dynamics
AIAA/ASME/SAE/ASEE
22nd Joint Propulsion Conference

3) Aberdeen
Nielson R D. Barr ADS
Spectral Features of the Response of a Rigid Rotor
Mounted on Discontinuously Non-linear Supports
Proceedings 7th World Congress Theory of
Machines and Mechanisms 17-22 Sept 1987
Seville Spain, Pages 1799 to 1803 Vol.3

3) R M Stewart Stewart Hughes Ltd
Application of Signal Processing
Techniques to Machine Health Monitoring
Source: Noise & Vibration (Book) by
R G White and J G Walker
Published by ELLIS HORWOOD 1982

ACKNOWLEDGEMENTS

This work has been carried out with the support of the Ministry of Defence Procurement Executive.

Opinions of the authors are not necessarily those of Rolls-Royce, the UK MOD or the RAF.

The authors wish to express appreciation to Dr E K Armstrong who recently retired from Rolls-Royce plc and to colleagues and associates who have contributed directly or indirectly to this study.

DISCUSSION

G. KRISHNAPPA

Did you try to determine degradation in the performance of the aerodynamic components using vibration analysis?

Author's Reply:

We never use the vibration analysis as a diagnostic tool for the compressor or fan efficiencies. But in development one can relate some engine vibration levels to the aerodynamic disturbances as approaching surge.

J. HOUILLON

Quelle est la corrélation entre les défauts constatés par diagnostic et ceux réellement constatés par le réparateur? Pouvez-vous donner le pourcentage de réussite rencontré dans la R.A.F. et plus particulièrement sur un moteur technologiquement très complexe tel que le moteur à trois axes RB 211.

Author's Reply:

I show you the slide (fig 5 of my paper) where I indicate the number of signatures taken, and the success rate of these analysies.
Even if the RB211 is a three spool engine, it does not suffer much vibration problems. As shown on fig 5, on 13 tests there was one rejected engine which was indeed due to a HP turbine blade.

H. AHRENDT

1. Do you derive your spectrum information from one specific engine running point or does it cover the whole speed range?
2. Did you derive your information about malfunctions of internal components (i.e. oil squeeze bearings) by external mounted pick-ups?
3. Can you relate malfunction signature of a specific engine-aircraft configuration to a different one as a new engine on a new aircraft?

Author's Reply:

1. The spectrum looks over the whole speed range, idle to maximum, and is derived through a continuous acceleration taking 1 to 1½ min.
2. We can derive them from external pick-ups but it is not the best method. A very good way is to monitor the oil pressure in the supply line of the bearing.
3. The out of balance excited responses generate specific bands of vibration which vary with the engine type, because they are related to the design and dynamic characteristics of that structure. The combination of engine and airframe or engine and test bed produce these unique characteristics.

FAULT MANAGEMENT IN AIRCRAFT POWER PLANT CONTROLS

S. Mazareanu, A. Nobre
Pratt & Whitney Canada Inc
Box 10
Longueuil
Quebec
J4K 4X9

INTRODUCTION

The advent of Digital Electronics in aviation nas opened new doors to fault management as a tool to enhance aircraft operability and safety of flight. Today it is possible to integrate flight control systems with power plant management systems. Operability of a battle damaged aircraft can be enhanced under certain conditions through sophisticated fault management systems.

This paper reviews some of the considerations applicable to engine control fault management systems in commercial aviation. Engine control systems have evolved inthe last decade from being primarily hydromechanical to being primarily electronics. This rapid growth in acceptance of the electronic systems by the aviation industry was due to the improvement in reliability of the digital systemsover analogue systems, which were previously in use.

The fault management system is a powerful tool to organize and optimize the maintenance logistics. Operating costs can be significantly reduced with an appropriate fault management system on board.

The paper presents:

- A Brief Review of the Evolution of Engine Controls.
- The Emergence of Fault Management Systems (as part of Engine Control Systems)
- Maturity of Fault Management Systems (Still in Evolution).
- Future Potential.

EVOLUTIVE PROCESS

The fault management in hydro-mechanical controls is simple in concept and difficult in implementation compared to its counterpart microprocessor based digital electronics with their massive memory and computing capability.

The perceived high reliability of the mechanical components drove some engineers to design their control systems without back-up or independent protections and accepting an engine out (or a loss in power) in the case of an engine control failure.

Hydro-mechanical controls have a major handicap, they do not detect failures. Due to this, the concept was to surround the control system with autonomous devices that will prevent critical parameters from being exceeded (example: overspeed protection). Also, these control systems are unable of deciding if they still are in condition to control the engine. If a back-up control exists the system relies on the pilot to diagnose the failure and transfer to the back up control.

The engine control industry could not stay indifferent to the "invasion" of electronics. Analog circuits started to be used in instrumentation and ancillary functions. As engineers became satisfied with the reliability of these electrical components they started to expand their utilization to the main control. As a result, analog controllers started to be used as supervisory units with limited authority or as protective systems and later stepped up to full authority control, with its pinnacle on the"Concorde" Twin channel application. These systems having limited fault detection restricted to checks on voltage thresholds and still rely heavily on pilot detection and action.

The last decade has witnessed a giant leap forward in control concepts. Making use of the digital technology and microprocessors, the control laws became more elaborate and the fault detection, isolation and accommodation, which constitutes the fault management was called to play a major role.

Fault detection on todays Full Authority Digital Electronic Controls (FADEC) is extensive. Levels of fault coverage range from 80 to 100%. Levels on the high 90 are possible with internal checks. However, fault coverage of the remaining (up to 100%) can not be achieved internally. The most common configuration to achieve this level is the voting agreement between two out of three control channels to isolate the faulty controller.

The microprocessor based digital control system gives to the engineer extensive power with which to configure the control system to optimize fault management. Controls that use internal checks as a mean of fault detection have two possible philosophies when it comes to fault accommodation. One of the philosophies advocates that cross talk between the channels should be reduced to its minimum and that when a fault is detected the channel in control should give up control, transferring the control to an identical second channel. The other approach defends that the channel in control should remain in control for as long as it can before transferring to a second channel. To sustain control after a fault, the channel in control has to borrow parameter inputs from the second channel (if it lost its own).

This second approach increases substantially the cross talk between channels and the complexity of the software.

AIRFRAME INTEGRATION

There has always been a degree of integration of the power plant control with the airframe. Its complexity, as expected rises with the number of engines. On single engine aircraft the interaction is limited to the aircraft and the engine control. However in the case of a multi-engine application interactions exist between the engine and the airframe as well as between engines.

The functions that have a degree of interaction between two (or more) engines need to be restricted to a very limited authority such that a failure on one engine does not have detrimental effects on the other engine(s). Typical examples are syncrophasing (on Turboprops), Torque matching (Helicopters), etc.

Mechanical controls often have a reduced number of parameters interacting with the airframe. Usually, these parameters are confined to control requirements and minimal if any are dedicated to fault annunciation. Mostly, fault analysis relies on the pilot report and subsequent interpretation of it by the maintenance crew and available troubleshooting charts.

Microprocessor based digital controls have demonstrated their potential for fault management and for information transfer to the maintenance crew. The transfer of information between the control and the maintenance crew can be done in many different ways. They start with simple interrogation devices which are connectable to the Engine Electronic Control (EEC) unit allowing the crew to read the memory locations where the fault identification is stored. In the more sophisticated applications the EECs are linked with the aircraft EICAS-Engine Indication and Crew Alerting System and/or a Central Maintenance Computer (CMC). Using a serial data bus the fault information is downloaded to these aircraft computers. The maintenance or flight crew can then interrogate the CMC with the faults being displayed in plain language through multi-function displays.

In recent years there has been increasing demand for the implementation of systems that are able to detect and identify failures not only internal to the EEC but also external. External failure can be detected to the level of Line Replacement Units (LRU) associated with the EEC (i.e. input sensors and output effectors) as well as other power plant LRU's.

Potentially, a well designed fault management system improves not only the maintainability of the control system but also reduces pilot workload and extends the life of the engine. With FADEC controls it is becoming common place to configure systems which enable aircraft take offs with the engines producing 90% of the maximum takeoff power capability. In the case of a detected power plant failure the remaining engine is automatically commanded by its EEC to raise its power to 100%. This take off configuration extends substantially the life of the engines but it requires a health status of the opposite engine to be acknowledged by the local engine control. Failures that are immediately identified and automatically accommodated result in a significant reduction in pilot workload compared to that required in fault handling using hydro-mechanical controls.

CERTIFICATION REQUIREMENTS

For all practical purposes the various civil certification regulations are not significantly different with respect to power plant controls.

As an example the certification requirements imposed on an Engine Control System are part of the following FAA regulations:

FAR 33
FAR 25
FAR 27
FAR 29
TSO C77a

If integration of the propeller and engine control is considered then FAR 35 requirements have to be considered.

The purpose of this section is not to give a detailed description of certification requirements and procedures but to highlight what is considered to be the main impact of certification requirements on the hardware and software Fault Management Configuration.

For the purposes of this discussion we will consider FAR 33 that addresses the engine certification as such and FAR 25 that addresses a transport category airframe certification. An Engine Control System that complies with these requirements is basically certifiable to FAR 27 and 29 for helicopters or TSO C77a for APU's.

Given the trend towards greater integration of airframe systems the airframe certification has an impact on the Engine Control System configuration.

The advent of such functions like engine-to-engine synchronization, Automatic Takeoff Thrust Control System (ATTCS), Autofeather etc increases the complexity of the Engine Control System and their certifiability is one of the important drivers for the hardware and software configuration.

Some typical requirements that are specified for a twin engine commercial aircraft Engine Control System are:

a) Unprotected overspeed (O/S) of the engines rotors must be extremely improbable (<1 failure per 10^9 hours).

b) Dual engine in flight shutdown (IFSD) must be extremely improbable (<1 failure per 10^9 hours).

c) Single engine IFSD shall be improbable (<1 failure per 10^5 hours).

d) Loss of thrust of one engine in the takeoff phase and failure to uptrim the other engine must be extremely improbable (<1 failure per 10^9 hours).

e) Complete inability to shut the engine down must be extremely remote (<1 failure per 10^7 hours).

f) Faults in either the Engine Control System or the Airframe Instrumentation System resulting in hazardous operation of the other system must be extremely remote (<1 failure per 10^7 hours).

If the Engine Control System also includes an integrated propeller control, the additional set of requirements that are typically specified are:

a) Unprotected overspeed of the propeller must be extremely improbable (<1 failure per 10^9 hours).

b) Unwanted travel of the propeller blade pitch to a position below the normal flight low pitch stop must be extremely improbable (<1 failure per 10^9 hours).

c) Unwanted travel of the propeller blade pitch to a position higher than the maximum angle of attach causing blade stalling must be improbable (<1 failure per 10^5 hours - similar to single engine IFSD).

d) Complete inability to feather the propeller blades must be improbable (<1 failure per 10^5 hours).

OPERATIONAL REQUIREMENTS

Typical operational requirements specified for a commercial aircraft Engine Control System are:

a) Probability of the inability to dispatch <1 failure per 10^4 hours.

b) Built-in-Test-Equipment (BITE) functional test capability in the maintenance mode to test more than 95% of the system's components/LRUs.

c) Scheduled maintenance for possible dormant faults at time intervals greater than 500 hrs.

FAULT MANAGEMENT CONFIGURATION

To meet the Safety and Certification requirements and the operational requirements both aspects of the configuration hardware and software are equally important and in many cases trade offs between them can be made.

The Fault Management Configuration discussion will center on a FADEC System since these systems have become more common.

FADEC is a system where the processor based digital electronics have full authority on the effectors (without mechanical constraints), therefore being able to drive the engine from low to maximum limits.

A typical FADEC system comprises the following (see also figure 1):

- Input sensors (engine parameters and feedbacks).
- Engine Electronic Control (EEC) unit with input interfaces, processing hardware and output drivers.
- Effectors

The Engine Electronic Control (EEC) unit processes all the signals from various engine and airframe sensors and controls a fuel flow motor in the Hydromechanical Unit (HMU), one or two variable geometry motors and various solenoids and relays. Modern FADEC Systems are Fly-By-Wire (FBW) systems where all signal acquisition (including the pilot command signals) and effectors control are done through electrical links.

HARDWARE CONFIGURATION RESULTING FROM CERTIFICATION REQUIREMENTS

The hydromechanical part of a FADEC system can be substantially simplified because all the computations, altitude, temperature compensations etc are implemented in Software based algorithms and tables.

The simplicity of the hydromechanical part makes it very reliable with an IFSD rate of typically 3 to 4 x 10^{-6}/hr.

This allows for an IFSD rate of 6 to 7 x 10^{-6}/hr for the electrical part of the system to achieve the single IFSD Certification requirement.

The failure rate of the electrical/electronic part of a FADEC channel generally falls in the 150 x 10^{-6}/hr range. For 70% of this failure rate i.e. 100 x 10^{-6}/hr (CPU, drivers, effectors etc), there is no possible accommodation within the channel.

This points to a major configuration impact: with today's electronics reliability, a FADEC system has to have at least a dual independent channel configuration for its electrical/electronics part (See Fig. 2). In fact, a dual channel FADEC system has a significantly lower IFSD rate than a complex hydromechanical system.

If it is assumed that all faults are detected, the IFSD rate of such a system will be:

$$\lambda_{\text{IFSD}}^{\text{Hydromechanics}} + \lambda_{\text{IFSD}}^{\text{Electronics}\,2} = 4 \times 10^{-6} + (100 \times 10^{-6})^2$$

$$= 4 \times 10^{-6} + 1 \times 10^{-8} = 4 \times 10^{-6}/\text{Hr}.$$

The dual channel configuration means that there has to be no common mode failures between the two channels including:

a) Common Signal Sources

b) Common Processing Hardware

c) Power Supply

d) Lightning and Electromagnetic Interference

e) Software

The dual IFSD requirement of 1×10^{-9}/hr results in the same common mode failure requirements applied to the two Engines Control Systems.

To comply with the unprotected O/S or other protection requirements of 1×10^{-9}/hr, independent protections are considered mandatory.

The above common mode failure requirements apply again this time between the control channel and the independent protection.

These considerations point to the following optimized FADEC hardware configuration (See Fig. 1):

- Two well isolated FADEC electrical channels, each with its own power supply, CPU, sensors, interfaces and drivers.
- Dedicated electrical generator for each engine Control System/Dual winding, one winding for each channel.
- Independent protection hardware for each control channel with its own internal power supply, sensors, computational core and effectors.

The airframe power supply can be used as a back-up of the dedicated generator providing it does not become a source or path for transmitting common mode faults from engine to engine (on line when the dedicated generator is out of operation).

If a functional link between the two engines is necessary (ATTCS, Synchronization) this has to be implemented in hardware such that no engine-to-engine common mode failure is possible (for instance local engine EEC reads directly from dedicated sensors the remote engine parameters).

To comply with the engine shutdown requirement, two independent shutdown means have to be provided.

To comply with the requirement for segregation between the Engine Control System and the Instrumentation System, the two systems have to be independent to the extent that failures in one of them will not result in hazardous effects in the other one.

HARDWARE CONFIGURATION RESULTING FROM OPERATIONAL REQUIREMENTS

A dual channel FADEC System has typically the following reliability for the functions that make the system non dispatchable:

$$\lambda \text{ Hydromechanics} < 40 \times 10^{-6}/\text{Hr}$$

$$\lambda \begin{matrix}\text{Electrical} \\ \text{One Channel}\end{matrix} < 100 \times 10^{-6}/\text{hr}$$

If a twin engined airframe is considered and all components have to be operational to dispatch, then the non dispatch rate will be:

$$2 \times \lambda \text{ Hydromechanical} + 4 \lambda \begin{matrix}\text{Electrical} \\ \text{One Channel}\end{matrix} =$$

$$= 2 \times 40 \times 10^{-6} + 4 \times 100 \times 10^{-6} = 480 \times 10^{-6}/\text{Hr}$$

This figure is higher than the required 10^{-4}/Hr (100×10^{-6}/Hr) and the major contributors to the non dispatchability of the airframe are the 4 electronic FADEC channels.

The interest of having an Engine Control System configuration that allows the dispatch of a twin engined airframe with 3 channels operational out of 4 (1 channel operational on one engine and 2 channels operational on the other engine) is obvious. In this case only single failures in both HMUs or dual Electrical Channel failures will prevent the dispatch.

Therefore the non dispatch rate will be:

$$2 \times 40 \times 10^{-6} + 6 \times (100 \times 10^{-6})^2 = 80.06 \times 10^{-6}/Hr$$

This result shows that the hydromechanical part dominates the system non dispatch rate.

The dual IFSD rate of a 3-out-of-4 dispatch configuration has to be less than 1 in 10^9 hours as for the normal dispatch situation.

If a 100% Fault Detection Coverage is assumed this rate can be achieved even if the airframe is dispatched continuously with 3-out-of-4 channels operational, as shown in Fig. 3.

The single IFSD requirement of 10×10^{-6}/hr results in limitation of the time the airframe is allowed to dispatch with one channel out as described below.

Given an IFSD of 100×10^{-6}/hr for the electrical part of the channel, it means that every 2500 hrs an airframe will dispatch with one FADEC channel incapable of control:

$$\frac{1}{4 \times 100 \times 10^{-6}/hr} = 2500 \text{ Hrs}$$

To limit to 10×10^{-6}/hr the average Engine Control System IFSD rate, and continuing to assume a 100% Fault Coverage, will result in limitation of the time the airframe is allowed to dispatch with one channel out to no more than 150 hrs:

$$\frac{(2500-150)\ 4 \times 10^{-6} + 150 \times 104 \times 10^{-6}}{2500} = 10 \times 10^{-6}/Hr$$

Where 4×10^{-6}/Hr is the IFSD rate of the fully operational system and 104×10^{-6} is the IFSD rate of the system dispatched with one channel inoperative (see also Fig. 3).

SOFTWARE CONFIGURATION

In practice not all the faults resulting in IFSD can be detected or accommodated in a dual FADEC channel configuration (case under discussion).

Hardware independent protection functions (O/S protection for instance) or dual channel redundancy can not prevent the Engine Control System from controlling the engine in an undesired way (flame out, large thrust excursions within red limits, etc) if a fault occurs and that fault can not be detected and accommodated (system reconfigured).

The fault detection and accommodation are components of the system's Fault Coverage that can be defined as the conditional probability that the system continues to perform in an acceptable manner, given that some internal part has failed.

The Engine Control System overall Fault Coverage is calculated as a weighted average as follows:

$$C = \frac{\lambda_1 C_1 + ... + \lambda n Cn}{\lambda_1 + ... + \lambda n}$$

Where λn is the failure rate of component n, Cn is the Fault Coverage of component n and C is the system's Fault Coverage.

Given the high reliability and safety requirements imposed on Engine Control Systems and the present reliability of a single channel FADEC system, fault tolerance capabilities (achieved through Fault Coverage and redundancy) must be built into the system.

If only the dual IFSD rate certification requirement was considered and only dispatch with 4 channels operational was allowed, then the required Fault Coverage could be as low as 73% (see Fig. 4).

If in addition the single IFSD rate certification requirement is considered anc only dispatch 4 channels operational was allowed, then the Fault Coverage has to be greater than 94%:

$$4 \times 10^{-6} + \frac{100-94}{100} \times 100 \times 10^{-6} = 10 \times 10^{-6}/\text{Hr}$$

If in addition the dispatch of the airframe with one channel inoperative (out of 4) is considered, and the dispatch time in this configuration is to be a meaningful figure of at least 25 hrs, then a Fault Coverage of at least 95% is mandatory.

$$\frac{\left[4 \times 10^{-6} + \frac{100-95}{100} \times 100 \times 10^{-6}\right] (2500-25) + 104 \times 10^{-6} \times 25}{2500} =$$

$$= 10 \times 10^{-6}/\text{Hr}.$$

With a dual lane FADEC System a 95% Fault Coverage is considered to be a challenge for today's techniques in Fault Detection and Accommodation design.

The FDA techniques described below are considered necessary to achieve this goal.

The FDA requirements are classified in two categories:

- Fault Detection Requirements
- Fault Accommodation Requirements

Fault Detection needs are primarily defined by the 95% Fault Coverage requirement and by the Control System Failure Modes and Effects Analysis (FMEA).

Fault Accommodation needs are defined by IFSD and dispatchability requirements and the goal to make the Control System fail-operational as much as possible.

FAULT DETECTION:

In a dual channel configuration each channel must be basically responsible for the detection and containment of its own failures, and for handing over control to the other channel.

With this configuration it is clear that a 100% fault coverage can not be obtained, even if complete redundancy is available, because of the fault detection aspect.

This fault coverage can be achieved via a combination of self tests and comparison tests.

When a certain component is hardware replicated in both channels its failure can be detected in two ways:

a) Self tests only using the channel's internal resources (range, rate, etc) - No-Cross-Talk configuration.

b) Self tests as in (a) and comparison tests between the two channels sensors - Cross-Talk configuration.

Our experience shows that the Cross Talk configuration is much more complex than the No-Cross-Talk configuration and offers only marginal benefits.

The point of departure in the design of a self test is a Failure Modes and Effects Analysis (FMEA).

A FMEA defines the various failure modes of a device, as well as their effects on the performance of the device and the system.

Based on this analysis, a self test is designed to detect those failure modes which have an unacceptable impact on the performance of the system.

To quantify the level of coverage inherent in a self test, the FMEA must be examined to determine the fraction of the failures of the device which are detectable by the self test (which is associated with that device).

A large part of the Fault Detection logic is primarily based on EEC input/output Self Tests, i.e. range and rate tests to detect out-of-range and out-of-rate faults.

With some exceptions, in-range Fault Detection may be necessary for some EEC inputs depending on the effect of their failures at the high and low limits of the range check. Simulation of these failures is performed to estimate if in-range Fault Detection for these parameters is worth implementing.

A typical Fault Detection Configuration for a turbofan application is shown in Table 1.

For the EEC internal faults a mix of Software and Hardware logic is used under the name of Built-In-Test (BIT). The BIT tests are performed in the engine normal operation modes (Start and Run) and in engine static modes (initialization, maintenance) modes.

Typically the following internal EEC checks are performed:

- PROM – Checksum, Parity
- RAM – Read/Write, Parity
- EEPROM – Erase Upon a Power Down, Parity
- CPU – Watchdog Timer, Activity Monitor, Loss-of-clock Detector, Instruction Test.
- Effectors Drivers – Current Wraparound (W/A), Initialization Test
- A/D Converter – Test Input
- F/D Converter – Test Input
- ARINC – W/A
- Spool-Up Channel Switchover

A short description of each of the above tests is given below.

BUILT-IN TEST DEFINITIONS

PROM CHECKSUM:

Programmable ROM is divided into blocks, each block having a standard checksum test value location. This process adds all locations and verifies that the sum is consistent with the checksum location.

PROM PARITY:

A fault in the main application program is detected by a parity check circuit which is enabled by the action of the processor in fetching the next instruction. The result of this fault is a reset of the application program tc the starting location.

RAM READ/WRITE TEST:

RAM read/write tests can be performed on all RAM locations:

1. WRITE/READ address value
2. WRITE/READ alternating "1"-"0" parity
3. WRITE/READ alternating "0"-"1" parity
4. WRITE/READ any odd parity pattern

Also a test pattern can be written into fixed RAM locations and the result reac during normal operation EEC mode.

RAM PARITY:

A fault in the scratchpad memory will be detected by a parity check circuit which is enabled by the action of the processor in fetching the desired piece of data. The result of this fault is a reset of the application program to the starting location.

EEPROM PARITY:

A fault in the electrically eraseable memory can be detected by a parity check circuit which is enabled by the action of the processor in fetching the desired piece of data. The result of this fault is a reset of the application program to the starting location.

EEPROM ERASE CHECK:

This initialization process checks for a single EEPROM location that is erased or incompletely written. This would happen if an ERASE/WRITE cycle was in process when ECU power was last interrupted.

WATCHDOG TIMER:

The watchdog timer is basically a counting circuit which is used to keep track of the overall application program. The application program will issue a command to the watchdog timer at scheduled intervals which are designed to correspond with an acceptable hardware window. The processor will be reset to the starting location if the watchdog timer command does not occur in the allowable windows.

ACTIVITY MONITOR:

The activity monitor circuit is used as a crude backup to the watchdog timer. A command to this monitor switches between one and zero on a regular basis. The channel outputs are depowered if this switching sequence is interrupted.

LOSS-OF-CLOCK DETECTOR:

The hardware circuit detects the loss of the CPU clock and resets the software to its starting location upon clock recovery.

INSTRUCTION TEST:

A subset of the processor instructions is executed and proper execution verified. The subset is designed to exercise all instruction code bits through an "0" and "1" state and extensively test all critical and frequently-used instructions.

CURRENT WRAPAROUND FOR DRIVERS:

Fault detection for the effector drivers is accomplished by measuring the voltage across an accurate resistor in the output driver. This voltage is directly proportional to current and is compared to the commanded value in order to detect faults such as opens and ground short circuits.

INITIALIZATION TEST FOR DRIVERS:

The initialization test for actuators allows each channel to enable its output drivers for a preset time, so that the output logic can test the electrical integrity of each driver.

ANALOG-TO-DIGITAL (A/D) TEST INPUT:

A known voltage is input to the A/D converter. The voltage is converted by the CPU and compared to a known value to verify correct A/D operation.

FREQUENCY-TO-DIGITIAL (F/D) TEST INPUT:

A known frequency is input to the F/D converter. The frequency is converted by the CPU and compared to a known value to verify correct F/D operation.

ARINC WRAPAROUND TEST:

The control verifies that what it has sent out through the ARINC transmitter is what it receives at the wraparound receiver. All messages which are transmitted appear in the wraparound buffers. The ARINC link is disabled if the wraparound does not match the intended transmission.

LVDT/RVDT CHECKSUM:

The sum of the two LVDT voltage signals is range checked.

SPOOL-UP SWITCHOVER:

The secondary channel starts the engine up to a certain N_2 speed and then switches to the primary channel for the completion of the spool-up. This switchover detects possible dormant failures in the secondary channel.

FAULT ACCOMMODATION

The main goal of the Fault Accommodation logic is to make the system fail operational upon the detection of all first single electrical faults when the system is dispatched with two channels up.

When a certain component is duplicated in each channel and the one in the channel in control fails the action can be:

a) To switch to the back-up channel that will assume control of the engine (no-cross-talk configuration).

b) To "borrow" the failed component from the back-up channel (cross-talk configuration). However the cross-talk configuration is far more complex and its benefits in terms of IFSD rate, dispatchability etc. are marginal.

In the case of single parts of the system (a single P_3 probe for both channels for instance), analytical redundancy must be achieved when possible. For single items that can not be analytically replaced, safe defaults or alternative Control Modes that do not need these parts must be created.

Table 2 gives an overview of a typical Fault Accommodation configuration for a turbofan application.

CHANNEL SWITCHOVER

The channel switchover logic determines the relative health of each channel and uses this as a basis for determining which channel shall be in control. A channel in control is a channel that has its outputs enabled.

Some of the rules for the channel switchover are the following:

1. The two channels must not simulataneously have their outputs enabled (this function to be implemented in hardware independent of the software controlled hardware).

2. The pilot can use a cockpit channel select switch that overrides the automatic channel selection. This will be achieved through hardware means independent of the software controlled hardware.

3. Each channel asseses its own health status and cross-talks this information to the other channel.

4. If the channel in control is less healthy, it must give up control. If the standby channel does not assume control within a reasonable period, the channel that gave up control must resume control.

5. The standby channel cannot enable its outputs unless the channel in control allows it.

FAULT ACCOMMODATION WITHIN THE CHANNEL

EEC input single failures will be accommodated through the following processes:

1. Input Processes

   - Default to a Safe Value
   - Default to a Synthesised Value

2. Control Processes

   - Modified (Lower) Nominal Schedules
   - Back-up Modes that do not use the failed inputs

3. Output Processes

. Fail-Safe

The input single faults accommodation will result in possible degraded performance but not shutdown.

Double failures will be accommodated to the extent that no more logic is required than that necessary for each single failure accommodation.

All the other cases will result in Shutdown and fail safe position of the effectors during flight operation.

COST AND COMPLEXITY CONSIDERATIONS

The costs associated with the development of a FADEC control system as well as the purchase cost are still high. There are several factors contributing to the high prices to be paid for a FADEC control.

The question is, why are FADEC's so expensive when the cost of home computers is in a steep downtrend? A close look to the hardware and software procedures will help to understand the reasons. Electronic hardware used in EECs are often qualified to military standards that include more stringent acceptance tests and tolerances to a wider range of temperatures. Components complying with these procedures can cost up to eight times more than similar mass production components. Due to weight, reliability and processing speed requirements, it is not uncommon to find in the FADEC systems components which are custom made and therefore very expensive. The cost of generating software is also very high due to the documentation and testing required to substantiate and validate the coding. Testing which in non aeronautical applications is minimal, in this case is extensive and well documented due to its criticality.

If a system follows more complex algorithms because its capacity allows it, the cost involved in developing more elaborate algorithms is proportionally less than the increase in benefits to the end user, in fact performance versus cost improves. This is a strong motivation for producing more sophisticated control systems.

The end user, the operator, how does he see this new technology from the point of view of a business that has a fierce competition and high costs of operation? The FADEC systems improve engine operation, reduces pilot workload and perform accurate troubleshooting reducing aircraft downtime. On the other hand, these systems are more complex than their mechanical counterparts and have smaller Mean Times Between Failures (MTBFs). But once more, the increase in complexity is proportionally less than the penalty in MTBF.

In summary, although the FADEC systems are more expensive, more complex and have smaller MTBFs they perform valuable complex functions not only in the field of engine control but also in fault management.

HARDWARE/SOFTWARE TRADE OFFS

The optimization of a complex system like a power plant FADEC represents a challenging task for the engineer responsible for its configuration. He has to study the options and the trade offs involved such that the final configuration is the most cost effective without any safety compromise. The major item involving possible trade offs that normally arises during the conceptual phase concerns redundancy.

The selection between the use of a second sensor as a back up or a parameter synthesis has to be made in the design phase. The decision is made based on the assessment of the criticality of the parameter.

In other cases trade offs are not permissible, for example a speed sensor that can not be shared by the "control" and the "protection". The reason for this is that if an overspeed condition results from the failure of the speed sensor to the "control", the "protection" will see itself prevented from operating because it also lost its speed input.

In the EEC internal hardware trade offs involve the selection between the use of "off the shelf" discrete components versus highly integrated custom made components. In this case the cost will rise but the reliability improves because instead of having many components failing at their own rates, they are replaced by a single device with a failure rate better than the compound effect of the discrete components.

The end result is a very challenging task where safety, cost, reliability and weight are the variables to be optimized by the designer.

FUTURE TRENDS

To accurately predict what the future will bring is not an easy task, however trends are precious indicators that point to where the industry is going.

The use of electronic controls is now widely accepted and its potential is recognized. It is believed that the move towards electronics is irreversible. Improvements in the reliability of the FADEC systems must be made by increasing the reliability of the individual components and moving towards higher system integration.

The continuing demand from airlines to reduce the cost of ownership will drive to systems which are not only more reliable but also with enhanced fault detection and isolation. Aircraft downtime (as it relates to cost of ownership) is one of the biggest airline concerns, therefore systems that will accurately isolate and identify the faults, speeding the troubleshooting process, will be continuously improving. Also, there already exist fault tolerant configurations that allow airplanes to be dispatched for revenue flight with faults.

Higher system integration is an area where it is expected that major progress will be made. The integration in the EEC of functions like Propeller Control, Propeller Synchrophasing, Engine Synchronization, Autofeather, Uptrim, etc., is not only possible in terms of safety and certification but also desirable from the point of view of control performance, fault management, reliability, weight and cost.

In summary, within a decade fault management in FADEC engine controls has gained major significance and when integrated with airframe controls/diagnostics is expected to evolve as a major factor to enhance aircraft operation related to safety, reliability and cost.

TABLE 1

	INPUT/OUTPUT/ COMPONENT	FAULT DETECTION
FAN SPEED	NF (CONTROL CH.)	Range, Rate
GAS GEN SPEED	NG (CONTROL CH.)	Range, Rate
PRESSURE-TOTAL	PT (ADC)	Range, Rate, Comparison to Engine PT
TEMP.-TOTAL	TT (ADC)	Range, Rate
PRESSURE-STATIC	PS (ADC)	Range, Rate, Comparison to Engine PS
	PT (Engine)	Range, Rate
	TT (Engine)	Range, Rate, Comparison to ADC TT
	PS (Engine)	Range, Rate
TEMP. STATION 45	T45	Range, Rate, Model Checks (T45 > x·c when N_2 > y%)
FB - FUEL FLOW	WFPOS	Range, Rate
		Checksum (Va + Vb = K_1)
FB - IGVs	IGVPOS	Range, Rate
		Checksum (Va + Vb = K_2)
THROTTLE LEVER ANGLE	TLA	Range, Rate
		Checksum (Va + Vb = K_3)
PRESSURE STATION 3	P3	Range, Rate, Model Checks
	WF TM	LVDT W/A
		Current W/A, Initialization
	IGV TM	RVDT W/A
		Current W/A, Initialization
	NF TRIM	Illegal Combination
	IGV TRIM	Illegal Combination
	T45 TRIM	Illegal Combination
	DISCRETES	Illegal Combination
	NF (O/S PROT.)	Checked every Normal Shutdown
	NG (O/S PROT.)	Checked every Normal Shutdown
	EEC-INTERNAL	Various Methods - See BIT

FB = FEEDBACK
TM = TORQUE MOTOR
ADC = AIR DATA COMPUTER (AIRFRAME)

TABLE 2

FAULT	ACCOMMODATION
. Loss of a hardware redundant input (NF, NG, TLA, feedbacks, discretes, Power Supply)	Automatic switchover to the other channel
. Loss of output driver (all are redundant)	Automatic switchover to the other channel
. Loss of channel capability (internal Power Supply, CPU, memory)	Automatic switchover to the other channel
. Loss of aircraft redundant input used as a primary source for engine control (ADC PT and PS)	Switch to Engine Control System input if this is not failed.
. Loss of control system input backed up by an aircraft input (ADCTT)	Switch to aircraft input if validated by control system tests.
. Loss of a hardware simplex input that has analytical back-up (P_3)	Use of analytical redundancy - synthesize lost input or, - switch to a back-up mode that does not use the lost input
. Loss of a hardware simplex input that does not have analytical back-up (only mechanical parts of the control system: metering valve common to both channels).	Fail-safe the outputs (Shut-off Fuel Flow, IGV open).

For common (to both channels) mode covered faults or for multiple covered failures resulting in loss of both channels or not enough parameters available to run the engine properly the accommodation consists in going to a fail safe condition for all effectors.

HARDWARE CONFIGURATION BLOCK DIAGRAM

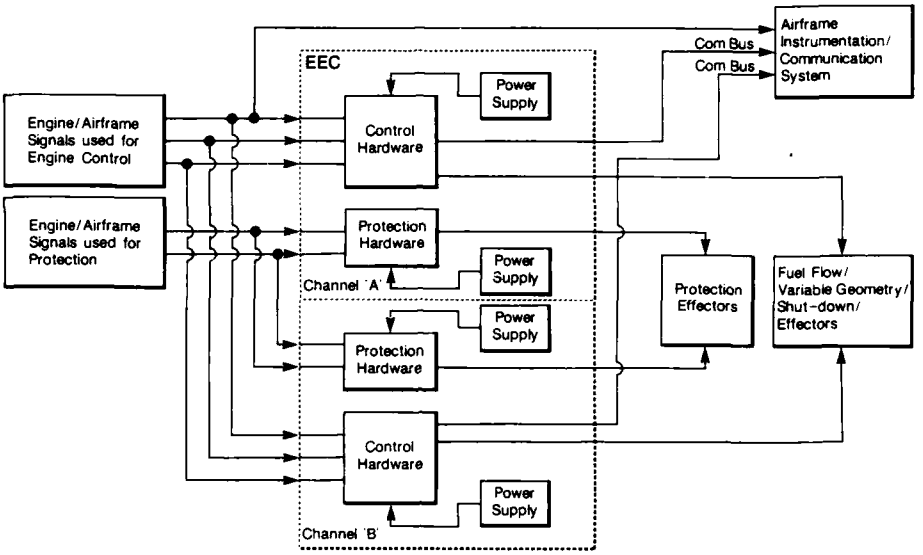

Figure 1

I.F.S.D. RELIABILITY BLOCK DIAGRAM

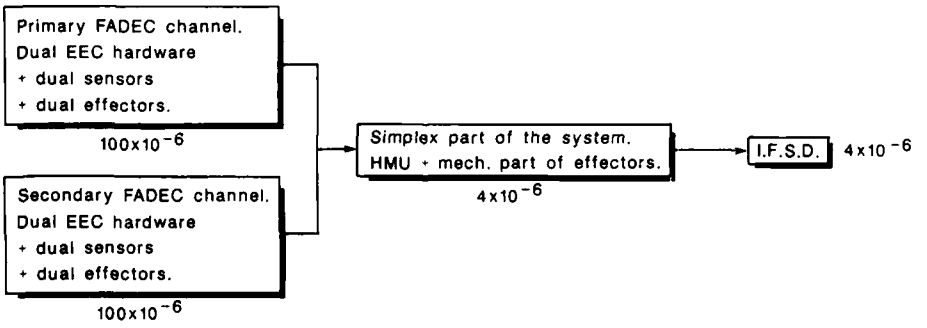

100% fault coverage assumed

Figure 2

I.F.S.D. FAULT TREE
100% FADEC FAULT COVERAGE

I.F.S.D. Analysis:
- 1 channel out prior to dispatch.
- All faults resulting in I.F.S.D. are detected.
- When a fault resulting in I.F.S.D. occurs, switchover to the standby channel is performed.

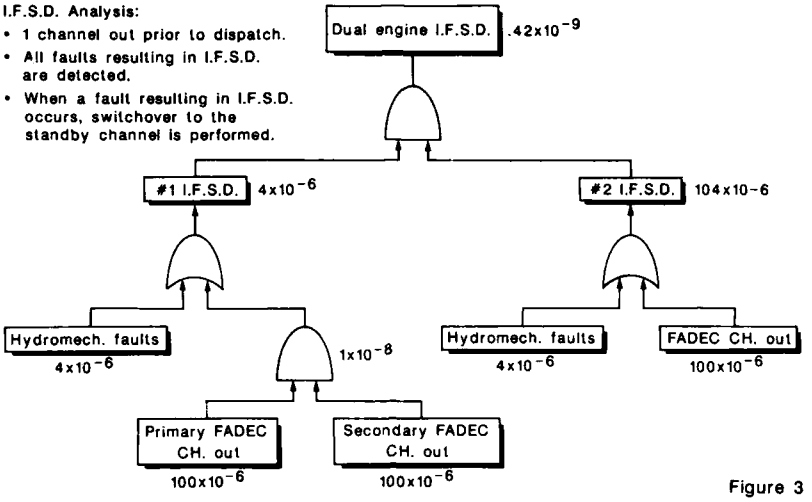

Figure 3

I.F.S.D. FAULT TREE
73% FADEC FAULT COVERAGE

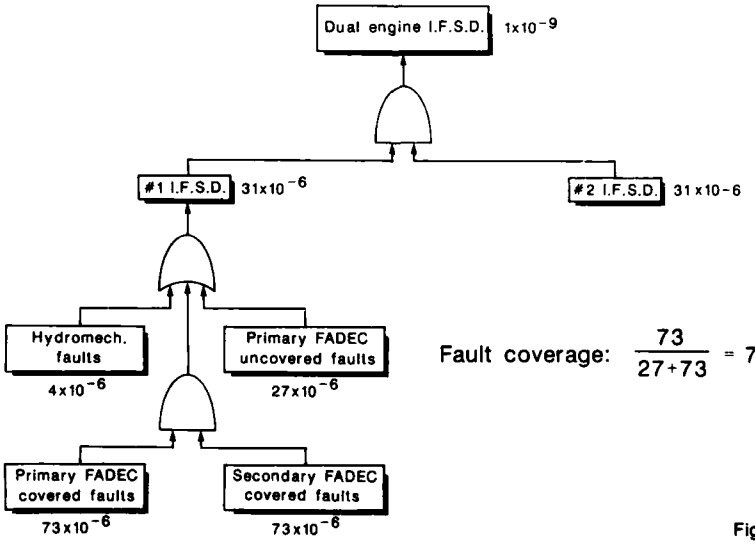

Fault coverage: $\frac{73}{27+73} = 73\%$

Figure 4

DISCUSSION

G.TANNER

Does the EEC perform other checks apart from essential safety checks in order to isolate faults to LRU level?

Author's Reply:

Yes, the EEC performs other checks that are dedicated to fault isolation to the LRU level when possible. A large part of these checks are the same as the safety related checks.
However some of them are performed only in the EEC maintenance mode (BITE). Typically 90 to 95% LRU fault isolation levels are achieved for the control system.

DISCRETE OPERATING CONDITIONS GAS PATH ANALYSIS

By

STAMATIS, A., Res. Assistant
PAPAILIOU, K.D., Professor

Laboratory of Thermal Turbomachines
Athens National Technical Univ.,
Athens, Greece.

ABSTRACT

The implementation of a reliable Diagnostic System based on a Gas Path Analysis (GPA) approach is not always feasible. Extra instrumentation is required in order to predict, detect and isolate failures. Discrete Operating Conditions Gas Path Analysis (DOCGPA), which is presented here, is an extended version of the conventional GPA algorithm, providing the capability of increased reliability when using only existing sensors for estimating engine mulfunctions.

LIST OF SYMBOLS

Δ	Percentage change from an initial value
$E\{\}$	Expectation operator
$\underline{f}$	Fault parameter vector
(ICM)	Influence Coefficient Matrix
J	Scalar defined in eq.(21)
M	Information Matrix
n_f	number of estimated fault parameters
$\underline{p}$	vector of performance parameters
P	Covariance Matrix of estimated fault parameters
P_o	A priori Covariance Matrix of estimated fault parameters
PEUI	Performance Estimation Uncertaincy Index (equal to J)
R	Covariance Matrix of measured variables
$tr\{\}$	trace of a matrix
$\underline{v}$	sensor non-repeatability noise vector
u	operating conditions vector
$\underline{y}$	Measurement vector

SUPERSCRIPTS

$(\ )^T$	Transpose Matrix
$\hat{(\ )}$	Estimated value

1. INTRODUCTION

Gas Path Analysis (GPA) can be considered as a procedure for evaluating the operational condition of a Gas Turbine, using measurements of performance variables, at a certain number of flowpath stations. Aging or specific engine failures reflect on engine performance deterioration, which results in deviations of the values of the measured variables from the ones corresponding to a healthy operation (baseline values). The existing correspondance between the set of deviations from the healthy situation and the performance deterioration constitutes the standard basis for any diagnostic system development /1/. Although a considerable amount of work has been done in this field, during the last two decades (recent work is presented in references /2/ to /4/), many practical limitations are encountered when diagnostic systems based on GPA are used.

These limitations appear when, in an effort to develop an effective diagnostic system, a satisfactory trade-off is searched between the following issues:

i. Reliability
ii. Extent of detailed diagnosis
iii. Integrity of the powerplant
iv. Cost of implementation

In order to increase the confidence levels on performance estimation as well as to isolate mulfunctioning components of the engine, one has to increase the volume of the information concerning its state.

This may be done either by increasing the measured quantities, by installing additional sensors, or by making use of additional measurements realized by the already installed ones. Integrity of the powerplant and cost of implementation restrict usually the installation of additional sensors. Making use of information coming out of the already existing ones will be the subject of the present work.

This information coming out of measurements at different operating points, the corresponding procedure was named Discrete Operating Conditions Gas Path Analysis (DOCGPA). This particular GPA procedure is conditioned by our ability to correlate correctly the engine observed behaviour with that of each one of its components, at all operating points.

2. THEORETICAL PRINCIPLES

2.1 Conventional GPA

Traditional GPA methodology is based on the sequence of events presented in Fig.1. Physical problems affect the values of characteristic performance parameters (e.g. component efficiencies), which, in turn, alter the expected values of (measurable) engine variables, provided that the engine operates in a steady state mode at a given operating point. The most popular mathematical formula-

tion of the problem is expressed by the following linear model equation (5).

$$\Delta\vec{Y} = (ICM)\vec{f} + \vec{v} \qquad (1)$$

where the vector of the deviations of the measured quantities $\Delta\vec{Y}$ is related to the vector of the deviations of characteristics performance parameters (fault parameter vector), $\vec{f}$, through the Influence Coefficient Matrix (ICM), allowing for a random noise $\vec{v}$.

The noise is assumed to possess a Gaussian distribution with mean and covariance:

$$E\{\vec{v}\} = 0$$
$$E\{\vec{v}\vec{v}^T\} = R$$

Having established baselines (either from theoretical modelling and simulation or from measurements on a "healthy" engine), it is possible to construct the (ICM) by perturbing sequentially all performance parameters and calculating the resulting percentage changes in measured variables.

An estimate $\hat{\vec{f}}$ for $\vec{f}$, based on minimum variance considerations, can be calculated according to ref./6/ from the following expression:

$$\hat{\vec{f}} = M^{-1}(ICM)^T R^{-1}\Delta\vec{Y} \qquad (2)$$

where M is the information matrix defined as:

$$M = (ICM)^T R^{-1}(ICM) \qquad (3)$$

Then the estimate error covariance, P is resulting from equation (2) as:

$$P = M^{-1} \qquad (4)$$

Previously established statistical information on $\hat{\vec{f}}$ associated with a covariance P_o, may be taken into account in this procedure (ref./7/). The expression for the information matrix becomes then:

$$M = P_o^{-1} + (ICM)^T R^{-1}(ICM) \qquad (5)$$

and the corresponding expression for the estimate error covariance reads:

$$P = \{P_o^{-1} + (ICM)^T R^{-1}(ICM)\}^{-1} \qquad (6)$$

Equation (6) implies that the estimate f becomes more "oblivious" to sensor noise, when the a priori covariance P_o is considerably "small". This scenario is appropriate for aging deterioration monitoring. In cases where previous information about f is not available or lost, for example, following a serious damage, the resulting information matrix must be well conditioned, in order to avoid false alarms from sensor noise.

In practice, the following measures are taken:

a) The number of measured variables is at least equal to the number of parameters for estimation, and
b) The chosen measured variables are sensitive to the ones chosen for diagnostic purposes.

2.2 Generalized GPA

An arbitrary gas turbine configuration may be considered as a system for which the measured output $\vec{Y}$ is a function of the system parameter vector p and the input vector $\vec{u}$:

$$\vec{Y} = G(\vec{p},\vec{u}) \qquad (7)$$

The input vector in our case defines the operating conditions (i.e. altitude, aircraft Mach number, power setting, etc.) and the system parameter vector $\vec{p}$ contains characteristic performance parameters (i.e. efficiencies etc). Linearization of equation (7) with respect to $\vec{p}$ leads to the equation:

$$\Delta\vec{Y} = \{ICM(\vec{u})\}\,\Delta\vec{p} \qquad (8)$$

Since by definition f are the percentage changes of p i.e.

$$\vec{f} = \Delta\vec{p} \qquad (9)$$

we get

$$\Delta\vec{Y} = \{ICM(\vec{u})\}\,\vec{f} \qquad (10)$$

The classical formulation of GPA (equation (1)) is nothing but the application of the equation (10) at a single operating point.

From the above expression of equation (10) it can be easily seen that, if the (ICM) is sensitive to the vector $\vec{u}$, then the measurement deviation vector $\Delta\vec{Y}$ will be different for different operating conditions, when the fault vector remains the same.

The practical consequence of the above statement is that, when information is missing, it can be supplied by measurements at other operating conditions (different values for the input vector $\vec{u}$).

Consider, as an illustrative example, the following single input-output model equation:

$$\Delta y = uf_1 + u^2 f_2 \quad , \quad u \in |0.8,1| \qquad (11)$$

or in vector notation:

$$\Delta y = (u \; u^2)\begin{pmatrix} f_1 \\ f_2 \end{pmatrix} \tag{12}$$

For input u=1, it implies:

$$\Delta y(1) = f_1 + f_2 = c_1 \tag{13}$$

and there is a family of fault vectors satisfying equation (11) as we can see from Fig.2a.

Taking into account one more measured output with input u=0.8, we have:

$$\Delta Y(0.8) = 0.8 f_1 + 0.64 f_2 = c_2 \tag{14}$$

It is obvious from Fig. 2b that the direction of the fault vector is uniquely determined.

In reference /8/ engine simulation codes were developed for three specific cases (two aircraft and one ground gas turbine engines), for which sufficient data were available. Analysis using these codes has demonstrated that the (ICM) is sensitive to operating conditions. The same fact is stated explicitely in reference /9/, where it is reported that operating a gas turbine at constant speed conditions and under a specific fault situation, the deviations of the performance variables were found to be considerably different from those corresponding to a constant output power operation.

We can, now, return to the formulation of our problem, when different operating conditions are considered.

3. DISCRETE OPERATING CONDITIONS MODEL

Consider equation (8), including sensor noise error readings. For N different operating conditions we can write:

$$\begin{aligned} \Delta\vec{Y}_i &= \{ICM(i)\}\,\vec{f} + \vec{v}_i \\ E\{\vec{v}_i\} &= 0 \qquad\qquad i = 1,N \\ E\{\vec{v}_i \vec{v}_i^T\} &= R_i \end{aligned} \tag{15}$$

The vector $\vec{f}$ may be viewed as the state, at time t_N, of the dynamical system:

$$\begin{aligned} \vec{f}_{i+1} &= \vec{f}_i \\ \Delta\vec{Y}_i &= \{ICM(i)\}\,\vec{f}_i + \vec{v}_i \end{aligned} \tag{16}$$

provided that time intervals $t_{i+1}-t_i$ are long enough to assume that a steady state is reached, but small enough compared with the time required for further deterioration of the state. Suppose that $\vec{f}_N$ is completely observable with respect to $\{\Delta\vec{Y}_1, \ldots \Delta\vec{Y}_N\}$ or, equivalently, the matrix:

$$\sum_{i=1}^{N} \{ICM^T(i)\}\, R_i^{-1}\, \{ICM(i)\}$$

is positive definite.

The unbiased minimum variance estimate of f_N is given by Gauss-Markov theorem /10/. It reads:

$$\hat{\vec{f}}_N = M_N^{-1} \sum_{i=1}^{N} \{ICM(i)\}\, R_i^{-1} \Delta\vec{Y}_i \tag{17}$$

where

$$M_N = \sum_{i=1}^{N} \{ICM^T(i)\}\, R_i^{-1}\, \{ICM(i)\} \tag{18}$$

is the Information Matrix.

The covariance of $\hat{\vec{f}}_N$ is:

$$P_N = M_N^{-1} \tag{19}$$

The model that has been built from N discrete operating conditions, is called the order N model. Refering back to the example of par. 2.2, it is easy to deduce that the order 1 model possesses an indefinite covariance for the estimated parameters, while for the order 2 model the covariance (assuming $R_i = I$) gets the form:

$$P_2 = \begin{pmatrix} u_1^2 + u_2^2 & u_1^3 + u_2^3 \\ u_1^3 + u_2^3 & u_1^4 + u_2^4 \end{pmatrix} \tag{20}$$

We can remark that from this point on, it is possible to search for the most appropriate inputs u_1, u_2 in order to have some norm of P_2 minimum, which will insure an optimal estimate.

Following the above reasoning, for any order N Discrete Operating Condition Model, along with its covariance P_N, we may consider as a diagnostic effectiveness measure for the Model, the norm defined in ref./5/ as:

$$J = \sqrt{\frac{1}{n}\, tr\, \{P_N\}} \tag{21}$$

which is named Performance Estimation Uncertaincy Index (PEUI), in this study.

Since the main diagonal elements of the covariance matrix P_N are the variances of the estimation errors, J is just the square root of the average variance and is like an RMS error for the order N model. Roughly speaking, a value of J of 1.5 means that the standard deviations of the estimation error for each of the fault parameters considered are "close" to 1.5%. Clearly, the smaller the value of J, the more accurate is the estimate, using the order N model.

4. CASE STUDY

We have already mentioned that analytical studies on different engine simulations, which are discussed in /8/, have proved that the Influence Coefficient Matrix depends on operating conditions. With this in mind, we shall proceed to demonstrate the DOCGPA capabilities, considering a commercial turbofan engine for which data for the (ICM) were available for three operating conditions.

Table 1 defines the measurement vector $\vec{Y}$ and the fault parameter vector $\vec{f}$ used for the engine.

Tables 2-4 present the values of the (ICM) matrix for the three different operating conditions (Engine Pressure Ratio, flight Mach number and ambient conditional mentioned above).

These values will be used in order to investigate improvements that the DOCGPA approach can offer in respect to an ordinary GPA method.

Even before starting this investigation, the strong dependance of the (ICM) elements on varying operating conditions can be remarked.

The calculation results that will be presented, have been obtained with the assumption that all measured values of the variables (N_1,N_2,W_F,EGT) have been made with an accuracy characterized by a standard deviation equal to 0.5%, if not stated otherwise.

Figure 4 presents the values of the performance estimation uncertaincy index (PEUI), when the order of the model (number of operating points taken into account) is varied as well as the number of the estimated parameters (number of components of the fault vector).

Case 1 considers the estimation of four fault parameters under one, two or three operating conditions. Cases 2 and 3 consider, successively, five and eight fault parameters for two and three operating conditions. Case 4 considers nine fault parameters and three operating conditions.

It can be seen from Fig.4 that nine fault parameters can be estimated only when all three operating conditions are used. On the other hand, the overall accuracy and reliability is improved when the number of operating conditions considered is increasing, for a given number of fault parameters.

An idea about the influence of the measuring accuracy can be deduced from the calculation results presented in Fig.5. The evolution of the PEUI is presented in this Figure for case 4, when the measurement accuracy varies from 0.5 to 1.0%.

An interesting feature of the DOCGPA is demonstrated by the calculation results presented in Fig.6. For cases 1 and 3, one or two measurements were disregarded when estimating the fault parameters. It can be seen that using less measured variables, it is still possible to estimate the required fault parameters, of course, with a loss in accuracy.

In order to complete the picture we can add that additional calculations were performed, which demonstrated that:

a) The prediction accuracy is not considerably changing, when different sets of fault parameters (the total number remains constant) are estimated.
b) The choice of measurement variables influences the accuracy of the estimation, when their number is reduced. In fact, the variables N_1,N_2 for this case, cannot be disregarded without a dramatic increase in estimation uncertainty.

Finally, in order to give an idea about the estimation accuracy for each fault parameter, when a DOCGPA procedure is used, we shall consider the Table 5. Row A of this Table contains typical errors in the estimation of the nine fault parameters (Case 4). For the same number of operating conditions, row B of Table 5 presents the corresponding errors for Case 3 (eight variables are estimated, that is the value of $\Delta\eta_f$ was considered as known).

The variation in estimation accuracy for each parameter is evident. It is worthwhile noting that changes in efficiency are estimated more accurately than the other parameters (except from the fan efficiency, for which the estimation uncertaincy level is unacceptably large).

5. CONCLUSIONS

A method named Discrete Operating Conditions Gas Path Analysis was described above. The method is an extension of the ordinary Gas Path Analysis. It takes advantage of the non linear behaviour of a gas turbine engine and gives the possibility to increase information coming out of a number of sensors, which are positioned on the engine.

This additional information may be used for:

a) Decreasing the uncertainty of the estimation of parameters, which are used for diagnostic purposes and, thus, increase the reliability of the diagnosis itself.
b) Performing a diagnosis, when the number of measured quantities is smaller than the number of variables used for diagnostic purposes.
c) Performing a check on the values of the measured variables.

The requirements in order to render the DOCGPA more effective are the following:

a) Realistic modeling of the engine and adaptation of the model to predict actual engine behaviour at all operating conditions.
b) Knowledge of the (ICM) sensitivity over the whole operating range in order to choose the optimum testing profile.

c) Improvement of existing instrumentation characteristics, which is a general GPA requirement.
d) Determination of minimum deterioration limits for each fault parameter so that, when these limits are exceeded, they are estimated with sufficient accuracy.

REFERENCES

/1/ - "Diagnostics and Engine Condition Monitoring", AGARD CP 165.

/2/ CHAMBLEE,C.E., BURWELL,A.E.,"Effectiveness of Turbine Engine Diagnostic Systems", AIAA-83-0535.

/3/ SMITH,C., BROADIE,M.,"Turbine Engine Fault Detection and Isolation Program: Turbine Engine Performance Estimation Methods", AFWAL-TR-2058, Aug. 1982.

/4/ SMITH,C., DE HOFF,R.L.,"Developments in Performance Monitoring and Diagnostics in Aircraft Turbine Engines", SAE 821400.

/5/ KOS,J.M., "Multiple Fault Gas Path Analysis Applied to a Twin-Spool Mixed Flow, Variable Geometry Turbofan Engine", AD-A019 183, Oct. 1975.

/6/ GOODWIN,G.C., PAYNE,R.L.,"Dynamic System Identification: Experiment Design and Data Analysis" ACADEMIC PRESS, 1977.

/7/ BIERMAN, "Factorization Methods for Discrete Sequential Estimation", ACADEMIC PRESS, 1977.

/8/ STAMATIS, A.G., "Diagnostics and its Application to Preventive Maintenance", PhD Thesis in Preparation.

/9/ SARAVANAMUTOO,H.I., MAC ISAAK,B.D.,"Thermodynamic Models for Pipeline Gas Turbine Diagnostics" ASME 83-GT-235.

/10/ JAZWINSKI "Stochastic Processes and Filtering Theory", ACADEMIC PRESS.

j	Y_j	
1	N_1	Fan spool rotational speed
2	N_2	High Pressure Compressor spool rotational speed
3	W_F	Fuel Flow rate
4	EGT	Exhaust Gas Temperature

Table 1a Measurement vector

j	f_j	
1	$\Delta\eta_F$	Fan efficiency change
2	$\Delta\eta_{IPC}$	Intermediate Pressure Compressor efficiency change
3	$\Delta\eta_{HPC}$	High Pressure Compressor efficiency change
4	$\Delta\eta_{HPT}$	High Pressure Turbine efficiency change
5	$\Delta\eta_{LPT}$	Low Pressure Turbine efficiency change
6	ΔW_{BLF}	Fan Bleed Overboard
7	ΔW_{BLCDV}	High Pressure Compressor Bleed into Fan Duct
8	ΔW_{BLCOB}	High Pressure Compressor Bleed Overboard
9	ΔA_N	Effective Nozzle Area change

Table 1b Fault Parameter vector

	$\Delta\eta_F$	$\Delta\eta_{IPC}$	$\Delta\eta_{HPC}$	$\Delta\eta_{HPT}$	$\Delta\eta_{LPT}$	ΔW_{BLF}	ΔW_{BLCDV}	ΔW_{BLCOB}	ΔA_N
ΔN_1	0.06	0.133	0.1	0.04	0.267	0.267	-0.133	0.15	0.6
ΔN_2	-0.1	-0.233	0.933	0.517	-0.4	0.067	0.267	0.333	0.14
ΔWF	-0.5	-0.55	0.833	-0.7	-1.0	0.333	1.833	2.483	0.533
ΔEGT	-0.2	-0.7	-0.6	-0.667	-0.667	0	1.333	1.5	0.033

Table 2. Influence Coefficients for Engine Pressure Ratio, ERP=1.74, Sea level static.

	$\Delta\eta_F$	$\Delta\eta_{IPC}$	$\Delta\eta_{HPC}$	$\Delta\eta_{HPT}$	$\Delta\eta_{LPT}$	ΔW_{BLF}	ΔW_{BLCOV}	ΔW_{BLCOB}	ΔA_N
ΔN_1	0.133	0.267	0.233	0.333	0.383	0.433	-0.167	0.133	1
ΔN_2	-0.1	-0.267	1	0.6	-0.267	0.067	0.133	0.433	0.267
ΔW_F	-0.333	-0.4	-0.333	-0.767	-0.733	0.333	1.667	1.667	1.267
ΔEGT	-0.167	-0.6	-0.433	-0.933	-0.800	0	1.467	1.6	0.433

Table 3. Influence Coefficients for EPR=1.96 Sea Level static.

	$\Delta\eta_F$	$\Delta\eta_{IPC}$	$\Delta\eta_{HPC}$	$\Delta\eta_{HPT}$	$\Delta\eta_{LPT}$	ΔW_{BLF}	ΔW_{BLCDV}	ΔW_{BLCOB}	ΔA_N
ΔN_1	0.1	0.1	0.1	0.15	0.3	0.3	-0.1	0.1	0.8
ΔN_2	-0.05	-0.1	0.4	0.5	-0.1	0.05	0.25	0.3	0.2
ΔW_F	-0.25	-0.15	-0.65	-0.8	-0.65	0.35	1.85	2.4	1.1
ΔEGT	-0.311	-0.415	-1.141	-1.348	-1.037	0	1.244	1.452	0

Table 4. Influence Coefficients for EPR=2.00
Altitude 35000 ft, Mach 0.8

	$\Delta\eta_F$	$\Delta\eta_{TPC}$	$\Delta\eta_{HPC}$	$\Delta\eta_{HPT}$	$\Delta\eta_{LPT}$	ΔW_{BLF}	ΔW_{BLCDV}	ΔW_{BLCOB}	ΔA_N
A	10.7	1.7	1.6	2	3.4	3.7	3	3.7	3
B	-	1.3	1.5	1.6	1.8	3.3	1.5	1.1	2

Table 5. Typical percent errors in estimated fault parameters, using 3-order DOCGPA model.

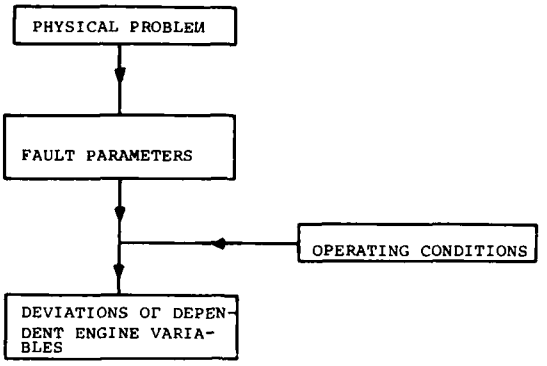

FIGURE 1 Gas Path Analysis flowchart.

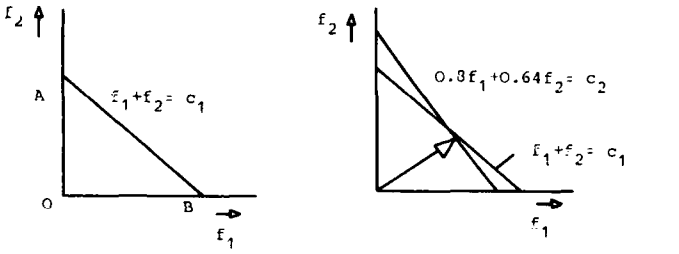

(a) $\hat{f}$ may be any vector with origin O, ending at line AB.

b) The vector $\hat{f}$ is uniquely defined.

FIGURE 2 An illustrative example.

CONSTANT POWER	T_4	P_2/P_1	$N/\sqrt{\theta_1}$	W_f	EPR
Fouled compressor	≶	≶	↑	≶	≶
Excess leakage	↑	↓	↓	≶	≶
$\eta_{gas\ gen\ turbine}$	↑	↓	↓	↑	≶
A_{LPT}(increase)	↓	↑	↑	≶	≶

CONSTANT SPEED	T_4	P_2/P_1	SHP	W_f	EPR
Fouled compressor	↓	↓	↓	↓	↓
Excess leakage	↑	≶	↑	↑	↑
$\eta_{gas\ gen\ turbine}$	↑	↑	↑	↑	↑
A_{LPT} (increase)	↓	↓	↓	↓	↓

FIGURE 3 Fault Matrices for a Two Shaft Engine (from /9/)

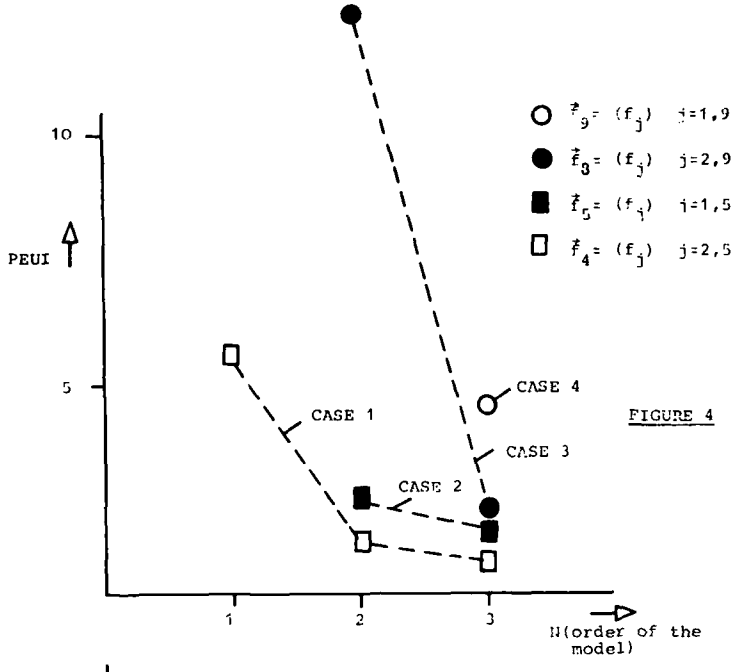

FIGURE 4

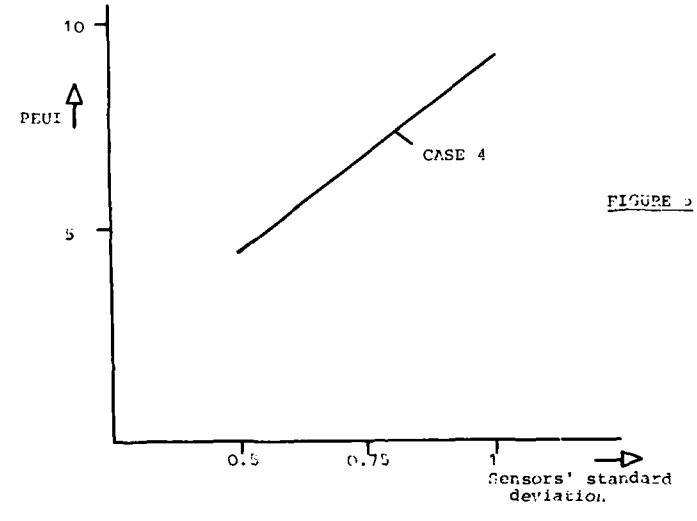

FIGURE 5

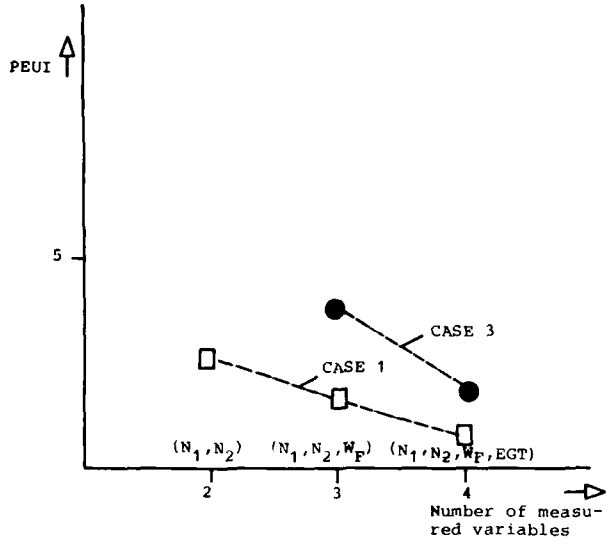

FIGURE 6

DISCUSSION

F. HOERL

Which methods have you used to determine observability?

Author's Reply:

For the observability we use the standard definition and the theorems given by systems control theory.

H.CIKANEK

What is the method by which you determine your ICM (influence sensitivity) matrices?

Author's Reply:

ICM is extracted from existing engine simulation codes by calculating the deviation of the measured variables that results when cash fault parameter is perturbed by one percent and the other parameters remain unchanged.

GAS PATH MODELLING, DIAGNOSIS AND SENSOR FAULT DETECTION

by

Prof. Dr.-Ing. R. Lunderstädt
and
Prof. Dr.-Ing. K. Fiedler
University of the German Armed Forces Hamburg
Holstenhofweg 85
D-2000 Hamburg 70
FRG

SUMMARY

The gas path analysis (GPA) becomes more and more an important method for the diagnosis of jet engines. Therefore in this paper a fundamental way of finding the mathematical engine model is shown, especially with regard to the adaptation of the coefficients of the system matrix to the gradients of the characteristic curves of the turbomachines.

The theoretical fundamentals are applied to a two-shaft jet engine. In order to test the method some faults in the engine are simulated. All faults are detected very accurately and the method shows by this its efficiency.

For practical use of the method also the faults of the measuring device (sensors) are to be taken into consideration. Therefore filter algorithms are outlined to diminish the stochastic parts of these faults. For the systematic parts (offsets) a special and new theory is developed for compensation. For both simulation results are given based on actual test stand data.

1. INTRODUCTION

The high requirements both in the civil and military field of air traffic, which may be characterized by the keywords of "safety, reliability, and economy" have lead at an early stage to the development of methods of engine condition monitoring.

Back in the early thirties, visual inspections were carried out. Later on, there came up operational tests, ultrasonic tests, and lubricant checks as well as vibration analyses. The first automated diagnostic systems were introduced in the early sixties. Those systems were designed to supervise mainly the life cycle of important engine components by counting load cycles and temperature strains. A detailed compilation hereto can be found among other subjects in [1]. System theory regarding diagnostic procedures for jet engines was first considered in the early seventies [2], [3]. Those considerations were based on steady-state models for engine dynamics, having been obtained from working procedure data processing. Special achievements in that field have been contributed by URBAN who was the first to develop analytical programs which have stood the test of practice and allow a high-quality diagnosis with the aid of the digital computer. They are used with success for example by several airline companies [4], [5].

Based thereon and moreover on [6] and [7], an example of a diagnostic procedure for up to date two-shaft jet engines has been composed. Due to measuring noise and also to systematic measuring errors, the diagnosis comprises the employment of estimation procedures. Referring hereto, algorithms for state evaluation are indicated and checked for their reliability. Especially for the systematic sensor errors a new theory is developed which is outlined in detail in [8] and which will be published separately in [9].

2. DEVELOPMENT OF MATHEMATICAL ENGINE MODEL

As stated in the introductory context, a diagnosis oriented towards system theory requires a detailed model development. In the following, this is elaborated for a two-shaft jet engine, based on working process computations.

2.1 Generalities

Corresponding to an up-to-date concept of jet engines, a modular structure of the engine is assumed. The modules to be considered are: the compressors, the combustion chamber, the turbines, and the thrust nozzle.

Different characteristics serve at describing the condition of those components. In the sense of the terms related to control technology, they are referred to as state variables. For the turbo engines, they are efficiency and mass flow rate, for the combustion chamber, efficiency and relative pressure loss, and for the nozzles, efficiency and cross section of outlet. Those characteristics and state variables are not directly measurable, but they must be calculated from measured values. Those measured values are the pressures and temperatures at inlet and outlet of each module, furthermore the speeds of the turbo engines, the fuel flow rate and, as a desirable further magnitude, the thrust. If parts of the jet engine are of variable geometry, the position indicators describing the change of geometry are comprised with the measured values.

The correlation between measured values and state variables is established by reference to thermodynamics and the characteristics of the components, with the aid of similitude theory. Those linkages are in general non-linear, and procedures of system theory would not be applicable therewith. For that reason, the describing equations in the area of a predetermined operational point are linearized, and only the changes in that working point, as referred to nominal state, are considered.

If a variable of state X_i is a function of m measure values Y_j, the total differential of X_i is

$$dX_i = \left(\frac{\partial X_i}{\partial Y_1}\right)_0 \cdot dY_1 + \left(\frac{\partial X_i}{\partial Y_2}\right)_0 \cdot dY_2 + \ldots + \left(\frac{\partial X_i}{\partial Y_m}\right)_0 \cdot dY_m \quad , \tag{1}$$

wherein $dY_j = Y_j - Y_{j0}$ and $dX_i = X_i - X_{i0}$, the nominal state being identified by index 0.

For later evaluatation as well as for generalization, it is of advantage to pass over to non-dimensional description. This is reached by referring the variations to the nominal state itself. At the same time, there shall be considered that finite deviations Δ from the nominal state are allowed. Herewith Eq. (1) changes to

$$\Delta x_i = \frac{Y_{10}}{X_{i0}} \cdot \left(\frac{\partial X_i}{\partial Y_1}\right)_0 \cdot \Delta y_1 + \frac{Y_{20}}{X_{i0}} \cdot \left(\frac{\partial X_i}{\partial Y_2}\right)_0 \cdot \Delta y_2 + \ldots + \frac{Y_{m0}}{X_{i0}} \cdot \left(\frac{\partial X_i}{\partial Y_m}\right)_0 \cdot \Delta y_m \quad , \tag{2}$$

wherein

$$\Delta y_j = \frac{Y_j - Y_{j0}}{Y_{j0}} \text{ and } \Delta x_i = \frac{X_i - X_{i0}}{X_{i0}} \quad .$$

In the compressors, direct determination of the coefficients

$$a_{ij} = \frac{Y_{j0}}{X_{i0}} \cdot \left(\frac{\partial X_i}{\partial Y_j}\right)_0$$

corresponding to the structure of Eq. (2) is possible and sufficient for description, as will be shown in the following section by the example of the compressor efficiency. The reason hereof is that all measured values required are available at the entry and exit of a compressor.

In the case of turbines and possibly also of combustion chambers and thrust nozzles mostly not all of the necessary measured values are realized. This applies above all to the entry temperatures of turbines, the measurement of which inevitably leads in any case to dubious results on account of a radial temperature profile and of the mixing effects between main gas stream and cooling air stream. Applying the balance of power for the corresponding shafts of the engine, the not measurable values can, however, be obtained by calculation, based on the measurable values in the compressor portion. It is true that hereby the clear composition of the formula is somehow affected.

2.2 Efficiency of compressor

The use of Eq. (2) and in particular the calculation of its coefficients shall be explained by the example of the compressor efficiency.

The efficiency η of a compressor, which is compressing from total state 1 to total state 2, is determined under consideration of the variability of the specific heat c_p from the relation

$$\eta = \frac{c_{p1} \cdot T_1 \cdot \left[\left(\frac{p_2}{p_1}\right)^{R/c_{p1}} - 1\right]}{h_2 - h_1} \quad . \tag{3}$$

In that equation p is the pressure, T is the absolute temperature, h is the enthalpy, and R is the gas constant. The linkage between temperature and enthalpy is supplied by the equation of definition of the specific heat

$$dh = c_p \cdot dT \quad . \tag{4}$$

With Eq. (4) and application of Eq. (2) one gets from Eq. (3)

$$\frac{d\eta}{\eta} = \frac{-\frac{R}{c_{p1}}}{1-\left(\frac{p_1}{p_2}\right)^{R/c_{p1}}} \cdot \frac{dp_1}{p_1} + \left(1 + \frac{c_{p1} \cdot T_1}{h_2 - h_1}\right) \cdot \frac{dT_1}{T_1} + \frac{\frac{R}{c_{p1}}}{1-\left(\frac{p_1}{p_2}\right)^{R/c_{p1}}} \cdot \frac{dp_2}{p_2} - \frac{c_{p1} \cdot T_2}{h_2 - h_1} \cdot \frac{dT_2}{T_2} \quad . \tag{5}$$

This variation of efficiency has now still to be compared with the one to be expected from the characteristics of the compressor. This is necessary because the diagnosis shall indicate failures as compared to a failure-free state, and not deviations referred to another working point [6]. For comparison, the efficiency η must be known as a function of two similarity characteristics. A description of the efficiency and of the pressure ratio as a function of the reduced flow rate is widely known. That kind of reference is, however, not so useful for the evaluation intended here, because when employing Eq. (2) it will become necessary to differentiate those characteristics. In the case of transonic compressors with vertical characteristics, as used in modern jet engines, it would hereby result in infinitely high values. Therefore, the efficiency is expressed as a function of the pressure figure ψ with the circumferential Mach number M as a parameter. Hereby, the numeral values for the differential quotients of $\partial\eta/\partial\psi$ and $\partial\eta/\partial M$ remain unique and finite [7].

Using the equations of definition for the two similarity parameters

$$\psi = \frac{2 \cdot c_{p1} \cdot T_1 \cdot \left[\left(\frac{p_2}{p_1}\right)^{R/c_{p1}} - 1\right]}{u^2} \tag{6}$$

and

$$M = u \cdot \sqrt{\frac{1 - R/c_{p1}}{R \cdot T_1}} \quad , \tag{7}$$

with u as the circumferential speed of reference, which is proportional to the rotational speed n, one obtains the difference between the efficiency of a compressor found by measuring and the one to be expected according to the characteristics, in a non-dimensional description for finite differences

$$\frac{\Delta\eta}{\eta} = \frac{\frac{R}{c_{p1}}}{1 - \left(\frac{p_1}{p_2}\right)^{R/c_{p1}}} \cdot \left(\frac{\psi}{\eta} \cdot \frac{\partial \eta}{\partial \psi} - 1\right) \cdot \frac{\Delta p_1}{p_1} + \left(1 + \frac{c_{p1} \cdot T_1}{h_2 - h_1} - \frac{\psi}{\eta} \cdot \frac{\partial \eta}{\partial \psi} + \frac{1}{2} \cdot \frac{M}{\eta} \cdot \frac{\partial \eta}{\partial M}\right) \cdot \frac{\Delta T_1}{T_1} +$$

$$+ \frac{\frac{R}{c_{p1}}}{1 - \left(\frac{p_1}{p_2}\right)^{R/c_{p1}}} \cdot \left(1 - \frac{\psi}{\eta} \cdot \frac{\partial \eta}{\partial \psi}\right) \cdot \frac{\Delta p_2}{p_2} + \left(\frac{-c_{p2} \cdot T_2}{h_2 - h_1}\right) \cdot \frac{\Delta T_2}{T_2} + \left(2 \cdot \frac{\psi}{\eta} \cdot \frac{\partial \eta}{\partial \psi} - \frac{M}{\eta} \cdot \frac{\partial \eta}{\partial M}\right) \cdot \frac{\Delta n}{n} \quad . \tag{8}$$

Now there are set $\Delta\eta/\eta = \Delta x_1$ and $\Delta p_1/p_2 = \Delta y_1, \ldots, \Delta n/n = \Delta y_5$, so that Eq. (8) corresponds to the general description of Eq. (2), and the correlation between the variables of state Δx_i and the measured values Δy_j, j=1,...,5, as searched for, is established. The description in the form of Eq. (8) is similar for all state variables of a jet engine, but in most cases its structure is of much greater volume.

In the coefficients a_{ij} belonging to the measured values in Eq. (8), there are to be considered besides the gas properties (R and c_p) and the state of the medium of operation upstream and downstream of the compressor (p_1, T_1, p_2, T_2) the gradients of the characteristic curves $\partial\eta/\partial\psi$ and $\partial\eta/\partial M$ to be taken from the map of characteristics. Finding those values at the required accuracy causes sometimes certain difficulties. By calculation, they can, however, be found precisely enough by a few test runs of the engine.

2.3 Two-shaft jet engine

The considerations of the foregoing section shall be applied to a two-shaft jet engine with by-pass and fixed geometry. General structure and sections of the modules are shown in Fig. 1. The jet engine thus comprises seven modules:

Module 1: Low pressure compressor (LPC).
Module 2: Compressor case - transition piece.
Module 3: High pressure compressor (HPC).
Module 4: Combustion chamber (CC).
Module 5: High pressure turbine (HPT).
Module 6: Low pressure turbine rotor (LPT).
Module 7: Turbine case.

The procedure of diagnosis has now to be arranged in a way that a defective module is detected. The precondition is that the state variables are selected to describe sufficiently, either single or in groups, the physical state of each separate module. There are selected:

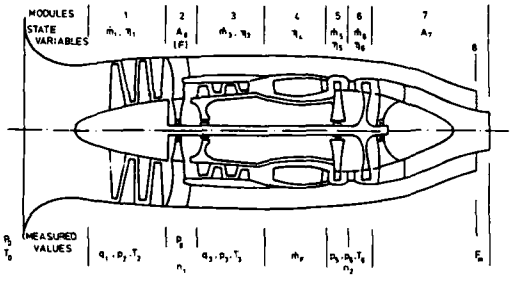

Fig. 1 Cross section with denotations for a two-shaft jet engine.

Module 1: Mass flow rate $\dot{m}_1$,
efficiency of the low pressure compressor η_1.

Module 2: Ring area A_8.

Module 3: Mass flow rate $\dot{m}_3$,
efficiency of the high pressure compressor η_3.

Module 4: Combustion chamber efficiency η_4.

Module 5: Mass flow rate $\dot{m}_5$,
efficiency of the high pressure turbine η_5.

Module 6: Mass flow rate $\dot{m}_6$,
efficiency of the low pressure turbine η_6.

Module 7: Outlet area A_7.

Additionally: Thrust F (as the case may be, for module 2 as well).

Corresponding to the former designations (state variables), the following order is set:

$$X_1 = \dot{m}_1,\ X_2 = \eta_1,\ X_3 = \dot{m}_3,\ X_4 = \eta_3,\ X_5 = \dot{m}_5,\ X_6 = \eta_5,\ X_7 = \dot{m}_6,\ X_8 = \eta_6,$$

$$X_9 = \eta_4,\ X_{10} = A_7,\ X_{11} = A_8,\ X_{12} = F.$$

This means that n = 12 state variables are available for diagnosis. For selection from X_1 to X_{12}, the criteria detailed below are of significance.

Modules 1, 3, 5 and 6 are turbomachinery. Those are characterized particularly well by efficiency η_i and mass flow $\dot{m}_i$. The use of both the efficiency and the mass flow has been provided because disturbances are imaginable, which concern just one of the two state variables. For example it is possible that a defective or a missing blade is perceptible only by fluid flow capacity, i.e. in mass flow, without any notable change of efficiency. Therefore, the combined evaluation of efficiency and mass flow provides in any case a reliable statement on the working state of the engine module concerned (LP, HP compressor; HP, LP turbine).

Module 4 - combustion chamber - is evaluated by its efficiency η_4 only, because there is to be expected that in case of disturbances, e.g. asymmetric distribution or changes of cooling air flow, the efficiency will be influenced. A similar additional evaluation, such as in case of the turbomachinery by mass flow, could be realized by supervising and computing the pressure loss. As, in general, no measuring point has been provided to that purpose in the hardware of the jet engine, this procedure must be desisted from. Anyhow, it may be assumed that variations in efficiency will describe sufficiently the combustion chamber for the purpose of diagnosis.

For module 2, only the ring area A_8 is available as a state variable. It allows, however, only a limited statement on functioning of this module. From the point of view of fluid flow, this module is not subject to a particular strain. Therefore, this reduced diagnostic statement should be sufficient.

For module 7 - the turbine case - only the outlet area A_7 can be referred to. As regards diagnosis, the same considerations as those to module 2 are applicable.

In addition to the state variables which can be clearly attributed to each of the indicated modules, the thrust value measured on the test stand is also referred to as a state variable. Although it does not allow any direct statement with regard to a determined module, nevertheless it provides a possibility to check the accuracy of the measured values and, possibly, an indirect statement on the condition of module 2, i.e. an evaluation of the dividing ratio between the primary and secondary mass flow.

The measured values Y_j must now be selected in a way allowing the intended state variables X_i distinctly to be calculable based thereon, i.e. the relation between state vector $\underline{X} = [X_1,\ldots,X_n]^T$ and the measuring vector $\underline{Y} = [Y_1,\ldots,Y_m]^T$ must be arranged that in terms of system theory an observable problem will be presented. For good conditioning of the system of equations to be set up, it will, therefore, be favourable to make available such measured values Y_j which influence as many states X_i as possible, i.e. which will grant an intense coupling within the system of equations. In detail, the measured values chosen are the following:

1) Environmental conditions:

- Ambient pressure p_0,
- Ambient temperature T_0.

The measured values of p_0 and T_0 will fix the inlet conditions for the jet engine. Thus they influence practically the overall state of the latter.

2) Compressor (module 1, module 3):

- Differential pressure q_1 at inlet,
- Pressure p_2 between low pressure and high pressure compressor,
- Temperature T_2 between low pressure and high pressure compressor,
- Differential pressure q_3 downstream of high pressure compressor,
- Pressure p_3 downstream of high pressure compressor,
- Temperature T_3 downstream of high pressure compressor.

The differential pressure q_1 measured at inlet provides a statement on mass flow through the jet engine. Herewith nearly all of the state variables X_i are influenced by this measured value.

Pressure p_2 and temperature T_2 are measured at the interface between low pressure and high pressure compressor. Whereas pressure p_2 influences decisively the compressor efficiencies and mass flow $\dot{m}_3$ only, temperature T_2 concerns nearly all of the state variables.

The differential pressure q_3 resulting from the difference between the total pressure and the static pressure at the outlet of the high pressure compressor characterizes mainly the primary mass flow.

Pressure p_3 and temperature T_3 at the high pressure compressor outlet influence, except X_1 and X_2 (low pressure compressor), all the other state variables in question.

3) Compressor case transition piece (module 2):

- Pressure p_8.

Pressure p_8 is measured upstream of the ring nozzle. It serves at evaluation of area A_8 and at calculation for checking thrust F, i.e. for the state variables X_{11} and X_{12}.

4) Combustion chamber (module 4):

- Fuel flow $\dot{m}_F$.

Measuring of fuel flow $\dot{m}_F$ serves mainly at evaluation of combustion chamber efficiency η_4.

5) Turbine (module 5, module 6):

- Pressure p_5 between high pressure and low pressure turbine,
- Pressure p_6 downstream of low pressure turbine,
- Temperature T_6 downstream of low pressure turbine.

Pressure p_5 at the interface between high pressure and low pressure turbine serves essentially at evaluation of the turbine section. Though in some jet engines not available as a measuring point, for a safe diagnosis on the turbine section it represents a particularly significant measuring value. From the thermodynamic point of view, this is convincing as for considering the output equilibrium of the two shafts of the engine, only the temperature T_5 can be obtained at that point. A result about pressure p_5 is not obtainable by recalculation.

Pressure p_6 and temperature T_6 are measured values downstream of the low pressure turbine. Both of them serve at evaluation of the turbine section.

6) Compressor/Turbine (module 1,3 ; module 5,6):

- Speed of low pressure shaft n_1,
- Speed of high pressure shaft n_2.

The speeds of n_1 and n_2 of low and high pressure shafts concern the state variables of all turbomachinery.

7) Thrust measurement (module 2):

- Thrust F_m.

Thrust measurement F_m serves at the check of the state variable of thrust F and possibly at evaluation of module 2. That measurement is only possible in case of diagnosis at the test stand, in flight it is not available.

In total there are thus available m = 16 measured values Y_j; based on the previous designations, they are identified as follows:

$$Y_1 = p_0,\ Y_2 = T_0,\ Y_3 = q_1,\ Y_4 = p_2,\ Y_5 = T_2,\ Y_6 = q_3,\ Y_7 = p_3,\ Y_8 = T_3,$$

$$Y_9 = p_5,\ Y_{10} = p_6,\ Y_{11} = T_6,\ Y_{12} = p_8,\ Y_{13} = n_1,\ Y_{14} = n_2,\ Y_{15} = \dot{m}_F,\ Y_{16} = F_m\ .$$

If one now proceeds according to the sections 2.1 and 2.2 and establishes, via working process computing, the relation between measured values and state variables, referring the applicable equations to failure-free nominal conditions and then normalizing them, one obtains

$$\Delta x_i = q_{i,1}\cdot\Delta y_1 + \ldots + q_{i,16}\cdot\Delta y_{16},\quad i=1,\ldots,12 \tag{9a}$$

or in terms of vector and matrix, respectively

$$\underline{\Delta x} = \underline{Q}\cdot\underline{\Delta y}\ . \tag{9b}$$

By Eq. (9b) the (12,1) dimensional state vector $\underline{\Delta x}$ is linked with the (16,1) dimensional measuring vector $\underline{\Delta y}$. The system matrix, therefore, has the dimension of (12,16). In some cases it may be more suitable to write Eq. (9b) in terms of a real measuring equation. Then

$$\underline{\Delta y} = \underline{C}\cdot\underline{\Delta x}\ ,$$

with

$$\underline{C} = \underline{Q}^T\cdot(\underline{Q}\cdot\underline{Q}^T)^{-1} \tag{9c}$$

as a (16,12) dimensional measuring matrix, which results from $\underline{Q}$, from the righthand side as a pseudo-inverse matrix [10].

2.4 Application

The outlines having been so far of general validity, shall now be put into more concrete terms. The jet engine of LARZAC will, therefore, serve as an example.

In jet engine diagnosis, usually one applies Eq. (9) to three different working points: full load (FL), partial load (PL - approx. 75 % of FL), idling (LP). As a first step, in the formulae, the coefficients of the matrix are calculated for the LARZAC jet engine, assuming realistic values for the empirical map characteristics. In the case of full load, this procedure leads to matrix $\underline{Q}$ of Table 1. For the two other load conditions, [7] is referred to. By the given $\underline{Q}$, as an example, a failure of -2 % in x_1, i.e. in the mass flow of the low pressure compressor, and in x_8, respectively, i.e. in the efficiency of the low pressure turbine, shall be diagnosed. The corresponding results are shown in Fig. 2 and Fig. 3.

-0.9988	0.75	0.465	0.1348	0	0	0	0	0	0	0	0	-1.5	0	0	0
0.378	3.83	0	-0.376	-4.22	0	0	0	0	0	0	0	2.34	0	0	0
0	0	0	-1	1.3	0.498	0.588	-0.5	0	0	0	0	0	-1.6	0	0
0	0	0	0.232	1.095	0	-0.232	-2.58	0	0	0	0	0	2.8	0	0
0.0388	-0.213	0.0268	0	0.1383	0.583	-0.59	-0.272	0	0	0.332	0	0	0	0.0166	0
-0.0686	0.418	-0.0525	0	-1.518	0.0616	-1.084	1.709	1.036	0	-0.653	0	0	0	-0.01306	0
0.0383	-0.264	0.0333	0	0.362	0.448	0.463	-0.455	-1	0	0.412	0	0	0	0.016	0
0.425	-2.95	0.369	0	3.36	-0.386	-0.398	0.392	-2.635	2.635	-1.155	0	0.8	0	-0.0155	0
0.131	-0.91	0.114	0	0.555	0.292	0.484	-0.397	0	0	1.42	0	0	0	-0.98	0
0	0	0	0	0	0.463	0.498	-0.49	0	-1	0.5	0	0	0	-0.0194	0
1	-0.935	0.87	0	0.5	-0.427	-0.441	0.436	0	0	0	-1	0	0	0	0
-0.26	-0.419	0.375	0	-0.225	0.885	0.888	-0.8865	0	0.43	0.288	0.277	0	0	0.011	-1

Table 1 System matrix $\underline{Q}$ for the load state of full load (FL).

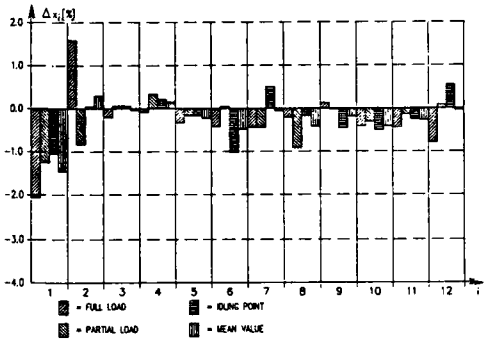

Fig. 2 Diagnosis of an error in module 1 ($\Delta x_1 = -2$ %).

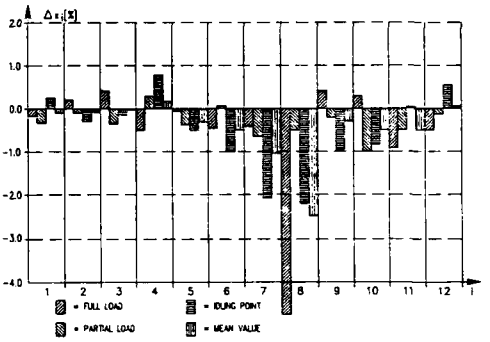

Fig. 3 Diagnosis of an error in module 6 ($\Delta x_8 = -2$ %).

There are indicated all the twelve state variables for the three different working points and moreover *the linear mean values* of the state variables over the three working points. It can be seen from Fig. 2 that each error is sufficiently well detected. Nevertheless there are still defects in the mathematical model, for in the case of (FL), the state of Δx_2 is affected and also in the further failure-free states, there may occur indications up to $\pm$ 1 %, which should not exist. This becomes even more obvious in Fig. 3, where the detection in state Δx_8 is useful only under a qualitative aspect and the "basic noise" of the failure-free states attains roughly the range of $\pm$ 1 %. This behaviour is founded on an inaccurate determination of matrix $\underline{Q}$, in particular with regard to the partial derivatives of the empirical map characteristics as mentioned in section 2.2. It is, therefore, recommendable to readjust the system matrix $\underline{Q}$. This can be carried out by a procedure at a mathematical model of a jet engine, at which prescribed errors are simulated. The way of proceeding is as follows:

A detailed analysis of the 12 equations (9a) shows that their coefficients $q_{i,j}$ for the first eight equations are of the type of

$$q_{i,j} = a_{i,j} + b_{i,j}\cdot\rho_i + c_{i,j}\cdot\varepsilon_i \quad , \quad i=1,\ldots,8; \quad j=1,\ldots,16 \quad , \tag{10}$$

where $a_{i,j}$, $b_{i,j}$, and $c_{i,j}$ being accurately known figures, whereas ρ_i and ε_i are the rather inaccurately known gradients of the map characteristics (cf. Eq. (8)).

With

$$a_i = \sum_{j=1}^{16} a_{i,j}\cdot\Delta y_j \quad , \quad b_i = \sum_{j=1}^{16} b_{i,j}\cdot\Delta y_j, \quad c_i = \sum_{j=1}^{16} c_{i,j}\cdot\Delta y_j \tag{11}$$

Eq. (9a) can then be rewritten as

$$\Delta x_i = a_i + b_i\cdot\rho_i + c_i\cdot\varepsilon_i \quad , \quad i=1,\ldots,8 \quad . \tag{12}$$

If now failure-free measurements of Δy_j are assumed, the case <u>without</u> model defects is described as

$$\Delta x_{i,0} = a_i + b_i\cdot\rho_{i,0} + c_i\cdot\varepsilon_{i,0} \tag{13a}$$

or the model defects themselves result from the difference of Eq. (12) and Eq. (13a) in

$$(\Delta x_i - \Delta x_{i,0}) = b_i\cdot(\rho_i - \rho_{i,0}) + c_i\cdot(\varepsilon_i - \varepsilon_{i,0}) \quad . \tag{13b}$$

By the linear approximation of

$$\rho_{i,0} = \rho_i + \Delta\rho_i \quad , \quad \varepsilon_{i,0} = \varepsilon_i + \Delta\varepsilon_i \tag{14a}$$

as well as by

$$\delta\Delta x_i = \Delta x_i - \Delta x_{i,0} \tag{14b}$$

Eq. (13b) results in

$$\delta\Delta x_i = b_i \cdot \Delta\rho_i + c_i \cdot \Delta\varepsilon_i \quad , \qquad i=1,\ldots,8 \quad . \tag{14c}$$

If now in the jet engine model $k \geq 2$ different errors are simulated, Eq. (14c) passes over to the superposed equation system of

$$\delta\underline{\Delta x}_i = \underline{Y}_i \cdot \begin{bmatrix} \Delta\rho_i \\ \ldots \\ \Delta\varepsilon_i \end{bmatrix} \quad , \qquad i=1,\ldots,8 \tag{15}$$

with $\delta\underline{\Delta x}_i$ as the (k,1) dimensional model defect vector and $\underline{Y}_i$ as the (k,2) dimensional "measuring" matrix. For the corrections of $\Delta\rho_i$ and $\Delta\varepsilon_i$ one obtains then at once from Eq. (15)

$$\begin{bmatrix} \Delta\rho_i \\ \ldots \\ \Delta\varepsilon_i \end{bmatrix} = (\underline{Y}_i^T \cdot \underline{Y}_i)^{-1} \cdot \underline{Y}_i^T \cdot \delta\underline{\Delta x}_i \quad , \; i=1,\ldots,8 \quad . \tag{16}$$

By Eq. (14a) improved parameters of $\rho_{i,0}$ and $\varepsilon_{i,0}$ can herewith be determinded, and they yield, by Eq. (10), improved elements of $q_{i,j}$ for system matrix $\underline{Q}$ in Eq. (9).

$\underline{Q}$ =

-0.7361	0.8389	0.463	0.2731	0	0	0	0	0	0	0	0	-1.6779	0	0	0
-0.6724	3.7948	0	0.6724	-4.22	0	0	0	0	0	0	0	0.9984	0	0	0
0	0	0	-1.1612	1.5486	0.492	0.6692	-0.5	0	0	0	0	0	-2.8807	0	0
0	0	0	-0.7856	2.5095	0	0.7856	-2.59	0	0	0	0	0	-0.0292	0	0
0.0338	-0.234	0.0294	0	0.143	0.4797	-0.039	-0.2421	-0.5267	0	0.3647	0	0	-0.1862	0.0163	0
-0.3693	0.4763	-0.0502	0	-1.5557	0.0674	-0.9855	1.7212	0.9569	0	-0.7472	0	0	0.3087	-0.0131	0
0.0384	-0.2659	0.0334	0	0.3026	0.4471	0.4619	-0.4545	0.0869	-1.0866	0.4147	0	-0.0054	0	0.016	0
0.4543	-3.1456	0.3948	0	3.5797	-0.4127	-0.427	0.4198	-0.879	0.8879	-0.8197	0	-0.0128	0	-0.0167	0
0.131	-0.91	0.114	0	0.586	0.392	0.406	-0.397	0	0	1.42	0	0	0	-0.98	0
0	0	0	0	0	0.483	0.498	-0.49	0	-1	0.5	0	0	0	-0.0196	0
1	-0.935	0.87	0	0.5	-0.427	-0.441	0.434	0	0	0	-1	0	0	0	0
-0.26	-0.419	0.375	0	-0.225	0.085	0.088	-0.0865	0	0.43	0.288	0.277	0	0	0.011	-1

Table 2 Improved system matrix $\underline{Q}$ for the load state of full load (FL).

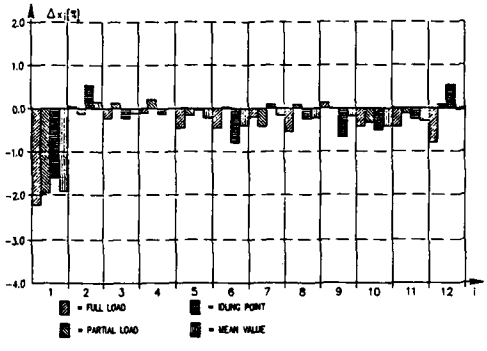

Fig. 4 Diagnosis of an error in module 1 ($\Delta x_1 = -2$ %) for improved model.

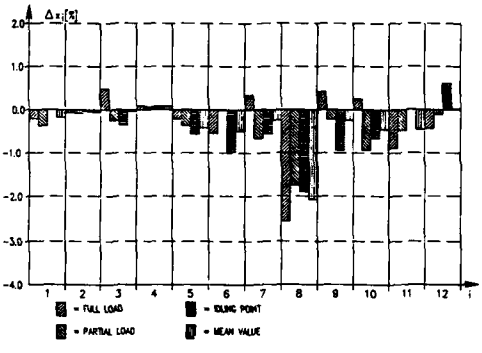

Fig. 5 Diagnosis of an error in module 6 ($\Delta x_8 = -2$ %) for improved model.

The procedure described was carried out for k = 20 error simulation runs and has made available the new improved system matrix $\underline{Q}$ in Table 2. The corresponding error detection of Fig. 2 and Fig. 3 with the new $\underline{Q}$ is shown in Fig. 4 and Fig. 5. The comparison between Figures 2 and 4 clearly evidences that the affection of Δx_2 in the case of (FL) has been eliminated and that also the other failure-free states are situated distinctly below $\pm$ 1 %. In Fig. 5, the diagnosis of state Δx_8 is now also quantitatively useful, the "basic noise" of the failure-free states has remained in its order of magnitude. There is to be noted that the measuring technology used for the error simulation runs has an accuracy of $\pm$ 1 % only with regard to the Δx_i, i.e. the validation of the mathematical model can then on principle not be more accurate than that value.

The used procedure of readjusting the system matrix $\underline{Q}$, i.e. solution of Eq. (15), is nothing else than proceeding in terms of minimizing according to the least squares method. If you refer to the weighted version of the procedure [11], Eq. (16) passes over to

$$\begin{bmatrix}\Delta\rho_i\\ \dots\\ \Delta\varepsilon_i\end{bmatrix} = (\underline{Y}_i^T\cdot\underline{W}_i\cdot\underline{Y}_i)^{-1}\cdot\underline{Y}_i^T\cdot\underline{W}_i\cdot\delta\Delta\underline{x}_i \quad , \qquad i=1,\dots,8 \quad . \tag{17}$$

Herein $\underline{W}_i = \mathrm{diag}(w_{jj})$, $j=1,\dots,k$, is a (k,k) dimensional weighting matrix, through which particular simulation runs with sensor errors, which are more precisely known than others, can be weighted more intensely. This leads to a further improvement of accuracy of the model, i.e. to still more qualified system matrices $\underline{Q}$. If, however, the physical basis of modelling is deficient to an extent that the linear approximation of Eq. (14a) will not be good enough, one may use for iteration Eq. (16) or (17). In general two iterations will do to achieve a model accuracy below $\pm$ 1 %.

The procedure outlined above for the improvement of the mathematical engine model says nothing by now regarding the last four equations of Eq. (9a). These equations are independent of the gradients of the map characteristics, and the coefficients $q_{i,j}$ are pure constants. Nevertheless, they can be included in an algorithm for improvement. The procedure is a little bit different from that given for the first eight equations. Details for this are outlined in [7] and in [12].

The corrections $\Delta\rho_i$ and $\Delta\varepsilon_i$ obtained from Eq. (16) and Eq. (17) are so large in some cases that the new gradients in Eq. (14a) are outside of their physical meanings. In order to avoid this the calculation procedure for $\Delta\rho_i$ and $\Delta\varepsilon_i$ has to be modified in such a way that $\Delta\rho_i$ and $\Delta\varepsilon_i$ are constrained. This can be done by introducing penalty functions. By this the calculation procedure becomes nonlinear, thus requiring an iterative solution. For this a comprehensive computer program is developed published in [13]. The program is suitable for engines with any n and any m state and measurement variables, respectively. Additionally, the case of any p equations independent of the gradients of the map characteristics is considered. One can say that with this computer program an automated modelling for any class of modern jet engines can be achieved.

3. ESTIMATION OF STATE

The model shows the relation between the state vector $\Delta\underline{x}$ and the measurement vector $\Delta\underline{y}$ by the structure of Eq. (9b) and, derived from there, by Eq. (9c). If $\Delta\underline{y}$ is known, $\Delta\underline{x}$ can, therefore, be found immediateley from Eqs. (9), as has been practised before. The assumption in that case is, however, that $\Delta\underline{y}$ is free of failures. As this is not the rule, Eq. (9b) has in fact to be written as follows:

$$\Delta\underline{x} = \underline{Q}\cdot[\Delta\underline{y} - \underline{v} - \delta(\Delta\underline{y})] \tag{18a}$$

and Eq. (9c) goes over in

$$\Delta\underline{y} = \underline{C}\cdot\Delta\underline{x} + \underline{v} + \delta(\Delta\underline{y}) \quad . \tag{18b}$$

Herein, the (16,1) dimensional vector $\underline{v}$ considers the measuring noise in $\Delta\underline{y}$. By the (16,1) dimensional vector $\delta(\Delta\underline{y})$ systematic sensor errors are described in $\Delta\underline{y}$, which have been caused by d.ift of the zero point for example. As $\underline{v}$ and $\delta(\Delta\underline{y})$ are unknown, now $\Delta\underline{x}$ can no more be determined directly from (18). Consequently, an estimation algorithm has to be applied, which allows for $\Delta\underline{x}$, with reference to the algorithm used, the best possible estimation $\Delta\hat{\underline{x}}$ of $\Delta\underline{x}$. As in that context stochastic and deterministic (systematic) sensor errors must be treated distinctly, in the following at first $\delta(\Delta\underline{y})$ is set to zero and only $\underline{v}$ will be considered.

3.1 Stochastic sensor errors

If only stochastic sensor errors (noise) occur with $\underline{v}$, Eq. (18b) is written as follows:

$$\Delta\underline{y} = \underline{C}\cdot\Delta\underline{x} + \underline{v} \quad . \tag{19}$$

A general way of estimating $\Delta\underline{x}$ by $\Delta\hat{\underline{x}}$ can now be taken from

$$\Delta\hat{\underline{x}} = \underline{b} + [\underline{B}+\underline{C}^T\cdot\underline{A}\cdot\underline{C}]^{-1}\cdot\underline{C}^T\cdot\underline{A}\cdot(\Delta\underline{y}-\underline{C}\cdot\underline{b}) \quad . \tag{20}$$

Here we first assume that only one single measurement vector $\Delta\underline{y}$ exists, which means that the estimation by Eq. (20) is based on a so-called "snapshot".

According to selections of vector $\underline{b}$ as well as of matrices $\underline{A}$ and $\underline{B}$, various procedures of estimation being known in literature [11] result from Eq. (20). If for example $\underline{b} = \underline{0}$ and $\underline{B} = \underline{0}$, there results with $\underline{A} = \underline{G} = \mathrm{diag}(g_{jj})$ the estimation of

$$\Delta\hat{\underline{x}} = (\underline{C}^T\cdot\underline{G}\cdot\underline{C})^{-1}\cdot\underline{C}^T\cdot\underline{G}\cdot\Delta\underline{y} \quad , \tag{21}$$

i.e. the weighted minimation of error by the least squares method (WLS) also referred to in Eq. (17), which for $\underline{G} = g\cdot\underline{I}$, g = const. passes over into its unweighted version. The estimator described by Eq. (21) is most easy. Moreover it has the advantage that nothing else has to be known about the noise vector $\underline{v}$ but the mean value freedom of its components. In case you know additionally that the realizations of the $\underline{v}$ components are normally distributed, you will obtain by $\underline{G} = \underline{R}^{-1}$ from Eq. (21) the Maximum Likelihood Estimator (MLS), wherein $\underline{R}$ is the matrix of covariances belonging to $\underline{v}$ and $\Delta\underline{y}$, respectively. Thus the estimators of (WLS) and of (MLS) distinguish themselves formally only by the choice of their weighting matrix $\underline{G}$.

The case of just one single measurement vector $\Delta\underline{y}$ is rare. As a rule, due to time-discrete scanning, several measurement vectors $\Delta\underline{y}_i$, $i=1,\dots,r$, arise. Assuming that the model characteristics as fixed by measuring matrix $\underline{C}$ remain unchanged during scanning from $i = 1$ to $i = r$, the measurement vectors $\Delta\underline{y}_i$ lead to the estimation of

$$\Delta\hat{\underline{x}} = \frac{1}{r}\cdot(\underline{C}^T\cdot\underline{G}\cdot\underline{C})^{-1}\cdot\underline{C}^T\cdot\underline{G}\cdot\sum_{i=1}^{r}\Delta\underline{y}_i \quad . \tag{22}$$

That is the non-recurrent formulation of the (WLS) or (MLS) estimator, respectively, which makes particularly clear that those procedures of estimation involve a mean value formation with a variable weighting of the different sampling chanels.

Based on Eq. (20), only estimation algorithms comprising no a priori information were considered so far with $\underline{b} = \underline{0}$ and $\underline{B} = \underline{0}$. If for example with $\underline{b} = \underline{x}_0$ an initial approach for $\Delta\underline{x}$ or $\Delta\hat{\underline{x}}$ is available, and with $\underline{B} = \underline{M}$ a weighting matrix is given for weighting the error between $\Delta\underline{x}$ and $\Delta\underline{x}_0$, then by

$$\Delta\hat{\underline{x}} = \Delta\hat{\underline{x}}_0 + (\underline{M}+\underline{C}^T\cdot\underline{G}\cdot\underline{C})^{-1}\cdot\underline{C}^T\cdot\underline{G}\cdot(\Delta\underline{y}-\underline{C}\cdot\Delta\hat{\underline{x}}_0) \tag{23}$$

an estimation according to the extended weighted minimation of error by the least squares method (EWLS) is described [11]. Apart from the requirement of mean value freedom of the components of $\underline{v}$, also for application of Eq. (23), no other conditions are claimed. However, in case there exists the additional information that $\underline{v}$ and $\Delta\underline{x}$ are normally distributed and the mean value of $\Delta\underline{x}$ is available by $\underline{b} = \bar{\underline{x}}$, with $\underline{M} = \underline{P}^{-1}$ and $\underline{G} = \underline{R}^{-1}$ the (EWLS) estimator of Eq. (23) passes over into the Bayes Estimator (BS)

$$\Delta\hat{\underline{x}} = \Delta\bar{\underline{x}} + (\underline{P}^{-1}+\underline{C}^T\cdot\underline{R}^{-1}\cdot\underline{C})^{-1}\cdot\underline{C}^T\cdot\underline{R}^{-1}(\Delta\underline{y}-\underline{C}\cdot\Delta\bar{\underline{x}}) \quad . \tag{24}$$

Herein - as formerly in the (MLS) estimator - $\underline{R}$ is the matrix of covariances of $\underline{v}$ and $\Delta\underline{y}$, and $\underline{P}$ is the corresponding covariance matrix of the error in $\Delta\bar{\underline{x}}$ or of $\Delta\underline{x}$ itself, respectively. There can be expected that estimators of the type of Eqs. (23) and (24) will lead to more efficient results than those obtainable by Eq. (21), provided that with $\Delta\underline{x}_0$ and $\underline{M}$ or $\Delta\bar{\underline{x}}$ and $\underline{P}$ adequate a priori information can be made available. Of course, also in Eqs. (23) and (24), there exist several measurement vectors $\Delta\underline{y}_i$, i=1,...,r, suitable for determination of $\Delta\hat{\underline{x}}$. If one assumes again that the model characteristics remain unchanged during generation of $\Delta\underline{y}_i$, i.e. that measuring matrix $\underline{C}$ is constant, for this case Eq. (23) becomes

$$\Delta\hat{\underline{x}} = (\frac{1}{r}\cdot\underline{M}+\underline{C}^T\cdot\underline{G}\cdot\underline{C})^{-1}\cdot(\frac{1}{r}\cdot\underline{M}\cdot\Delta\hat{\underline{x}}_0 + \frac{1}{r}\cdot\underline{C}^T\cdot\underline{G}\cdot\sum_{i=1}^{r}\Delta\underline{y}_i) \quad . \tag{25}$$

As an analogy to Eq. (22), this is the non-recurrent version of the (EWLS) estimator or, for $\Delta\hat{\underline{x}}_0 = \Delta\bar{\underline{x}}$ and $\underline{M} = \underline{P}^{-1}$, of the (BS) estimator. From Eq. (25) it appears with particular clearness that significance of the (EWLS) and (BS) estimators, as compared to the (WLS) and (MLS) estimators, refers to low values of r. For high values of r, there results

$$\frac{1}{r}\cdot\underline{M} \ll \underline{C}^T\cdot\underline{G}\cdot\underline{C} \quad , \quad \frac{1}{r}\cdot\underline{M}\cdot\Delta\hat{\underline{x}}_0 \ll \underline{C}^T\cdot\underline{G}\cdot\Delta\bar{\underline{y}} \quad , \tag{25a}$$

if $\Delta\bar{\underline{y}}$ is the vector of the mean values $\Delta\bar{y}_j$, j=1,...,16, from the individual measurements Δy_{ij}, i.e. Eq. (25) is in the limiting case $r\to\infty$ identical to Eq. (22). It may be summarized that we can assume to be able, in case of good a priori information in $\Delta\hat{\underline{x}}_0$ and $\underline{M}$, to reduce substantially the number r of the measurement vectors to be treated in order to obtain a determined accuracy in the state estimation.

In order to be able to judge the efficiency of the estimators in Eq. (22) and in Eq. (25) they are applied to the example given in Fig. 4, in which an error of $\Delta x_1 = -0{,}02$ (-2 %) has to be diagnosed. As a reference for judgement, the error scale of

$$e(r) = \sqrt{\frac{1}{12}\cdot\sum_{i=1}^{12}[\Delta x_i(r)-\Delta x_{i,0}]^2} \tag{26}$$

is used, in which $\Delta x_{i,0}$ are the set states and $\Delta x_i(r)$ are the real states. Via the squared mean value $e^2(r)$ the behaviour of convergence of the estimator is described. Furthermore $e(r\to\infty)$ yields a scale for model accuracy. Fig. 6 shows for the case of full load (FL) the course of e(r) for the two different standard deviations of $\sigma = 10^{-1}$ and 10^{-2}. It was assumed that all of the 16 sensors are subject to the same standard deviation and that, therefore, the (MLS) estimator passes over into an unweighted (WLS) estimator. The taken choice of σ means in consequence of the standardized Eq. (19) as noise of either 10 %, or 1 % referred to the physical measured values Y_j, j=1,...,16, of Eq. (1). In detail Fig. 6 points out that the (EWLS) estimator in comparison to the (WLS) estimator is throughout faster in the convergence. Both estimators meet the expectations which means that both estimators are consistent - as known from literature [11].

The difficulty in applying estimators with a priori information is due to selection and knowledge of that information itself. In the present case of error detection it seems useful to set $\Delta\hat{\underline{x}}_0$ to zero, i.e. to take the failure-free state as an a priori information. Fixation of the weighting matrix $\underline{M}$ or of the covariance matrix $\underline{P}$ is more difficult. Whereas in case of $\underline{G}$ and $\underline{R}$ the choice of diagonal matrices seems logical, since one can suppose that the meas-

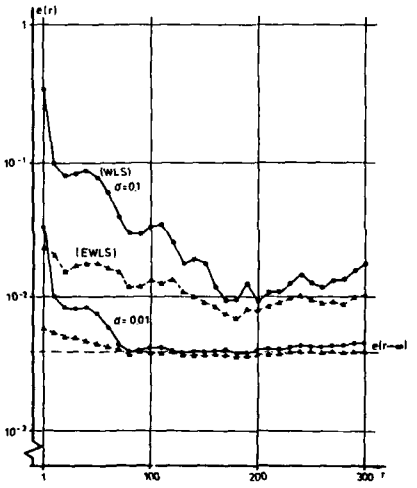

Fig. 6 Filter results for the example of Fig. 4.

urements Δy_j, j=1,...,16, are uncorrelated, there will certainly be correlations between the various states Δx_i, i=1,...,12. This means covariances different from zero in $\underline{P}$ and herewith fully filled-in matrices of $\underline{P}$ or $\underline{M}$, respectively. As the covariances are not known, $\underline{M}$ has here been used also as a diagonal matrix. By simulation it was found that for the example of Fig. 6 it is suitable to set $\underline{M} = \mathrm{diag}(m_{ii})$; $m_{ii} = 10$. This value results from an easy coordination by numbers to $\underline{C}^T \cdot \underline{R}^{-1} \cdot \underline{C}$ in the first bracket of Eq. (25) and is valid also for errors to be diagnosed in other states Δx_i. If the measuring matrix $\underline{C}$, however, changes for example due to another case of load, $\underline{M}$ must be newly found. This makes evident that the use of Eq. (25) is likely to put some problems, at least the fixing of $\underline{M}$ may require lasting preparatory work.

3.2 Systematic sensor errors

Systematic sensor errors exceeding the introductory remarks of chapter three have not been treated so far with regard to jet engine diagnosis. This shall be done now.

In Eq. (18) systematic sensor errors were modelled by means of vector $\delta(\Delta\underline{y})$. In fact, $\delta(\Delta\underline{y})$ comprises further model defects, too, as can be gathered from Fig. 4 and Fig. 5 for example. Before a detailed calculation is carried out, there are to be mentioned some matters of principle regarding the detection of systematic sensor errors. Considering the historical development, hardware solutions, by which a technical redundancy was generated by several sensors, have been of prime interest so far. This way of proceeding is of high expenditure regarding work and cost. Also in consequence of high weight, among other subjects, for aircraft jet engines its use is possible in rare exceptional cases only. Procedures with analytical redundancy, in which sensor errors are determined by software, via appropriate algorithms of detection, are more favourable in this aspect. A detailed survey to the subject is to be found in [14]. According thereto, at the present state of the art, three different ways of proceeding for detection of sensor errors are used, i.e. detection by error sensitive filters, by multiple hypothesis filters and by innovative filters. In the case of error sensitive filters, the method of state vector extension has proved particularly successful. It is suitable for detection of model defects and of systematic sensor errors. Compared to other methods it has the advantage of finding out also creeping errors, such as those occurring by ageing. The drawback is that the determination of errors lacks observability. The multiple hypothesis filters are based in general on bancs of filters and observers, respectively. The filter which shall detect an error will be especially sensitized with regard to that error, in relation to the other filters. Thereupon, in a decision logic, the results of the estimates produced under different hypotheses are evaluated. This may for example take place via the residues belonging to the estimators [15]. The method, which on principle is effective, requires a high expenditure of software and has the drawback that only such sensor errors are detected that occur during data monitoring. A priori errors are not discoverd. Innovative filters have the same drawback, and moreover they only respond to errors in form of jumps. It is true that regarding their expenditure they are more favourable than multiple hypothesis filters. When using innovative filters, error detection is reached by the aid of statistical tests, in which the employment of a generalizing likelihood ratio has proved useful [16].

The systematic sensor errors contained in $\delta(\Delta\underline{y})$ shall now be determinded in detail by the method of state vector extension in combination with a hypothesis test. To that purpose one takes recourse to Eq. (18), and it is assumed that all stochastic components of error $\underline{v}$ are eliminated. Then $\Delta\underline{x}$ and $\delta(\Delta\underline{y})$ are unknown in Eq. (18). Thus the (16,1) dimensional measurement vector $\Delta\underline{y}$ allows besides the determination of the (12,1) dimensional state vector $\Delta\underline{x}$ additionally the determination of four components of $\delta(\Delta\underline{y})$ at maximum, if Eq. (18b) for determination of $\delta(\Delta\underline{y})$ is used. In the case of Eq. (18a) first no sensor error can be determined.

For reasons of generality it is now assumed that m sensors are present and that the number of sensor errors is $k \leq m$. If these errors are pure offsets and this is supposed, then they can be modelled by

$$\delta(\Delta\underline{y}) = \underline{G} \cdot \underline{s} \quad . \tag{27}$$

In Eq. (27) $\underline{G}$ is a (m,k) dimensional weighting matrix and $\underline{s}$ is the (k,1) dimensional vector of the sensor errors. Using Eq. (18b) in combination with Eq. (27) one gets

$$\Delta\underline{y} = [\underline{C} : \underline{G}] \cdot \begin{bmatrix} \Delta\underline{x} \\ \cdots \\ \underline{s} \end{bmatrix} \quad . \tag{28}$$

From this follows for the (n,1) dimensional state

$$\Delta\underline{x} = [(\underline{C}^T - \underline{\Omega}) \cdot \underline{C}]^{-1} \cdot (\underline{C}^T - \underline{\Omega}) \cdot \Delta\underline{y} \quad , \tag{29a}$$

and for the sensor errors

$$\underline{s} = (\underline{G}^T \cdot \underline{G})^{-1} \cdot \underline{G}^T \cdot (\Delta\underline{y} - \underline{C} \cdot \Delta\underline{x}) \quad , \tag{29b}$$

where with

$$\underline{\Omega} = \underline{C}^T \cdot \underline{G} \cdot (\underline{G}^T \cdot \underline{G})^{-1} \cdot \underline{G}^T$$

a (n,m) dimensional auxiliary matrix is introduced. Under the assumption of maximal rank of $\underline{C}$ in Eq. (28) $k = m - n$ sensor errors are admissible. In relation to the jet engine there are several working points available. If the number of working points is r and the normalization of the measurement equation is done in such a way that one gets in each working point the same state vector $\Delta\underline{x}$, it then follows from Eq. (18b)

$$\Delta\underline{y}_i = \underline{C}_i \cdot \Delta\underline{x} \quad , \quad i=1,\ldots,r \tag{30}$$

for the sensor error-free case. If one now normalizes the sensor errors on the working point 1 (arbitrarily

chosen) it is

$$\delta(\Delta\underline{y}_i) = \underline{N}_i \cdot \delta(\Delta\underline{y}_1) \tag{31a}$$

and with Eq. (27)

$$\delta(\Delta\underline{y}_i) = \underline{N}_i \cdot \underline{G} \cdot \underline{s} \quad , \quad i=1,\ldots,r \quad . \tag{31b}$$

The matrices $\underline{N}_i$, i=1,...,r, in (31) are (m,m) dimensional normalization matrices with $\underline{N}_1 = \underline{I}$. If one now puts together Eqs. (30) and Eqs. (31) one gets

$$\begin{bmatrix} \Delta\underline{y}_1 \\ \vdots \\ \Delta\underline{y}_r \end{bmatrix} = \begin{bmatrix} \underline{C}_1 & : & (\underline{N}_1 \cdot \underline{G}) \\ \vdots & : & \vdots \\ \underline{C}_r & : & (\underline{N}_r \cdot \underline{G}) \end{bmatrix} \cdot \begin{bmatrix} \Delta\underline{x} \\ \cdots \\ \underline{s} \end{bmatrix} \quad . \tag{32}$$

The solution of Eq. (32) is

$$\begin{aligned} \Delta\underline{x} &= \left[\sum_{\kappa=1}^{r} (\underline{C}_\kappa^T - \underline{\Omega}_\kappa) \cdot \underline{C}_\kappa\right]^{-1} \cdot \sum_{i=1}^{r} (\underline{C}_i^T - \underline{\Omega}_i) \cdot \Delta\underline{y}_i \quad , \\ \underline{s} &= \left[\sum_{j=1}^{r} (\underline{N}_j \cdot \underline{G})^T \cdot (\underline{N}_j \cdot \underline{G})\right]^{-1} \cdot \sum_{i=1}^{r} (\underline{N}_i \cdot \underline{G})^T \cdot (\Delta\underline{y}_i - \underline{C}_i \cdot \Delta\underline{x}) \quad . \end{aligned} \tag{33}$$

Similar to $\underline{\Omega}$ in Eq. (29a) now the auxiliary matrices $\underline{\Omega}_i$ are defined by

$$\underline{\Omega}_i = \sum_{\nu=1}^{r} \underline{C}_\nu^T \cdot (\underline{N}_\nu \cdot \underline{G}) \cdot \left[\sum_{j=1}^{r} (\underline{N}_j \cdot \underline{G})^T \cdot (\underline{N}_j \cdot \underline{G})\right]^{-1} \cdot (\underline{N}_i \cdot \underline{G})^T \quad .$$

Because of the several working points r, now the admissible number k of sensor errors is

$$k \leq r \cdot m - n \quad . \tag{34}$$

For k = m, i.e. all m sensors have offsets,

$$r \geq 1 + \frac{n}{m} \tag{35a}$$

working points are necessary. In the other case with k = 0 it is

$$r \geq \frac{n}{m} \quad . \tag{35b}$$

By this it is seen that the number r of working points reduces the number of sensors m in order to solve the diagnosis problem, the solution of which is the state vector $\Delta\underline{x}$. If one takes into account Eq. (18a) a similar theory with similar results can be found. This case it is referred to in [9].

For k = m the diagnosis problem is completely solved by Eq. (33). However, generally it is k < m and because of this it is not known how to choose the weighting matrix $\underline{G}$ and how the number k. Therefore Eq. (33) now is combined with a hypothesis test. If one assumes that with k = 1 only one sensor error is present then one has with H_q, q=1,...,m, a number of h = m hypotheses that in one of the m sensors is an error or not. If we have two sensor errors, then there exist

$$h = \frac{m!}{2 \cdot (m-2)!}$$

hypotheses $H_{p,q}$, p=2,...,m; q=1,...,m-1, and for an arbitrary number k it is

$$h = \frac{m!}{k!(m-k)!}$$

for the hypotheses $H_{p,\ldots,q}$, p=2,...,m; ...; q=1,...,m+1-k. As decision criterion for the different hypotheses Eq. (30) can be used. This equation namely bases on the fact that in a sensor error-free case the state is always $\Delta\underline{x}$. If sensor errors are present this cannot be true anymore. This can be taken into mathematical equations in the following way: For each hypothesis $H_{p,\ldots,q}$ there exist for r working points r state vectors $(\Delta\underline{x}_{p,\ldots,q})_i$, i=1,...,r, which have a vector of mean values

$$(\Delta\underline{x}_{p,\ldots,q})_M = \frac{1}{r} \cdot \sum_{i=1}^{r} (\Delta\underline{x}_{p,\ldots,q})_i \quad . \tag{36}$$

To this and to the different $(\Delta\underline{x}_{p,\ldots,q})_i$ belongs a (n,n) dimensional covariance matrix $\underline{R}_{p,\ldots,q}$, which has the trace

$$\text{trace } \underline{R}_{p,\ldots,q} = \frac{1}{r-1} \cdot \sum_{j=1}^{n} \sum_{i=1}^{r} [(\Delta x_{j,p,\ldots,q})_i - (\Delta x_{j,p,\ldots,q})_M]^2 \quad . \tag{37}$$

Thereby the index j in Eq. (37) denotes the components of the vectors $(\Delta\underline{x}_{p,\ldots,q})_i$ and $(\Delta\underline{x}_{p,\ldots,q})_M$, respectively. If there are no sensor errors available it is $\Delta\underline{x}_i = \Delta\underline{x} = \Delta\underline{x}_M$ and

$$\text{trace } \underline{R}_{p,\ldots,q} = \text{trace } \underline{R} = 0 \quad . \tag{38}$$

This is also the case for a correct choice of the hypothesis $H_{p,\ldots,q}$, that means when the sensor errors are placed in the right sensors. In the practical realization the condition of Eq. (38) will be fulfilled only approximately because of the fact that there are small model defects yet. Nevertheless, the relating trace will become very small. The task of finding the correct hypothesis therefore finally consists in detecting the minimum

$$\min_{p,\ldots,q} \{\text{trace } \underline{R}_{p,\ldots,q}\} \quad . \tag{39}$$

Eq. (39) delivers the right combination of sensors in which errors are present.

For this an example: In [8] a reduced model of the two-shaft jet engine LARZAC with n = 9 state and m = 13 measurement variables is considered. In this model an error of 1 % is simulated related to the measurement value in the sensor 7 which measures the temperature behind the high pressure compressor. The traces $\underline{R}_p$ of the 13 sensors are given in Fig. 7 and it can be seen that the defective sensor 7 is isolated in an impressive manner.

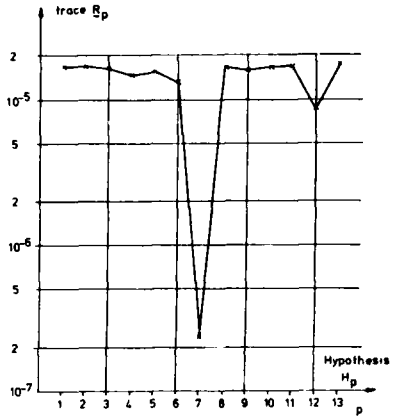

Fig. 7 Detection of sensor errors in the case of one defective sensor.

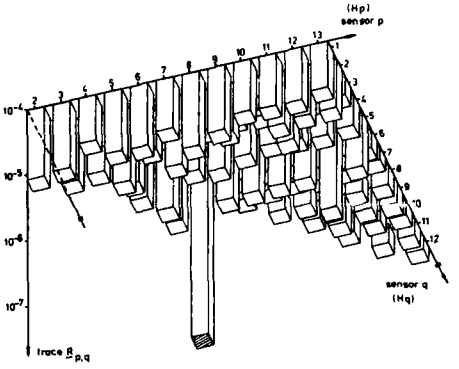

Fig. 8 Detection of sensor errors in the case of two defective sensors.

In addition to the example in Fig. 7 a second sensor error in sensor 5 is simulated. This error has also a value of 1 % related to its measurement value. Sensor 5 is the temperature sensor between the low and the high pressure compressor. Now, 78 hypotheses have to be proven. The traces $\underline{R}_{p,q}$ of all these combinations are illustrated in Fig. 8. Similar to Fig. 7 also in the case of two sensor errors the isolation of the right sensor error combination is perfect.

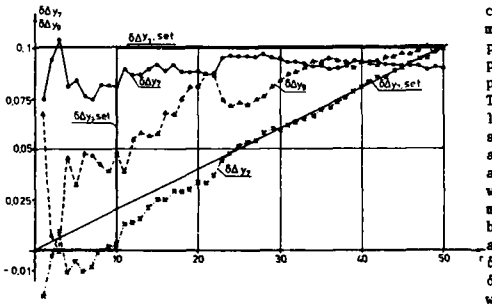

Fig. 9 Filter results for stochastic and systematic sensor errors.

Detection of systematic sensor errors can, of course, be combined with filtering of noise affected measuring data as referred to in section 3.1. This is particularly simple due to the fact that a linear problem is concerned, and the solution of the two parts of the task will be achieved by superposition. To demonstrate this, the example of Fig. 4 was selected to be simulated for stochastic and systematic sensor errors at the same time by the aid of a (WLS) algorithm. For all sensors, a uniform standard deviation of $\sigma = 0{,}01$ was fixed, and systematic errors were assumed in sensors 7 and 9. For sensor 9 a measuring error in form of a jump of $\delta\Delta y_9 = 0{,}1$ to begin with the tenth scanning step, and for sensor 7 alternatively a measuring error in form of a jump of $\delta\Delta y_7 = 0{,}1$ or a growing linear measuring error of $\delta\Delta y_7 = 0{,}1 \cdot r/50$ to begin with the first scanning step were set. The results are to be found in Fig. 9. Here it becomes evident that the sensor errors in form of a jump are very well detected and that also the linearly variable error is discoverd.

4. OUTLOOK

In the present investigation, the diagnostic problem is treated and also analytically solved by the example of a modern aircraft two-shaft jet engine. A diagnosis is particularly effective in case it can be made on-line, i.e. in real time. To that purpose, for trial on the test station, a FORTRAN diagnosis program fulfilling the mentioned task was developed [7]. For the future, an inflight diagnosis has been envisaged. This requires as well a satisfactory equipment with instruments as a sufficiently large computer capacity on board of the aircraft. One can count upon that equipment in future aircraft generations. Then it will become worth-while to reconsider the replacement of steady-state models by dynamic ones. This will provide substantial advantages regarding the data available for a diagnosis, but it will require a further increase of computer capacity.

REFERENCES

[1] De Hoff, R.L.; Hall, W.E.jr.: Advanced Fault Detection and Isolation Methods for Aircraft Turbine Engines. Office of Naval Research Report ONR-CR-215-245-1, Arlington, USA, 1978.

[2] Barschdorff, D. (Ed.): Verfahren und Systeme zur technischen Fehlerdiagnose. GMR-Bericht 1 zum Ausprachetag "Diagnosesysteme", 2.-3. April, Langen 1984.

[3] Isermann, R.: Diagnosemethoden mit Modellbildung. In: [2].

[4] Urban, L.A.: Gas Path Analysis Applied Turbine Engine Condition Monitoring. AIAA/SAE 8th Joint Propulsion Specialist Conference, New Orleans, 1972, AIAA-Paper 72-1082.

[5] Urban, L.A.: Gas Path Analysis - A Tool For Engine Condition Monitoring. 33rd Annual International Air Safety Seminar, Flight Safety Foundation Inc., Christchurch, New Zealand, 1980.

[6] Roesnick, M.: Eine systemtheoretische Lösung des Fehlerdiagnoseproblems am Beispiel eines Flugtriebwerkes. Dissertation, Fachbereich Maschinenbau der Hochschule der Bundeswehr Hamburg, 1984.

[7] Fiedler, K.; Lunderstädt, R.: Diagnoseverfahren für LARZAC-Triebwerk. 1. und 2. Teilbericht, Hochschule der Bundeswehr Hamburg, 1983.

[8] GFE mbH: Studie über Integrierte Diagnostik. BMVg-Auftrag Nr. T/R423/H0006/F2419, Hamburg 1987.

[9] Lunderstädt, R.: Zur Kompensation systematischer Sensorfehler.
To be published in Automatisierungstechnik (at), 1988.

[10] Takahashi, Y.; Robins, M.J.; Auslander, D.M.: Control and Dynamic Systems.
Addison-Wesley Publ. Comp., Reading 1970.

[11] Sage, A.P.; Melsa, J.L.: Estimation Theory with Applications to Communications and Control.
Mc Graw-Hill Book Comp., New York 1971.

[12] Hillemann, Th.: Diagnoseverfahren für LARZAC-Triebwerk. Diploma Thesis, Institute of Automation of the University of the German Armed Forces, Hamburg 1984.

[13] Willan, U.: Modellbezogene Diagnose. In: [8].

[14] Willsky, A.S.: A Survey of Design Methods for Failure Detection in Dynamic Systems.
Automatica, Vol. 12, S. 601-611, 1976.

[15] Tylee, J.: On-Line Failure Detection in Nuclear Power Plant Instrumentation.
IEEE Transactions on Automatic Control, Vol. AC-28, No. 3, S. 406-415, 1983.

[16] Willsky, A.S.; Jones, H.L.: A Generalized Likelihood Ratio Approach to State Estimation in Linear Systems Subject to Abrupt Changes. Proceedings IEEE Conference on Decision and Control, S. 846-853, Phoenix, 1974.

ACKNOWLEDGEMENT

The authors are grateful to Dipl.-Ing. U. Willan for his encouragement in working for the programming and the simulation on the computer. Furthermore they acknowledge the support given by Mrs. U. Barkmann and Mrs. I. Czechatz, who typed and otherwise prepared the manuscript.

SYSTEM-THEORETICAL METHOD FOR DYNAMIC ON-CONDITION MONITORING OF GAS TURBINES

by

F. Hörl, G. Kappler, H. Rick
Technische Universität München
Institut für Luft- und Raumfahrt / Flugantriebe
Arcisstraße 21, D-8000 München 2

Summary

In order to ensure the reliability and safety of such complex technical systems as aero-engines, model-related diagnostic techniques must be applied. The basis for this is a linear, time-invariant, dynamic engine state space model derived from system analysis. Due to the model order and the associated difficulties, order reduction procedures are used. The diagnostic parameters to be taken into account are integrated into a dynamic disturbance model. This disturbance model and the reduced engine model form the extended dynamic engine state space model. A detailed investigation of the dynamic system for observability and disturbability is essential. Because of measuring/process noise and other system disturbances, dynamic state estimation methods are applied in the diagnosis, whereby the synthesis of such observer systems is a crucial point. The usefulness of the dynamic monitoring method is demonstrated on the example of a helicopter engine using computed simulations. A sensitivity analysis allows the accuracy of the diagnostic results to be estimated.

List of symbols

$\mathbf{A}$		system matrix
$\mathbf{B}$		input matrix
$\mathbf{C}$		output matrix
$\mathbf{D}$		direct connection matrix
$\mathbf{H_B}$		observer gain matrix
$\dot{m}_B$	kg/s	fuel mass flow
$\dot{m}_r$	kg/s	corrected mass flow
n	U/s, U/min	rotor speed
n_r	$-$	corrected speed
p, p_t	Pa	pressure
P	W, kW	shaft power
t	s	time
T, T_t	K	temperature
$\mathbf{w}$		command signal vector
η_{is}	$-$, %	isentropic efficiency
λ		eigenvalue
σ		scatter
MTO-0/0		Max. Take Off SLS
MCR-0.2/1500		Max. Cruise ($M_0 = 0.2, H_0 = 1500m$)

1. Introduction

The increasing power of advanced aircraft makes the use of extensive monitoring systems imperative. Since recently, assessment of the costs for the three main sections of an aircraft — airframe, engine and avionics — has no longer been limited solely to development and production costs, but rather the life cycle costs are of primary interest to the aircraft operator /1/. The high proportion of the maintenance costs of an aircraft attributable to the engine alone stresses the necessity for meaningful and reliable engine monitoring.

With the modular contruction of modern engines, it is possible, if suitable diagnostic methods are available, to localize disturbed components and correct the defect without having to dismantle the entire engine. Possible methods for determining the condition of an engine or for identification of engine faults are

- radiography
- borescope inspection

- lube oil system monitoring
- life cycle monitoring
- vibration engine monitoring
- thermodynamic engine monitoring

The actual problem in the diagnosis of component faults which alter the thermodynamic cycle is that the flow parameters and the parameters characterizing the conditions of the individual components have a very complex aerothermodynamic relationship to each other via the flow in the gas path of an engine. Therefore, a useful engine model must also be capable of taking into account the changes due to damage and defects besides the actual dynamics of the engine. The addition of the engine dynamics to the system description permits fault diagnosis even in dynamic operation.

It is possible to make a direct statement on component faults if the deviations from the specified operating behaviour of the components can be determined quantitatively. This requires in particular module-specific parameters which relate the generated disturbances in engine behaviour to a component, and which are independent of operating point shifts, changes in the internal engine geometry and external margin conditions. System failures with short-term causes such as mechanical or thermal overload, or those which arise in the long term due to fouling and wear, are equivalent to changes in the component parameters. In contrast to most component parameters, e.g. efficiency and mass flow, functional parameters are, in principle, measurable, although this is not possible in certain cases, or only with insufficient accuracy, for purely technical reasons. Since defects in main path components affect the thermodynamic characteristics, the changes, or the measurable characteristics, are themselves the starting point for determining the component faults that caused them. The "diagnostic task" of thermodynamic engine monitoring is illustrated in Figure 1.

2. Dynamic Engine Model

The prerequisite for system-theory orientated fault diagnosis in complex technical systems is a comprehensive mathematical process model. In order to include dynamic operation in the monitoring, the system dynamics must be accounted for in the model. Furthermore, the quantitative examination of a dynamic system, be it only a simulation, a theoretical analysis of its characteristics, or the synthesis of a controller or observer, requires an accurate system description.

2.1 System Analysis

The engine model to be considered bears great similarity in its layout to the 250-C20 turboshaft engine of ALLISON GAS TURBINES, which is installed in a range of helicopters (e.g. MBB BO 105). The scheme in Figure 2 shows the engine's modular construction and its major components.

2.1.1 Theoretical Modelling

In theoretical model design, the mathematical engine model is generated by way of the elementary processes taking place in the components, using technical data (e.g. component maps), the physical laws of conservation, material laws and system-specific models.

The steady-state and dynamic behaviour of a gas turbine engine is the product of the behaviours of its components working together. The components of the gas turbine affect the working fluid flowing through it in a variety of ways, changing its physical state (pressure, temperature etc.). The sequence of these changes of state is called the working or cyclic process. The work cycle calculation performed here is limited to a unidimensional consideration, taking into account detailed dynamic modules.

Analytical inclusion of steady-state and dynamic engine behaviour requires a subdivision into static and dynamic calculation modules which are described using general forms of the laws of conservation, among other things /3/. The dynamic calculation modules take into account the four basic effects of

- energy storage in rotors
- thermal exchange between working fluid and engine parts
- gas storage in the various engine volumes
- dynamic combustion

It would be too complicated to calculate the behaviour of the multi-stage turbocomponents compressor and turbine in an engine cycle calculation. Therefore, the behaviour of these components is described in the form of corrected maps.

Fault diagnostic methods not only include fault detection but also defect localization and quantity determination. The component characteristics Φ_Z (e.g. $\eta_{is,V,Z}$) are parameters which indicate both the location and the extent

of any change in component, independent of the operating condition of the engine. In order to achieve this, a real component parameter Φ (e.g. η_{isV}) resulting from the cyclic calculation must be compared with the ideal parameter from the map of the undisturbed component Φ_{KF} (e.g. $\eta_{isV,KF}$). Due to operating point shifts, the component parameter Φ_{KF} depends on various engine (functional) parameters $\mathbf{Y}$. The undisturbed component state is taken as the reference component parameter Φ_{ref}. The following non-linear formulation stands for the general mathematical disturbance model

$$\Phi = \Phi_{KF}(\mathbf{Y})\frac{\Phi_Z}{\Phi_{ref}} \tag{1}$$

The complete mathematical description of a helicopter engine includes not only the thermodynamic process model but also the dynamic load model — the helicopter rotor system. In connection with the low-pressure turbine, therefore, it includes the main rotor, tail rotor and transmission /3/.

The combination of the unidimensional static and dynamic calculation models results in a base equation system describing the operating behaviour /3/. This base eqation system provides a non-linear, time-invariant, continuous, dynamic engine model with lumped parameters in the general form

$$\dot{\mathbf{X}} = \mathbf{f}(\mathbf{X}, \mathbf{U}) \tag{2}$$
$$\mathbf{Y} = \mathbf{g}(\mathbf{X}, \mathbf{U}) \tag{3}$$

The $[n]$-vector of the physical state variables $\mathbf{X}$ for the twin-spool helicopter engine is given in Table 1. The input quantities $\mathbf{U}$ are composed of the control signals $\mathbf{U}_S$ and disturbances $\mathbf{U}_Z$. The part input vector $\mathbf{U}_Z$ contains various different types of disturbance:

External margin conditions

$T_{0,Z}, p_{0,Z}$	: ambient conditions
$M_{0,Z}$	: flight Mach number

Component parameters

$\pi_{E,Z}$	: inlet
$\eta_{isV,Z}, \dot{m}_{rV,Z}$	: compressor
$\eta_{BK,Z}, \pi_{BK,Z}$	: combustion chamber
$\eta_{isHT,Z}, \dot{m}_{rHT,Z}$	: high-pressure turbine
$\eta_{isNT,Z}, \dot{m}_{rNT,Z}$	: low-pressure turbine
$\pi_{R,Z}$	: duct
$\eta_{D,Z}, A_{D,Z}$	: nozzle (exhaust duct)

Air system

$\dot{m}_{BLV,Z}$	: acceleration bleed air
$\dot{m}_{ZV,Z}$	: bleed air (external accessories)

Power take-off

$P_{exHR,Z}$	: power take-off (HR)
$P_{exNR,Z}$	: power take-off (LR)
$P_{L,Z}$	: load (load change)

The output vector $\mathbf{Y}$ comprises measurable and non-measurable flow parameters, performance characteristics and other important engine parameters.

In view of the difficulty in analysing non-linear systems, such mathematical models are linearized to steady-state operating points. The steady-state and dynamic operating behaviour of the controlling system "ENGINE" is described completely in the vicinity of the stationary operating point $[\mathbf{X}_R, \mathbf{U}_R, \mathbf{Y}_R]$ by the linear, time-invariant state space model

$$\dot{\mathbf{x}} = \mathbf{A}\mathbf{x} + \mathbf{B}\mathbf{u} \tag{4}$$
$$\mathbf{y} = \mathbf{C}\mathbf{x} + \mathbf{D}\mathbf{u} \tag{5}$$

By subdividing the inputs $\mathbf{u}$ into control variables $\mathbf{u}_S$ and disturbances $\mathbf{u}_Z$, the following equivalent state space equations are obtained

$$\dot{\mathbf{x}} = \mathbf{A}\mathbf{x} + \mathbf{B}_S\mathbf{u}_S + \mathbf{B}_Z\mathbf{u}_Z \tag{4a}$$
$$\mathbf{y} = \mathbf{C}\mathbf{x} + \mathbf{D}_S\mathbf{u}_S + \mathbf{D}_Z\mathbf{u}_Z \tag{5a}$$

2.1.2 System Identification

In system identification, the structure (model order n) and the parameters of a suitable mathematical model are determined. This is performed in three stages:

- establishment of the model form

- specification of a quality criteria
- selection of an algorithm to determine the model parameters in accordance with the specified quality criteria, and calculation of the model parameters.

Besides the model structure, the theoretical system analysis also provides the model order n. To estimate the model parameters there are various estimation algorithms /4/. The non-recursive least square method was successfully applied /3/.

2.2 System Order Reduction

The problem in the generation of a model is finding an appropriate compromise between the conflicting requirements of simplicity and closeness to reality of the model. A common form of model simplification is the linearization of the non-linear state equations (2-3) around an operating point $[\mathbf{X}_R, \mathbf{U}_R, \mathbf{Y}_R]$. The more accurately a model — original system in the following — is required to describe reality, the higher the system order n will be. However, this is detrimental if the mathematical model (4-5) is intended as the basis for a simulation or for synthesis of a controller or observer. The memory capacity of even large computer systems can be too small, and computing times can become extremely long. In the synthesis of a controller or observer, one is still faced with the problem of having to predetermine sensible weighting matrices or suitable eigenvalues for a higher order model. Therefore, it is often necessary to approximate the high-order model with a model of lower order.

The requirement imposed on a reduced model is to reproduce as accurately as possible the progressions of the major state variables of the original system, i.e. the progression of the n_r-dimensional state vector $\mathbf{x}_r$. The reduced model is formulated as the state equation

$$\dot{\tilde{\mathbf{x}}}_r = \mathbf{A}_r\tilde{\mathbf{x}}_r + \mathbf{B}_r\mathbf{u} \tag{6}$$

$$\tilde{\mathbf{y}} = \mathbf{C}_r\tilde{\mathbf{x}}_r + \mathbf{D}_r\mathbf{u} \tag{7}$$

where $\mathbf{u}$ is the input vector of the original system and $\tilde{\mathbf{x}}_r$ represents an n_r-dimensional state vector. The time-invariant matrices $\mathbf{A}_r$, $\mathbf{B}_r$, $\mathbf{C}_r$ and $\mathbf{D}_r$ shall be selected such that an optimum approximation of $\mathbf{x}_r$ by $\tilde{\mathbf{x}}_r$ is achieved.

Numerous methods of order reduction for time-invariant systems have been presented in recent years /2/. They can be categorized according to their objectives:

- singular perturbation (SP)
- equation error minimization (GLF)
- modal order reduction (MOD)

Application of the various order reduction methods to the linear engine state space model of the 22nd order, i.e. the original system, requires the selection of the state variables of the reduced model. With the modal reduction method, the eigenvalues of the reduced model must also be determined. The dominant eigenvalues and dominant state variables of the orignal system can be determined by dominance analysis /3/. Based on the results of the dominance analysis /3/ a 6th order model with the reduced state vector

$$\mathbf{x}_r = (x_1, x_2, x_{18}, x_{19}, x_{20}, x_{21})^T$$

and a 2nd order model with

$$\mathbf{x}_r = (x_1, x_2)^T$$

are calculated. The eigenvalues of the 6th and 2nd order models reduced by the various methods are given in Table 2. The step responses of n_{HR} and n_{NR} of the original system (22nd order), the reduced 6th and 2nd order systems (SP-S) and the identified 6th and 2nd order models (ID-L) for a fuel mass flow change of 10 % are shown in Figure 3.

The singular perturbation method (SP-S) gave rise to useful reduced linear engine models in all cases. It also has the advantage that the physical structure of the original system is largely maintained, facilitating the observation of the system behaviour.

Both the step response progressions and the frequency response characteristics /3/ show the good approximation of the engine behaviour by the 6th order model over a broad frequency range. This model accounts for both the energy storage of the two rotors and the thermal exchange between the working fluid and the engine components. In an engine of this size and configuration, the effect of gas storage in the various engine volumes on the time cycle operation is negligible.

For the 2nd order reduced engine model, which only accounts for the rotor dynamics, clear deviations from the original system are seen in step responses. However, it can still provide a sufficient description of the dynamic engine behaviour for certain engine monitoring problems.

3. Dynamic Engine Monitoring System

Starting from the state space description of the controlling system and the measured or measurable input and output variables, the monitoring system should establish estimated values for the component characteristics representing the engine state. The engine state must be determined using a state estimation method due to additional deterministic and stochastic process and measuring disturbances. The monitoring system can also provide the controller with additional information on the operating condition of the engine. The structural integration of the control and monitoring system is shown in Figure 4.

3.1 Extended Dynamic Engine Model

Besides the actual engine dynamics, the dynamic engine model only contains control variables $\mathbf{u}_S$ and deterministic disturbances $\mathbf{u}_Z$. The disturbances $\mathbf{u}_Z$ comprise the external margin conditions ($T_{0,Z}$, $p_{0,Z}$, $M_{0,Z}$, $P_{L,Z}$) and the relevant component characteristics for the engine diagnosis. In practice, additional disturbances affecting the control range and the measurement must be taken into account.

The linear, time-invariant system with process disturbances $\mathbf{w}_P$ and measuring disturbances $\mathbf{b}$ and $\mathbf{v}$ is described by state equations

$$\dot{\mathbf{x}} = \mathbf{A}\mathbf{x} + \mathbf{B}_S\mathbf{u}_S + \mathbf{B}_Z\mathbf{u}_Z + \mathbf{B}_P\mathbf{w}_P \tag{8}$$

$$\mathbf{y} = \mathbf{C}\mathbf{x} + \mathbf{D}_S\mathbf{u}_S + \mathbf{D}_Z\mathbf{u}_Z + \mathbf{b} + \mathbf{v} \tag{9}$$

For the disturbances, a distinction must be made between

- process- and measuring disturbances $\mathbf{w}_P$ and $\mathbf{v}$, which can be represented as Gaussian White Noise with the familiar covariance matrices $\mathbf{Q}$ and $\mathbf{R}$.
- measuring bias $\mathbf{b}$ and disturbances $\mathbf{u}_Z$, which are considered as deterministic disturbances.

The measuring bias $\mathbf{b}$ and disturbance vector $\mathbf{u}_Z$ can be combined to an extended disturbance vector $\tilde{\mathbf{u}}_Z$ for further consideration.

For deterministic disturbances, it is necessary to extend the model of the actual system – the controlling system – plus the dynamic disturbance models with state equations

$$\dot{\mathbf{x}}_D = \mathbf{A}_D\mathbf{x}_D + \mathbf{B}_D\mathbf{u}_D \tag{10}$$

$$\mathbf{y}_D = \mathbf{C}_D\mathbf{x}_D + \mathbf{D}_D\mathbf{u}_D \tag{11}$$

in order to reduce the resultant state estimate errors to an acceptable minimum. In addition, the deterministic disturbances $\mathbf{u}_Z$ contain the component characteristics sought for in case of engine diagnosis.

For engine diagnosis, the deterministic inputs

$$\mathbf{u} = [\mathbf{u}_S \mid \tilde{\mathbf{u}}_Z]^T$$

are subdivided, giving the state equations

$$\dot{\mathbf{x}} = \mathbf{A}\mathbf{x} + \mathbf{B}_a\mathbf{u}_a + \mathbf{B}_b\mathbf{u}_b + \mathbf{B}_c\mathbf{u}_c + \mathbf{B}_P\mathbf{w}_P \tag{8a}$$

$$\mathbf{y} = \mathbf{C}\mathbf{x} + \mathbf{D}_a\mathbf{u}_a + \mathbf{D}_b\mathbf{u}_b + \mathbf{D}_c\mathbf{u}_c + \mathbf{v} \tag{9a}$$

where

$\mathbf{u}_a$: directly measurable input variables (e.g. $T_{0,Z}$, $p_{0,Z}$, ...)

$\mathbf{u}_b$: not directly measurable but reconstructable input variables (e.g. component characteristics)

$\mathbf{u}_c$: not directly measurable nor reconstructable input variables (e.g. component characteristics, measuring bias)

The inputs $\mathbf{u}_b$ of the linear engine model can, for example, be described by a dynamic disturbance model for jumpy signals

$$\dot{\mathbf{x}}_{D_b} = \begin{bmatrix} 0 & \dots & 0 \\ \vdots & \ddots & \vdots \\ 0 & \dots & 0 \end{bmatrix} \mathbf{x}_{D_b} + \begin{bmatrix} 1 & \dots & 0 \\ \vdots & \ddots & \vdots \\ 0 & \dots & 1 \end{bmatrix} \mathbf{u}_{D_b} \tag{10a}$$

$$\mathbf{u}_b = \mathbf{y}_{D_b} = \begin{bmatrix} 1 & \dots & 0 \\ \vdots & \ddots & \vdots \\ 0 & \dots & 1 \end{bmatrix} \mathbf{x}_{D_b} \tag{11a}$$

If special knowledge of individual disturbances is available at the start (e.g. sinusoidal measuring bias), the disturbance processes of differing signal forms can be arranged at will in a model.

The engine model extended by the dynamic disturbance model

$$\dot{\mathbf{x}}_e = \mathbf{A}_e\mathbf{x}_e + \mathbf{B}_{ue}\mathbf{u}_e + \mathbf{B}_{ze}\mathbf{z}_e + \mathbf{B}_{Pe}\mathbf{w}_{Pe} \tag{12}$$

$$\mathbf{y} = \mathbf{C}_e\mathbf{x}_e + \mathbf{D}_{ue}\mathbf{u}_e + \mathbf{D}_{ze}\mathbf{z}_e + \mathbf{v} \tag{13}$$

$$\mathbf{u}_b = \mathbf{C}_{De}\mathbf{x}_e \tag{14}$$

$$\mathbf{y}_b = \mathbf{C}_{e_b}\mathbf{x}_e + \mathbf{D}_{ue_b}\mathbf{u}_e \tag{15}$$

is the starting point for the reconstruction of the state variables $\mathbf{x}_e$ using state estimation methods. With the estimated state variables $\mathbf{x}_e$ the component characteristics, measuring system faults $\mathbf{u}_b$ relevant for the engine diagnosis and non-measurable engine parameters $\mathbf{y}_b$ (e.g. T_{t4}) can be determined via the output equations (14-15).

3.2 Application of State Estimation Methods for Dynamic Engine Monitoring

State estimation methods are used in dynamic engine monitoring /3/. The state variables of the extended engine model contain indirectly non-measurable or inaccurately measurable input variables besides the physical state variables which describe the actual engine dynamics. These input variables can comprise component characteristics, margin condition parameters, inputs whose measured values have a high noise content, and deterministic measuring errors.

Thermodynamic engine monitoring is more difficult in practice because measuring inaccuracies, poor measurability and sensor failures can effect limitations in observability or give rise to misinterpretations. In addition, internal and external engine disturbances can often cause changes in the temperature and pressure profiles of the various flow sections. Depending on the measuring system used, the effects of the sensor dynamics must also be taken into account in dynamic engine monitoring.

3.2.1 Observability and Disturbability Analysis

A prerequisite for the use of a state estimation system is that the extended system (12-13) must be observable from measuring vector $\mathbf{y}$. Since the extended controlling system displays unstable behaviour because of the dynamic disturbance models, the question of observability becomes crucial for stability, and therefore for estimation error behaviour in case of uncertainties in the knowledge of the initial condition of the state variables.

A diagnostic model in the form of an observer system should allow faults in the engine components, air system and margin condition parameters to be determined. The measuring effort, i.e. the number of sensors, should be kept to a minimum in estimating these disturbances. In selecting the measuring variables $\mathbf{y}$, measurability and technical effort shall be considered with respect to measuring accuracy.

The reduction of the extended engine model is closely associated with the selection of the measuring parameters, i.e. neglection of non-measurable inputs. Table 3 shows different diagnostic variants for the testbed case (MTO-0/0) and flight case (MCR-0.2/1500).

Since an engine on the testbed is equipped with a standard inlet (e.g. bellmouth), and no external bleed air is taken off, the disturbances $\pi_{E,Z}$ and $\dot{m}_{ZV,Z}$ are irrelevant. The margin condition parameters $T_{0,Z}$ and $p_{0,Z}$ are considered as measurable input variables (E). In the flight case, the margin condition parameters $T_{0,Z}$, $p_{0,Z}$, flight Mach number $M_{0,Z}$ and the component characteristic $\pi_{E,Z}$ must be considered in the extended model. All diagnostic methods contain the component characteristics for compressor and turbines, load change $P_{L,Z}$ and control variable $\dot{m}_B$. Because of the high noise content in the measurement, a dynamic disturbance model is used for the fuel mass flow $\dot{m}_B$.

With only a few exceptions, the temperatures and pressures in the various engine sections, the shaft speeds, shaft torques, power outputs and the fuel mass flow are generally measurable. Especially at the combustion chamber outlet which is the hottest part of the engine, the flow parameters T_{t4} and p_{t4} are not measurable with sufficient accuracy. In the testbed case also, component parameters and mass flows are considered in principle as non-measurable quantities.

Besides the state variables of the disturbance models, the state vector of the extended engine model includes the actual engine dynamics. Firstly, the engine dynamics are described by the reduced, 6th order model established in section 2.2 by the physical state variables

$$\mathbf{x} = [n_{HR}, n_{NR}, T_{MatV}, T_{MatBK}, T_{MatHT}, T_{MatNT}]^T$$

and secondly by the 2nd order model with the state variables

$$\mathbf{x} = [n_{HR}, n_{NR}]^T$$

Since the physical state variables of the engine dynamics must be observable, differences arise in the selection of the measuring parameters in conjunction with the engine diagnosis for the 6th and 2nd order models. The differing measuring value sets for the diagnostic variants of Table 3 for the 2nd and 6th order models are summarized in Table 4. Quantitative observability analysis and the selection of the necessary measuring value sets is performed using standardized "deterministic" and "stochastic" measures of observability /3/.

3.2.2 Observer Synthesis

The essential factors in the selection of the observer dynamics and therefore the gain matrix $\mathbf{H}_B$ for a dynamic engine diagnostic model are as follows:

- dynamics of the controlling system
- robustness with respect to parameter deviations
- observability
- measuring noise
- process noise
- required accuracy of estimation
- type of monitoring

There are in principle two possibilities for calculating the matrix $\mathbf{H}_B$ that is pole placement and optimization. Table 5 summarizes the eigenvalues of the observers for three suboptimal configurations for the testbed case – diagnostic variant (PF2) and measuring value set (MP2/2).

3.2.3 Simulation and Analysis of Results

The working principles of the various dynamic diagnostic models are tested by examining all of the faults that have been accounted for. In order to simulate the observer, the necessary "measuring values" $\mathbf{y}$ are determined from the state space equations of the 22nd order original system with preset inputs. For the inputs containing component characteristics, load changes and margin condition parameters, step signals are used.

The results of the dynamic engine diagnosis for simulated component characteristics and load changes (testbed case) are shown in Figure 5. In spite of the rarity of the combination of simulated multiple disturbances in practice, the estimated values of the observer agreed exactly with the preset values after some 20 sec. During the various transient phases, the estimated component characteristics are not usable for engine diagnosis.

In order to simulate the diagnostic model in Figure 6, a measuring noise, which is always present in practice, is superimposed onto the "measuring data". A direct comparison of the time curves shows the measuring noise sensitivity of the observer. There are clear deviations from the deterministic case, especially for the compressor efficiency $\eta_{is,V,Z}$. The desired filter effect of the observer can be seen in the estimated fuel mass flow $\hat{m}_B$. The computed simulations show that the synthesis of an observer for the preset conditions must be orientated towards noise sensitivity.

Figure 7 shows the diagnostic results of various observer designs based on the 6th order reduced engine model. It can be seen from the progressions that, for the deterministic "measuring values", lower observer dynamics during the transient phase give rise to poorer estimated values. Due to the low heat exchange dynamics, the response time of observer DPF/6, for example, is considerably greater than that of observer DPF1/2. Direct comparison of the time curves of Figure 6 and 7 shows that better estimation values in the transient phase are obtained from the observers based on the 2nd order reduced engine model. The reason for this is the poorer observability of the component characteristics, since the material temperatures, which are inert as far as dynamics are concerned, are measured instead of the gas temperatures (DPF/2).

Even with noisy "measuring data", the various n-observer gave very good diagnostic results in the testbed and flight case, especially in built up condition. In the transient phase, the observer based on the 2nd order reduced engine model proved to be slightly the better one. With noisy measuring values, covariance analysis is indispensable for establishment of the observer dynamics and for checking the estimation results.

3.2.4 Covariance Analysis

Covariance analysis of an observer system provides the estimation error variances or scatters, i.e. the static data required for assessment and specification /3/. In particular with dynamic engine diagnosis, the case arises in which, on the one hand, disturbances are present in the form of process and measuring noise, and on the other, even minor changes in component characteristics must be detected in order to assess the engine's condition.

The scatters of the estimated values (in built up condition) for various observer designs are shown in Figure 8. The results underline the effect of observer dynamics on measuring noise sensitivity already mentioned in the previous sections. However, measuring noise has a varied effect on the estimation values. The greatest scatters are obtained

with the diagnostic parameters of the compressor section $\eta_{isV,Z}$, $\dot{m}_{rV,Z}$ and $\dot{m}_{BLV,Z}$. Each of the various observer concepts gives rise to good estimations. The advantages of an n-observer can be clearly seen when measurable, noisy input variables are included in the observer model as state variables. For example, in estimating the fuel mass flow $\dot{m}_B$ with observer DPF1/2, the scatter is only half as great with respect to the measured value.

3.2.5 Deterministic Error Analysis

The proposed engine monitoring models do not contain all of the possible component characterisics (e.g. combustion section) which would be necessary for complete engine diagnosis. This is due to non-measurable or barely measurable engine parameters for which observability cannot be achieved. Furthermore, the scope and complexity of measurement systems are limited on grounds of cost. Sensor failures or systematic measuring errors, which give rise to incorrect diagnostic results, cannot be discounted in practice. Insufficiencies in the modelling of the physical process, such as linearization errors, and imprecisely known or fluctuating parameters, can distort estimated values or even make them completely useless. By way of a deterministic error (sensitivity) analysis, the above effects on the engine diagnosis can be estimated.

In Figure 9, the effects of non-modelled, deterministic disturbances on the estimated values of diagnostic model DPF2/2 are shown in the form of stationary sensitivity coefficients. The results clearly show the problems of engine diagnosis. For example, a real change of -1 % in the component characteristic $\pi_{BK,Z}$ gives rise to distortions in the HP turbine component characteristics $\eta_{isHT,Z}$ and $\dot{m}_{rHT,Z}$ of 0.74 and 1.04 % respectively. The component characteristics of the exhaust duct $\eta_{D,Z}$ and $A_{D,Z}$ do not cause any additional estimation errors and can, therefore, be ignored in diagnostic systems for turboshaft engines.

The estimation errors arising from systematic measuring errors of T_{t3} and p_{t3} are shown in Figure 10. For example, a deterministic measuring error in T_{t3} of 1 % gives rise to $\eta_{isV,Z}$, $\eta_{isHT,Z}$ estimation errors of 1.66 % and -1.71 % respectively. The results show that great demands must be made on the accuracy of the measurement system in order to ensure a meaningful diagnosis.

Conclusion

A system-theoretical method for dynamic, thermodynamic on-condition monitoring of gas turbine engines has been presented.

The basis of the monitoring system is a mathematical model describing the steady-state and dynamic operating behaviour of the engine. In order to be able to apply practicable analysis and synthesis procedures, besides linearization, a system reduction is required for simplification of the model.

The dynamic engine monitoring system is a state estimator which reconstructs the engine state values from the measured input and output variables. Diagnosis parameters to be taken into account are included in a dynamic disturbance model. This disturbance model and the reduced engine model form together the extended dynamic engine state space model, the controlling system of the state estimator.

Very good results are obtained with deterministic measuring values for all diagnostic models, using simulated single and multiple disturbances in the open and closed loop control circuit. With noisy measuring values, only n-observers are suitable diagnostic models because of their filtration effect. Besides the transient response, the dynamic of the n-observer determines the measuring noise sensitivity.

The results of the covariance analysis show the immediate relationship between observer dynamics, the variance of the measuring noise and the scatter of the diagnostic parameters. The effects of non-modelled component characteristics and systematic measuring errors on the diagnostic results can be estimated by determinstic error analysis.

Possible further developments in the field of systems monitoring are a decentralized, linear state estimator or a non-linear, dynamic engine model in conjunction with a non-linear state estimator. In the future, however, parallel to theoretical modelling, mathematical models based on real engine data must be established by identification. Theoretical investigations have shown that the measurement system is crucial for the meaningfulness of a monitoring system.

References

/1/ BREE H.-G., BACKMANN G. :
Future Requirements for Helicopter Propulsion Systems.
AGARD-CP-302, Helicopter Propulsion Systems, Paper No. 25, May 11-14, 1981, Toulouse, France

/2/ FÖLLINGER O. :
Reduktion der Systemordnung.
Regelungstechnik 30, Heft 11, 1982

/3/ HÖRL F. :
Systemtheoretische Methode zur dynamischen Zustandsüberwachung von Gasturbinen.
Dissertation, Lehrstuhl für Flugantriebe, TU München, 1987
/4/ ISERMANN R. :
Prozeßidentifikation.
Springer-Verlag, Berlin-Heidelberg-New York, 1984

Tables

i	X_i	i	X_i
1	n_{HR}	12	T_{t5}
2	n_{NR}	13	p_{t5}
3	T_{t3}	14	$\dot{m}_5$
4	p_{t3}	15	T_{t7}
5	$\dot{m}_3$	16	p_{t7}
6	T_{t4}	17	$\dot{m}_7$
7	p_{t4}	18	T_{MatV}
8	$\dot{m}_4$	19	T_{MatBK}
9	T_{t41}	20	T_{MatHT}
10	p_{t41}	21	T_{MatNT}
11	$\dot{m}_{41}$	22	$\dot{Q}_{BK}$

Table 1 State variables **X** of the engine state space model

k	eigenvalues λ_k (Real/Imag)			
	(SP-S)	(SP-E)	(GLF)	(MOD)
1	-0.176/ 0.000	-0.176/ 0.000	-0.190/ 0.032	-0.176/ 0.000
2	-0.197/ 0.000	-0.197/ 0.000	-0.190/-0.032	-0.197/ 0.000
3	-0.237/ 0.000	-0.237/ 0.000	-0.232/ 0.000	-0.237/ 0.000
4	-0.344/ 0.000	-0.344/ 0.000	-0.363/ 0.000	-0.344/ 0.000
5	-0.763/ 0.000	-0.764/ 0.000	-0.820/ 0.000	-0.764/ 0.000
6	-2.760/ 0.000	-2.660/ 0.000	-2.070/ 0.000	-2.660/ 0.000
1	-0.762/ 0.000	-0.757/ 0.000	-0.491/ 0.032	-0.764/ 0.000
2	-2.670/ 0.000	-2.160/ 0.000	-2.300/ 0.000	-2.660/ 0.000

Table 2 Eigenvalues λ_k of the 6th and 2nd order reduced models; MTO-0/0

input variable u	diagnostic variant: test bed case PF1	PF2	PF3	PF4	flight case PF1	PF2
$T_{0,Z}$	X	X	X	X	X	X
$p_{0,Z}$	X	X	X	X	X	X
$M_{0,Z}$					X	X
$\pi_{B,Z}$					X	X
$\eta_{isV,Z}$	X	X	X	X	X	X
$A_{kV,Z}$	X	X	X	X	X	X
$\eta_{BK,Z}$			X	X		X
$\pi_{BK,Z}$				X		
$\eta_{isHT,Z}$	X	X	X	X	X	X
$A_{kHT,Z}$	X	X	X	X	X	X
$\eta_{isNT,Z}$	X	X	X	X	X	X
$A_{kNT,Z}$	X	X	X	X	X	X
$\pi_{B,Z}$						
$\pi_{D,Z}$				X		
$A_{D,Z}$				X		
$A_{kV,Z}$						
$\dot{m}_{BLV,Z}$		X	X	X	X	X
$P_{exHR,Z}$				X		
$P_{L,Z}$	X	X	X	X	X	X
a_n	X	X	X	X	X	X

Table 3 Diagnostic variants for the testbed case (MTO-0/0) and flight case (MCR-0.2/1500)

measuring variable y	measuring value set: test bed case MP1/6	MP2/6	MP3/6	MP4/6	flight case MP1/6	MP2/6	test bed case MP1/2	MP2/2	MP3/2	MP4/2	flight case MP1/2	MP2/2
T_{t0}												
P_{t0}					X	X					X	X
T_0	X	X	X	X	X	X	X	X	X	X	X	X
P_0	X	X	X	X			X	X	X	X		
T_{t2}					X	X					X	X
P_{t2}					X	X					X	X
T_2												
P_2		X	X	X	X	X		X	X	X	X	X
T_{t3}							X	X	X	X	X	X
P_{t3}	X	X	X	X	X	X	X	X	X	X	X	X
T_3												
P_3												
T_{t4}				X						X		
P_{t4}				X						X		
T_{t41}							X	X	X	X	X	X
P_{t41}	X	X	X	X	X	X	X	X	X	X	X	X
T_{t5}			X	X		X			X	X		X
P_{t5}				X						X		
P_{t7}												
P_{t9}				X						X		
T_9				X						X		
α_{HR}	X	X	X	X	X	X	X	X	X	X	X	X
π_{HR}	X	X	X	X	X	X	X	X	X	X	X	X
T_{HatV}	X	X	X	X	X	X						
T_{HatBK}	X	X	X	X	X	X						
T_{HatBT}	X	X	X	X	X	X						
T_{HatNT}	X	X	X	X	X	X						
M_{DNT}					X	X					X	X
P_{NT}												
P_B												
P_L	X	X	X	X			X	X	X	X		
a_n	X	X	X	X	X	X	X	X	X	X	X	X

Table 4 Measuring value sets for the testbed case (MTO-0/0) and flight case (MCR-0.2/1500); 6th and 2nd order models

k	eigenvalues λ_k (Real/Imag)		
	observer		
	DPF1/2	DPF2/2	DPF3/2
1	-2.672 / 0.0	-2.672 / 0.0	-2.672 / 0.0
2	-0.762 / 0.0	-0.762 / 0.0	-1.238 / 0.0
3	-0.500 / 0.0	-1.000 / 0.0	-2.000 / 0.0
4	-0.500 / 0.0	-1.000 / 0.0	-2.000 / 0.0
5	-0.500 / 0.0	-1.000 / 0.0	-2.000 / 0.0
6	-0.500 / 0.0	-1.000 / 0.0	-2.000 / 0.0
7	-0.500 / 0.0	-1.000 / 0.0	-2.000 / 0.0
8	-0.500 / 0.0	-1.000 / 0.0	-2.000 / 0.0
9	-0.500 / 0.0	-1.000 / 0.0	-2.000 / 0.0
10	-0.500 / 0.0	-1.000 / 0.0	-2.000 / 0.0
11	-0.500 / 0.0	-1.000 / 0.0	-2.000 / 0.0

Table 5 Eigenvalues λ_k of the n-observer for the testbed case PF2-MP2/2; 2nd order model; MTO-0/0; system eigenvalues: $\lambda_k = \{-2.672 | -0.762 | n_D \cdot 0.0\}$

Illustrations

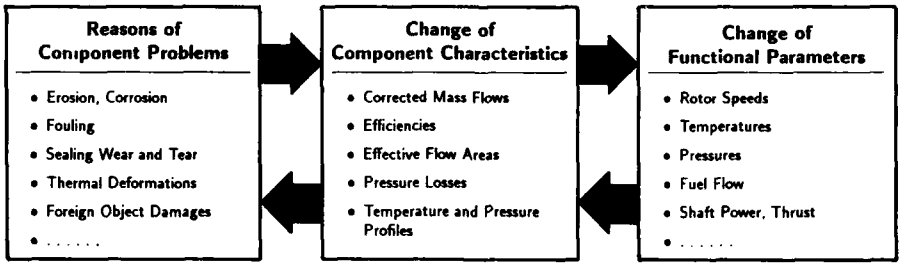

Figure 1 Thermodynamic engine monitoring

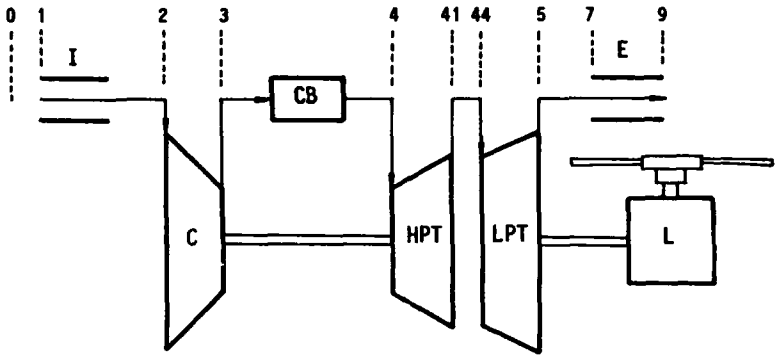

Figure 2 Turboshaft engine scheme

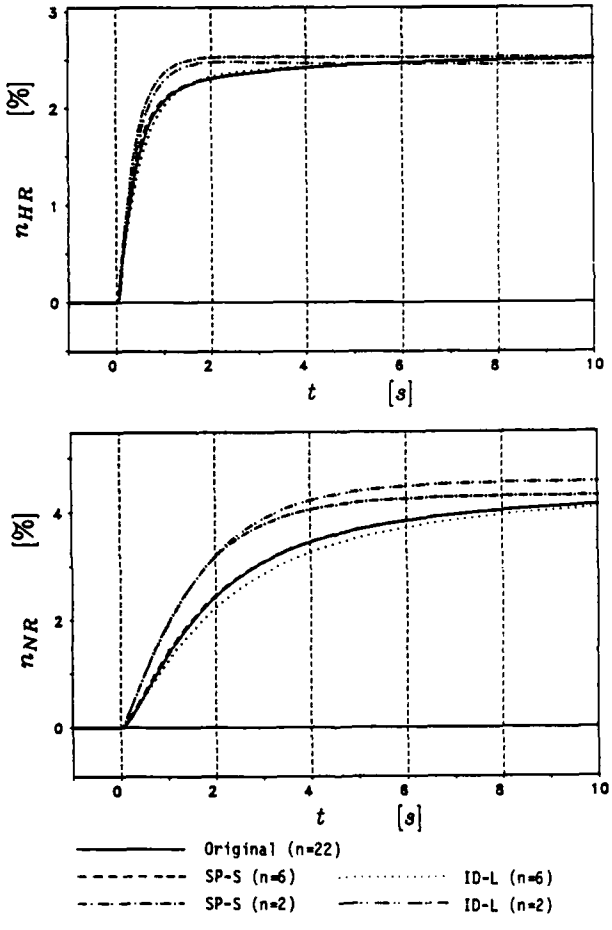

Figure 3 Transient functions of n_{HR} and n_{NR} with jumpy excitation via $\dot{m}_B$; $\Delta\dot{m}_B = 10$ %; MTO-0/0

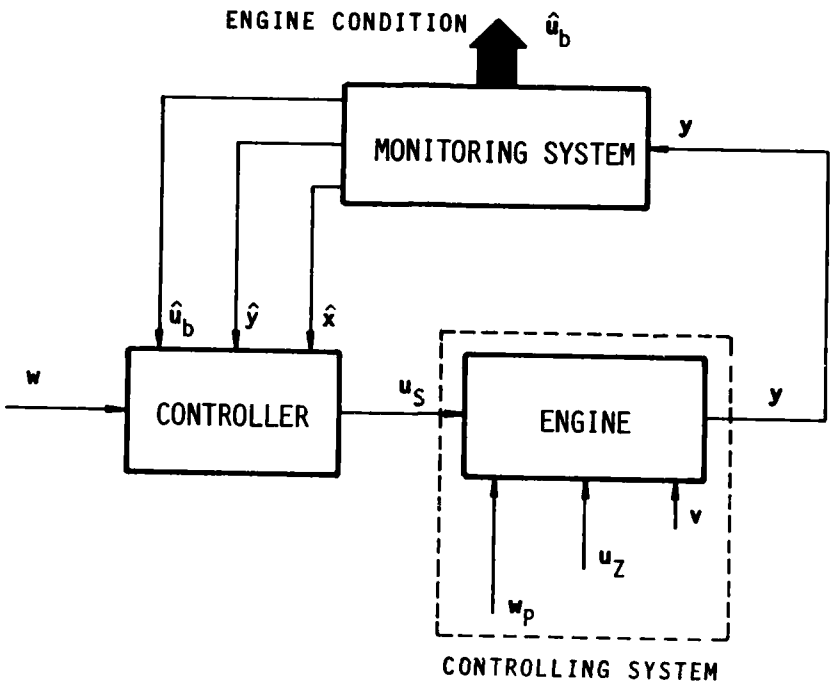

Figure 4 Control and monitoring structure

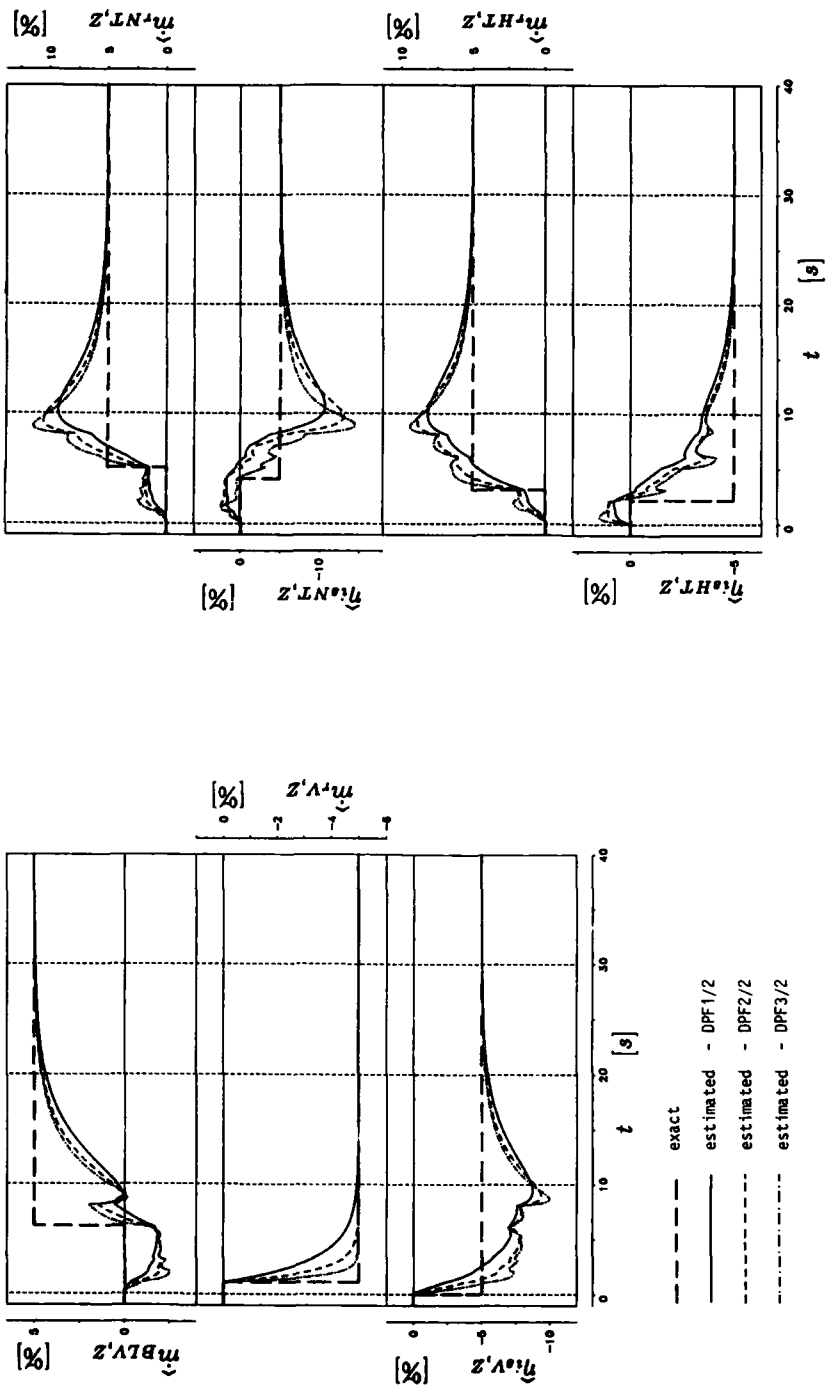

Figure 5 Exact and estimated state variables;
testbed case: PF2-MP2/2, deterministic "measuring data"

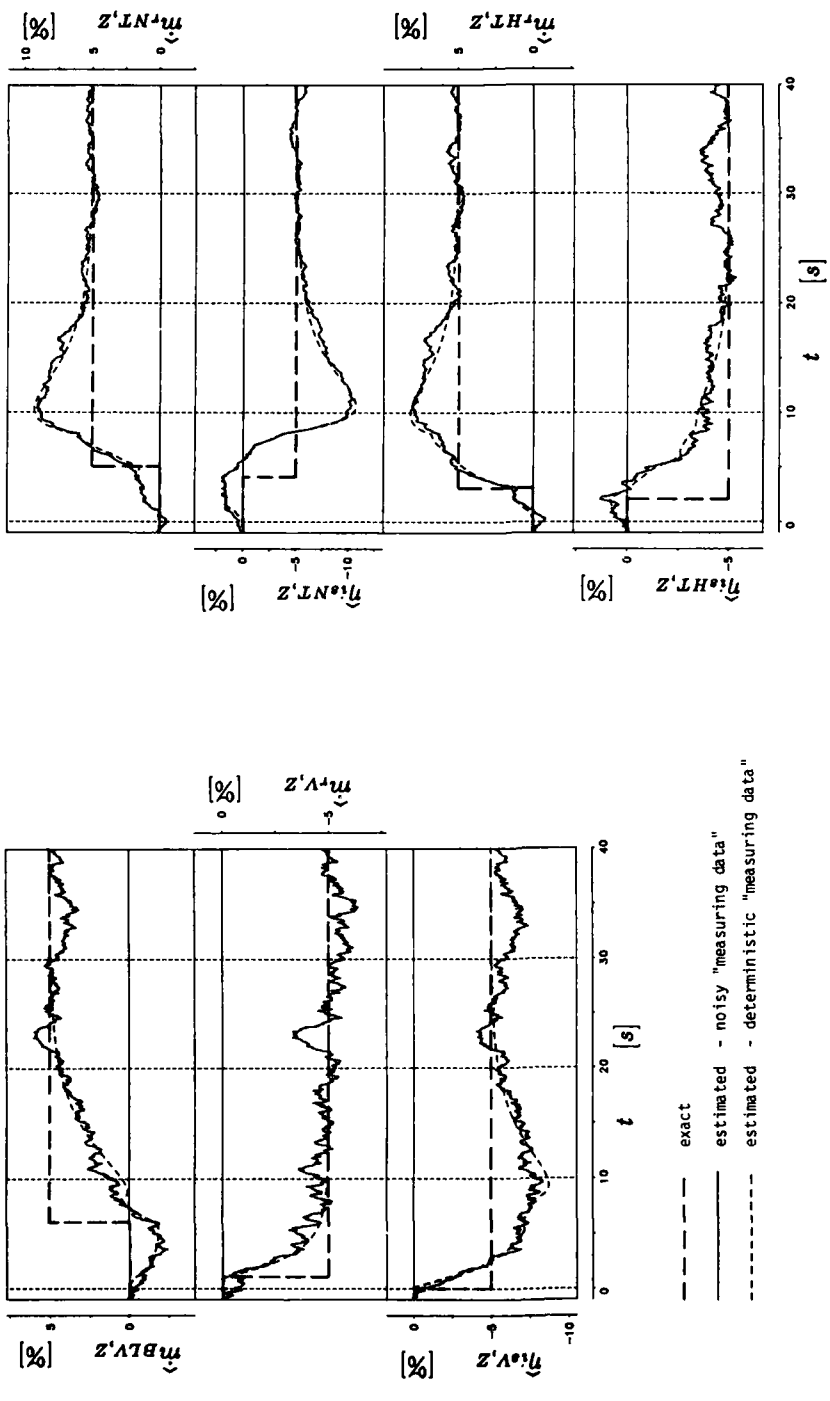

Figure 6 Exact and estimated state variables;
testbed case: PF2-MP2/2; n-observer DPF1/2

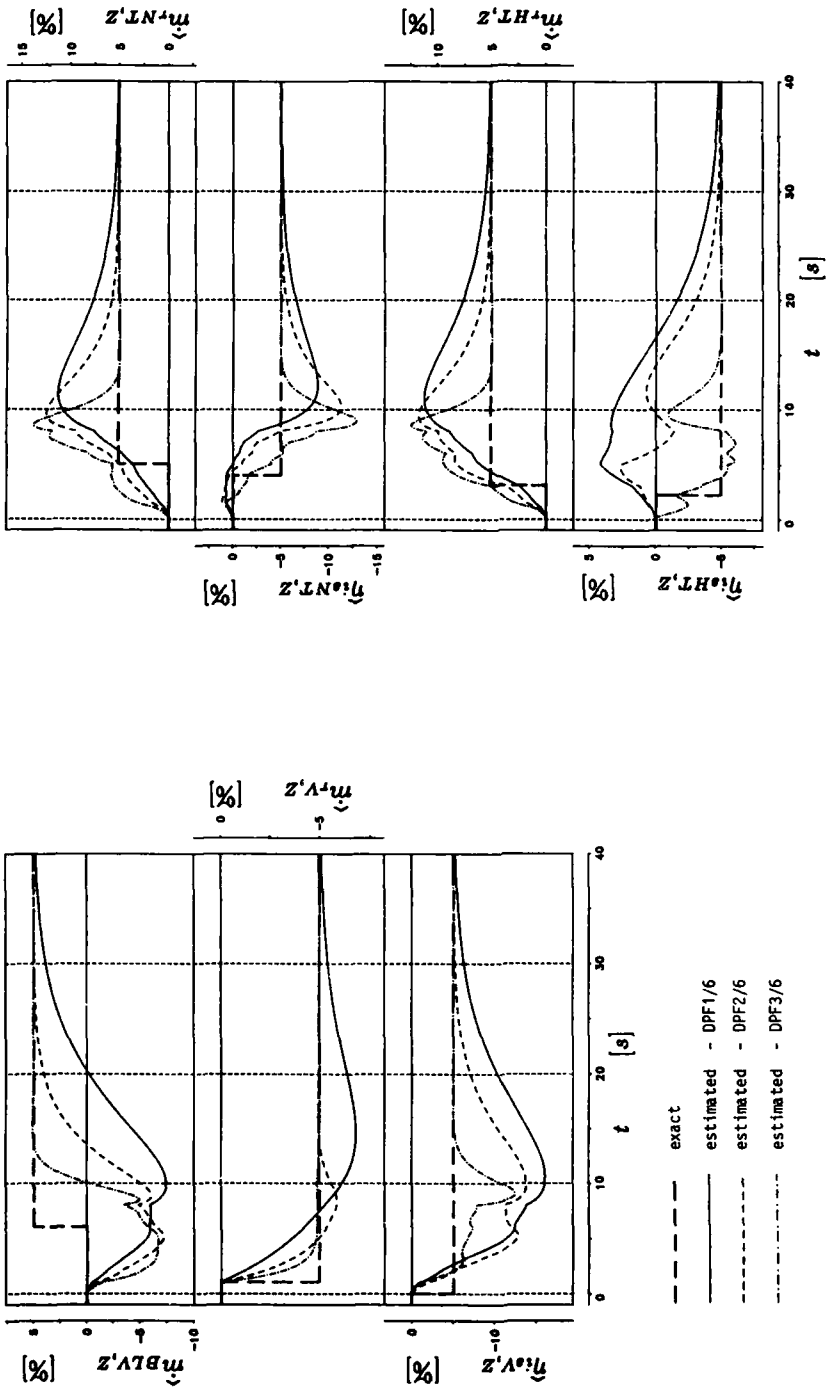

Figure 7 Exact and estimated state variables;
testbed case: PF2-MP2/6; deterministic "measuring data"

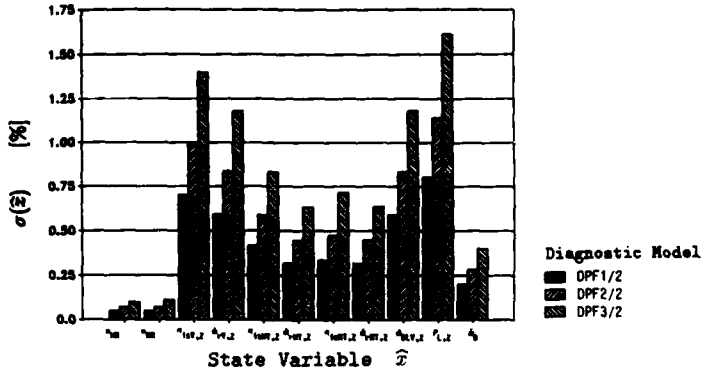

Figure 8 Scatter of the estimated values (built up conditions) for various observer designs; testbed case: PF2-MP2/2; *) [kW]

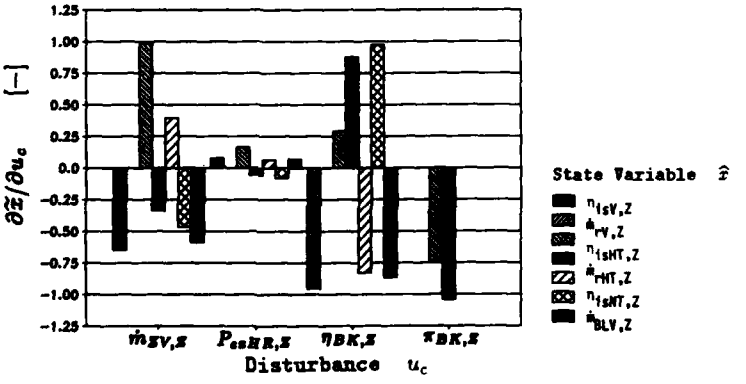

Figure 9 *Effects of non-modelled disturbances on the diagnostic results; n-observer DPF2/2; testbed case: PF2-MP2/2*

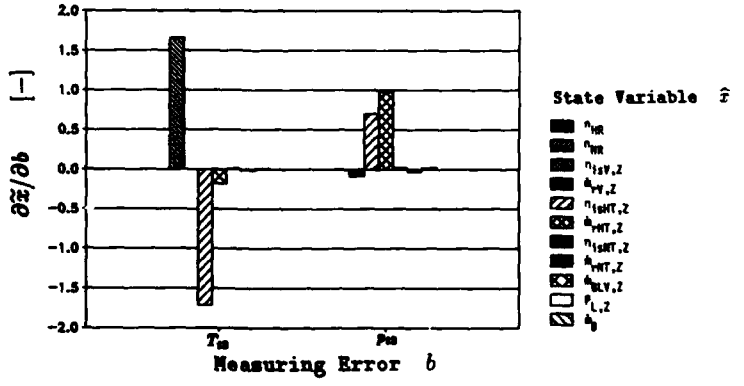

Figure 10 *Effects of systematic measuring errors of T_{t3} and p_{t3} on the diagnostic results; n-observer DPF2/2; testbed case: PF2-MP2/2*

IDENTIFICATION OF DYNAMIC CHARACTERISTICS FOR FAULT ISOLATION PURPOSES IN A GAS TURBINE USING CLOSED-LOOP MEASUREMENTS

G.L. Merrington
Aeronautical Research Laboratory
Defence Science and Technology Organisation
PO Box 4331 Melbourne 3001
Australia

SUMMARY

Combat aircraft, because of the mission profiles involved, tend to rarely operate with their engines in a steady-state condition for extended periods. Furthermore, current generation aircraft contain Engine Monitoring Systems (EMS) which automatically capture a record of important engine parameters when a parameter exceedance is detected. It follows then that any subsequent post-flight data analysis for fault isolation purposes will often necessitate the extraction of the required diagnostic information from transient data records. This generally contrasts with past practice where most of the available fault diagnostic procedures have been derived from steady-state information.

In an attempt to overcome this, and thereby provide effective tools for diagnosing faults from transient data records, a procedure is outlined to extract information about the dynamic characteristics of gas turbines from input/output measurements. The parameter estimator technique involved has the potential to provide a means of detecting changes in some unmeasured/unrecorded parameters, such as shifts in variable geometry schedules. Thus in essence, it provides a tool for identifying problems from simple transient test data which were previously inaccessible or difficult to obtain.

SYMBOLS

A	Parameter EQ(3)	S	Laplace operator
A8	Final nozzle area	SISO	Single input single output
B	Parameter EQ(3)	SLS	Sea level static
CPR	Compressor pressure ratio	S/N	Signal to noise ratio
EGT	Exhaust gas temperature	t	Time
EMS	Engine monitoring system	t_N	Spool time constant
f_s	Sample frequency	T	Temperature
FPR	Fan pressure ratio	WF	Engine fuel flow
K_N	Spool steady-state gain	WFE	Engine overfuelling (WF-WFSS)
LSE	Least squares estimator	WFSS	Steady-state fuel flow
IRP	Intermediate rated power	ΔN	$N_t - N_{t-1}$
N	Spool speed	Δt	Sample time
NL	Fan speed	$\varepsilon(t)$	Equation error
NH	Compressor speed	θ	Parameter vector
P	Pressure	σ	Standard deviation
PPER	Pre and post event recorder	ψ	Vector of observations

1. INTRODUCTION

Many current generation aircraft contain Engine Monitoring Systems (EMS) which have the capability to automatically capture selected engine/aircraft parameters inflight when a parameter exceedance is detected by an onboard computer. These data are then available to maintenance personnel to aid them in diagnosing engine faults. However, while careful consideration is given to the parameter selection and data acquisition aspects during the design/development phase of an EMS, surprisingly little thought appears to have been directed towards providing the user with an adequate inventory of analytical tools to diagnose faults from these data. This contrasts with the situation in the transport/commercial environment where considerable effort has been expended in devising fault diagnostic techniques based on nominally steady-state data. However, combat aircraft seldom operate with their engines in a steady-state condition for extended periods and, therefore, faults will probably have to be diagnosed from transient data records. It follows then that many of the analytical tools currently available are basically unsuitable.

The increasing trend towards the adoption of on-condition maintenance further emphasises the need for improved engine diagnostic techniques to facilitate the process of fault isolation to module and/or line replaceable unit level. It is generally accepted that many of the current fault isolating methods, based primarily on information contained in manufacturer supplied Technical Manuals, can give rise to an unacceptably high rate of false diagnosis. Therefore, in the military environment at least, there is considerable scope for applying new techniques to retrieve important diagnostic information from the EMS records.

In this paper, a method is outlined for analysing transient engine data records and thereby correlating changes in the engine dynamic characteristics with particular engine faults. Such a method has the potential to detect changes in some unmeasured parameters, such as shifts in variable geometry schedules, from input/output transient measurements.

2. ENGINE FAULTS AND TRANSIENT PERFORMANCE

Some engine faults impact upon the steady-state performance of an engine and the symptoms can usually be reproduced under sea-level-static (SLS) test conditions. Other faults, such as those leading to reduced surge margins in the compression system, may not necessarily be reflected in a loss of steady-state performance but could seriously degrade the operability of the engine especially at altitude, during aircraft manoeuvres and following missile release. For instance, misscheduled variable geometry within the engine or corrupted sensor signals can be cause for concern.

In the past, maintenance personnel have tended to rely on manufacturer supplied information in the form of procedures laid down in Technical Manuals, combined with experience, to diagnose common engine faults. In certain cases it may involve the use of trial and error methods and/or component substitution to eradicate the problem. However, the advent of relatively inexpensive computer-based data acquisition systems in many current generation aircraft provides a means of automatically capturing important engine/aircraft parameters in the form of a Pre and Post Event Record (PPER). Moreover, these records can contain crucial information on how the fault affects the transient response of the engine in addition to any steady-state effects. This is achieved by utilising sampling frequencies of 5-10 Hz or even higher depending on the particular EMS configuration. Thus, to fully utilise the PPER data and thereby increase the current level of engine fault diagnostic capability, there is a need to implement new analysis procedures in ground based computing facilities. The following procedure represents one such approach.

3. ANALYSIS PROCEDURE FOR EXTRACTING THE DYNAMIC CHARACTERISTICS

Parameter estimation and identification procedures are continually finding new applications in the field of fault detection and isolation including in gas turbines (Refs. 1-5). The primary aim of the present exercise is to develop techniques for application to in-flight recorded data and thereby aid engine fault diagnosis within the constraints imposed by existing EMS.

The transient response of a gas turbine can be identified in terms of well-defined dynamic characteristics, namely time constants and steady-state gains. These in turn are governed by aerothermodynamic states within the gas path in combination with mechanical considerations such as spool inertias. To simplify the problem for discussion, the present analysis is confined to the single-input/single-output (SISO) fuel-flow/spool-speed response. However, as matrix methods are employed in the analysis, additional inputs/outputs can be added when and if necessary.

In a gas turbine, the spool-speed/fuel-flow response over the normal operating speed range is characterised by a non-linear relationship of the form :

$$N = f(WF,\ t_N,\ K_N,\ P,\ T) \tag{1}$$

In the vicinity of a steady-state set point, the response is closely approximated by a simple lag

$$\Delta N = \frac{K_N}{1 + t_N S}\ \Delta WF \tag{2}$$

which in terms of the overfuelling becomes

$$\Delta N = \frac{K_N}{t_N S}\ \Delta WFE$$

or alternatively in discrete time

$$N_t = AN_{t-1} + BWFE_{t-1} \tag{3}$$

where $A \neq 1$ and $B = K_N\ \Delta t/t_N$

Some engine faults will modify the steady-state behaviour and can therefore be expected to appear as changes in K_N. Similarly, other faults will influence the transient performance characterised by changes in the effective t_N or a combination of K_N and t_N. Thus it follows that the embedded fault information will be associated with the fault parameter B. The basic problem reduces to estimating the parameters A and B in Eq.(3) from noisy transient measurements and correlating these with known fault conditions to ultimately form a fault library. A parameter estimation scheme was used to extract this information.

3.1 Parameter Estimation Procedure

Equation (3) being linear in the parameters is in a form suitable for regression analysis (Ref. 6), that is

$$N_t = \theta^T \psi(t) + \varepsilon(t)$$

where $\psi(t) = (-N_{t-1}, \ldots -N_{t-n}, WFE_{t-1} \ldots WFE_{t-m})$

$$\theta^T = (A_1 \ldots A_n, B_1 \ldots B_m)$$

The simplest estimator is the Least Squares Estimator (LSE) where the estimate for $\theta = (A, B)^T$ in Eq.(3) is given by

$$\hat{\theta} = \begin{bmatrix} \hat{A} \\ \hat{B} \end{bmatrix} = \begin{bmatrix} \frac{1}{n}\sum_{t=1}^{n} N_{t-1}^2 & \frac{1}{n}\sum_{t=1}^{n} WFE_{t-1}N_{t-1} \\ \frac{1}{n}\sum_{t=1}^{n} N_{t-1}WFE_{t-1} & \frac{1}{n}\sum_{t=1}^{n} WFE_{t-1}^2 \end{bmatrix}^{-1} \begin{bmatrix} \frac{1}{n}\sum_{t=1}^{n} N_t N_{t-1} \\ \frac{1}{n}\sum_{t=1}^{n} N_t\, WFE_{t-1} \end{bmatrix}$$

The LSE is known to produce asymptotically-biased estimates in the presence of measurement noise even for very large data samples(Ref. 6). The degree of bias depends on the signal to noise (S/N) ratio of the individual signals and for some applications small levels of residual bias can be tolerated. The present problem falls into this category in that relative differences between the fault/no-fault estimates of the parameter assume much greater importance than the absolute values of the individual estimates, provided the level of bias error is consistent.

Simulated turbofan data, derived from a modified version of a generic thermodynamic simulation (Ref. 7), superimposed with white measurement noise, were used in the analysis, together with SLS test cell data from a small turbojet. The LSE was found to yield satisfactory results for small levels of measurement noise. However, the bias and the associated uncertainty of the parameter estimates increased markedly in the presence of typical noise levels experienced in the test cell. This is illustrated in Fig. 1, where the predicted spool speed for a small turbojet, based on the measured fuel flow and the estimated model parameters, is compared with the actual measured data. It is immediately apparent that the correlation is poor for these noisy experimental data.

To overcome this, a modified estimator was proposed (Ref. 4), where improved estimates are obtained by using well-known hill-climbing techniques to obtain a new minimum variance fit of the predicted/measured speed profiles, Fig. 2. This method uses the LSE as a first estimate, from which improved estimates are subsequently obtained using the pre-filtering characteristics of the model. In essence, this technique resembles the Instrumental Variable (IV) method (Refs. 2,8,9) but with the important difference that conceptually at least, it is more easily understood by performance engineers. Monte-Carlo testing, using simulated turbo-fan test data superimposed with white measurement noise, indicated that the resultant bias errors were insignificant (<.1%) for levels of measurement noise normally experienced in the field. As a further test of the method, the linearised model Eq.(3) was configured with variable coefficients to predict the full non-linear idle/max power and max/idle power speed transients using the measured fuel as input, Fig. 3. The coefficients were estimated at a number of steady-state set points across the speed range from small accelerations/decelerations. The good agreement with the measured test data is justification for the use of the estimator as a tool for extracting the spool dynamic characteristics from noisy engine data. It therefore remains to evaluate the use of the estimator for diagnosing faults from transient data.

4. THE ESTIMATOR AS A FAULT DIAGNOSTIC TOOL

Two simple faults are chosen to illustrate the important features of the estimator as a fault diagnostic tool. The first, a biased exhaust gas temperature (EGT) sensor error in an engine controlled to an EGT schedule, can introduce significant transient and steady-state performance effects. The second, a changed final nozzle schedule during an acceleration does not impact upon the steady-state performance but can influence the transient performance. The method is applied to results obtained from the generic military turbofan simulation referred to previously, because it enables effects of measurement noise and data sampling rate to be investigated in a carefully controlled environment with the aid of Monte-Carlo testing techniques. In the case of the EGT sensor bias fault, the simulation results are supported by F404 engine test data. Back to back tests were performed on an F404, with and without a faulty EGT harness, which resulted in a set of fault/no-fault data suitable for analysis.

4.1 Exhaust Gas Temperature Sensor Bias Error

In gas turbines, EGT limiting can be effective in reducing engine over-temperatures and therefore preserving hot section component lives. In military turbofans, closed-loop control of the final nozzle is commonly employed to achieve this. Thus an EGT sensor bias error immediately impacts upon the transient/steady-state engine performance when the limiter loop becomes active.

Simulated turbofan results for an acceleration under closed-loop fan-speed control combined with an EGT limiter (similar control concept to that employed in the F404 engine near Intermediate Rated Power (IRP)) are given in Fig. 4. The positive sensor bias culminates in a steady-state performance decrement (reduced engine pressure ratio and therefore thrust) as a result of an increase in final nozzle area and reduced overfuelling. Moreover, transient profile trajectory changes indicating increased surge margin in the fan, as shown by the curve of fan pressure ratio in Fig. 5 and a corresponding marginal reduction in the compressor over part of the transient, as shown by the curve of compressor pressure ratio in Fig. 6, accompany the bias.

Normally, EGT forms an integral part of EMS output and therefore bias effects can be quickly identified from temporal and crossplot data. However, parameter estimation techniques which can extract information about the fault from other input/output measurements in isolation, that is without the need for measurements of the actual fault parameter, can provide an important additional degree of redundancy for fault diagnosis purposes.

Estimator results for the turbofan acceleration as a function of sensor bias are given in Fig. 7. The resultant trends in the LP spool dynamic characteristics constitute a useful fault signature where the uncertainty bands correspond to representative levels of measurement noise, namely NL ≈ 0.3%, WF ≈ 0.6% for a 50 Hz sampling frequency. More particularly, the trend in K_N confirms the effect of the bias error on the steady-state performance and similarly, trends in t_N and B correlate with the transient performance changes.

In the above, the estimator has been applied to accelerations where $\Delta NL > 5\%$, that is, higher than the normally accepted speed range about a steady-state set point where the linearised approximation usually applies. The resultant effective spool dynamic characteristics derived from these larger transients do not have the same physical meaning as those obtained for the smaller linearised responses, but they still provide a convenient way of monitoring changes in fault/no-fault transient profiles. It is this aspect that is appealing in the fault diagnosis application, in that, simple linear model structures can still provide useful diagnostic information even in the non-linear domain.

4.2 F404 EGT Sensor Bias Results

F404 back to back small acceleration test data, corresponding to a fan speed increment of $\Delta NL_c \approx 5\%$, are given in Fig. 8, with and without an EGT bias error of approximately 60^0C caused by a faulty EGT harness. The bias error is immediately apparent from the EGT trace prior to and during the transient but the discrepancy diminishes subsequent to the EGT limiter becoming operational, as expected. The effects of the EGT bias are then transferred to some of the other measured parameters, such as A8 and EPR, Fig. 8. This is illustrated most effectively by crossplotting the parameters against fan-speed as in Fig. 9, resulting in comparable trends to those observed with the simulation data, Fig. 5.

Estimator results for the corresponding fault/no-fault transients are given in Fig. 10. The values obtained for the characteristics, namely $K_N = 22.10$, $t_N = 2.11$ differ significantly from the equivalent no-fault values ($K_N = 8.41$, $t_N = 0.77$). This is highlighted in Fig. 11 where the EGT bias results can be compared with nominal values obtained over a wide operating speed range.

It is apparent from the results presented so far that the EGT sensor bias affects the transient as well as the steady-state performance. However, the next fault, consisting of a misscheduled final nozzle, only affects the transient response. In the event that the final nozzle position is not monitored by the EMS, such a fault can be difficult to isolate without additional testing. It will be shown that the estimator technique overcomes this.

4.3 Misscheduled Final Nozzle

Misscheduling of gas turbine variable geometry can be instrumental in promoting compression system instabilities by reducing available surge margins. Therefore, misscheduling resulting from actuator wear, incorrect adjustment and/or corrupted sensor input may not necessarily be apparent from steady-state results. Furthermore, if variable geometry position is not included in the normal EMS output, then it will be necessary to infer changes from the available transient engine data. A misscheduled final nozzle is selected to demonstrate this.

In some military turbofans, the nozzle is scheduled open at low power then ramped to the floor during accelerations until the EGT limiter loop becomes active, Fig. 12. For convenience, the nozzle closure trigger point for the simulated turbofan is chosen as a fixed percentage of NL and the fault is characterised in terms of a retardation in this (ΔNL %). Typical fault/no-fault profiles are displayed in Fig. 13 indicating no changes to the resultant steady-state performance. However, surge margins in the fan/compressor are increased/decreased respectively over at least part of the transient, Figs. 14, 15.

Estimator results given in Fig. 16 exhibit a clear correlation with trigger point delay except for K_n which is invariant as expected. In addition, the fault signatures, namely curves of K_N, t_N and B, differ significantly from the EGT bias results, Fig. 7. The estimator technique clearly discriminates between the two faults but many more fault signatures need to be compiled before definitive statements can be made as to the uniqueness or otherwise of the individual signatures.

The important point that emerges from the above analysis is that the estimator technique provides a convenient tool for extracting information on unmeasured fault parameters from available input/output transient data. Moreover, it will be shown that the sensitivity of the fault estimator technique is critically dependent on :

(a) level of measurement noise, and

(b) data sampling rate.

4.4 Effect of Measurement Noise

The performance of the fault estimator deteriorates in the presence of measurement noise due principally to increased uncertainty in the estimates as distinct from bias effects. The uncertainties in the estimated parameters, which are specified by the $\pm 2\sigma$ bands about the means, Figs. 7 and 16, determine the minimum variations in the actual unmeasured fault parameters that can be detected by the fault estimator. Therefore, the magnitude of the uncertainties ultimately establishes the sensitivity of the method and as a consequence, is more important than the effects of residual bias errors because the latter can reasonably be expected to be of similar magnitude in the fault/no-fault cases. Furthermore, the present results indicate that the noise on the input fuel signal can seriously degrade the overall performance of the estimator, Fig. 17. The reason for this is that the peak overfuelling becomes a more suitable choice of reference signal than the mean fuelling level. To summarize, performance constraints imposed by the measuring system set minimum obtainable estimator sensitivity levels and therefore the full potential of the method may only be realised if the measuring system is correctly designed in the first place.

4.5 Effect of Sampling Rate

Typical characteristic frequencies of interest in gas turbines, based on the spool time constants, are less than 5 Hz. The simulation results presented so far correspond to acquisition rates of 25 - 50 Hz. In some aircraft EMS, lower sampling frequencies 5 - 10 Hz are employed and therefore it is essential to briefly examine the effects of reduced sampling rates on the uncertainty of the fault estimator. Uncertainty estimates, derived from Monte-Carlo tests using white measurement noise (constantσ) are given in Fig. 18 for the no-fault acceleration results discussed previously. The following observations can be made :

(1) Uncertainty increases as sampling rate decreases.

(2) The rate of increase in the uncertainty begins to become unacceptably high as the sampling rate decreases below 10Hz.

(3) If reduced sampling rate is employed on the input fuel signal, as in some operational EMS, the uncertainty increases at an even higher rate. This stems from the resultant smoothing of the input signal which in turn provides improved estimates of the time constant at the lower frequencies.

Near optimum results are obtained using 25 - 50 Hz full rate sampling on each signal. However, if reduced rate sampling must be tolerated on the input signal then the uncertainty that prevails corresponds approximately to the level of uncertainty obtained for the full sampling rate on both signals but at the lower frequency, Fig. 18. The performance differences become insignificant as $f_s \geq 50$ Hz.

4.6 F404 Data Uncertainty

The uncertainty in the estimated values of parameter B derived from the F404 test cell data is of the order of ±5% (Fig. 11). It should be emphasised that the resultant uncertainty is based on a limited number of tests and therefore can only be taken as a guide. This uncertainty corresponds to measurement noise levels of NL≈ 0.2%, WF≈ 1.5 - 2.0% and sampling rates for fan-speed and fuel-flow of 20 and 5 Hz, respectively. The measurement noise and sampling rate data for the F404 measuring system can be combined with the simulation predictions given in Fig. 18 to provide another estimate of the uncertainty in the parameter B. This yields a figure of approximately ±5% which agrees

with the previous estimate. It confirms the suitability of using data of the type given in Fig. 18 to predict the performance of the estimator. Thus knowledge of the measuring system performance, namely noise levels and data sampling rates, is sufficient to predict apriori, the estimated parameter uncertainty.

5. CONCLUSIONS

A method has been outlined for extracting fault diagnostic information from gas turbine engine transient data records. The parameter estimator technique, because it can provide information about unmeasured parameters, such as changes in variable geometry schedules, from normal closed-loop input/output measurements, forms the basis of a useful diagnostic tool. Moreover, this diagnostic information can be extracted without the need for additional test instrumentation.

The performance of the fault estimator is closely related to the capabilities of the measuring system, namely sampling rates and the levels of measurement noise. Optimum performance is obtained at $f_s > 50$ Hz but it deteriorates significantly as the sampling rate falls below 10 Hz. Measurement noise, especially on the input fuel signal, has a significant influence on the sensitivity of the fault estimator. However, noise levels encountered in many operational EMS do not unduly compromise the resultant sensitivity of the fault estimator technique.

When the technique is combined with corrected data cross-plotting procedures, a powerful tool emerges for analysing transient data records. The input/output results used in the present analysis were restricted to fuel-flow and fan-speed respectively, but temperature and pressure data can readily be incorporated. Furthermore, information on new faults can be added to an existing fault library to improve and extend its capability. Finally, the method can be applied to in-flight recorded data where it may be difficult to reproduce the fault under SLS test conditions.

6. REFERENCES

1. Baskiotis, C., Raymond, J. and Rault, A. 'Parameter Identification and Discriminant Analysis for Jet Engine Mechanical State Diagnosis', Proceedings IEEE Conference on Decision and Control, Fort Lauderdale, 1979, pp 648-652.

2. Isermann, R. 'Process Fault Detection Based on Modelling and Estimation Methods - A Survey', Automatica, Vol 20, 1984, pp 387-404.

3. Merrill, W. 'Identification of Multivariable High Performance Turbofan Engine Dynamics from Closed-Loop Data', Journal of Guidance, Vol 7, No 6, 1984, pp 677-683.

4. Merrington, G.L. 'A Modified Least Squares Estimator for Gas Turbine Identification', ARL AAP TM 445, 1988.

5. Merrington, G.L. 'Fault Diagnosis of Gas Turbine Engines from Transient Data', Paper to be presented to 33rd ASME International Gas Turbine Congress, Amsterdam, June 5-9, 1988.

6. Goodwin, G.C. and Payne, R.L. 'Dynamic System Identification : Experiment Design and Data Analysis', Academic Press, New York, 1977.

7. Sellers, J.F. and Daniele, C.J. 'DYNGEN - A Program for Calculating Steady-State and Transient Performance of Turbojet and Turbofan Engines', NASA TN D-7901, 1975.

8. Ljung, L and Soderstrom, T. 'Theory and Practice of Recursive Identification', MIT Press Cambridge, 1983.

9. Young, P. 'Recursive Estimation and Time Series Analysis', Springer Verlag, 1984.

7. ACKNOWLEDGEMENTS

The author is grateful to the RAAF for making an F404 engine available for testing and to his colleagues within ARL for their assistance with the experimental work.

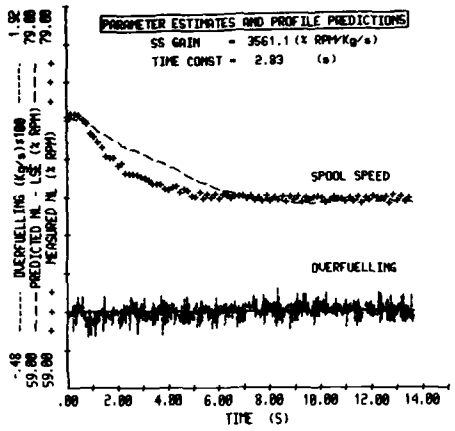

FIG. 1. *LSE PREDICTION - NOISY MEASURED TURBOJET DATA*

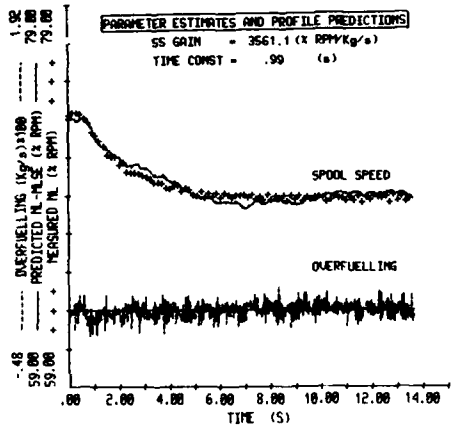

FIG. 2. *PREDICTION USING MODIFIED ESTIMATOR*

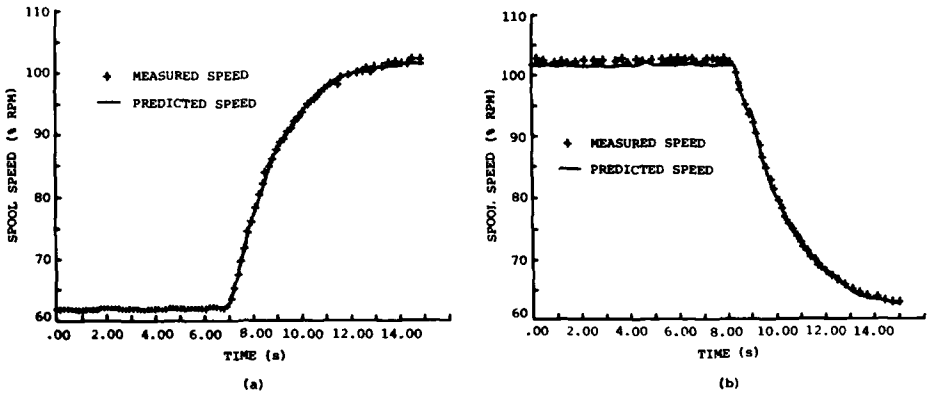

FIG. 3. **FULL TURBOJET TRANSIENTS**

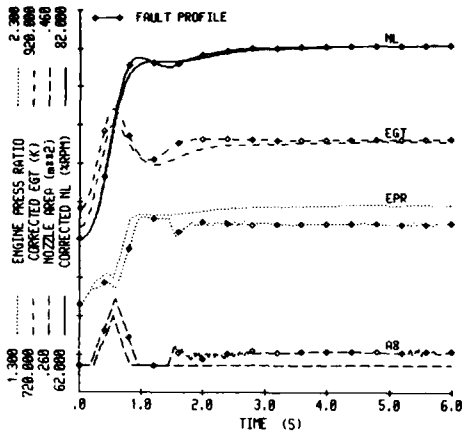

FIG. 4. TURBOFAN WITH EGT SENSOR BIAS

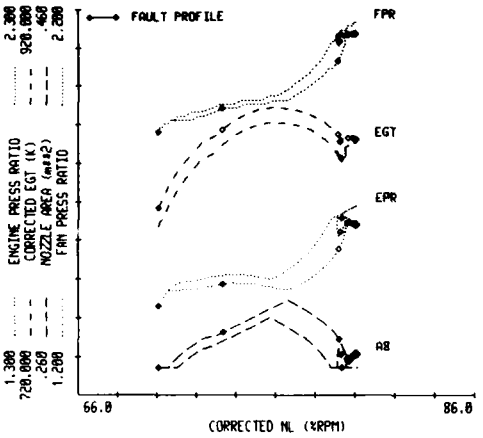

FIG. 5. EGT SENSOR BIAS DATA VERSUS NL

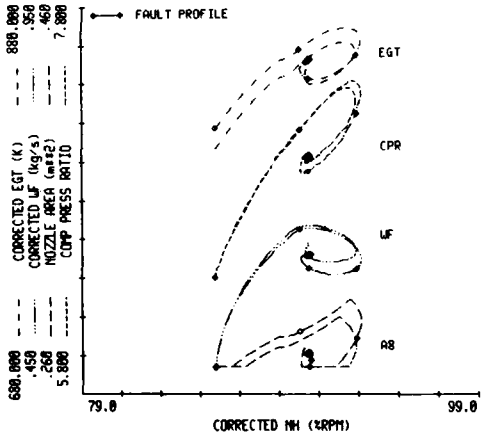

FIG. 6. EGT SENSOR BIAS DATA VERSUS NH

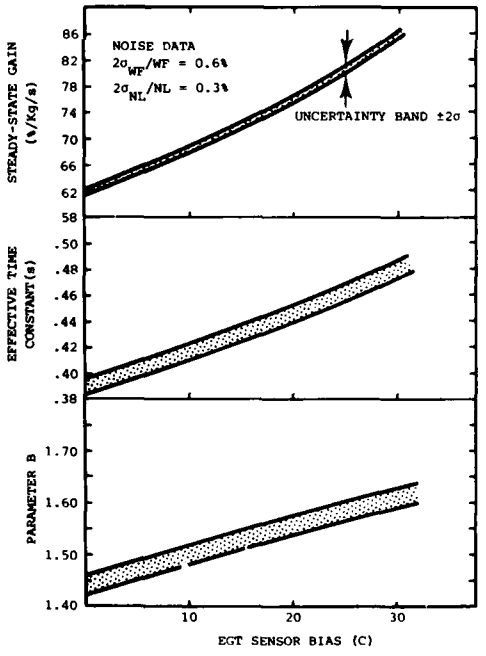

FIG. 7. PARAMETER FAULT SIGNATURES - EGT SENSOR BIAS

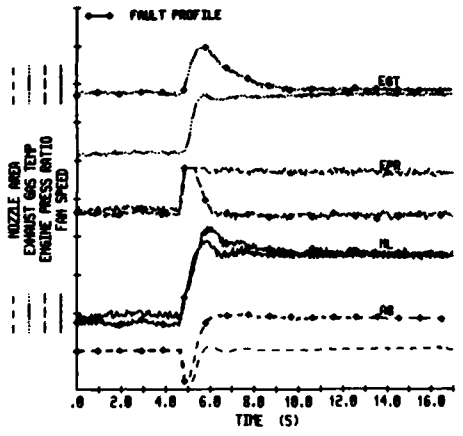

FIG. 8. F404 ENGINE ACCELERATION WITH 60°C EGT SENSOR BIAS

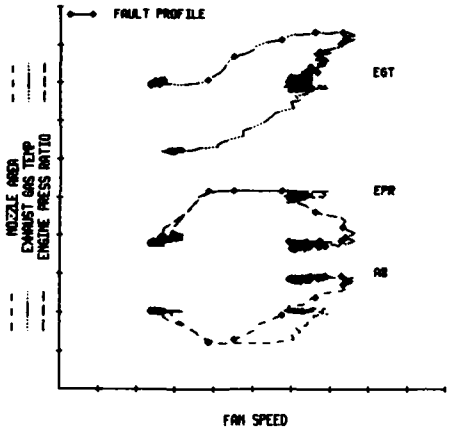

FIG. 9. F404 ENGINE SENSOR BIAS DATA VERSUS NL

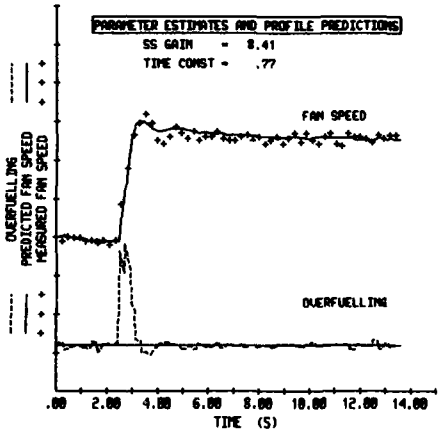

(a) NO EGT SENSOR BIAS

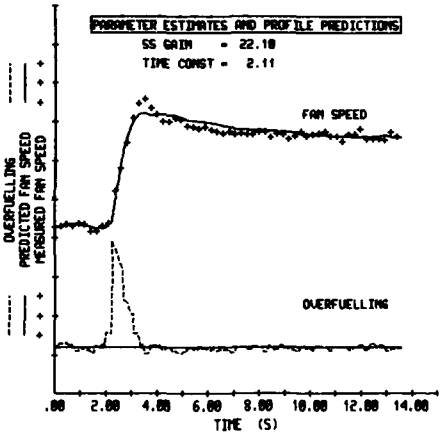

(b) 60°C EGT SENSOR BIAS

FIG. 10. F404 ENGINE PARAMETER ESTIMATES AND PROFILE PREDICTIONS WITH AND WITHOUT AN EGT SENSOR BIAS

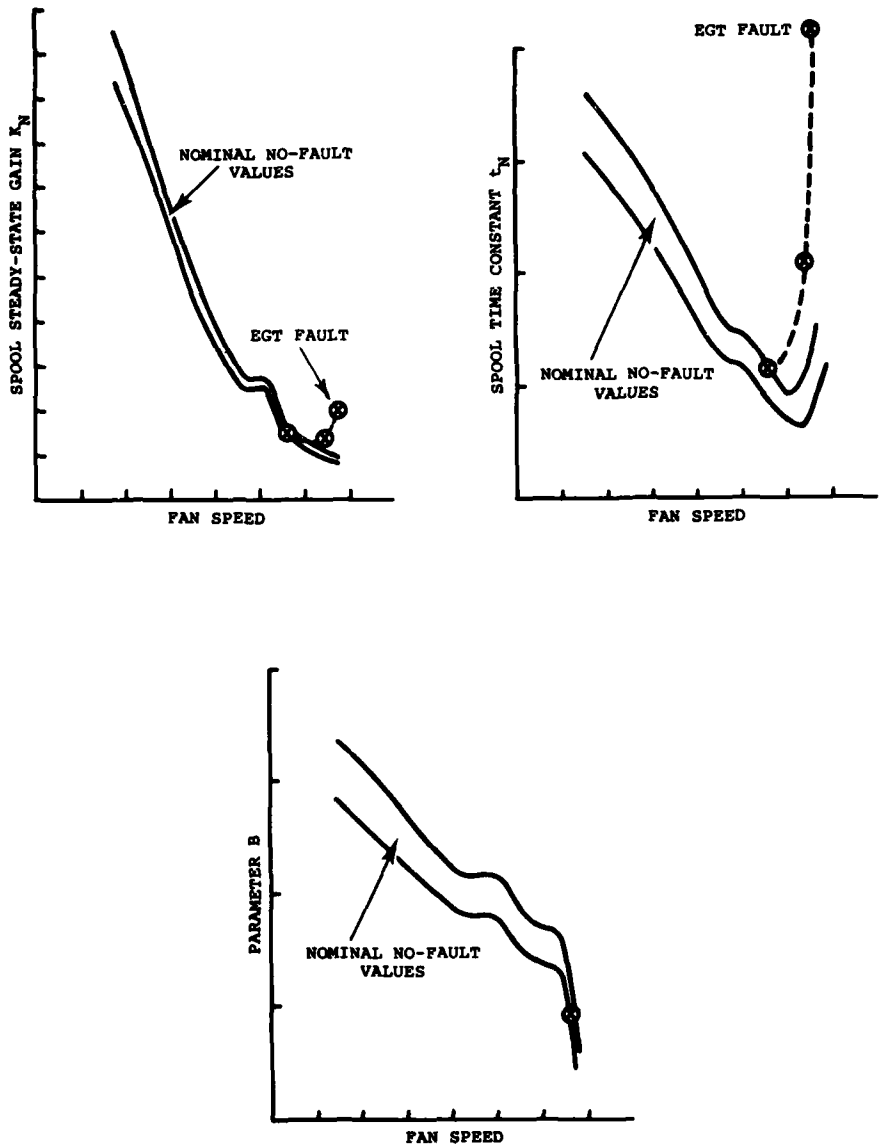

FIG. 11. EFFECTIVE FAN SPOOL DATA FOR THE F404 ENGINE

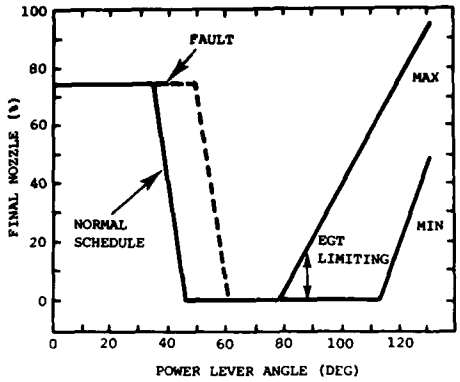

FIG. 12. TYPICAL NOZZLE SCHEDULE FOR A MILITARY TURBOFAN

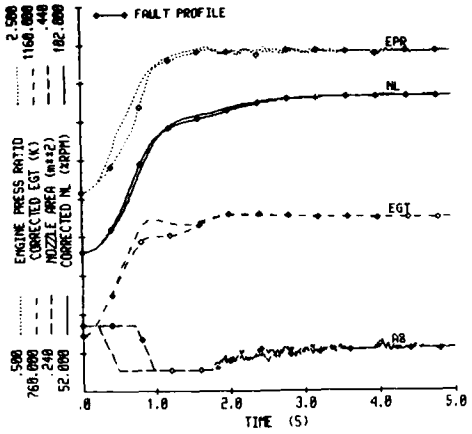

FIG. 13. TURBOFAN WITH MISSCHEDULED FINAL NOZZLE

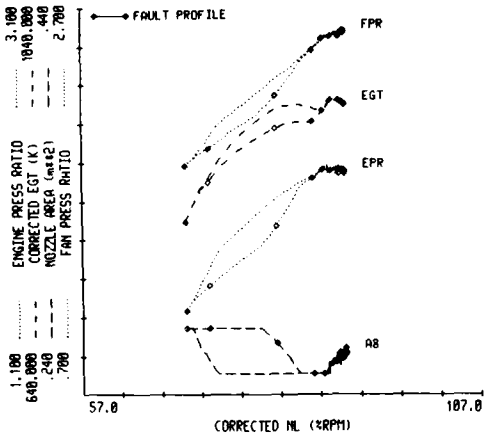

FIG. 14. MISSCHEDULED FINAL NOZZLE VERSUS NL

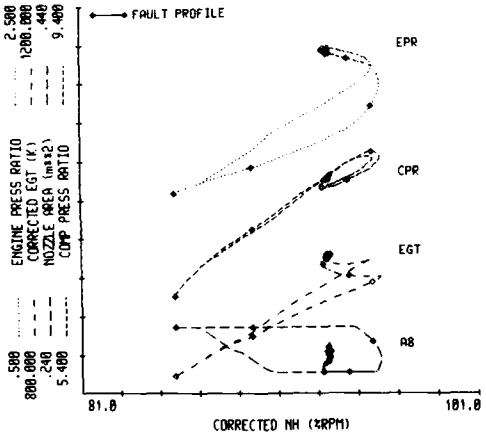

FIG. 15. MISSCHEDULED FINAL NOZZLE DATA VERSUS NH

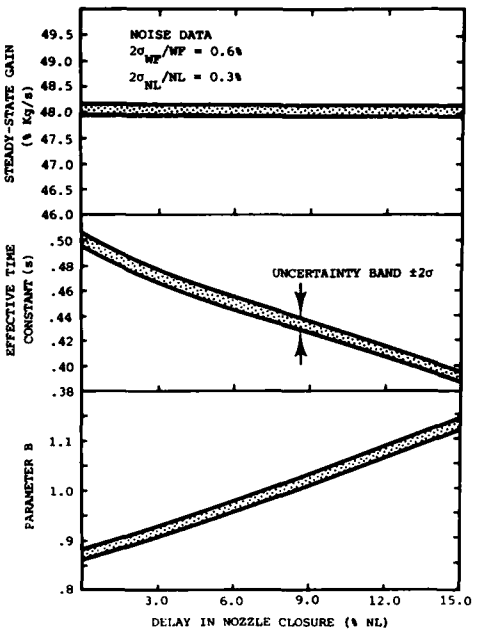

FIG. 16. PARAMETER FAULT SIGNATURES - MISSCHEDULED FINAL NOZZLE

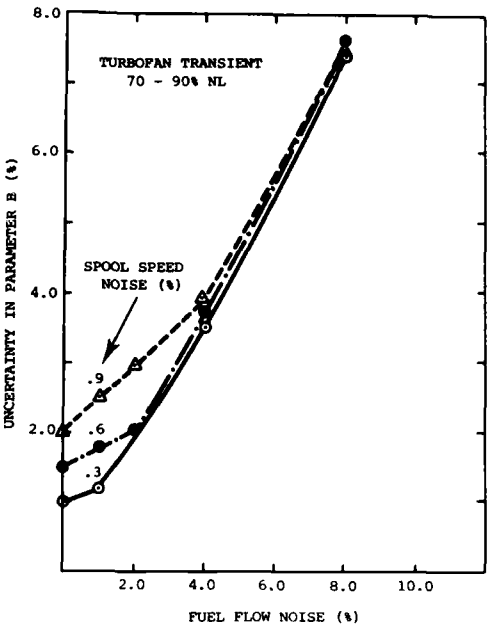

FIG. 17. EFFECT OF MEASUREMENT NOISE ON ESTIMATOR PERFORMANCE

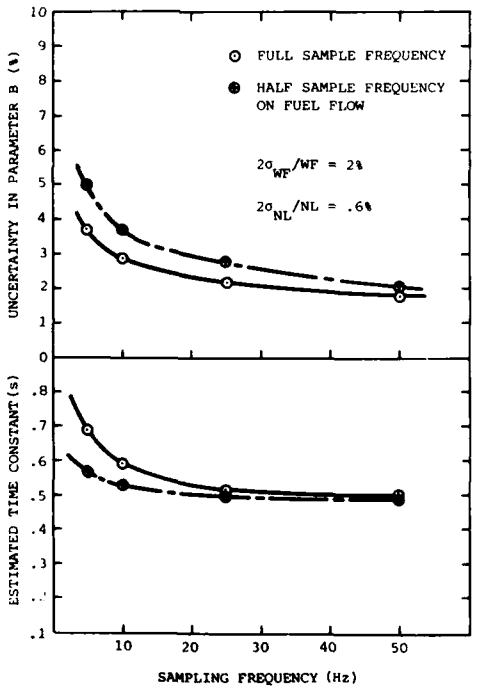

FIG. 18. EFFECT OF SAMPLING RATE ON ESTIMATOR PERFORMANCE

DISCUSSION

F. HOERL

How do you define the effective time constant for a twin spool engine?

Author's Reply:

The effective time constant is evaluated from eq (3):

$$t_N = K_N . \Delta t/B$$

It represents an effective time constant because some of the transients used correspond to spool speed changes $\Delta N > 5\%$, the normal limit for determining actual time constants from such simple linear model structures. However, for fault diagnostic purposes the relative differences between the predicted fault/no fault values of T_N are more important than the actual values themselves. Thus effective time constants obtained from larger transients ($\Delta N > 5\%$) can still provide useful information.

M. TOBIN

The diagnostic method appears to be predicated on the assumption that engine faults will manifest themselves as changes in dynamic characteristics. For the examples shown(i.e. EGT bias and A8 shedule change) a transient behaviour change seems reasonable to expect since the faults directly affect the engine control system. The question is, have you any experience which indicates that turbomachinery faults will similarly affect dynamic behaviour?

Author's Reply:

You are correct in that the faults examined affects the controller directly. However we are currently investigating ways of detecting small changes in component performance, typically efficiency changes of the order of 2% in the compressor or the turbine. This work is being performed at an Australian university under a DSTO research agreement. While the work so far is still in its formative stage, the results obtained look encouraging.

CF-18/F404 TRANSIENT PERFORMANCE TRENDING

by

Captain J.R.Henry
Aerospace Maintenance Development Unit
Canadian Forces Base Trenton
Astra, Ontario, Canada K0K 1B0

SUMMARY

The "on condition" concept of aircraft engine maintenance has led to intensive analysis of the data recorded by Engine Health Monitoring systems during steady-state operation of the engine. To date however the transient data acquired during take-off or in-flight have received far less attention. This paper presents the results of an investigation into the feasibility of utilizing engine data acquired during take-off to trend the performance of a modern turbofan engine (GE-F404). Factors influencing the repeatability of take-off data such as throttle rate, variable geometry and instrumentation effects are discussed. Using engine data from operational aircraft, various trending parameters are evaluated using a data capture window developed to minimize the scatter of nominal engine performance. A statistical tool to identify performance shifts is briefly described, and is shown to successfully detect a shift in the take-off performance of a recently repaired engine. It is concluded that the trending of transient performance data is a viable means of detecting certain engine faults and recommendations are made concerning the implementation of such a program for the F404 engine.

NOTATION

AMAD	airframe mounted accessory drive
EHM	engine health monitoring
HPC	high pressure compressor
IECMS	inflight engine condition monitoring system
MFC	main fuel control
MSDC	maintenance signal data converter
PS3	static pressure at high pressure compressor exit, lbf/in^2
P5	total pressure at low pressure turbine exit, lbf/in^2
T1	total temperature at inlet, deg K
T5	total temperature at low pressure turbine exit, deg K
VEN	variable exhaust nozzle
VG	variable geometry
XN1	low pressure spool speed, rpm
XN2	high pressure spool speed, rpm
δ	P/P standard
θ	T/T standard

ENGINE STATION NOTATION

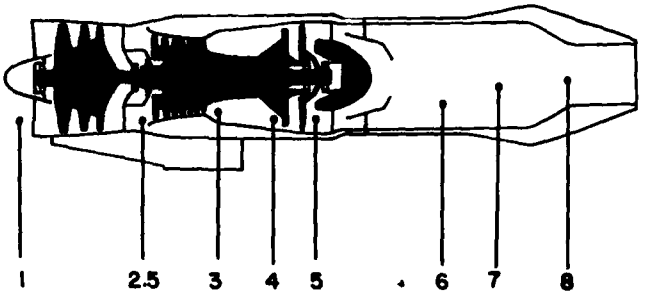

INTRODUCTION

The recent acquisition of the CF-18 aircraft by Canada has forced managers to re-evaluate maintenance policies and procedures. Due to the high cost of modern weapon systems, ways of reducing operating expenditures while improving aircraft availability must be found. To help achieve this goal, the F404 engine used in the CF-18 is maintained using on-condition maintenance.

As an engine fleet ages, one's ability to assess an engine's health will be a significant factor in determining engine reliability and availability. If time-dependent failures can be detected early-on, fewer failures and unscheduled maintenance actions may be expected during installed operations. The early detection of faults may also reduce operating costs by allowing the user to replace damaged components before repairable limits are exceeded and before severe secondary damage occurs.

A considerable, concerted effort has gone into the development of a wide range of Engine Health Monitoring (EHM) technologies suitable for application to the F404 engine. To date however, only borescope inspections of the F404 have produced tangible results. In an attempt to meet the need of Field Units for a simple EHM technique to complement borescope inspections, an investigation was started into the possible use of existing CF-18 data for EHM purposes.

Each CF-18 is equipped with an Inflight Engine Condition Monitoring System (IECMS) designed to record engine and aircraft parameters on a magnetic tape at various times throughout a flight. Figure 1 is a block diagram of the CF-18 IECMS. Detailed engine data are recorded whenever:

a. an engine parameter exceedance is sensed;

b. the pilot manually depresses a 'record' button located on the aircraft instrument panel; and

c. the aircraft takes-off.

Information from the magnetic tape is then archived, maintaining a record of every CF-18 take-off. As the recording of take-off data is software initiated, personnel are not involved in the data collection process. These two factors clearly make take-off records one of the most attractive sources of EHM data.

METHODOLOGY

GENERAL

When initially considering the transient behaviour of a modern military turbofan engine, one cannot help but immediately conclude that transient performance data are non-repeatable. Variations in throttle handling alone dictate that an engine must accelerate at different rates. Variable geometry schedules and control system functions such as temperature or speed-limiting will also complicate the overall analysis picture. Clearly then, variables influencing the acceleration of an engine must be identified and wherever possible, eliminated. An equally important consideration is the measurement of transient data repeatability. A simple means of quantifying transient performance data scatter is needed.

REPEATABILITY CONSIDERATIONS

Several studies were carried out to identify factors that may influence the repeatability of transient data. The results of this survey are summarized below:

A. AMBIENT CONDITIONS. Although standard temperature and pressure corrections were employed, Zucrow (ref 1) points out that these terms do not account for all possible influences. As variations in Reynolds and Prandtl numbers are disregarded, changes in viscosity, specific heat ratio and thermal conductivity could contribute to data non-repeatability. Also, the correction of transient data can only modify parametric values; the spacing of data in time is not changed.

B. STARTING SPEED. The importance of initial speed was emphasized by Gold and Rosenzweig (ref 2). Treating the time response of an engine as a linear first order system, they found that the time constant for spool speed response was dependent upon both the initial and final speeds of an acceleration. Clearly then, CF-18 take-off data must be screened to ensure that the range of speed increase is consistent.

C. VARIABLE GEOMETRY (VG). The F404 incorporates fan, High Pressure Compressor (HPC) and exhaust nozzle variable geometry. Fan VG activation occurs approximately half way through a slam acceleration. As HPC VG activation occurs much earlier, compressor geometry is continuously adjusted during an acceleration. Examination of test data revealed that during a rapid

acceleration, the F404 Variable Exhaust Nozzle (VEN) immediately moved to and remained in the fully closed position for approximately 4 seconds. Thus, data collected over this period would essentially be from an engine with a fixed nozzle.

D. RATE OF THROTTLE MOVEMENT. The rate of throttle movement influences the rate and magnitude of fuel added by the Main Fuel Control (MFC). There exists a rate of throttle movement for which the maximum or limiting fuel schedule is engaged. If the throttle is moved at this rate or faster, engine transient performance becomes independent of throttle rate. This throttle rate threshold was estimated to be about 50 degrees per second. As the IECMS does not start recording take-off engine parameters until the throttle has been advanced to military power, it might appear that throttle rate cannot be inferred from the data. Analysis of preliminary results showed that the nozzle starts to close shortly after the throttle movement commences and that it takes about 1 second for the nozzle to fully close. Therefore, it was concluded that if the IECMS take-off record shows the nozzle closing to zero percent, then the duration of throttle movement was less than the nozzle response time. Consequently, throttle rate can be estimated using take-off records.

E. RESLAM EFFECTS. A 'reslam' occurs when two slam accelerations are carried out in quick succession. During the first slam engine components are heated and, without sufficient cooling time, the second slam takes place with less heat being transferred to the engine body. The pre-heating of engine components will cause changes in blade tip clearance and component efficiencies. Saravanamuttoo and Fawke in Reference 3 found, when using a dynamic model of a twin spool engine that speed response will be significantly improved during reslams. To eliminate reslam effects, care must be taken to ensure that sufficient cooling time was allowed between slams.

F. INSTALLATION. Whether an engine is installed in the left or right side of a CF-18 should make little difference to it's dynamic performance. Indeed, left and right engines are interchangeable and the large inlet ducts are similar in every way. Each engine powers an Airframe Mounted Accessory Drive (AMAD) which uses generators and hydraulic pumps to support aircraft systems. Electrical and hydraulic loads are split between the two AMADs and bleed air is extracted equally from the two engines. Therefore, it is concluded that the side of the aircraft in which an engine is installed should not constitute a major influence on engine performance.

G. INSTRUMENTATION. The precisions of the aircraft data recording system and related instrumentation are significant factors in determining the repeatability of transient engine data. Using analytical and experimental techniques described in reference 4, data confidence intervals may be found and levels of nominal or background scatter determined. Furthermore, careful scrutiny of experimental data repeatability may provide valuable information about instrumentation and data processing deficiencies.

H. OTHER EFFECTS. Several other phenomena that occur during accelerations such as changing seal clearances and combustion time lag were considered. It was concluded however, that these effects should be repeatable from slam-to-slam.

DATA CAPTURE WINDOW

The objective of defining a data capture window was simply to reduce the number of variables affecting the F404's transient performance in the hope that the amount of data scatter would be reduced. The data capture window employed during this study was simply:

a. the use of transient data only during the period of time for which the VEN was closed. This was intended to eliminate the influence of the variable nozzle; and

b. the acceptance of take-off data from only those records where the VEN closure was shown. In this way, the effect of variations in throttle movement rate could be eliminated.

By this means, repeatability limiting factors(c) and (d) in the preceding section were eliminated.

COMPARING TRANSIENT DATA

When attempting to compare time response traces for engine parameters collected during different accelerations, the problem of synchronizing the data becomes readily apparent. Indeed, a benchmark must first be established to help define the start of an acceleration. Preliminary results indicated that fairly broad variations in the rate of throttle movement may be expected and consequently, it was decided not to align response curves on the basis of thrcttle position. Instead, an attempt was made to synchronize the response traces by defining an arbitrary

transient starting speed. The results from this trial were not acceptable as temperature and pressure responses tended to display significant amounts of scatter. It became clear that to overcome this problem, the elimination of time as a variable was required. To accomplish this, engine parameters were plotted as functions of one another, rather than as functions of time.

RESULTS

IECMS VALIDATION

Before attempting to detect engine faults, it was first necessary to identify and quantify sources of precision error within the IECMS. This was accomplished by reading data directly from engine-mounted sensors using a test cell data acquisition system of known precision. Consequently, the entire IECMS with it's associated precision errors was bypassed. By comparing data repeatability between test cell and IECMS data and through the use of error propagation theory (ref 5), it was possible to assess the precision error contribution of the Maintenance Signal Data Converter (MSDC).

The results of this effort are shown in Table 1. Engine sensor precision (Column (d)) was found by subtracting the test cell system precision (col. (c)) from the measured data precision (col. (b)) using the square root of the sum of the squares method described in ref 5. Similarly, MSDC precision (col (g)) was found by subtracting engine sensor precision (col. (d)) from the overall aircraft data precision (col (f)).

TABLE 1

PRECISIONS OF SELECTED PARAMETERS
(PRECISION VALUES BASED ON TWO STANDARD DEVIATION CONFIDENCE LIMITS)

PARAMETER	TEST CELL RESULTS				AIRCRAFT RESULTS			MSDC DIGITAL RESOLUTION (h)
	TARGET VALUE (a)	DATA PRECISION (b)	TEST CELL SYSTEM (c)	ENGINE SENSOR (d)	TARGET VALUE (e)	DATA PRECISION (f)	MSDC PRECISION (g)	
T1 K	266	0.22	0.2	0.1	296.1	1.3	1.3	1.0
XN1 RPM	10962	9.6	0.4	9.6	10560	154	153.6	16
XN2 RPM	14215	7.2	0.5	7.2	14204	138	138	16
PS3 PSIA	209.1	0.7	0.05	0.7	137.9	1.2	0.9	0.5
P5 PSIA	34.5	0.09	0.01	0.09	24.7	0.14	0.11	0.06
T5 K	834.3	0.84	0.6	0.6	871.0	2.0	1.9	1.0

By comparing the MSDC precision (col. (g)) to that of the engine sensors (col. (d)), it is evident that the MSDC is a significant source of precision error for temperature and speed measurements. A review of the analog to digital conversion process within the MSDC revealed that the MSDC digital resolution (col. (h)) for temperature and pressure terms was not high. In fact, most of the temperature and pressure readings fell within one bit 'toggle' of the mean value. This finding suggests that the precision of the IECMS would not be significantly improved by using more precise engine sensors. The number of bits assigned to each parameter must be increased if overall data repeatability is to be improved.

The large MSDC precision values for rotor speeds suggest that the MSDC is incapable of precisely converting frequency signals to digital outputs. In addition, it was discovered that the engine fuel flow meters are sampled by the IECMS at a rate greater than the response time of the flow meters.

ASSESSING TRANSIENT DATA SCATTER

Recognizing that scatter exists in transient data, it was necessary to quantify this non-repeatability so that true performance shifts could be distinguished from the nominal scatter. This was accomplished by carrying out a series of slam accelerations in aircraft under controlled conditions. For each acceleration, engine parameters were cross plotted and curve fitted. Using all the curve fits from a particular set of accelerations, it was possible to quantify the amount of nominal curve fit scatter by applying a statistical distribution (Figure 2) to the data. Assuming a normal statistical distribution, a confidence interval or band for each cross plotted pair of parameters was found. Examination of these

results revealed that confidence intervals for transient data were quite narrow. Also, these intervals were repeatable from engine-to-engine and aircraft-to-aircraft.

OPERATOR AND INLET TEMPERATURE EFFECTS

During the analysis of aircraft back-to-back slam acceleration data, it became apparent that despite the use of a data capture window, several variables were still influencing transient data repeatability. Some of the observed performance shifts not caused by engine faults were:

a. Throttle Overshoot. Figure 3 clearly shows that even a momentary throttle overshoot into the afterburner range can cause a shift in a performance baseline.

b. Inlet Screens. Two sets of slams were carried out on the same airframe/engine combination under virtually identical ambient conditions except that anti-personnel screens were left installed during one set. Figures 4 and 5 show that the effect of the inlet screen is quite noticeable at higher inlet Mach numbers.

c. Reslam Effects. During one of the tests, insufficient cooling time was allowed before the second slam was made. Figure 6 shows that a significant baseline shift was observed for the reslam acceleration.

d. Throttle Rate. At the end of each set of back-to-back slams, technicians were asked to perform an acceleration at a different rate of throttle movement. Analysis of these data indicated that throttle rates greater than 45 deg/sec produced repeatable transient performance. Furthermore, it was demonstrated that take-off records showing the nozzle closure were also take-offs with throttle rates greater than 45 deg/sec. This finding clearly supports the earlier data capture decision.

e. Inlet Temperature. It was found that changes of inlet temperature resulted in significant baseline shifts (Figures 7 and 8). These results strongly suggest that the correction scheme employed was not adequate to remove all ambient effects. Inlet temperature constitutes a major influence on transient data repeatability. This phenomenon requires further work so that ambient effects may be quantified and better correction schemes developed.

f. Starting Speeds. A survey of seven sets of back-to-back slams indicated that rotor speeds at the start of accelerations were very repeatable. The standard deviations of fan and core speeds were 4% and 2% respectively. This is quite remarkable when one considers that these speeds were established using only the throttle ground idle stop. The better repeatability of HP spool starting speed is significant in that engine transient behaviour is most sensitive to HP spool disturbances (ref 6).

DETECTING AN ENGINE FAULT

During a routine borescope inspection, Engine number 376020 was found to have extensive High Pressure Compressor (HPC) damage. During the repair process, it was determined that the damage was likely caused by the failure of a hook-bolt locking tab in the HPC. Prior to the borescope inspection, this engine was installed in the right side of an aircraft and following repairs, it was installed in the left side of another aircraft. Several records were obtained for both pre-repair (and possibly faulted) and post-repair take-offs, and the data were curve fitted and cross plotted. For this set of take-off records the inlet temperature range was approximately 30 deg C. Some of these results are shown in Figures 9 and 10.

The significance of the observed shifts is more evident in Table 2. Note that for each of the six cross plotted parameters shown, the observed shift in the curve fits exceeded the amount of nominal curve fit scatter. An automated means of detecting shifts in transient behaviour was developed. This technique uses the curve fit confidence interval obtained from the back-to-back slam acceleration tests and Kalman Filter Theory (ref 7) to determine when a shift has occurred. Although fully described in reference 4, this method has the following features:

a. successive, nominal take-off data are used to update the curve fits formed by cross plotting engine parameters. In this way, the estimated mean relation between two parameters is improved;

b. the confidence interval about the curve fitted line may be reduced in width as additional, nominal transient data are obtained. As more is learned about the transient behaviour of an engine, sensitivity to performance shifts is improved; and

c. the filter automatically identifies those take-offs for which data lie outside the acceptable confidence interval.

TABLE 2

CURVE FIT SHIFT SUMMARY FOR
ENGINE WITH DAMAGED COMPRESSOR

PLOT			TARGET ABSCISSA VALUE	SHIFT IN ORDINATE VALUE	NOMINAL SCATTER
ORDINATE		ABSCISSA			
$\frac{P5}{\delta}$	vs	$\frac{PS3}{\delta}$	125.0 psia	+2%	±1.0%
$\frac{T5}{\theta}$	vs	$\frac{PS2}{\delta}$	150.0 psia	+3%	±0.8%
$\frac{XN2}{\sqrt{\theta}}$	vs	$\frac{PS3}{P5}$	5.75	+3%	±1.0%
$\frac{T5}{\theta}$	vs	$\frac{PS3}{P5}$	5.5	+5%	±2.0%
$\frac{T5}{\theta}$	vs	$\frac{P5}{\delta}$	35.0 psia	+2%	±0.8%
$\frac{T5}{\theta}$	vs	$\frac{XN1}{\sqrt{\theta}}$	11500 rpm	+2%	±0.8%

While it has been shown that a performance shift occurred, it has not been proven that this change was exclusively caused by flow path damage in the HPC. However, several factors indicate that this was the most likely cause. These are:

a. the changes believed to be caused by damage to the HPC were compared with results from a F404 steady state computer model with an embedded compressor fault. None of the predicted, steady state baseline shifts conflicted with the observed transient results;

b. in reference 6 MacCallum employed a transient model of a twin spool bypass engine to study the effects of component faults on engine performance. Among other things, MacCallum's analysis predicted a slower XN1 and PS3 response for a damaged engine, both of which were observed in the present data. MacCallum also predicted that the XN2 transient response would be significantly slower, but this was not observed. With regard to observed shifts in cross plotted data, none were contradicted by MacCallum's results. Overall then, it is believed that the fault characteristics were generally supported by the work of MacCallum;

c. a fault 'signature' was constructed by noting the observed direction of shift for each cross plotted pair of parameters. Similar signatures were obtained for the documented operator and ambient temperature effects. Comparing these sets of cross plot shifts, it was determined that the faulted engine exhibited an unique set of baseline shifts, and therefore operator and/or ambient effects could not satisfactorily explain the faulted engine data. Superposition of ambient temperature effects was also used and it was concluded that the observed changes could not be explained by operator effects such as throttle overshoot or throttle reslam.

Overall then, it was concluded that the detected change in performance was consistent with the known HPC damage. Furthermore, it was demonstrated that the dynamic characteristics of such a fault could not be confused with other non-fault related performance changes.

CONCLUSIONS

From this brief investigation of CF-18/F404 IECMS data, it may be concluded that:

a. transient F404 IECMS parameters were repeatable within ± 1% during rapid accelerations from ground idle to military power given that:

   i) throttle rate is at least 45 deg/sec;

   ii) analysis is carried out while the nozzle is closed;

   iii) the ambient temperature did not change significantly; and

   iv) a cool down period was allowed prior to the accelerations.

b. overall, the existing IECM system has sufficient precision to permit the detection of changes in the F404's dynamic performance;

c. difficulties in synchronizing time-dependent data can be resolved by cross plotting engine variables directly;

d. engine faults can be detected by analyzing automatically recorded CF-18/F404 take-off data;

e. a statistical treatment of transient data proved to be a reliable means of detecting shifts in performance; and

f. if improved precision of IECMS data is desired, attention should be focused on improving the data handling qualities of the MSDC rather than on increasing sensor precision.

RECOMMENDATIONS

The monitoring of F404 transient performance appears to be a feasible means of passively detecting engine faults, however, additional work is needed before such a system could be implemented on a fleet-wide basis. These continuing efforts should include:

a. development of better correction methods to remove ambient temperature influences in transient data;

b. a review of IECMS sensor and data processing characteristics with the aim of improving the repeatability of engine data;

c. development of a dynamic F404 computer model capable of having faults embedded; and

d. expansion of the statistical methods developed to analyze transient data. New curve fitting algorithms and filtering techniques could be employed to increase the sensitivity of this method to performance changes.

ACKNOWLEDGEMENTS

The author wishes to thank Dr W.C. Moffatt of the Royal Military College and Mr J. Bird of the National Research Council of Canada for their assistance throughout this investigation. Also, the Repair and Propulsion organizations at Canadian Forces Bases Cold Lake and Bagotville are to be commended for their cooperation in providing data for this study. The technical advice and data reduction assistance provided by GasTOPS Ltd is gratefully acknowledged. The work was supported under ARP Grant 3610-147 and DND Contract FE220786FRMC4.

REFERENCES

1. Zucrow, M.J. *Aircraft and Missile Propulsion Vol II.* John Wiley and Sons, New York, 1958

2. Gold, H. and Rosenzweig, S. *A Method for Estimating Speed Response of Gas Turbines.* NACS RM E51K21, Lewis Flight Propulsion Laboratory, Cleveland, Ohio, 23 Jan 1952.

3. Saravanamuttoo, H.I.H. and Fawke, A.J. *Digital Computer Methods for the Prediction of Gas Turbine Response.* Society of Automotive Engineers 710550, 1971.

4. Henry, J.R. *CF-18/F404 Transient Performance Trending.* MENG Thesis, Royal Military College of Canada, May 1987.

5. Abernethy, R.B. and Thompson, J.W. *Handbook - Uncertainty in Gas Turbine Measurement.* Arnold Engineering Development Center report AEDC-TR-73-5, 1973.

6. MacCallum, M.R.L. *Further Studies in the Influence of Thermal Effects on the Predicted Acceleration of Gas Turbines.* American Society of Mechanical Engineers 81-GT-21, 1981.

7. Leach, B.W. *An Introduction to Kalman Filters.* National Research Council Repair NAE Misc 57, 1984.

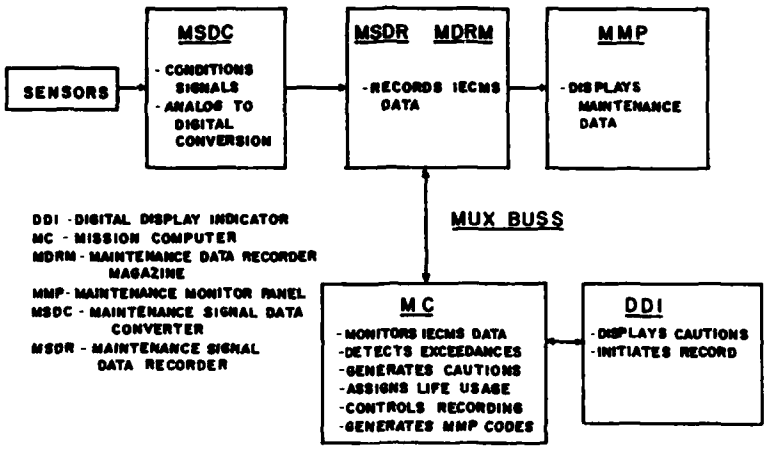

FIG. 1 - CF-18 IECMS - BLOCK DIAGRAM

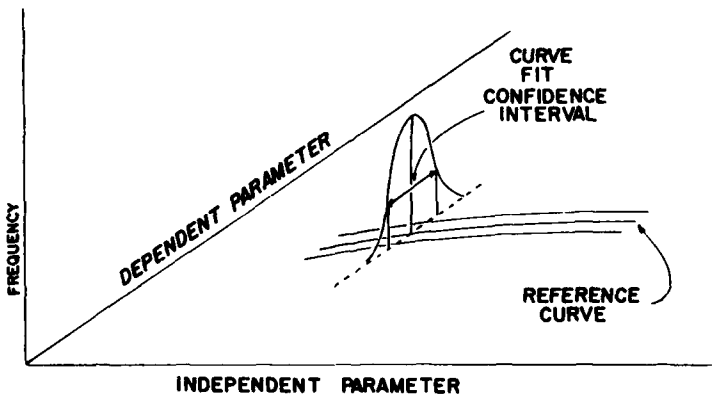

FIG. 2 - TRANSIENT DATA CONFIDENCE INTERVAL

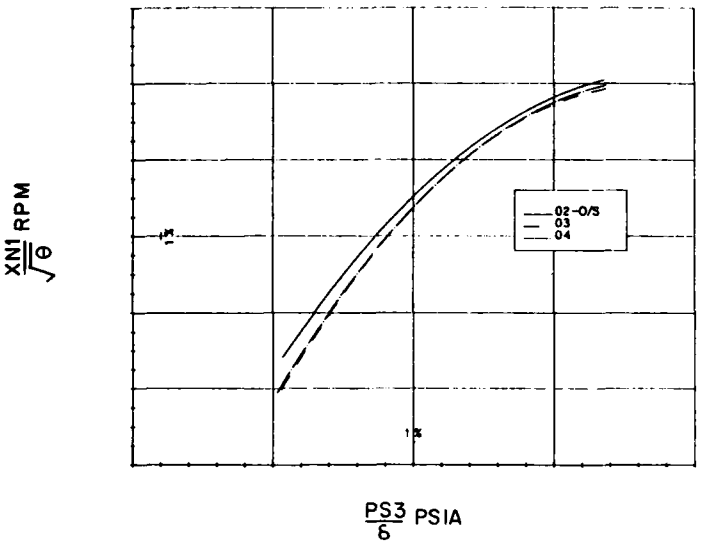

Figure 3 - F404 Transient Data -
Effect of Throttle Overshoot
(O/S)

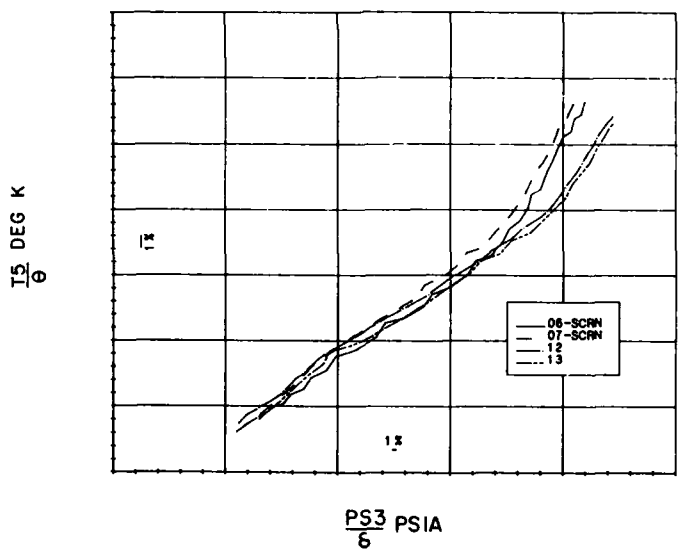

Figure 4 - F404 Transient Data -
Effect of Inlet Screens

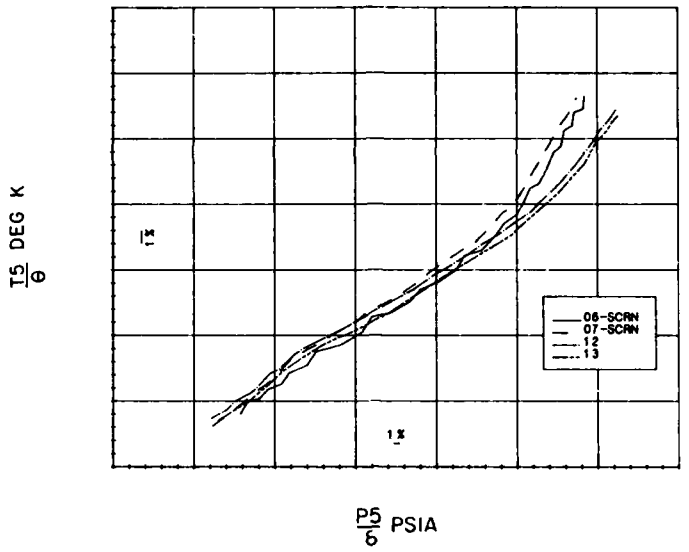

Figure 5 - F404 Transient Data -
Effect of Inlet Screens

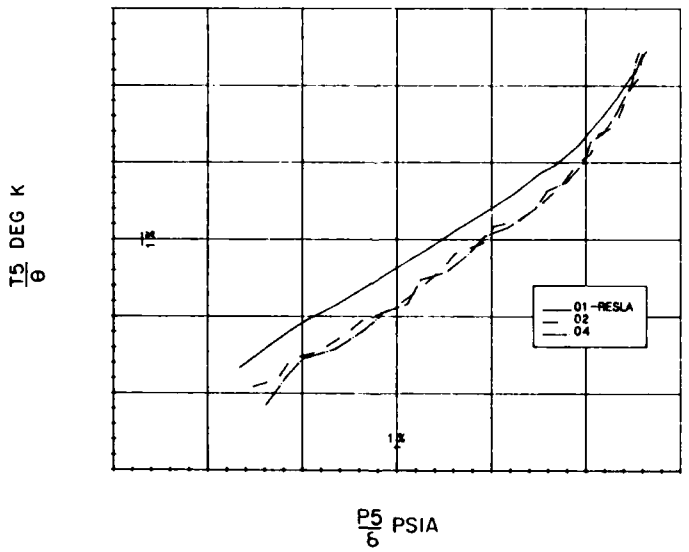

Figure 6 - F404 Transient Data -
Effect of Reslam

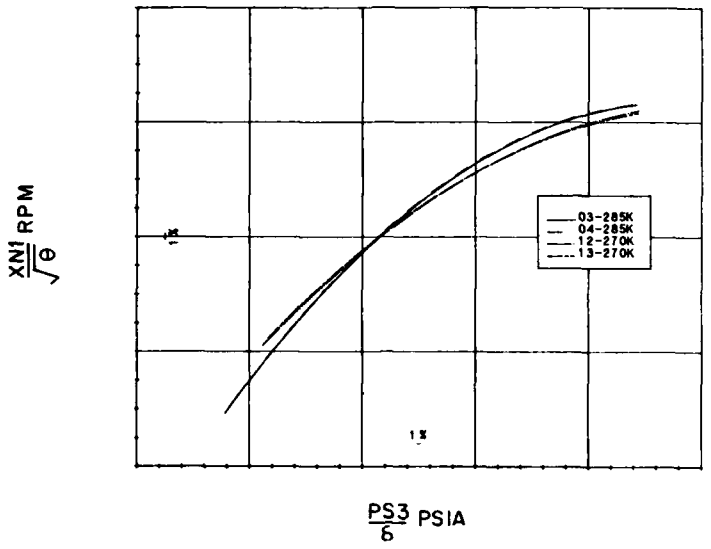

Figure 7 - F404 Transient Data -
Inlet Temperature Effects

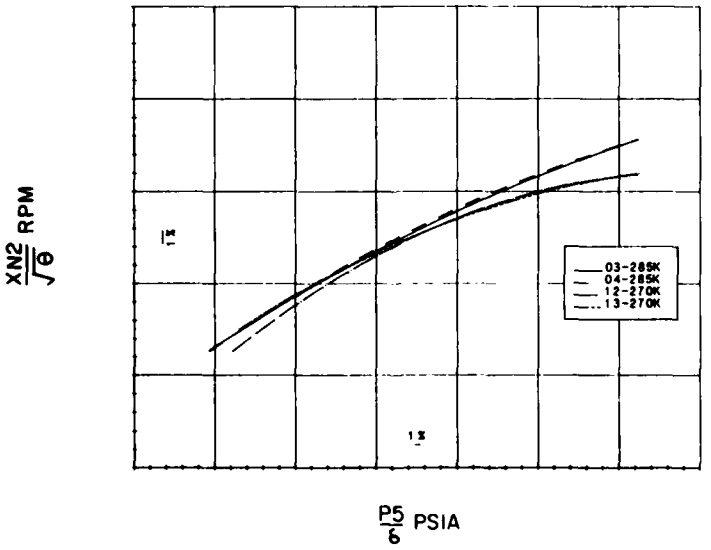

Figure 8 - F404 Transient Data -
Inlet Temperature Effects

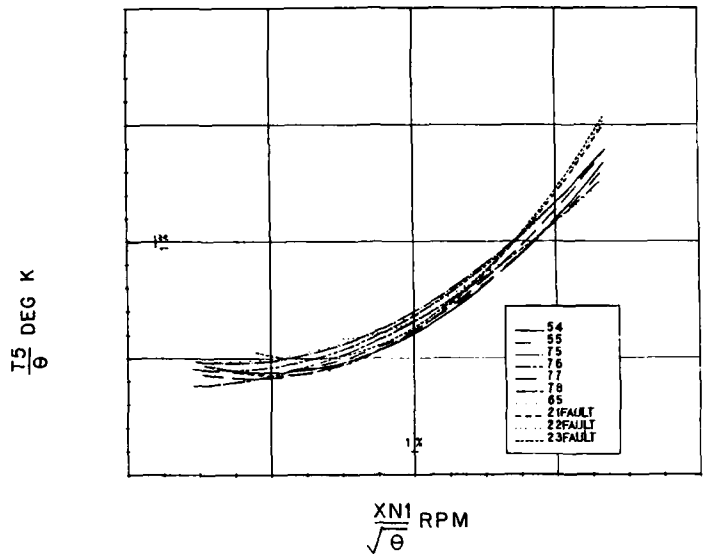

Figure 9 - F404 Transient Data - Effect of Compressor Damage

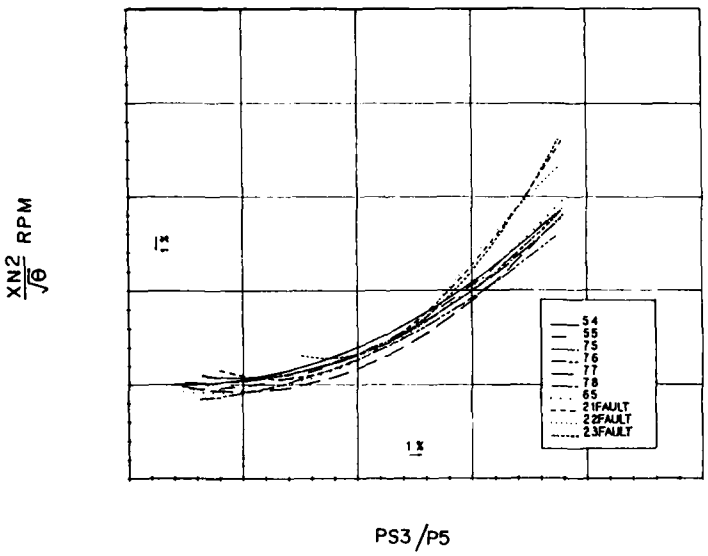

Figure 10 - F404 Transient Data - Effect of Compressor Damage

DISCUSSION

G. MERRINGTON

Some of your results show significant shifts with inlet t° T2? The measured value on the F404 is compensated for variations in fan speed. Did you use this compensated value or actual true inlet t°? If you used the compensated value, how would you expect this to affect the correlation?

Author's Reply:

During the initial stages of my study I acquired a large amount of steady state test cell data from the NRCC. I compared the bellmouth t° with the fan inlet t° measured on the F404 and observed the dependence of T2 on fan speed. A compensation scheme for T2 was developed and employed in all subsequent data analysis. Consequently, I do not believe that the dependence of T2 on fan speed affects cross-plot correlations.

M. HAMER

The P5 measurement is a single probe. How well does it track the turbine exit profiles, especially at various Mach/altitude conditions?

Author's Reply:

The technique is intended to be applied only to the take-off engine data. Consequently, Mach/altitude effects should not be significant.

D. DOEL

Do you have a transient model for the F404 engine and if so have you run it to try to understand the T2 effects?

Author's Reply:

Unfortunately CANADA does not yet have a F404 transient model.

M. BEAUREGARD

Have you considered changing/modifying the MSDC to improve data accuracy/repeatability of transient data?

Author's Reply:

My report recommended that the Canadian Air Force consider improvements to the CF18 IECM system. Modifying/changing the MSDC would be part of such an improvement program. Although the implementation of modifications to IECMS is the responsability of our headquarters, the ultimate decision to modify IECMS will be dependent upon overall requirements of the CF18 weapon system.

SPACE SHUTTLE MAIN ENGINE MONITORING EXPERIENCE AND ADVANCED MONITORING SYSTEMS DEVELOPMENT

Harry A. Cikanek, III
Mechanical Systems Control Branch, ED14
NASA, George C. Marshall Space Flight Center
Marshall Space Flight Center, Alabama 35812, USA

SUMMARY

Advanced space transportation systems must provide improved availability, reliability, safety, and reduced cost in order to make a new, more vigorous level of space activity economically feasible. Earth-to-Orbit (ETO) propulsion monitoring systems are a major factor in progress toward these improvements, and in the success of current systems. Operational experience with the Space Shuttle Main Engine (SSME), the first reusable ETO rocket engine, is valuable for examining current rocket engine monitoring capability and technology developments. This paper surveys SSME monitoring practice and experience. Unique aspects of rocket engine mission requirements are highlighted to provide improved understanding of engine monitoring practices and technology needs. Current ETO engine monitoring technology development goals and their relation to SSME experience and future transportation system mission needs are outlined. With this foundation, the techniques and components addressed within current technology programs are discussed to complete a picture of ETO propulsion monitoring status and development.

INTRODUCTION

For many reasons, out of all ETO liquid rocket engines which have been built and operated, the SSME is the most instructive engine to examine for monitoring experience. In many characteristics, the SSME is representative of other pump fed liquid rockets and thus encompasses many past rocket engine monitoring requirements. But, the demands of the shuttle vehicle and mission distinguish the SSME in many other ways. Manned operations, 3g maximum vehicle acceleration limits, approximately 33.5 kPa (700 psf) maximum vehicle dynamic pressure limits, high performance, accurate propellant utilization through engine mixture ratio control to ±1%, and reuseability design goals of 55 starts and 27,000 sec of operation are some of those demands. Resulting unique characteristics include a staged combustion cycle, closed loop digital computer control of thrust and mixture ratio, a vacuum specific impulse of 453 sec, a throttle range from 63 to 111% of rated power level, extended development and certification, extensive self test, and extensive monitoring [1]. These characteristics place many demands on monitoring capability; demands which in many cases will remain for future engines. SSME development began in the early 1970's. The engine has been utilized reliably and safely for flight operations since 1981. Monitoring has played a major role in these successful operations. Therefore, this paper will review SSME monitoring history and experience to provide a status of ETO engine monitoring practice and a view of new monitoring technology.

Monitoring takes many different forms, all very intensive, when applied to an engine such as the SSME. Much of the monitoring effort requires human expertise, specialized equipment, substantial computational power, large data management capacity, sophisticated communications resources, and significant operational time. Monitoring systems can be viewed as a series of layers. Engine monitoring includes, at the core, extracting and utilizing the data necessary for engine control, e.g., valve position feedback for error determination and correction. In the second layer, it involves real time acquisition and use of various Control and Monitoring System (CMS) parameters and engine parameters to determine if the engine is operating properly. If the system is not operating properly, then monitoring also involves determining the necessary action to respond safely to anomalous operation. In the third layer, monitoring is employed to determine the condition of the engine for maintenance requirements and to assess readiness for another mission. At the fourth and outermost layer, monitoring is utilized to assess trends which may indicate that design changes are necessary. This paper will discuss the latter three layers, with concentration on the last two. To appreciate the nature, scope, and intensity of ETO engine monitoring, it is necessary to first provide background information on the SSME.

BACKGROUND

The SSME is undoubtedly the most complex and highest performance propulsion system ever built. For example, the High Pressure Fuel Turbopump (HPFTP) weighs approximately 340.8 kg (750 lbs), and yet at full engine power it generates approximately 58.2 MW (78,000 hp) of power. The engine utilizes liquid hydrogen and liquid oxygen as propellants. The hydrogen enters the engine at approximately 21 K (38 R) and 310 kPa (45 psia), and the oxygen enters at 94 K (170 R) and 689 kPa (100 psia). The propellants leave the engine at over 1222 K (2200 R) and 17.9 kPa (2.6 psia) with a speed of 4441.5 m/sec (14572 ft/sec) after being expanded from 3611 K (6500 R) and 20726 kPa (3006 psia) to produce 2090.6 kN (470,000 lbs) of vacuum thrust at nominal Rated Power Level (100% RPL). A schematic of the engine cycle and typical 109% operational parameters are provided in Figure 1. In the SSME cycle, low pressure fuel and oxidizer turbopumps, located at propellant inlets, provide the proper head for the two high pressure pumps. Fuel from the High Pressure Fuel Pump (HPFP) discharge is routed to cool the Main Combustion Chamber (MCC), nozzle, and other hot gas flow path components of the engine. The main chamber coolant discharge is used to power the Low Pressure Fuel Turbine (LPFT). The nozzle

coolant discharge is mixed with bypass flow and fed to the two preburners. Oxygen is routed from the High Pressure Oxidizer Pump (HPOP) to drive the Low Pressure Oxidizer Turbine (LPOT) and feed the main injector. It is also fed to a Preburner Boost Pump (PBP) which provides oxidizer at the necessary higher pressure to the two preburners. The two preburners provide fuel-rich combustion gasses to each respective high pressure turbine. The turbine discharge is then routed through the Hot Gas Manifold (HGM) and fed to the main injector where it is mixed with oxygen from the HPOP outlet. Final combustion occurs in the MCC and the resulting gases are expanded through the supersonic nozzle. The engine also includes a POGO suppression accumulator with associated controls; tank repressurization discharges with an associated oxygen heat exchanger; a pneumatic controller to manage engine purges and the failsafe shutdown system; and avionics to control, manage, and monitor the engine.

During flight and in ground test, the SSME operates in one of three possible modes: start, mainstage, and shutdown. Closed loop control of the main combustion chamber pressure and the mixture ratio is utilized throughout the normal engine power range. Thrust control is effected through the Oxidizer Preburner Oxidizer Valve (OPOV) and mixture ratio control is effected through the Fuel Preburner Oxidizer Valve (FPOV). Prior to start, a series of functional self tests are run, followed by turbomachinery thermal conditioning and a series of four purge sequences. The purge sequences are run until an engine ready condition is reached. The engine may be fired from approximately 1 hr to 24 hr after start preparation begins. Proper thermodynamic conditions and operating states are automatically monitored for and must be met prior to start. During the low power level portions of start and shutdown, preprogrammed open loop sequences are used to command all five main propellant valves. Start lasts approximately 5 sec while shutdown (which may be entered at any time after the start signal) lasts approximately 3.5 sec. Other engine operating modes include electrical valve lockup, hydraulic valve lockup, and pneumatic shutdown to provide various levels of CMS system fail-operate and failsafe options. During shutdown, purges are initiated to clear the engine of combustibles and various control devices are returned to their shutdown state. After shutdown, engine drying purge lines are installed and purges are operated to remove all water remaining from the combustion process. Dew point checks indicate when drying is complete, at which time, the engine is ready for turnaround operations necessary to prepare it for another firing.

Each SSME is assembled as a combination of Line Replaceable Unit (LRU) components. These components consist of the major assemblies such as the valves, turbopumps, ducts, manifolds, injectors, nozzle, main combustion chamber, and many others which can form any particular engine build. Each LRU that is flight qualified has met many stringent requirements for integrity and quality which culminate with the ground test program. Requirements placed on flight components include that they be ground test fired and that there be two equivalent components within the ground test program that have at least twice the accumulated firing time as the highest accumulated flight component firing time. Because of these requirements, the SSME has operated cumulatively 281,770 sec in ground test versus 37,930 sec in flight. Since ground testing is so extensive, so fundamental to flight reliability, and has an operational nature, monitoring experience from ground firing is equal in importance to flight experience. Because ground test goals, requirements and capabilities differ somewhat from those in flight, ground test monitoring differs from flight monitoring. These differences will be noted throughout this paper.

The ground test program has required six types of engine tests. These are development tests, certification tests, green run tests, acceptance tests, Main Propulsion Test Article (MPTA) tests, and Flight Readiness Firings (FRF). Development tests are run primarily to solve problems and investigate improvements to design or operation. Certification tests expose an "all up" improved configuration to a simulated flight series of firings to qualify design improvements for flight. Green run tests expose new or newly overhauled components to a first firing. Acceptance tests verify that new hardware meets the requirements for admission to the fleet. MPTA tests provide cluster firings to qualify the three engine cluster, feed subsystem, and external tank as a system. FRF's qualify new vehicles along with their main engines on the launch pad. Engine operation during flight varies little from one mission to the next unless a failure occurs.

Engine monitoring starts with onboard systems to provide data and monitoring functions. The engine mounted SSME avionics system includes, in a single package, two identical cross strapped engine mounted digital computers, input electronics, output electronics, and timers, with redundancy allowing no single point failures. This package, known as the controller, interfaces with the vehicle or test stand to receive commands and to transmit 128 standard engine measurements in the Vehicle Data Table (VDT). The input electronics convert signals for performance instrumentation including: a turbine fuel flowmeter, shaft speed detectors, platinum wire resistance temperature sensors, pressure transducers, and both rotary and linear variable differential transformers. The output electronics condition commands for the five hydraulically actuated main propellant valves, the propellant augmented electrical spark ignitors, electronic servoswitches, and the helium-actuated pneumatic failsafe shutdown system. Software implements the control laws, control logic, threshold failure detection logic (redlines), and much of the self test and monitoring logic.

During typical engine testing, on the order of 500 measurements are taken and recorded from both the engine and the facility. These include the 128 VDT parameters at a sample rate of one sample every 40 msec (every other major cycle). An additional set of digital data is sampled every 20 msec through the facility data handling system. Analog parameters are recorded on facility systems for acceleration, strain measurements and, on occasion, high frequency pressure measurements. Additional engine test information is available from

video coverage. Fewer data are available from a typical flight. Standard flight data consists of the VDT data and measurements from six turbopump accelerometers. Special instrumentation such as strains or additional accelerometer units are often placed onboard for additional monitoring. Some engine compartment measurements are also available. These include temperatures, pressures and engine compartment vent flow gas samples from a pyrotechnic actuated grab bottle system for post-flight leakage analysis. Prior to engine ignition, leakage is detected by a hazardous gas detection system built into each launch pad. With this system, concentrations of various gasses are provided to launch personnel in near real-time.

A typical flight thrust profile is shown in Figure 2. It includes a 5 sec start period, approximately 25 sec of 100% power level operation, a 10%/sec throttle down to 65% power to reduce MAX Q orbiter aerodynamic loads, throttle up to 104% after 30 sec at 65%, 430 sec at sustained 104% operation, then a slow 1%/3 sec throttle down to 65% to limit acceleration loads on the vehicle, and finally an approximately 3.5 sec shutdown sequence. A simulated flight throttle profile is often utilized for test firings. However, ground tests can and have taken advantage of the many different power levels and durations that the engine is capable of providing. Propellant inlet conditions vary during a mission, allowing pump net positive suction pressure to drop as low as 41 kPa (6 psi) on the fuel side and 138 kPa (20 psi) on the lox side.

SSME MONITORING SYSTEMS

Discussion of SSME monitoring experience would not be complete without an introduction to the methods, techniques, and systems utilized to perform data reduction, translation, storage, transmittal, presentation, and archiving. Although much of the data handling, storage, and processing is automated, significant expert engineering talent is required to follow and diagnose engine condition on a day to day basis. The scope of the monitoring effort has grown since the initial testing of the engine. This is because of the learning that has occurred with respect to hardware condition that results from the demands placed on engine hardware by the engine cycle and operating conditions. Of course, compared to a typical jet engine, rocket engine monitoring is always far more intense due to the criticality of the mission and the higher cost of the hardware itself. Much of the condition monitoring process is implemented on general purpose computing equipment and data/communications equipment. This has evolved during the SSME program due both to the increased scope of monitoring and the tremendous explosion in electronics technology. Computer and software technology has allowed monitoring manpower requirements to remain nearly constant. A learning curve effect also plays a role in increased monitoring efficiency. A general overview of current SSME condition monitoring methods, techniques and systems will begin with flight systems.

The typical monitoring process for flight starts with a series of Flight Readiness Reviews. The reviews begin with project management and work up to Senior NASA management. During the reviews, all problems or special conditions are discussed, component history is covered, results of past operations summarized, and, in general, readiness is decided upon including a clear course of action to resolve any questionable conditions. This review process typically takes place less than a month prior to launch. If, during any of the prelaunch processing operations, a failure occurs, a team is formed to resolve the failure and return the system to flight status. For example, prior to flights 41-D and 51-F, launch attempts were aborted when abnormal main propellant valve actuator responses were detected in the engine self-monitoring circuitry while the engines were in start mode. The abnormal responses caused a switchover to redundant channels and invoked Major Component Fail (MCF) logic which leads to a shutdown if all levels of redundant systems are not operable prior to launch commit. After these failures, extensive investigations were undertaken, including teardowns, functional tests, laboratory tests, analytic investigations, simulations, and failure reconstruction. Probable causes were found and solutions were generated, agreed to, and implemented. Launch occcurred within one to two months after each abort. The MCF logic is part of a formal Launch Commit Criteria which is reflected in all of the automatic launch logic leading up to the time of Solid Rocket Booster ignition.

During powered flight, VDT data is telemetered to the Kennedy Space Center in Florida at 1 sample/second. During prelaunch preparations, which start with tank loading and carry through to engine start, low rate data is obtained from the engine systems mentioned earlier plus many ground systems. Expert engineering personnel (numbering about 20) follow the process in the firing room near the Vehicle Assembly Building. The data is also linked via satellite to the Huntsville Operations Support Center (HOSC) at Marshall Space Flight Center in Huntsville, Alabama; to Rockwell in Downy, California, from there to Rocketdyne in Canoga Park, California; and to Mission Control at Johnson Space Center in Houston, Texas. Up to the time the vehicle clears the tower, control of the mission rests with the firing room at Kennedy. Then control is handed over to Johnson for the duration. HOSC is on-line in an advisory capacity. During powered flight, all engine VDT parameters are followed by humans even though most processes are fully automatic onboard. In limited circumstances, though, certain functions can be overridden. Such an override occurred on mission 51-F when two HPFTP turbine discharge temperature sensors failed in quick succession. The exact sequence of failure led to an erroneous engine shutdown. A brief time later, another sensor failed on one of the two remaining engines. Ground controllers at the engine panel in Houston noticed the second sensor on that same engine begin behaving erratically and called for a redline inhibit which cancelled the authority of all automatic redline shutdown logic, allowing the mission to proceed successfully. Once the shuttle achieves orbit, full resolution engine VDT data is telemetered to ground receiving stations in the NASA tracking network. From there, the data is placed

on a data network for transmittal via satellite to the user sites at NASA Marshall and at Rocketdyne. High frequency data is stored onboard the orbiter until landing, at which time the data tapes are off-loaded and shipped. Flight data processing, analysis and review is similar to ground test processing and will be outlined later.

The typical monitoring process for ground testing begins with a test readiness review held via teleconference between the manufacturer, test personnel, NASA project personnel, Chief Engineer's representatives, and engineering personnel representing various technical disciplines. The review covers the results of the previous test, any hardware changes made, any software changes made, any special investigations, the time on components, the test procedures, the test goals and objectives, and any special conditions for the test. Particular attention is given to components with extensive firing time. High time components are flagged by how close they are in starts and/or accumulated time to fleet leader (highest time) components. Accumulated cycles are tracked and various hardware limits are imposed. All problems identified by problem tracking systems are also reviewed. Action items are assigned to the various subsystem experts for resolution of any outstanding questions or problems. Once everything has been reviewed, and a risk assessment made, the manufacturer and NASA project managers certify firing readiness.

At the test site, tests are observed by NASA personnel and are conducted primarily by the manufacturer. The firing crew includes a test conductor, facility observers/operators, periscope observers, and video observers. The firing team is located in the test control center which is a small distance from the test stand. Bunker observers are utilized to obtain different views of the engine. The VDT is provided to various computer displays including the test conductor's. Some strip charts, oscillographs, analog gauges, and digital readouts are also provided, particularly to report facility conditions and special parameters. The total test firing crew numbers about 15 to 20. Call to stations, followed by propellant drop into the engine (for thermal conditioning), usually occurs about 3 hr prior to test. Pretest data, to cover the period during the engine purge sequences, are taken at low rates. Once proper conditions are achieved and engine ready has been reached, engine start is initiated. During the firing, each member of the crew monitors critical parameters as assigned. Most of the test process is automated, but there are conditions and operations that must be manually performed. Most firing crew members have kill switches which can initiate early shutdown if necessary. Much of the automated real time monitoring utilized during firings consists of the built-in test, redundancy management and redlines built into the controller. However, other redlines are implemented on facility computers for additional engine parameters and for all critical facility parameters.

Engine test firings take place at National Space Technology Laboratories (NSTL) in Mississippi on four test stands and at Rocketdyne's Santa Susanna Field Laboratories on one test stand (scheduled to close in early 1988). An upgrade to a new engine data handling system is in progress. Already, the test sites send most data via satellite. A diagram of the new engine data network is shown in Figure 3. Low frequency data is stored on digital computer tape. High frequency data is recorded on analog tape, and the most critical measurements are digitized and stored on disk in real time. Before leaving NSTL, the analog data is processed into Power Spectral Density format. All data are archived at NSTL on tape. Once transmitted to the user sites, the data are archived on tape and placed on disk for use on data reduction computers. Perkin Elmer 3254s are utilized for performing simple data reduction, plotting, and statistical analysis. Masscomp 5000 series systems are utilized for real time digitizing, later PSD transformation at NSTL, and for analysis and correlation of the data at Marshall. A new Engineering Analysis and Data system at Marshall allows improved access to the data at many sites throughout the center over a fiberoptic network. This network allows a wide variety of terminals and computers to be interconnected on programmable baud rate links. Special high rate links are also available for computer to computer connections to transmit large files. Transmittal of data between dedicated engine data computers and general purpose analysis computers is also facilitated by the network. Generally, full fidelity data is available within a few hours of a firing.

Other data are also available from firings including video and film coverage of the engine and plume, inspections, functional test data, special test data, and condition reports for abnormal inspection/review findings. Video and film coverage provides multiple views of the vehicle during flight. Figure 4 shows the coverage requirements for the first shuttle flight. During ground test, full 360 degree coverage of the engine powerhead is available. Other cameras view the plume and nozzle. Ground test imaging systems were converted from film to high speed video over two years ago. Typical requirements for inspection after every firing include external inspections, internal borescope inspections, and main chamber wall/nozzle inspections. Dew point checks are required after every firing. Additional inspections and functional tests are required at 5000 sec of engine operation and at turbopump removal. 5000 sec requirements include: fuel turbopump internal seal integrity checks, minor-valve seal integrity checks, helium system leak checks (actuators and pneumatic controller), MCC to nozzle joint integrity checks, propellant valve shaft seal integrity checks, nozzle hot wall leak checks, and operation of engine controller software implemented automatic checkout modules for avionics components. Additional inspections/tests called for upon HPFTP removal include: FPB lox post concentricity checks, FPB liner gap dimensional checks, HGM transfer tube dye penetrant inspections, FPB injector element support point integrity checks, main injector heat shield integrity checks, lox post shield integrity checks, and lox post retainer integrity checks. Inspections/tests required upon High Pressure Oxidizer Turbopump (HPOTP) removal include heat exchanger visual checks and OPB lox post eddy current inspections. Post certification inspections can include destructive evaluation and radiographic inspection techniques. Inspection points are shown in Figures 5 and 6.

Typical functional tests required for every firing include: a heat exchanger leak test, a nozzle cold wall leak test, turbopump torque tests, turbopump axial shaft travel tests, preburner and main oxidizer valve seal leak tests, Main Fuel Valve (MFV) seal leak tests, and fuel turbopump lift-off seal leak tests. Typically, inspection results and functional test results are recorded on paper and summaries are transmitted by telefacsimile. Video is reviewed at the firing sites and shipped only for unusual occurrences. Data other than time series data are typically sent via express mail. High frequency data is utilzied for many sophisticated analyses which often require that dubbed tapes be shipped because the PSDs are not always suitable for the analyses due to lack of phase information. Standard reports, called Unsatisfactory Condition Reports (UCRs), are written for any problems found by the monitoring process. These are entered into a computer data base. Once a problem has been analyzed, a Failure Analysis Report is generated and added to the UCR. Both of these reports typically are one page in length. Conditions entered into the system are held open until a Problem Review Board accepts the resolution of the condition. A similar system, called Material Reviews, tracks manufacturing or rework conditions. In some instances, it is permissible to operate with nonstandard engine conditions. Deviation Approval Requests are generated and tracked for such instances. If conditions tracked by the systems above are recurrent and are not acceptable, Engineering Change Proposals may be generated to define a design or process change. A change control board headed by the project manager determines the acceptability of the proposed changes. If engine/vehicle interfaces are affected, then the review occurs at higher level.

When engine firing data is received, it is reviewed by teams of engineers both at Marshall and at Rocketdyne. As inspections are completed, the results are provided to the NASA and Rocketdyne engineering teams for correlation to data. Methods utilized for low frequency data evaluation include plots of various parameters with overlays of similar conditions from previous tests, calculation of performance parameters with a performance data reduction program, cross plots, and calculations of parameters such as pressure differences. Data averaging is utilized to reduce the number of data points for statistical analysis. The statistics are calculated to observe test-to-test variations, component-to-component variations, and to assess fleet characteristics. Some of the calculated parameters are also utilized to generate individual performance map adjustments for pre-firing predictions and component performance matching. Matching is required when some of the major LRUs are replaced. Vibration data are presented in terms of maximum g levels, time histories, in frequency domain at a selected time, and also in cascade plots showing frequency and amplitude versus time. Many statistical and correlation analyses may be run to determine the source and character of unusual signals. Within all of the data, a search for various characteristics which could be indicative of an anomaly or degradation is undertaken. These conditions are tracked by the engineers responsible for each engine technical discipline, i.e., engine systems, turbomachinery, combustion devices, avionics, and dynamics. The analysis process usually takes one day. After the analysis, a NASA data review is held by the chief engineer or his representative. A similar review is held by the manufacturer. This is a meeting where the analysis team convenes to review their results and form an assessment of the test. Generally, a NASA engineering representative at the test site is involved in the review by telephone. The inspection results and functional test results are fed into the review. If problems are found which are not resolved prior to the review, additional investigative work may be ordered including laboratory investigations, additional inspections (which may include various exotic Non Destructive Evaluation methods), use of engine steady state and transient prediction models to test hypotheses, a review of all manufacturing data, additional review of video and film data, etc. Many of the inspection techniques can be performed at the firing sites. Teardown inspections however are cconducted in clean rooms at the manufacturer's plant.

SURVEY OF MONITORED CONDITIONS AND EXPERIENCE

As stated during the description of the data review process, the engine is analyzed in terms of various engine subsystem disciplines and types of resulting data. The demarcation between each of these subsystems is necessarily blurred, and in order to analyze and resolve any anomalies, interaction is continually required. Interaction is also required with personnel conducting inspections and tests at the test sites and plant. Comparisons between manufacturer's review results and NASA review results are often made, and interaction between the two engineering teams is common. Many anomalous signatures that may be found in the data have been determined from the careful analysis and resolution of past anomalies by these teams. Examples of these conditions and the monitoring system techniques to detect them will be described in order.

Engine Systems

The engine systems group reviews overall engine performance during prestart, start, mainstage, and shutdown. A first screen checks all critical engine parameters against Interface Control Document defined acceptance limits. The group also checks all redlined parameters against redline values. All measurements are reviewed for obvious sensor failures such as noise, bias, total loss of signal, etc. Failure identification signals from the controller are also noted. Avionics personnel investigate and resolve the sensor and other avionics anomalies. When reviewing engine performance, start characteristics are reviewed first. Parameters indicative of start conditions include turbomachinery speeds, turbine discharge temperatures, main pump discharge pressures and main chamber pressure. Priming time for each burner is checked and tracked. Turbine discharge temperature oscillations and maximums are also checked and tracked. Turbine damage and degradation is known to be related to start, and so the OPOV sequence may be slightly adjusted when major components such as turbopumps are changed.

Another set of engine systems monitoring activities include monitoring the performance of ancilliary systems such as the POGO suppressor, the augmented spark ignitor systems, the pneumatic systems, tank repressurization systems, chamber and nozzle cooling circuit flows, hydraulic systems, drain lines, and the various solenoids and switches necessary to actuate many of the devices mentioned. Component variations are analyzed because after replacement of an engine LRU, the engine balance may be altered. For balancing, there are various system orifices which must be selected for flow legs that do not contain active valves for control. The selection is made based on the performance measurements. Leaking valves are detected by reviewing downstream temperatures prior to start. If temperatures are abnormally low, cryogenic propellant is likely leaking past valve seals. In mainstage, general control response is checked to assure that all commands are followed properly and all expected operating conditions are met. Because there have been past difficulties with instrumentation, turbomachinery, and other components which affect controls and safety monitoring, parameters relating to these components are carefully tracked. For example, fuel flowmeter output is reviewed for low frequency oscillation. In the past, this phenomenon was found to be either due to bent blades, dropped bits in computation of flow rates, or shaft precession due to mounting flexibility. Once indicated, the cause of such a problem is isolated in order of the least impact to schedule and cost. Turbine discharge temperatures are another example.

Turbine discharge temperature sensors provide key redlines. They also provide varying readings during engine operation which can be related to inlet conditions, change in internal flow conditions (the sensors are located 90 degrees apart on the outer flow wall of each high pressure turbine discharge turnaround duct which has extremely complex flow patterns that affect the sensor output), or sensor failure. The variations can also be related to turbopump anomalies. Some of the more common anomalies include fuel leaks from any fuel flow passage, loss of turbine performance, flow blockage, and loss of pump performance. Cavitation, rubbing, dragging, cracks, erosion, abnormal clearances, and contamination are phenomena which may result in loss of turbine or pump performance. The signatures for these various phenomena are analyzed by experts to determine the likely underlying cause. They are also tracked to determine the efficacy of the turbine discharge temperature redlines. Turbine discharge temperature is a good indicator of many engine problems because of the nature of the engine cycle and control system. Essentially, any loss of power can only be made up through increased preburner combustion temperatures. Unfortunately, the discharge turbine temperature is also a very poor discriminator, and, therefore, diagnosis of an indicated problem must take advantage of other engine data. The discharge temperature redlines have shut down many tests successfully, preventing damage and progression to catastrophic failure. They have also reduced the consequences of catastrophic (termed major incident) failure in 9 of 24 applicable cases.

Turbopump coolant liner pressure, a bi-stable preburner pump operating condition, and a preburner diffuser crack are three more conditions that require tracking. The coolant liner is located between turbine discharge flow liner sheetmetal and the turbopump structural wall. Interactions between internal seal flows and coolant cavity discharge flows have allowed pressure fluctuations that, in one instance, collapsed the liner, causing extensive engine damage. Design changes were made and a redline was added to prevent overpressure of the cavity. The design changes have proved successful and the coolant liner redline has not yet signaled an engine shutdown. The bi-stable operating point of the preburner pump impeller occurs at low engine power level. Not all fleet preburner pump units exhibit the phenomenon which is thought to be due to an aerodynamic instability. When present, pressure oscillations are induced into the preburners. These can be detrimental to control stability and pogo stability. Pumps are checked for this condition by a cross plot of main pump to preburner pump discharge pressures which will exhibit loops if bi-stability is present. Spikes in main chamber pressure at low power level are also searched for as an indication of the bi-stable problem. After shutdown, combustion chamber temperature measurements are checked for residual high temperatures which are indicative of oxidizer leaks causing continued combustion. A crack in the fuel preburner oxidizer diffuser is one common problem that has a particular post test temperature signature. During engine operation, the crack allows oxygen to fill a normally void cavity. After shutdown, the oxidizer trickles out and fuel turbine discharge temperatures rise, indicating the crack. Abnormal coolant liner pressure behavior, bi-stable pumps, and cracked fuel preburner diffusers are not allowed for flight but are acceptable for test.

A different aspect of the systems review involves monitoring for external leaks at any location in the engine system. Leaks are a critical problem with machinery such as the SSME because of the high internal pressures, the small size of the hydrogen molecules, the insidiousness of liquid oxygen, the volatility of both propellants, and the destructive potential of engine combustion products. Small propellant leaks, in addition to being serious problems themselves, can also be indicators of structural problems. During a 1985 engine ground test, a small blowing hydrogen leak developed at the MCC outlet duct neck. The leak continued for approximately 10 sec until a large section of the duct failed causing massive fuel loss and severe internal and external engine damage due to the resulting rise in mixture ratio and combustion temperatures. Subsequent to that failure, diesel engine glow plugs were added to an array of engine powerhead thermocouples which were (and are) mounted for each engine ground test firing. This system will ignite any hydrogen leaks, causing external temperature to rise enough to trip redlines set for each of the powerhead thermocouple measurements. The thermocouple/glowplug system has successfully initiated shutdown for three hydrogen leaks this past year. This thermocouple data is of course reviewed after every test. The addition of the high speed video coverage was also a result of the same failure. Video observers with kill switches back up the thermocouple system.

Figure 7 illustrates engine leak detection methods used between firings. Helium is utilized as the leak test pressurant because of its inertness and its small molecule size. Various major sections of the engine are pressurized as shown in Figures 8, 9, and 10. Then, large volume flow meters are utilized to ascertain if any internal leakage exists. Ultrasonic probes and mass spectrometers are utilized to check joints and welds for leaks. Soapy leak solutions are utilized to check for joint, nozzle and chamber leaks. Mass spectrometry is utilized to check for oxygen heat exchanger leaks. An SSME designated for the first post 51-L flight was recently disqualified because an extremely minute heat exchanger leak was detected by spectrometry. Engine system leak tests are performed at acceptance, and at other times if required under special conditions. The system check utilizes an impermeable "big bag" enclosure with mass spectrometer detection. Flight leak detection depended only upon all of these same methods until the sixth Shuttle flight. Flight six was the first flight of the orbiter Challenger and so there was a flight readiness firing before the scheduled launch. The engines passed all of their leak checks prior to the FRF. Grab bottle sampling during the FRF indicated hydrogen concentrations in the engine compartment higher than allowable levels. After the firing, the source of the leaks could not be fully isolated. A second FRF was ordered with additional instrumentation to isolate the leak source(s). The inability to detect leaks prior to the firing clearly identified a need for a sensitive system level leak test. In response to the need, a test called the Helium Signature Test [2] was developed. The test is conducted with engine and propellant feed systems pressurized to 276 kPa (40 psi) with helium. The engine compartment is then sealed and purged with substantial nitrogen gas flow. The compartment gas is vented and sampled at one of two available vent doors. Sensitivity of this method has been found to be 98.3 sccm (6 scim) minimum detectable leakage, and accuracy was found to be ±49.16 sccm (3 scim). Since being instituted, two instances of leaks above allowable limits were detected by the Helium Signature Test after not being detected by other methods. In each case, the leaks were tracked down and corrected.

Turbomachinery

Turbomachinery performance and mechanical design personnel review the data derived by the systems group and add to that effort a detailed review of the operation of seals, bearings, internal cooling flow processes, overall turbopump performance, and the relation of these parameters to inspection results. Turbomachinery dynamics personnel carefully review and analyze dynamic data processed by the dynamics group for rotordynamics anomalies such as subsynchronous whirl, bearing wear, or rubbing. These results are correlated to the performance and the inspection data. To determine seal performance, the barrier seals and purges (which prevent liquid oxygen from mixing with hot gas in the HPOTP) are checked for proper delta pressures and steady operation. The coolant liner pressure is tracked for expected response to events such as liftoff seal actuation, engine inlet pressure changes, axial shaft movement, power level changes, etc. Cavitation is checked for by head/flow characteristics and turbine power requirements.

SSME experience has had a tremendous impact on the science of analyzing, understanding, and monitoring the dynamics of high speed flexible turbomachinery. During the early days of the SSME program, two major HPOTP failures led to the instigation of a number of research, technology development, monitoring improvement, and redesign efforts. Early monitoring consisted of much of the instrumentation utilized today such as external accelerometers and some internal strain gauges, but generally, only overall loads and vibration levels were plotted and reviewed in the time domain. Efforts to analyze and model rotor dynamics concentrated on determining loads on bearings, stiffness and damping characteristics of the rotor and case, stability margins, and parameters which affect loads and stability. From the analyses, it was eventually determined that one of the early engine failures was most likely caused by rotordynamic instability in the HPOTP. Turbomachinery redesign efforts concentrated upon increased damping, altered stiffness characteristics, and better quality assembly. One valuable result of the redesign effort was the invention of damping seals for turbomachinery and their incorporation into the SSME. As stability characteristics and their driving parameters became understood, and as redesign efforts met success, attention became more focused upon loads because as the operational life of the machinery steadily was increased in the test program, bearing wear and condition became critical life limiting issues.

Both the HPFTP and the HPOTP have had bearing wear limitations, but the more critical have been found on the HPOTP. Because the HPOTP bearings are bathed and cooled in lox, any degradation leading to high temperatures, particle shedding, or induced vibration could be instantly catastrophic because of the ignition potential. Inspections, including visual, borescope, and teardown, are key methods in tracking the condition of the bearings and other turbomachinery components. Only one bearing set, the HPOTP number 3 bearing set, is borescope inspectable. Conditions that are tracked by borescope or teardown inspections include: ball coloration, size, roundness, microscopic surface condition; cage condition; and race wear patterns. In many cases, because of the stiffness and damping characteristics of the machine, bearing wear correlates with decreased housing vibration as measured by external accelerometers. HPOTP units that were a part of the development test program have been found with asymetrical balls, blue and black colored balls, damaged cages, destroyed cages, heavily worn races, and severely distressed balls; yet none of these conditions have lead to a major failure. Since all of these abnormal conditions, although so far self-limiting, are unacceptable for flight, a significant component of the engine development program has been the use of turbopumps instrumented with internal strain gauges placed on bearing mounts. The data obtained from these instruments has been finely combed with many different types of time series analysis and correlation methods in order to tie dynamic signatures to the onset of abnormal bearing conditions both in theoretical terms of what is occurring during operation and in terms of the results obtained from inspections.

Current monitoring techniques center on frequency domain analysis and in many cases utilize time as a third variable on cascade plots for enhanced event correlation. An example plot is shown in Figure 11. Analysis consists of searching for fundamental frequencies and harmonics. Amplitudes are also observed. In normal operation, vibration consists of broad low amplitude noise with only shaft rotation synchronous frequency feeding through. As bearings wear, case (or ball train) frequencies become evident. The geometry of the system constrains the balls to run at a fixed fraction of rotor speed. In the case of the HPOTP, that fraction is 43%. Because wear changes the bearing system dynamics, the fractional frequency gradually shifts higher with increased wear. The array of strain gages utilized allows determination of the maximum ball wear in any orientation. Amplitudes of the various harmonics show how uneven the wear is from ball to ball. For example, 2N (twice synchronous) would indicate two heavily worn balls. The balls tend to travel in a groove on the race. Over time, amplitude increases with wear; however, if for some external influence such as a change in axial loading, the balls begin to run in a different groove, the amplitude may substantially decrease. In all cases, the reduction is temporary, for once wear begins, it progresses.

Unfortunately, the internal strain gauges are not very reliable and, therefore, are not built into every machine. To improve turbomachinery monitoring capability, a near-term objective is to relate the internal measurements with signals taken from external accelerometers. As had been hinted at before, external accelerometers are relatively poor indicators of bearing and rotordynamic problems in the turbomachinery. Although efforts are still being made to extract useful information from their signals, only gross problems can be reliably detected by them. However, a recent finding that was chanced upon has provided external means to sense at least the condition of the pump end HPOTP bearing pair. Due to concerns over a housing weld, a strain gauge was mounted on the housing of some of the HPOTP units in the fleet to examine loads at that location. In analyzing the weld strain gauge data, it was found that bearing characteristics could be determined. Standard monitoring depends upon external accelerometers (at least 3 uniaxial units per high pressure turbopump). Ground data systems implement redlines on RMS filtered output from these units. A Flight Accelerometer Safety Cutoff System (FASCOS) has been developed, but has yet to be implemented in flight. However, accelerometers have been successful in improving safety during ground test. One failure that most likely would have proved catastrophic was prevented by a timely automatic shutdown initiated by the ground redline accelerometer cutoff system. That case was a HPFTP first stage impeller crack. During engine failures that have been catastrophic, the accelerometer cutoff systems were, at minimum, successful in limiting damage through providing the initial cutoff signal in 7 of 24 applicable cases.

In the turbomachinery monitoring process, many functional tests are undertaken. After every firing, all turbopumps undergo shaft push-pull tests to determine axial looseness of the rotor. Looseness can indicate some bearing wear and other rotor problems. Measurements of axial travel are logged and acceptable ranges have been established. Turbopump torque checks are run to determine breakaway torque values and dry run-in values. These provide indications of any binding or other irregularity which would prevent free rotation. Acceptable limits of both of these parameters have been established. In addition to the rotor support system, the hot gas flow path of the turbomachinery is a carefully monitored subsystem. Sheet metal cracks are noted for repair if they grow beyond a designated size. Seals are monitored for signs of rubbing and proper dimensional tolerances. Hydrogen embrittlement protection is checked for any wear or flaws. Most careful attention is given to turbine blades in the high pressure turbines. SSME turbomachinery has a history of blade cracking. Over the development history of the engine, many design and process improvements have been instituted to alleviate the incidence of turbine blade problems, but the environment in which the blades operate presents a very difficult set of problems to solve. At the current time, many inspections are required and the blades are only certified for a relatively short duration of 5000 sec. Three turbine failures have been attributed to blade failure. The first two failures occurred early in the test program; the third occurred later and was the result of out-of-spec blades, and experimental burner alterations which significantly worsened nonuniformities in circumferential temperature profile. Current turbine blade monitoring has been very successful in providing safe engine operation.

Combustion Devices

Combustion devices monitoring depends upon system analysis of engine performance data, review of some combustion devices parameters, inspection results and upon dynamics analysis. Systems analysis can provide evidence of leaks, improper pressure drops across injectors and some cracks, such as the FPB injector diffuser crack. Unless anomalies are severe, system monitoring usually does not provide indication of combustion devices anomalies. A couple of combustion device parameters do, however, provide significant information. Main chamber coolant discharge temperature correlates with chamber wall condition. Temperatures in excess of 500 R usually indicate presence of hot wall degradation. Chamber coolant liner pressure is also reviewed to irdicate any occurrence of overpressure. Inspections provide the best indication of combustion device distress and degradation. Visual inspections of the nozzle, chamber, and main injector face are made after every firing. Nozzle tube cracks are a common occurrence. The combination of a certain number and severity are acceptable for ground firings. Nozzle tubes are easily repaired with brazing equipment. Blanching of the main chamber copper alloy liner is another common minor problem. If left, blanching (a local surface roughness) causes flow disturbances which increase local heat transfer to the liner and eventually result in liner cracks. It is not known what causes blanching, but simple polishing of the blanched surface prevents deterioration. If necessary, film cooling can also be increased. Injector elements, the injector faceplates, and baffles are observed for erosion and/or

discoloration which is indicative of thermal distress. Similarly, preburners are borescope inspected for the same conditions. When turbopumps are removed and access is thus improved, additional similar inspections are undertaken for the preburners in locations that the borescope cannot view.

Among the problems that preburner inspections indicate are cracks in sheet metal, lox posts, the FPB lox diffuser, welds, and joints. Inspections also indicate concentricity, erosion, and contamination. Accelerometer data from devices mounted on or near the burners provides indications of detonation or low frequency combustion instability (pops or chugs). These measurements are traced on oscillograms and screened. Any suspected pops or chugs are picked out and the data is frequency analyzed. Anomalous vibration indicating structural degradation or abnormal structural/flow interactions are searched for within the vibration data. A phenomenon that occurs only on some main injector units has been closely tracked recently. It is theorized that a slight deviation on a lox inlet flow straightener vane might be producing a 4000 Hz resonance found on the abnormal units. Although bothersome, the resonance has not caused any serious problems to date. Design changes to eliminate it are being considered.

From these examples, it is obvious that the monitoring undertaken for an engine as complex, expensive, and mission critical as the SSME is an intensive, broad based, and detailed effort. SSME monitoring requires many resources in terms of manpower and equipment. Although many monitoring parameters are available, much of the process depends upon manual operations such as inspection techniques. The available onboard monitoring parameters, although valuable, do not provide information to indicate and/or discern many anomalies that have been present. The continuing developmental and experimental nature of the SSME requires that extensive human intervention and expertise be employed as a critical and fundamental component of the monitoring process. Because of the intensive and varied nature of SSME monitoring, and the experimental nature of the engine, the performance of the monitoring system is difficult to compile and judge. A false alarm rate or other such measure cannot be determined except for some small subsets of the process. The next section will attempt to provide some feel for the efficacy of SSME monitoring, and the maturation process that SSME monitoring has undergone.

SSME MONITORING EXPERIENCE SUMMARY

The optimum monitoring system will detect all failures that provide any kind of incipient indication prior to operation of the system being monitored. It will also predict the life remaining until, as the system condition and reliability degrades through wear, the minimum system condition and reliability requirement has been crossed. The optimal monitoring system will then call for maintenance to return the system to an acceptable condition. When a failure begins to occur during operation of the monitored system, an optimum monitoring system will recognize all possible signatures and promptly react to prevent catastrophe. When a number of similar failures occurs over a series of operations and a trend is established, the optimum monitoring system will recognize the trend and call for a design or process change as warranted. Of course, what is optimal in monitoring depends predominantly on what the monitored system is and how it will be operated and maintained. The SSME monitoring system, as described previously, is very extensive as befits a complex, expensive, high performance experimental propulsion system. Much of the significant and interesting flight monitoring experienced was related in the section on monitored conditions. In addition to that, one instance of a relatively minor failure in an augmented spark ignitor was detected during post flight inspection. Although interesting, the limited flight data cannot provide a good indication of SSME monitoring performance and experience. However, the extensiveness of ground monitoring experience does provide data sufficient to describe overall trends and to follow individual engines through their life cycle.

For ground test operations, statistics concerning premature or early shutdowns can be provided to illustrate how real-time SSME failure detection methods have performed These data are derived from a data base which summarizes the SSME test history. The base provides the test number, test duration, engine number, test date, turbopump unit numbers, shutdown method, and brief comments. Before presenting the data, factors concerning the validity of the results should be stated. The foremost factor is that the data base was not intended for use in determining monitoring performance. Since no ground rules are available for data entry into the base, and since the determination of whether a premature shutdown may be classed as erroneous is a partially subjective matter, the data accuracy is not easily confirmed. Where possible, the data was checked against other sources. In the data base, the shutdown method was entered with three simple possibilities. Either the test ran to programmed duration, was prematurely shutdown for cause by some means, or was prematurely shutdown erroneously by some means. In compiling statistics from the data base, if there was a question of whether a premature shutdown was erroneous, then for this paper, the shutdown was classed as erroneous. Thus, the data presented is conservative on how well the SSME safety monitoring systems operated. The comment section of the data base sometimes indicates the cause of a premature shutdown, and when erroneous, the method that produced the error. Because the notation which forms the data base comments is to a degree cryptic, there were a number of cases where the cause of premature shutdown could not be ascertained. The collective effect of these factors could cause the specific numbers quoted herein to be in error as much as 10%, but the data still provides interesting trends and a good indication of monitoring system performance. The statistics cover single engine testing only.

The table provides shutdown statistics for single engine SSME testing. It lists, for each year, the number of tests, the number of premature shutdowns, the percentage of tests that were premature shutdowns, the number of erroneous premature shutdowns, the percentage of all premature shutdowns which were erroneous, the number of major incident failures, the percent of all tests which were incidents, and the percentage of all necessary and proper premature shutdowns which ended in major incident failure. In the early years of testing (1975-1979), up to 50% of all engine tests were prematurely shutdown. In each of those years, 38% to 77% of the premature shutdowns were erroneous. During this period, the SSME was taken from initial start tests through rated power level testing. Numerous development problems were being tackled and solved. Liberal application of redline protection, conservative test procedures, sensor unreliability, and the engine development problems led to the high rate of premature shutdowns. Five particular types of sensors and their redline logic were responsible for the bulk of the erroneous shutdowns. The HPOTP speed sensor was responsible for 12 erroneous premature shutdowns and numerous sensor failures. As a result, this unit was eliminated from the HPOTP design in 1979. Accelerometers and their redline systems were responsible for 21 erroneous premature shutdowns through 1979. Design and manufacturing improvements since then have eliminated erroneous premature shutdowns due to accelerometers, and have greatly reduced accelerometer anomalies. Turbine discharge temperature sensors (platinum resistance wire thermometers) and their logic were responsible for 27 erroneous shutdowns up through 1979. A number of design and manufacturing improvements have gradually eliminated the temperature sensors as causes of erroneous shutdowns, and have reduced anomalies in the sensors. The latest generation of these sensors has not failed during engine testing. Facility systems have led to 13 erroneous shutdowns. These instances may or may not be monitoring system related. As a part of the facility systems, human observers provided 6 correct shutdowns versus 4 erroneous shutdowns. In 1978 and earlier, HPOP seal pressure parameters led to 15 erroneous shutdowns. Improvements in the redline logic and reduction in the number of seal parameters utilized for the protection system eliminated further erroneous cutoffs.

Table. Shutdown Statistics for Single Engine SSME Testing

Year	Tests	Prem. Shutdowns	Pct. Prem. Shutdowns	Err. Prem. Shutdowns	Pct. Err. Shutdowns	Incidents*	Pct. Incidents	Pct. Incidents Per Good Shutdown
1975	27	7	26	3	43	0	0	0
1976	108	55	51	21	38	0	0	0
1977	115	57	50	34	60	4	3.5	17
1978	144	63	44	37	59	6	4.2	23
1979	136	26	21	20	77	1	0.8	16
1980	80	9	7	5	56	2	1.6	50
1981	132	13	10	4	31	5	3.9	55
1982	128	16	13	0	0	3	3.1	25
1983	96	10	10	0	0	0	0	0
1984	29	12	41	0	0	1	3.4	8.3
1985	33	10	30	2	20	1	3.0	12.5
1986	34	4	12	0	0	0	0	0
1987	114	6	5	1	17	1	0.9	20
All Test Totals								
	1176	288	24	127	44	24	2	15
1980-87 Test Totals								
	646	80	12	12	18	13	2	19

*Does not include incidents that occurred after shutdown or during multiple engine testing.

Throughout the single engine test history, accelerometers have provided a total of 52 proper early shutdowns, turbine discharge temperatures have provided 42 proper early shutdowns, HPOTP seal parameters have provided 12 proper early shutdowns, facility monitors have provided 11 proper early shutdowns, and all other parameters have provided 6 or fewer proper early shutdowns. Altogether, there have been 288 premature engine shutdowns during SSME single engine testing, with 161 of those considered to be necessary and proper. The premature shutdowns occurred in a total test population of 1176 tests (up until 12/18/87). These figures show that 24% of all tests were shut down early, and 44% of all cutoffs were erroneous. After the SSME passed through initial development and was qualified for flight operations, the premature shutdown statistics changed significantly. In the period 1980 to 1987, there were 646 single engine ground tests run, of which 80 were terminated early. 68 of the early shutdowns were considered necessary and proper; 12 were not. These figures show that the percentage of tests shutdown early was 12% from 1980 to 1987 versus 24% for the whole population, and the percentage of erroneous shutdowns was 18% during the 1980-87 period versus 44% for the whole population. During SSME ground test operations, there have been a total of 28 failures classed as major. Of these 24 occurred during single engine testing prior to scheduled engine shutdown. That number represents approximately 2% of all tests. Thirteen of the major failures occurred in the 1980-87 period. The percentage of tests ending in major failure remained at 2% for the 1980-87 period. However, for the total test population, 15% of proper shutdowns ended in major failure, while for the 1980-87 period, 19% of proper shutdowns ended in major failure. If all premature shutdowns are considred, then 8.3% of all early shutdowns ended in major failure while for the 1980-87 period, 16% of all early shutdowns ended in major failure. Although this may show that the reduction in erroneous shutdowns came at the price of less protection, insufficient investigation has been undertaken to sustain that conclusion.

To judge how well the overall SSME monitoring system (including the non-real-time components) has operated, it is necessary to review major failure history in more detail. Of the 28 major failures, 7 tests have records which do not provide enough information to determine whether insufficient monitoring could be related to the failure. From the remaining 21 failure tests, the following 10 were monitoring deficiency related. The particulars of three cases follow. During test 901-249, a turbine blade failure resulted from steady degradation throughout the test. Turbine discharge temperature redlines were not active for this test, but if active, may have prevented the failure. During test 901-364, an experimental modification to the HPFTP turbine end cap resulted in abnormally high temperatures in the rotor support system which led to the failure. Vibration redlines were not active for the HPFTP during this test. Had they been active, they may have shut down the test prior to the severe damage. During test 902-120, an experimental speed probe structural deficiency led to an HPOTP internal fire. The probe had not worked properly prior to this test, but the monitoring system did not recognize that the probe structure was failing rather than the electronics. During MPTA test SF10-01, the HPFTP liner was eroded through by localized high mixture ratios due to a distorted faceplate and a canted lox post tip. Preburner inspection requirements were increased as a result of this failure. During test 750-160, cooling fluid remaining from a machining operation collected in a duct and froze when exposed to propellant during start. The frozen coolant blocked part of the internal fuel flow, resulting in high internal mixture ratios and temperatures which produced the damage. Dew point monitoring before the test did not detect the fluid due to a procedural oversight. During test 750-168, cumulative damage to the OPOV downstream seal caused by anomalous augmented spark ignitor operation resulted in high HPOT temperatures causing damage after shutdown. Similar damage was noted during teardown inspections on other OPOV units, but the damage was not recognized as a potentially serious trend. During test SF6-03, a nozzle feedline failed at shutdown because improper materials were utilized during fabrication but not detected prior to test. During test 901-222, the oxygen heat exchanger failed due to damage incurred during repair work. The damage was not detected prior to the firing. During test 902-132, an improperly indexed MOV caused the engine to be improperly controlled during start. Substantial damage occurred because the assembly error was not detected until after the failure. Finally, during test 901-284, the engine was miscontrolled when a chamber pressure sensor purge port jet was dislodged during start. The engine ran in a severely abnormal manner for 6 sec until destruction ensued. The abnormal operating state was not detected by monitoring until major damage occurred.

Inspection results provide another picture of SSME monitoring experience. Engine 2010 was utilized in a series of certification tests [3] with teardown inspection following the conclusion of the certification cycles. Three cycles of approximately 5000 sec each were run for a total of 38 tests and 15436.5 sec of operation. This certification series was part of a test program with the objective of extending flight certification to 15 missions. During this series, normal monitoring was conducted much as described in earlier sections except that some of the requirements now in effect were derived from the certification series. With the exception of turbomachinery (which does not have the life capability), the number of UCRs generated during each cycle were 33, 41, and 91 for the first, second and third cycles, respectively. All of the UCRs were closed and the conditions resolved. An outline of the more significant UCRs follows. During the test series, two instances of leakage and one instance of overstress were found which required extraordinary maintenance. Of these, one of the causes was contamination, a second was wear, and the third was due to inadequate design margins. These problems eventually led to one instance of redesign, one of rework, and one of a standard fix. Disassembly inspection led to UCRs for one instance of leakage, one of damage, three of contamination, two of looseness, one of corrosion, and one of cracks. Vibration was indicated as the cause of one of the conditions, mis-assembly was indicated in two of the cases, and causes were not specifically determined for six cases. Redesign ensued as a result of the inspections in one case, rework was initiated in five cases, and no action was taken for the other three cases. Hardware inspections led to UCRs for six cases of leakage, one of wear, one of damage, one out-of-tolerance dimension, one functional failure, one instance of corrosion, and five of cracks. The causes included two cases of vibration, three cases of contamination, three cases of wear, two cases of thermal overload, three fabrication errors, and three of indeterminant causes. These inspections led to five cases of redesign, one additional monitoring requirement, seven cases of no action, and three cases where actions taken were not delineated.

This experience overview and sampling illustrates the complexity of the SSME and the results of the intense monitoring required. Since the SSME was the first oxygen/hydrogen staged combustion engine ever developed and has the highest chamber pressure and required operating conditions, much of the development effort eventually required could not be anticipated. The relatively lean resources available for engine development constrained the design and development process. Materials properties were not completely defined, component testing allowed was less than planned, and early internal design environment definition was not verified to the extent possible by test. Missed predictions on orbiter weight and payload requirements further forced the engine design to push to the limits of unsubstantiated margins in the quest for increased thrust to weight ratios. Under such conditions, the eventual experienced hardware life capability did not meet design predictions. The monitoring system was thus geared to keeping careful track of the high performance, high maintenance hardware. In future engines, it is likely that although performance will be pushed, as it must be to achieve a positive payload, margins will be much more thoroughly defined through more knowledge of materials properties, better design tools, and improved internal environment definition. Such definition should lead to designs resulting in fewer maintenance, reliability, durability, and functional problems. In addition, more advanced materials and processes should alleviate many fabrication, quality, and rework difficulties that are present with the SSME.

Some of these improvements are expected to be applied to the SSME in component upgrades. Alternate high pressure turbopumps are being designed and developed by Pratt and Whitney. These new designs reduce the number of welds required in turbopump fabrication by orders of magnitude. They also eliminate many sheet metal components such as the HPFTP coolant liner. Further improvements are expected to accrue from improved bearing designs and the rotordynamics lessons learned with the original SSME turbomachinery. Advanced expendable and reuseable engines are currently under study to apply to a next generation U.S. launch vehicle. These engines will allow clean sheet capitalization upon SSME experience. Monitoring has received increased attention as a key discipline for the development of future engines and in the improvement of the SSME. The next section will discuss the goals of current monitoring technology development and will outline technology development activities under way and planned.

TECHNOLOGY DEVELOPMENT GOALS AND STATUS

Even though new engine and major component designs should reduce monitoring requirements, much of the monitoring task will remain. Major objectives for improving monitoring are as follows. First, an increase in the ability to sense direct component condition is required to reduce inspections and increase safety. For example, instead of inferring bearing condition from external accelerometers, a new technique should provide direct measurement of bearing deflection or vibration. Second, better reliability and performance is required of current and future sensors. Erroneous inflight shutdown is not tolerable, and the thermal drift and other inaccuracies of some current engine sensors limit their usefulness. Third, new parameters should be exploited to provide a more complete picture of condition. For example, plume contaminants are not currently monitored, although past failures had indications which were visible in the plume prior to failure. Fourth, analysis techniques, inspection techniques, functional tests and data management should be more automated and more efficient. One stated objective is to be able to analyze every test in the detail that incident tests are analyzed. Increased efficiency would support that goal [4]. Fifth, inspectability should be designed into critical components such as bearings to eliminate scheduled maintenance and reduce teardowns. Sixth, trending and tracking systems must be made more perceptive in order to minimize the chance that repeating problems will lead to catastrophic failure.

Future U.S. vehicle goals include an order of magnitude reduction in operations cost, reduced flight preparation time, increased availability, and less down time if recovery from failure is required. The extensive inspections, functional tests, and manual monitoring operations required by the SSME show that monitoring along with basically improved design, materials and processes are key development requirements necessary to meet the future vehicle goals. Technology efforts in sensors have been underway with NASA sponsorship since 1981. Other monitoring system components have been under development for a more brief period. Programs that support the effort to improve monitoring include the Civil Space Technology Initiative propulsion program. It includes base technology resources to support applied research, and component/engine system test resources to provide large scale/full scale validation of new techniques. A refurbished test stand, last utilized in the Apollo/Saturn program, will provide full scale experimental engine testing with modified SSME hardware. An expansion of technology development resources should allow new monitoring techniques and components which will meet the goals outlined above. A new technology program focused on the Advanced Launch System concept will provide some of that expansion. Up until the present time, much of the monitoring technology development has been directed at re-useable engines, however, the ALS concept has renewed interest in expendable engine monitoring. Expendable engines are not required to fire as many times as re-useable engines, but they must fire at least three or four times for green run, calibration, acceptance, and flight. This can require much of the same monitoring process as the SSME. Many of the fatigue and other long term re-useable engine operation problems should be eliminated in expendables to ease some of the monitoring burden.

Current plans and data point toward engine out capability being required for future vehicles. In order for engine out capability to provide benefit, monitoring must successfully detect engine failure and direct shutdown safely, i.e., without leading to catastrophy and without involving other engines or vehicle components. To meet this requirement, it follows that on board monitoring must be very capable and reliable in order to minimize the probability of catastrophic failure and of erroneous shutdown. Thus, in-flight monitoring will be as critical to mission success for advanced systems as for the SSME. The goal of increased vehicle availability also requires a capable monitoring system. Faults must be detected before engines reach the flight line. Detrimental trends must be corrected more rapidly. In the event of a major failure, key information necessary to determine the cause must be available in order to minimize investigation time. The 1985 Titan liquid engine failure provides a case in point. The vehicle mission was not accomplished due to an engine failure which could not be isolated from flight data. Corrective action was less certain, took more time, and involved more effort because a single failure point could not be determined. Monitoring improvements necessary to effect the flight goals also benefit the engine development program through reduced hardware attrition, and better evidence of the cause when failure occurs. For re-useable engines, another benefit also accrues: a good monitoring system will reduce the possibility that failure in an engine with many components near fleet leader life will lead to incidental loss of those high time components. The fleet leader and high time components are very valuable because of the testing invested in them.

The results of the SSME experience, the available technology program resources, and the motivation of advanced vehicle requirements have led to extensive monitoring technology development. The status of the development will be related here. From 1981 through 1983, Rocketdyne performed a study sponsored by NASA's Lewis Research Center on rocket engine condition monitoring [5] that set the early development course, particularly in sensor development. In that study, the history of many past rocket engine programs were reviewed for failure modes. Sixteen most frequent failure modes were identified. These include: bolt torque relaxation, coolant passage leakage, joint leakage (hot gas, pneumatic, hydraulic, and propellant), hot gas path cracks, high torque (binding), cracked turbine blades, bellows and convolutions cracks, loose electrical connectors, bearing damage, tube fracture, turbopump seal leakage, lubrication pressure anomalies, valve failure to actuate, internal valve leakage, regulator problems, and hydraulics contamination. After failure mode identification, sensing concepts were identified for potential to give direct indication of the failure modes, and to reduce inspection requirements. As a follow-on to that study, further work focused on developing improved monitoring for turbomachinery problems. Three sensor concepts were developed for the job. An optical pyrometer was selected for sensing turbine blade temperatures. From air breathing turbine experience, it was known that pyrometers provide very high useable response. For example, in addition to direct blade temperature measurement, gross turbine blade cracks could be detected by such devices through temperature differences stemming from the change in heat transfer in a cracked blade. Pyrometer development challenges include lower turbine temperatures than found in cooled blade air breathing engines. The lower temperatures reduce the radiance that can be detected. Materials compatiblity and mechanical design also create problems due to the high pressures, propellant compatibility, and high loads. Progress to date includes rig tests to simulate engine environments, and design for inclusion in a test bed turbopump. A second sensing concept was selected for bearing monitoring. This concept utilizes an optical deflectometer to track bearing race deflection. Test bearing samples with various wear characteristics have been run in bearing rigs instrumented with the deflectometer. Results have been promising. Some liquid nitrogen testing has been accomplished but no liquid oxygen or hydrogen testing has been run to date. This system is also being designed for inclusion into a test bed turbopump. A third system tagged for development by the study was radioactive isotope wear detection. Bearing races were irradiated, and wear correlated with changes in radioactivity. Selection of a safe, but long-lived isotope is a critical problem with this concept. So far, isotope wear detection has not been tested in rocket engine turbomachinery.

At the same time that the condition monitoring study was in progress, direct SSME experience led to development of improved pressure sensors, flow meters, and lox turbopump speed sensors. Numerous SSME sensor development problems were experienced with the MCC pressure sensors (used for control), including thermal drift. Isolation mounts were utilized to solve the problem at the expense of reduced response. Microelectronic sensors with on-sensor compensation were developed. These units are undergoing qualification for inclusion in a testbed engine. Vortex shedding flowmeters were developed to provide more durable and reliable sensing compared to turbine flowmeters. The original SSME design contained a lox turbine flowmeter in addition to the fuel turbine flowmeter. The lox flowmeter could not survive the environment downstream of the HPOP and was eliminated from the engine design. The vortex shedding flowmeters have been tested at dynamic similitude, and have been exposed to some simulated engine conditions. Provisions are being made for test bed engine testing. Speed sensing was eliminated from the HPOTP because the first sensor type that was tried could not produce reliable signals, and the second type that was tried caused an engine failure. A new non-intrusive speed sensor has been developed for high pressure lox turbomachinery application. This sensor has passed many rig and qualification tests and is being prepared for application to testbed turbomachinery.

Beginning in 1983, a study was conducted by Battelle Laboratories under the sponsorship of NASA Headquarters to survey the state of monitoring technology in other industries, and to search for promising technologies which could be developed for application to the SSME [6]. This study resulted in the confirmation of some of the technology efforts already underway, and also recommended many new techniques. Among those, specific techniques related to systems design and monitoring logic were pointed to as offering promising monitoring improvements. Partially as a result of this study, monitoring technology efforts were expanded. In 1984 and 1985, work was initiated in developing real time failure detection algorithms [7]. The first step of the effort was to develop signatures that the various types of SSME failures produced. Then, a three stage detection algorithm was formed with the objective of rapid detection of failure signatures. This work is still in an infant stage but is a promising first step toward improving upon redlines. Further monitoring logic development activity is being investigated for analysis of dynamic data by means of pattern recognition and expert system techniques [8]. Lewis will, in the near future, begin study to develop component life prediction algorithms based on structural durability research they have conducted over the past five years. Such algorithms would be implemented as part of an integrated life management system, the research for which is just beginning. This type of work would be particularly applicable to future space-based orbit transfer engines, as well as booster engines.

A unique new sensing medium has been under study and development since 1985. Optical spectrometry is being applied to the detection of anomalous combustion and wear/erosion which would be exhibited in the SSME plume [9]. Commercial and special laboratory spectrometric equipment has been utilized to survey and characterize the SSME plume during single engine testing. Instrument successes include detection of copper (in the form of copper tape inadvertently left from leak test procedures) in the plume which was burnt and expelled during engine start, the detection of calcium in the plume which is believed

to be related to bearing cage degradation that occurred during a test, and detection of superalloys in the plume arising from the erosion of a fuel preburner. A prototype Optical Plume Anomaly Detector specifically designed to meet engine requirements is under development based on the characterization data.

Other parameters not previously exploited include turbine torque and imaging of the engine exterior. Torque is valuable in determining turbomachinery performance and operating characteristics. A sensor to operationally measure torque has been under laboratory development at Rocketdyne. Imaging has potential application to leak detection. During the plume spectrometry studies, initial imaging data was acquired for further study. In a different monitoring realm, the ability to make predictions and analyze engine performance was identified as an important component of monitoring. A new Rocket Engine Transient Simulation System is under development to provide a flexible, modular, computer code which can perform steady and transient 1-dimensional aerothermal performance predictions. The code will allow much more efficient and accurate predictions for monitoring purposes. Many other technology projects which show promise are being planned to further enhance liquid rocket engine monitoring technology, but are not developed sufficiently for significant results to be reported.

SUMMARY AND CONCLUSION

SSME monitoring experience provides a rich base to build upon for future liquid rocket booster engine monitoring capability. The SSME features and characteristics, including its cycle, performance, mission, and development history, have led to the employment of very extensive and varied techniques for all aspects of monitoring. Growth in monitoring requirements has occurred as development testing provided increased experience with re-useable engine components. The systems employed to perform SSME monitoring are being upgraded as improved technology becomes available. Even though the SSME is an experimental, high performance, developmental engine with extreme operating parameters, many aspects of SSME monitoring experience are representative of, and applicable to, other large liquid rocket engines. Techniques employed in SSME real time monitoring include automatic parameter redlines, human observers, and avionics redundancy management. Condition monitoring techniques include visual inspections, borescope inspections, some eddy current, dye penetrant, and radiographic inspection techniques. They also include functional tests for avionics and actuating mechanisms. Leak detection is performed by a number of methods including mass spectrometry. Correlation, analysis, and condition determination is performed by expert engineering staffs supported by high capacity data and analysis systems, permitting rapid data transmission and reasonable turnaround. Analysis of dynamic data routinely used sophisticated methods and very high capacity computing capability. Trending depends upon a number of document tracking systems which are partially automated through conventional data base techniques.

During early engine testing, the SSME experienced a substantial rate of erroneous early shutdowns which were due to conservative test procedures and sensor unreliability. More recent test history exhibits a good record of accurate automatic monitoring. Flight history includes one erroneous engine shutdown due to sensor unreliability (which has since been resolved). Insufficient monitoring was related to only ten major failures in a test history that includes 1176 tests. Inspections with results such as those described for engine 2010 bear a significant portion of the credit for the good SSME monitoring record, and illustrate why the SSME monitoring process is extensive. Future launch vehicle designs must meet requirements for more economical access to space. Monitoring is a key technology category for development in the quest for the vehicle improvements necessary to meet advanced vehicle design goals. Improvements to monitoring technology currently in progress include alternate sensing concepts to provide more reliable and higher bandwidth information, exploitation of new parameters to provide improved engine condition information, better analysis methods for increased efficiency and higher quality information, and more sophisticated real time detection logic and systems. Based on SSME experience and future vehicle needs, monitoring technolgy goals have been defined to guide an expansion of efforts to improve monitoring development already underway and to tackle all other aspects of the monitoring problem. Recent results are beginning to prove the benefits of the effort, and the efficacy of the new techniques. Plans for the expanded monitoring effort are being established to quantatively define the goals and success criteria for each item and the systems as a whole. The plans will guide implementation of the research and technology development effort necessary to meet the needs of advanced engine systems. The future holds much in store for liquid rocket engine monitoring technology development.

REFERENCES

1. Rockwell International Corp., Rocketdyne Div., "Space Transportation System Training Data," SSME Orientation (Part A-Engine), 1986, ME-110(A) PIR.

2. Bilardo, Vincent J., Jr., Izquierdo, Francisco, National Aeronautics and Space Administration, Kennedy Space Center, "Development of the Helium Signature Test for Orbiter Main Propulsion System Revalidation Between Flights." 1987, AIAA-87-0293.

3. Rockwell International Corp., Rocketdyne Division, "SSME Return to Flight Design Certification Review - Systems, Book 1 of 2," 1986, BC 87-228-1.

4. Daumann, Al, Modesitt, Ken, Rockwell International Corp., Rocketdyne Division, "Space Shuttle Main Engine Performance Analysis Using Knowledge-Based Systems," at ASME Int. Conf. on Computers in Mech. Eng., 1985, pp. 1,2.

5. MacGregor, Charles A., Rockwell International Corp., Rocketdyne Division, "Final Report, Reuseable Rocket Engine Maintenance Study," 1982, NASA CR-165569.

6. Tischer, A. E., Glover, R. C., Battelle Columbus Division, "Studies and Analysis of the Space Shuttle Main Engine," 1987, BCD-SSME-TR-87-3, NASA Contract NASW-3737.

7. Taniquchi, M. H., Rockwell International Corp., Rocketdyne Division, "Failure Control Techniques for the SSME-Phase II Final Report," 1987, RI/RD87-198, NASA Contract NAS8-36305.

8. Pooley, J., Thompson, W., Homsley, T., Teoh, W., Sparta Inc., "Embedded Expert System for Space Shuttle Main Engine Maintenance," 1987.

9. Powers, W. T., Sherrell, F. G., "Plume Spectrometry for Liquid Rocket Engine Health Monitoring," 1988, Paper No. 39, at 71st Symposium of the Propulsion and Energetics Panel on Engine Condition Monitoring Technology and Experience.

ACKNOWLEDGMENTS

Several persons were instrumental in allowing this paper to cover the subject of SSME monitoring and technology in such a broad fashion. Their help is gratefully acknowledged. Contributions were made to the content of this paper by T. Fox, P. Lewallen, and S. Barkhoudarien in rotordynamics processing practice, dynamics analysis practice, and current status of sensor technology programs, respectively. Review of the paper was aided by W. Powers, M. Neeley, P. Lewallen, T. Fox, and P. Broussard. Other helpful contributions were made by K. Simmons, D. Leath, S. Ryan, and J. Douglas. Credit is also due Mr. E. Gabris of NASA Headquarters for the original idea and motivation behind this effort.

NOMENCLATURE

CMS - Control and Monitoring System
ETO - Earth-to-Orbit
f/s - Feet per second
FFT - Fast Fourier Transform
FPB - Fuel Preburner
FPOV - Fuel Preburner Oxidizer Valve
FRF - Flight Readiness Firing
g - Gravitational constant
hp - Horsepower
HGM - Hot Gas Manifold
HOSC - Huntsville Operations Support Center
HPFP - High Pressure Fuel Pump
HPFT - High Pressure Fuel Turbine
HPFTP - High Pressure Fuel Turbopump
HPOP - High Pressure Oxidizer Pump
HPOTP - High Pressure Oxidizer Turbopump
kg - Kilogram
kPa - Kilo-Pascal
°K - Degrees Kelvin
kN - Kilo-Newton
lbs - Pounds
lox - Liquid Oxygen
LPFT - Low Pressure Fuel Turbine
LPOT - Low Pressure Oxidizer Turbine
LRU - Line Replaceable Unit
m/s - Meters per second
Max Q - Mission Dynamic Pressure
MCC - Main Combustion Chamber
MCF - Major Component Fail
MFV - Main Fuel Valve
MOV - Main Oxidizer Valve
MPTA - Main Propulsion Test Article
msec - Milliseconds
MW - Mega-Watts
NASA - National Aeronautics and Space Administration
NSTL - National Space Technology Laboratories
OPB - Oxidizer Preburner
OPOV - Oxidizer Preburner Oxidizer Valve
psf - Pounds per square foot
psia - Pounds per square inch absolute
PBP - Preburner Boost Pump
POPO - Coupled engine/vehicle oscillation
PSD - Power Spectral Density
°R - Degrees Rankine
RPL - Rated Power Level
sccm - Standard cubic inches per minute
scim - Standard cubic centimeters per minute
SSME - Space Shuttle Main Engine
UCR - Unsatisfactory Condition Report
VDT - Vehicle Data Table

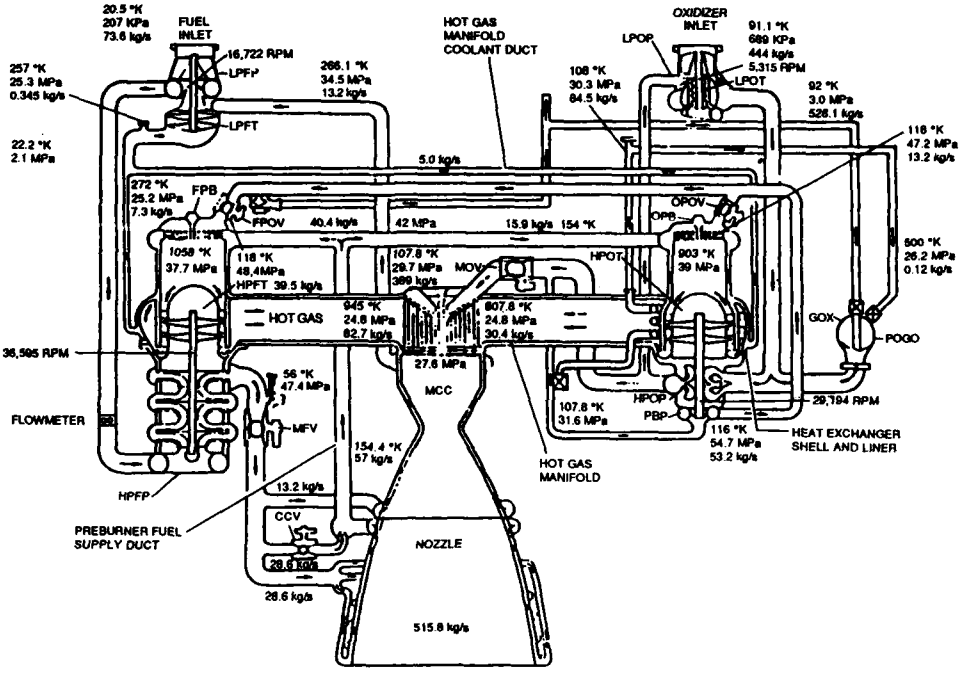

Figure 1. SSME Schematic with 109% Power Level Typical Operating Parameters.

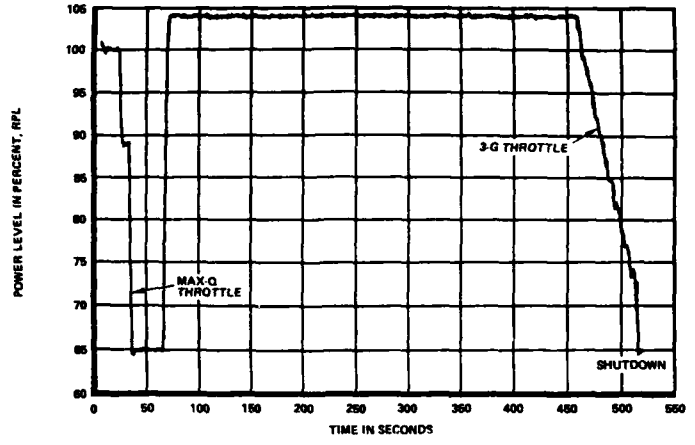

Figure 2. Typical SSME Flight Mission Thrust Profile.

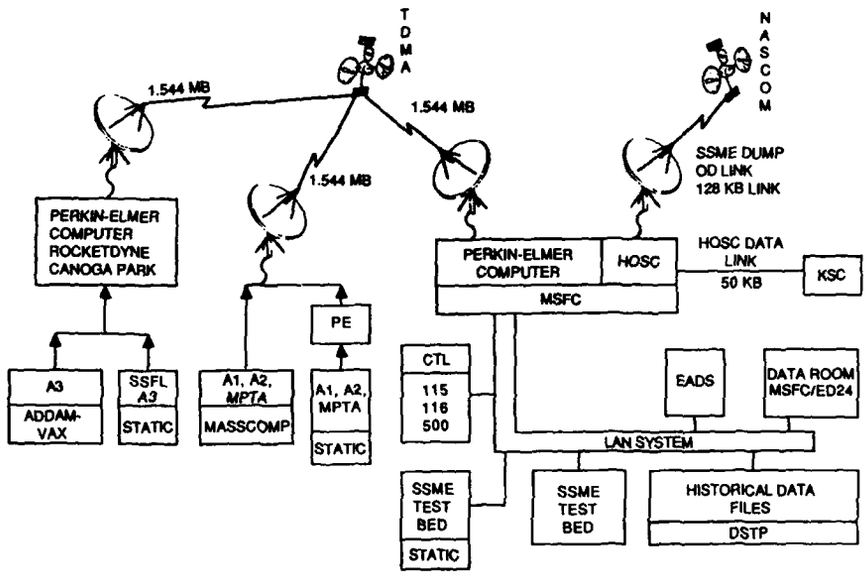

Figure 3. SSME Data Network.

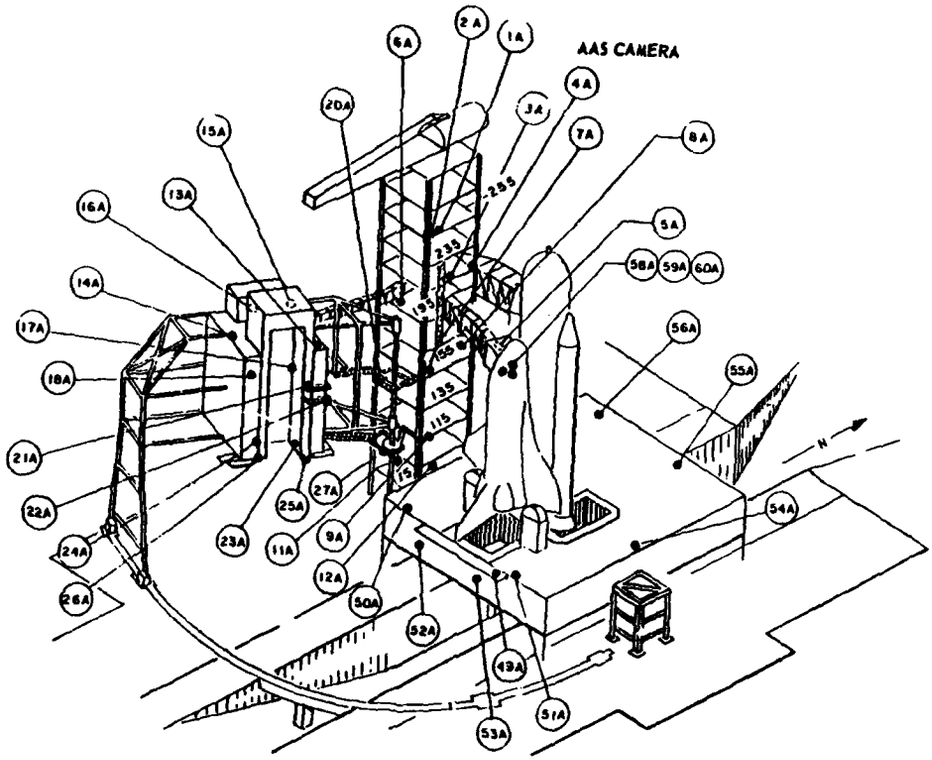

Figure 4. STS-1 Launch Pad Camera Positions.

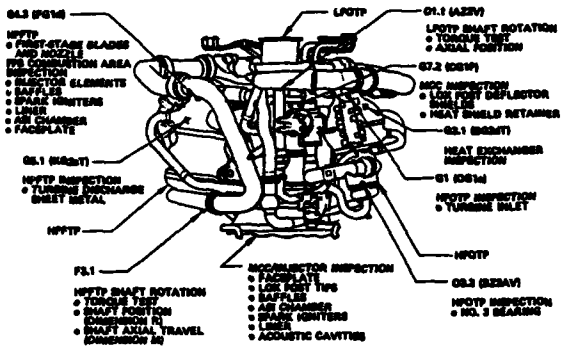

Figure 5. Internal Inspection Points on the Oxidizer Inlet Side of the SSME.

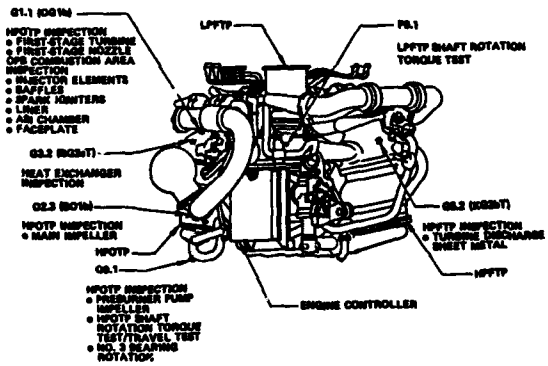

Figure 6. Internal Inspection Points on the Fuel Inlet Side of the SSME.

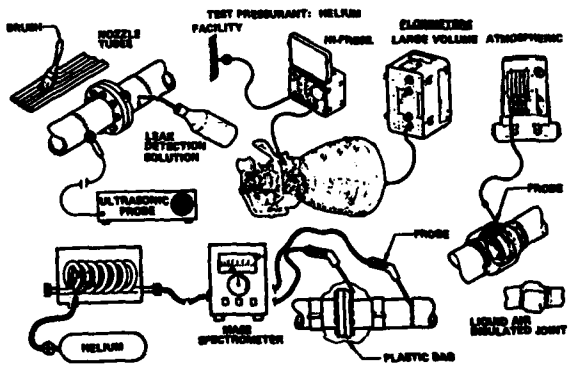

Figure 7. SSME Leak Detection Methods Used Between Firings.

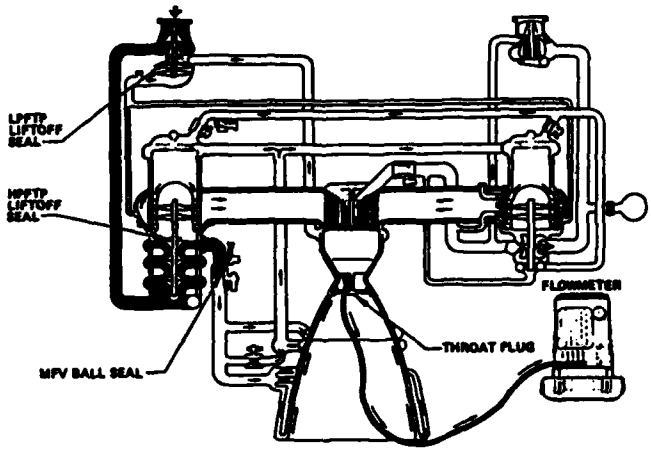

Figure 8. Combined Leak Test, LPFTP and HPFTP Liftoff Seals, and MFV Ball Seal.

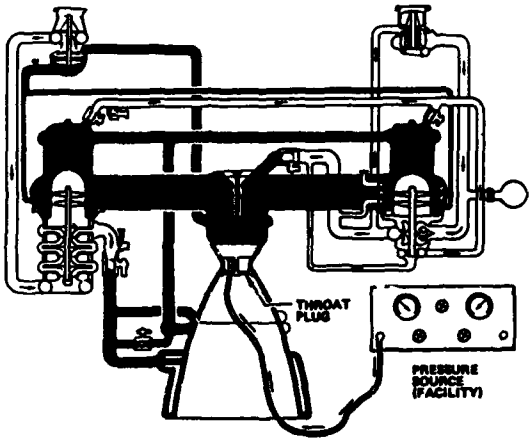

Figure 9. Thrust Chamber and Hot Gas System Leak Tests.

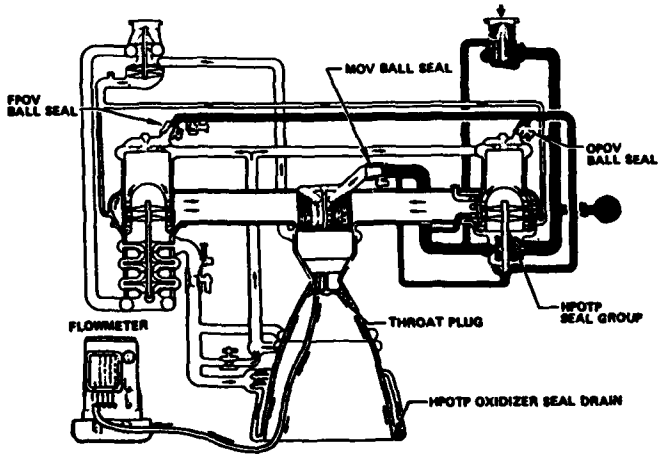

Figure 10. Combined Leak Test MOV, FPOV, OPOV Ball Seals.

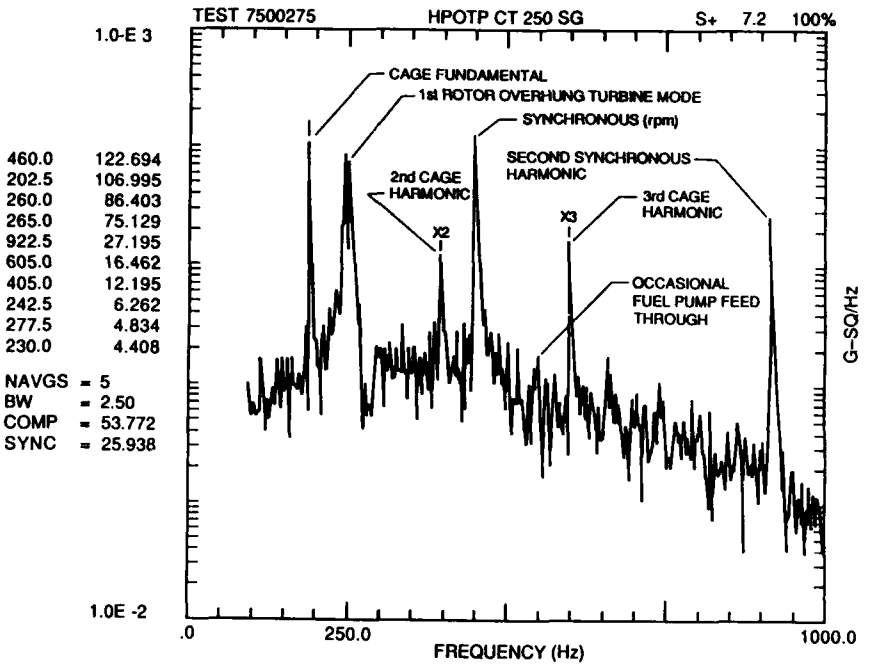

Figure 11. Example SSME Turbomachinery Dynamic Response Plot.

DISCUSSION

D. DAVIDSON

What sort of new sensor do you expect to be testing on the forthcoming Test Bed Engine Program?

Author's Reply:

The list of sensor types provided during the presentation and in the paper are those which are being developed to a maturity sufficient to engine testing.

PLUME SPECTROMETRY FOR LIQUID ROCKET ENGINE HEALTH MONITORING

by

William T.Powers
NASA Marshall Space Flight Center
Office Code EB 22
AL 35899, USA

and

F.G.Sherrell, J.H.Bridges III and T.W.Bratcher
Sverdrup Technology, Inc./AEDC Group
Arnold Air Force Base, TN 37389-9998, USA

ABSTRACT

An investigation of Space Shuttle Main Engine (SSME) testing failures identified optical events which appeared to be precursors of those failures. A program was therefore undertaken to detect plume trace phenomena characteristic of the engine and to design a monitoring system, responsive to excessive activity in the plume, capable of delivering a warning of an anomalous condition. By sensing the amount of extraneous material entrained in the plume and considering engine history, it may be possible to identify wearing or failing components in time for a safe shutdown and thus prevent a catastrophic event. To investigate the possibilities of developing an engine health monitor to initiate the shutdown procedure a large amount of plume data were taken from SSME firings using laboratory instrumentation. Those data were used to design a more specialized instrument dedicated to rocket plume diagnostics. The spectral wavelength range of the baseline data was about 220 nanometers (nm) to 15 microns with special attention given to visible and near UV. The data indicates that a satisfactory design will include a polychromator covering the range of 250nM to 1000nM, along with a continuous coverage spectrometer, each having a resolution of at least 5A°. The concurrent requirements for high resolution and broad coverage are normally at odds with one another in commercial instruments, therefore necessitating the development of special instrumentation. The design of a polychromator is reviewed herein, with a detailed discussion of the continuous coverage spectrometer delayed to a later forum. The program also requires the development of applications software providing detection, variable background discrimination, noise reduction, filtering, and decision making based on varying historical data.

INTRODUCTION

In the process of reviewing engine failures occurring during the testing program for the Space Shuttle Main Engine (SSME), a number of films of the operations were analyzed to discover possible clues to anomalous operation.[1,2] It was noted that in 8 of 27 major failures a visible artifact was present within milliseconds prior to the event. It was theorized that the visible artifacts might be preceded by less luminous traces distributed within specific spectral bands, perhaps characteristic of certain types of failures. A project was proposed and enacted to analyze and characterize the emitted spectrum from rocket plumes, with the subject of immediate interest being the SSME. The purpose of the project was to identify the spectral pattern of a normal plume and phenomenological spectra peculiar to verified mechanical anomalies, and to design a system to detect those spectra and provide a usable response to them. It is not the purpose of this paper to disclose the results of analyses of data thus far acquired, as those analyses are reported upon elsewhere,[3,4] but rather to review the equipment used to obtain the basic data and the system being designed as a result of those analyses. (Related work has been reported on an allied but independent study [5])

Having decided to effect the program, the Engine Test Facility, Propulsion Diagnostics Section at The Arnold Engineering Development Center (AEDC) was selected to provide the instrumentation support necessary to obtain the data. Tests were conducted at NASA's National Space Technology Labs (NSTL) in Southern Mississippi, since the A1 test stand there was the closest available location of an SSME (the other being the A3 stand at Rocketdyne's Santa Susanna Facility in California)[6]. The AEDC had been involved in spectrographic analytic work for some time and had the equipment available for this project.

REVIEW OF THE RADIOMETRIC TEST INSTRUMENTATION

The environment at the nozzle exit level on A1 is hardly conducive to easy use of laboratory optical equipment. Optical radiation measurements were made in the presence of heat, noise, vibration, moisture saturated air, wind currents, and even bright sunlight. The deck is not enclosed and is thus open to normal environmental conditions (weather). A sturdy steel table, 5 by 18 feet, was mounted to the concrete hard core of the tower, and braced to minimize vibration. The front edge of the table is about 25 ft. from the center of the SSME plume (see fig. 1). Environmental control boxes were designed to protect the instruments described below; the boxes provided acoustic, thermal, and general environmental protection. The boxes were equipped with appropriate windows (quartz or IRTRAN II) having high volume external air purges and internal dry gas purges; they were attached to the table via vibration isolators (fig. 6).

Instrumentation provided to support this effort (see fig. 1, 2, 6) included a pair of custom built 4-band filter radiometers, a custom high speed single channel filter radiometer, 2 single channel filter radiometers with UV active detectors (PMTs), a mechanical scanning 0.5M spectrometer having 3 detectors [4], a 3/4M spectrometer with a film attachment. Two EG&G-PARC OMA's (Optical Multichannel Analyzers) coupled to 0.33M Czerny-Turner Spectrometers - one of which was fiber optic remoted with only the foreoptic system outside, 4 video cameras - 3 with filters, an AGA Thermovision, a custom built UV auto ranging camera [7], and 2 IR spectrometers having circular variable filters (CVF) [8].

The 4 band filter radiometers were built by the AEDC. They have 4 separate sections mounted in one case and have co-aligned optical axes with provision to allow laser aiming. These units are equipped with PMT's and replaceable optical filters chosen to pass selected specie lines (see table 1). The electronics for each section include a five decade, fast switching, autoranging nanoammeter designed at the AEDC [7]. Filters were changed out several times during the course of the observations. The field of view was defined by the field stop to be 18 in. high by 84 in wide (see fig. 3).

The single channel high speed radiometer was originally designed to detect "hot particles" which were presumed to generate the orange streaking apparent in the plume; those hot particles were presumed to be material released from various internal locations which had become luminous upon passing through the Main Combustion Chamber (MCC) and remained in tight groups in the high speed portion of the outer plume. The radiometer was equipped with a PMT and an 850 Schott glass filter yielding a response optimist for the near IR (approximately 850 to 1000+ nM). Provision was made for cryogenic cooling of the PMT, although it was not necessary for our purposes. The field of view was stopped at 2 in. high by 9 ft. wide at the plume and the bandwidth was about 500khz (see fig. 5). It later became apparent that the water emission band around 950nM was so large that the detector was saturated and thus rendered ineffective. Also, the orange streaking apparently is due to sodium emission. For those reasons this radiometer was reconfigured to monitor other bands.

Two other single channel filter radiometers, having UV sensitive PMTs, were used to monitor the OH radiation (narrow filtered with the center at about 310 nM) from the plume just below the edge of the nozzle and from the mach "disc". These were to be used to try to obtain a verification of calculated specie populations in the plume (see fig. 4).

A custom built high resolution grating spectroradiometer was used to characterize the UV (200 to 320 nM). This unit utilized a 0.5M SPEX spectrometer having a scanning mirror (3 sec. per scan) with the focal plane covered by 3 slit-detector pairs, each slit-detector pair covering 40nM. Data were acquired and processed by a dedicated micro-computer system and raw output was fed to FM tapes.[4] (see fig. 1, 2, 3)

A 0.75M spectrometer with a film attachment at the exit plane was utilized. Exposures of many seconds were used. Data was reduced by using an optical densitometer to yield an amplitude versus wavelength plot (see fig. 1, 2).

Two IR spectrometers were applied. These units, built by the AEDC, have LN[2] cooled long wavelength detectors and motor driven circular variable filters. A micro-computer data system was used to acquire and process the data.[8] The range covered by the units was approximately 1.3 micron to 5 microns and 2.5 microns to 16 microns (see fig. 2, 3).

Two OMA's were used. These units have intensified 1024 element silicon diode arrays. The 0.33M spectrometer of one OMA was mounted on the support table with custom cabling connecting to the control computer assembly inside the hard core. This unit was usable from approximately 300 to 800 nM and was generally used in the near UV. The other OMA was set up with its spectrometer inside the hard core along with its data acquisition and control equipment. A fiber optic cable connected the spectrometer to a foreoptic assembly (two lenses and cable termination) (see fig. 1, 2). Since fiber optic cables do not transmit UV well this unit was usually used for visible range emissions. These units can have the scan rate and number of scans added for data intensification programmed. Due to memory constraints the OMA's could acquire only 90 spectrums at any time; therefore 90 sets would be taken, loaded to disc, during which time no data could be taken, followed by another 90 sets loaded to a second disc.

Several imaging systems were used. A total of 4 video cameras were used. Two GE TN2500 CCD solid state scanning array cameras were equipped with a Sodium filter (590 nM) and a Potassium (770 nM) filter. A standard video camera having an 850 Schott glass filter was used to observe the approximately 850 to 1100 nM band; this allowed viewing the plume in the 950 nM water emission band. A facility (NSTL) provided high speed video camera was also utilized.

An AGA Thermovision IR camera equipped with InSb detector and a 2.7 micron filter was used. This allowed imaging in another water emission band, although the spatial resolution is not high.

A UV camera, with an OH band filter (311 nM), was used. Some tests were configured with a simple pinhole to obtain a relatively wide field of view. This

camera utilizes a proximity focussed channel intensifier tube (PFCIT) with a Cesium telluride photocathode for use in the deep UV, below 320nM.[4]

Data from all radiometers were fed to FM tape recorders and the data from the cameras were fed to VCR's. The data acquisition is started remotely by a signal initiated from the NSTL test control center. Tapes were retrieved and digital discs backed-up immediately after each test.

Data acquired at the A3 location was obtained [5] using a Tracor-Northern TN-6500 Real Time Spectrometer having a 512 element unintensified detector array coupled to a 5 in. f/10 Schmidt-Cassegrain reflecting telescope. Wavelength range is 350 to 800 nM. This arrangement was located several hundred feet from the test stand. When used to view an Orbital Transfer Vehicle (OTV) engine, a different foreoptic system was used and a distance of about 65 ft. utilized.

EXPERIENCE FROM TESTING

Tests at NSTL have yielded little anomalous plume data, primarily because the engines are not operated in marginal condition and thus are not given to frequent major failure. The engines normally run at A3 are engineering evaluation units and are sometimes run in less than flyable condition. For instance, during a series of 3 runs on A3, analysis of the data revealed an onset of an erratic CaOH trace. The trace, normally showing about 5% variations, suddenly showed variations of about 25 to 50%. Mechanical inspection showed total failure of the bearing cages in one of the turbopumps. Other instrumentation was provided to monitor bearing failure but usable information was available from the spectrometer, which would permit cage failure detection, prior to more conventional methods. A similar event occurred during observation of an OTV engine; a bearing locked up, stopping the engine, but the CaOH trace showed a major deviation a few seconds before [5].

Another incident, fortuitous for the investigators, derived from the inadvertent failure to remove a piece of copper tape- used to seal cracks in the MCC to allow inerting pressurization during shipping- from the MCC of a SSME. As the tape was consumed during engine operation, an easily observable CuOH trace was seen. Similarly, an injector face plate failure permitted the detection of metallic species such as Ni and Fe.

While few instances of anomalous plume emissions were observed in this study, a large amount of baseline plume data was collected [5]. As shown in figures (7 and 8), high background radiation was observed in the ultraviolet . There is, in fact, an apparent continuum from OH emission in the range from 230 to 360nM. There is very strong emission from Na at 590 nM and K at 770 mN; CaOH at 556nM and 624nM are also evident as shown in figure (9). On selected tests other trace elements have been observed but no other species have been continuously present.

The high UV background radiation coupled with high daylight background and scatter from water vapor aspirated into the field of view generated high-level, noisy signals on all filter radiometers. To counter the effects of these high background signals, much higher optical resolution will be necessary to observe the desired line spectra. With the equipment used, the energy available from each specie of interest is a low percentage of the total presented within the resolution element, thus making difficult the detection of the desired signal. Combined with a requirement for fast response, and tempered by funding constraints limiting the end product, it is necessary to design a new piece of equipment which will provide 5A°, or better, resolution and wide adjustability in a multi-channel radiometric instrument.

Incidentally, it is strongly felt that the Na, K, and Ca base traces are due to material present in the fuel (H2). This was inferred because of the continuous presence of these species when H2 is burning. These species are seen in the plume edges and in the mach disc, and the disc is likely to contain only whatever is fed into the MCC. Fuels are analyzed for adherence to specification but levels of trace materials observable by optical sensors is considerably smaller than the standard chemical analyses permit. A program to identify the impurities in the fuels has been planned but has not been effected; for example, the observed Na concentration has been calculated at less than 1 ppb [4,5].

The references (1 through 5) provide more detail as to the reasons for the demand placed upon the new instrument. The rest of this paper will describe the Optical Plume Anomaly Detector (OPAD) and the high resolution optical spectrum analyzer.

OPAD CONCEPT DESIGN

As indicated in the previous section, the high background levels generated by OH radical emission, scattered light from the mach disc and daylight scatter combine to make detection of weak spectral lines very difficult. The most substantial countermeasure against high background levels is to acquire the best possible spectral resolution. Therefore, the design of an OPAD cannot be based on low resolution optical

filter radiometers such as the 4-band radiometers described in the previous section. Optical filters generally have pass bands of 3 to 5nM. Since the spectral lines of interest are essentially monochromatic, the OPAD signal-to-background-noise ratio will vary inversely with the pass band. Therefore, at least one order of magnitude improvement in signal-to-background can be realized by using a high resolution grating spectrometer to isolate spectral emission lines. As a result a polychromator based on the use of a ¼-meter grating spectrograph was chosen for use in the OPAD. The use of a grating spectrograph also provides for an essentially unrestricted selection of candidate spectral lines, which is not true with optical filters. Figure 11 is a diagram of the OPAD polychromator as it is currently being implemented.

The assembly consists of a manually-operated, ¼-meter, SPEX, grating spectrograph. The device was ordered without attachments. Customized input and output attachments are being developed.

The input attachment consists of a 1.25-inch diameter integrating sphere (see fig. 13) and associated lenses. The diagram shows the system aligned to analyze light emitted from the area of the shock structure (mach disc), although it may prove preferable to sample the light from the area between the nozzle exit and the shock structure. Either way the field of view of the OPAD is determined by the field stop aperture located immediately in front of the field lens. The field stop can be conveniently changed to meet specific field-of-view requirements. The field lens directs light coming through the field stop to an input aperture on the integrating sphere. The wall of the sphere has a high, diffuse reflectance and the sphere wall becomes uniformly illuminated by the input light. The relay lens magnifies an output slit in the sphere wall to uniformly fill the entrance slit and field of view of the spectrograph.

The dispersed spectrum at the output of the spectrograph is 4 inches long by 0.9 inches high. The grating has 333 lines/mm and is blazed at 600 nM in the first order.

The first order dispersion at the focal plane is 4.95nM/mm, which gives a focal plane coverage of 500 to 1000nM in the first order overlapped by 250 to 500nM in the second order.

The output attachment consists of a special, ruggedized assembly of sixteen discrete, photovoltaic, silicon detectors. The detectors are 1.1 x 5.9mm, Hamamatsu type S1227-1680, and are mounted on adjustable arms as shown in the exploded view of Figure 12. A 0.005 inch wide by 0.25 inch long, light exit slit and an order sorting filter are mounted in front of each detector. The arms are adjusted so that each slit intercepts a unique spectral line. Schott glasses are used as order sorting filters. One row of eight detectors is mounted along the bottom half of the dispersed spectrum and a second row of eight detectors is mounted along the top half of the spectrum; only twelve of the sixteen detectors will be utilized in initial applications. The positions of the mechanical arms are adjustable along the direction of the dispersed spectrum and the detector mounts for the two opposite sections are designed to clear each other along the middle of the spectrum. Since the spectral line images are long enough to overlap both rows of detectors, two spectral lines that are very close together can be monitored simultaneously by two opposing detectors. The position of each detector is adjusted by maximizing the signal generated with a monochromatic source of the desired wavelength. Hollow cathode spectral lamps are the primary monochromatic sources used for wavelength calibrations. During test stand applications nothing in the OPAD will move. Therefore, the instrument should maintain its calibration in the high noise environment.

OPAD POLYCHROMATOR ELECTRONIC SYSTEM

The photo-current from each detector is measured by an auto-ranging nanoammeter, which detects currents in the 10^{-11} to 10^{-5} amp range. The design of the electrometer is presented in Ref. 7. One auto-ranging nanoammeter is provided for each of the 12 detectors.

A block diagram of the electronic instrumentation in the OPAD system is presented in Figure 13. All analog signals from the autoranging nanoammeters are fed to four 4-channel ADC boards. Each channel per board has an input preamplifier, sample-and-hold amplifier, 12-bit ADC, output latches, and buffers. The analog signals are digitized at a 1 Khz rate. The digitized signal data and range data are transferred to the computers via the digital control board.

The digital control board was designed and built to control the digitizing process, to provide a first-in/first-out (FIFO) memory for the digital data, to implement the computer handshaking protocol and to provide a high speed digital comparator. The comparison process is implemented using a bipolar microprocessor and microprogrammable sequences. The microprocessor executes an instruction every on-board clock cycle and "builds" an overflow word from the results of successive comparisons made between the signal data and the stored Threshold Levels. The over flow word is then transferred to the computer performing the real-time analysis and is also available for real-time control of possible engine shutdown. The FIFO memory does not

represent a significant delay in the system, but rather, it is used to insure no loss of data due to computer bus contention which can occur during a synchronous data transfers. Another microprogrammed sequencer is used to perform the handshakes between the computer's direct memory access (DMA) interface and the FIFO memory.

Each computer is an 80286-based Zenith Z-248 system configured as follows: EGA color graphics card and monitor, 20 Mbyte hard disk drive, 1.5 Mbyte RAM, 80287 coprocessor, 360 Kbyte floppy disk drive, and DMA and programmed I/O interfaces. The system used to archive the data also contains an additional dual 20 Mbyte removable-disk cartridge drive. One computer acquires and stores spectral data and IRIG time data (data archiving), while a second computer is used for real-time analysis and display. The second computer also calculates and downloads the threshold levels to the microprocessor on the digital control board. The microprocessor serves as a digital comparator and supplies an overflow word back to the computer, as discussed above.

Assembly language software was written under DOS to acquire and store data on the first system at rates exceeding 170 Kbytes/second. Assembly language software was written to acquire data on the second system and display an on-line 12 channel histogram. The histogram Figure D shows signal range and magnitude for each channel (each channel represents a particular line source). Each channel is sampled once every millisecond.

The overflow word represents the fact that the detected signal has exceeded a predetermined threshold (downloaded from the real-time computer to the digital control board). The output of this overflow word is available to be fed to an external system capable of initiating a response to the detected anomaly. That response could be anything from a variation effected in operating conditions to shut-down of an engine.

A 4-band filter radiometer is to be mounted alongside the OPAD to capture wide range data. This is to allow the possibility to correct for variations in the background caused by disturbances such as vapor clouds in the field of view creating scattering or obscuration, variations in ambient light levels or other optical abnormalities. These levels can be fed to the real-time analysis computer and used to determine appropriate threshold levels on a real-time basis.

THE OPAD SPECTROMETER

The OPAD Spectrometer (a multi-channel high resolution radiometer) is intended to be a failure detection/prevention device. It is meant to detect anomalous species and, based on perceived levels and tempered by historical data, issue an output to the engine controller directing some corrective action. At the present time, however, limited information is available concerning the relationship between emitted spectra and their sources. Therefore, it is necessary to gather more spectroradiometric data on the engines being monitored. As mentioned previously,[2,3] high resolution is necessary, but with the wide range desired, 250nM to 1000nM, no commercially available instrument will do the job; thus, a custom instrument is being designed. The Optical design of the OPAD spectrometer is similar to the OPAD Polychromator (Figure 11) excepting that the detector assembly is replaced with an assembly carrying four 2048 element linear detector arrays. Using order sorting filters to separate the 4 arrays into 2 groups, the range and resolution requirements are approached. The arrangement gives 4096 elements to cover each of the two bands, 250 to 500nM and 500mN to 1000nM. These arrays, via their control boards, are connected to a Zenith 248 computer, which processes the data and stores it on an optical memory disc (approximately 120 Megabytes). The data may then be analyzed later.

COMMENTS

The two instruments reviewed in this paper are tools which may allow rocket engine systems to identify mechanical abnormalities in themselves before a catastrophic incident occurs, thus saving, at least, the engine and perhaps even the vehicle on which they are used. Several significant tasks remain before such protection can become a reality. One effort is that of correlating actual engine incidence with detected events; such a task will allow the development of proper software. Considering the diversity of construction among the several engine test stands, even the act of mounting the instruments to those stands is not trivial. Keeping track of the engines and the data applicable to each is also necessary. As more engines are made available, data tracking and correlation becomes a considerable task. None of the tasks are insurmountable but rather require in-depth attention.

ACKNOWLEDGEMENT

The authors gratefully acknowledge the efforts provided on behalf of this program by Mr. W. G. Spradlin of the MSFC Residents office at NSTL, members of the SSME engine project office at MSFC, facilities support personnel of NSTL and its supporting contractor, Severdrup technology, personnel of Rocketdyne Division, Rockwell International, and personnel from the AEDC and its operating contractor Sverdrup

Technologies - in particular Mr. V. A. Zaccardi, project coordinator, and W. K. McGregor, K. A. Dietz, R. G. McCoy, W. J. Phillips, and C. C. Limbaugh, and Lynn Wyett of Rocketdyne, Canoga Park, CA. This sort of project cannot be accomplished without the efforts of such people as these.

REFERENCES

1. Cikanek, H. A. III, "Failure Characteristics of Space Shuttle Main Engine Failures", in Proceedings of the Joint Propulsion Conference, June 1987.

2. Cikanek, H. A. III, Powers, W. T., et al., "Space Shuttle Main Engine Plume Spectral Monitoring - Preliminary Results", in Proceedings of Joint Propulsion Conference, June 1987.

3. McCoy, R.G., Phillips, W. J., McGregor, W.K., Powers, W. T., and Cikanek, H. A., "Analysis of UV-VIS Spectral Radiation From SSME Plume", JANNAF Propulsion Meet, San Diego, December 1987.

4. Limbaugh, C. D., Brown, D. G., Hiers, R. S. III, Gross, K., and Eskridge, R., "Analysis of SSME Plume Images Obtained During Ground Testing", JANNAF Propulsion Meet, San Diego, December 1987.

5. Wyett, L., Maram, J., Barkhoudarian, S., and Reinert, J., J., "Reusable Rocket Engine Optical Condition Monitoring", JANNAF Propulsion Meet, San Diego, December 1987.

6. Sherrell, F. G. & Neese, D. W., "Techniques for Rapid Scanning Spectroradiometry using a Grating Monochromator", AEDC publication TMR-84-E41, May 1985.

7. Sherrell F. G., "Autoranging Radiometric System", 33rd International Instrumentation Symposium, Las Vegas, NV, May 1987.

8. Sherrell, F. G. & Neese, D. W., "Circular Variable Filter (CVF) Radiometer Design with Digital Data Processing" AEDC Publication TR-85-11, April 1985.

9. Sherrell, F. G. "Ultraviolet Image Display System for Plume Radiometry", AEDC publication TR-85-8, March 1985.

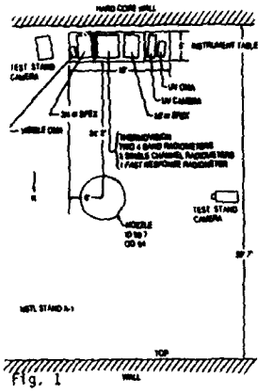

Fig. 1

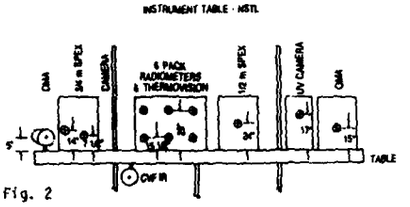

Fig. 2

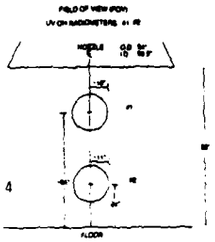

Fig. 4

Single channel UV radiometer FOVs.

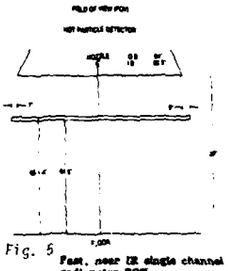

Fig. 5

Fast, near IR single channel radiometer FOV.

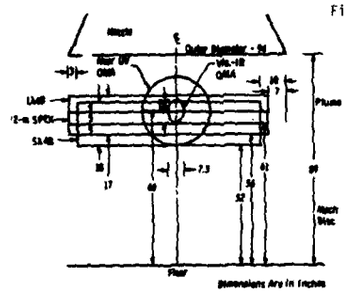

Fig. 3 Instrumentation Fields-of-View for SSME Tests at HSTL Test Stand A1.

RADIOMETER FILTERS

ELEMENT	FILTER BAND	BAND PASS
Ag	338.3 nm	5.0 nm
Al	396.2 nm	1.0 nm
Au	958.6 nm	5.0 nm
C	247.8 nm	5.0 nm
Cr	357.4 nm	4.0 nm
Cu	324.8 nm	2.4 nm
CuOH	548 nm	20 nm
Fe	372 nm	2.5 nm
Hf	385 nm	4.6 nm
Mn	279.5 nm	5.0 nm
Ni	352.5 nm	4.0 nm
Screen MG 850	850 nm	200 nm
Ag	350 to nm	8.12 nm
OH	310 nm	4.3 nm

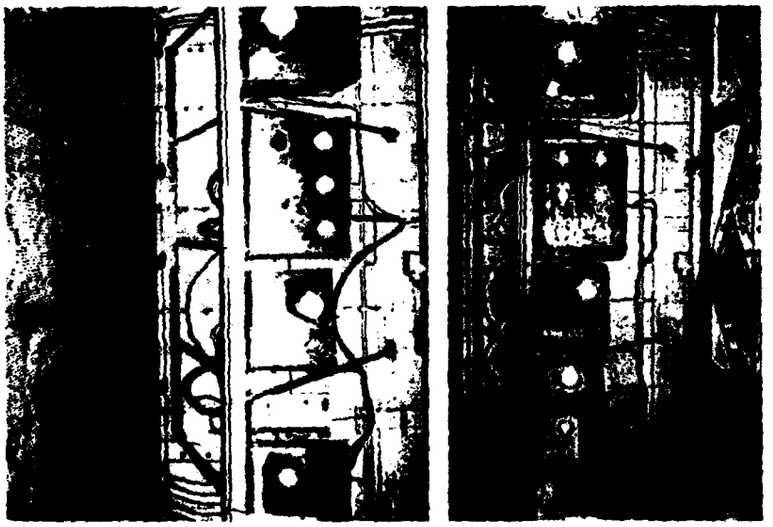

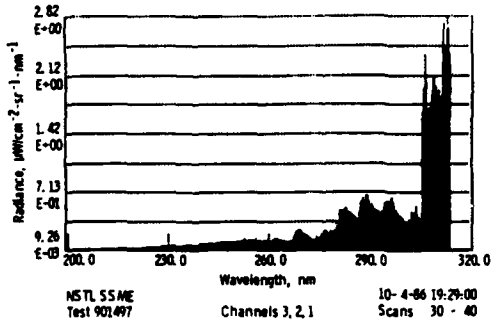

Fig. 7 a. Far UV

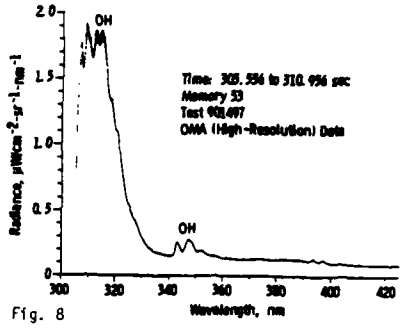

Fig. 8

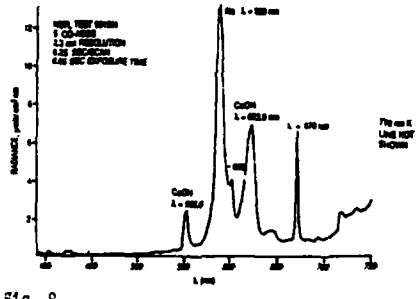

Fig. 9 Detail in the 500-700 nm band.

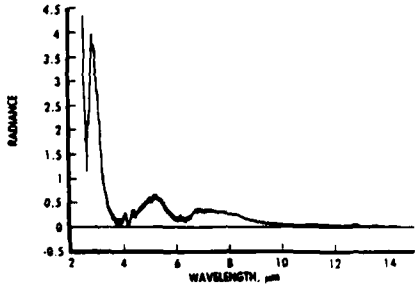

Fig. 10 CVF IR spectrometer response.

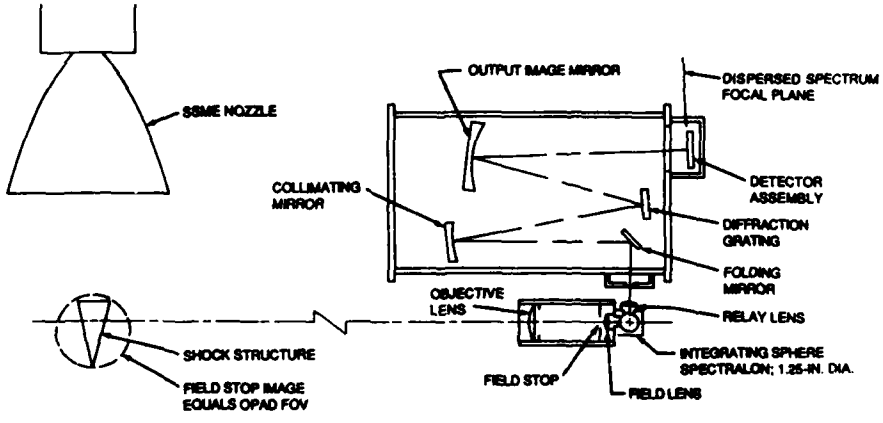

FIGURE 11 OPAD CONCEPT DESIGN IMPLEMETED WITH DICRETE DETECTOR ARRAY

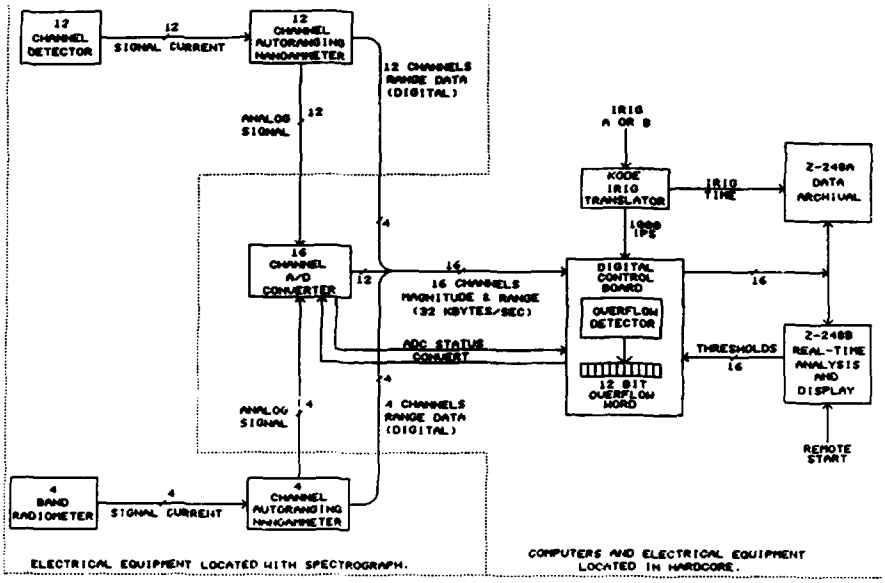

NASA/OPAD POLYCHROMETER
ELECTRONICS CONCEPT

Fig. 12

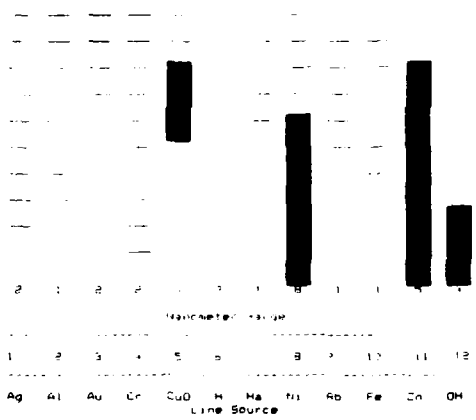

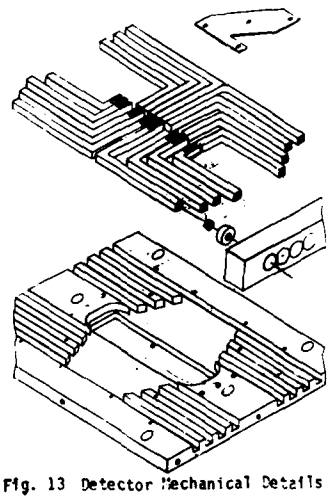

Fig. 13 Detector Mechanical Details

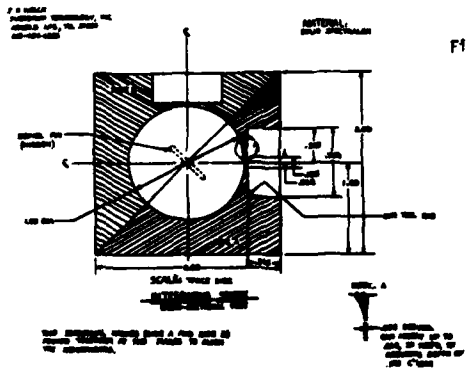

DISCUSSION

K. TAYLOR

1. Is the spectrometer intended to be an on-board system?

2. Would you describe how such an on-board system might be set up in the vehicle? Do you forsee any changes to the engine to accomodate such a monster?

Author's Reply:

1. Not this model, it is too large, too heavy and too fragile. This unit is a prototype engineering model.

2. No changes to the engine would be required. The instrument would be totally transparent to the engine system. It is not obvious at this time how to accomplish such a task. A high spectral dispersion system is necessary as well as a vibration insensitive one. The design of such an instrument is a future (near-term) task.

GAS PATH CONDITION MONITORING USING ELECTROSTATIC TECHNIQUES

by

Celia Fisher, BSc, CEng, MIMechE
Senior Applications Engineer
Stewart Hughes Limited
Centre for Advanced Technology
Chilworth Manor, Southampton SO9 1BX, UK

SUMMARY

The concept of condition monitoring using electrostatics offers the opportunity to monitor gas path faults as they occur. It is based on the assumption that gas path distresses, such as blade rubs and combustor burns, cause the production of minute particles of debris, which carry electrostatic charge, and can be monitored on suitable sensors mounted in the engine.

The engine has a normal level of charge, which produces a background signal. The debris produced by distresses causes a change in the signal which can be monitored using suitable signal processing techniques.

The paper describes the research work which was necessary to provide an understanding of the mechanisms involved. This forms the basis of the technique which is described, with examples of the application of the system to various engines.

1.0 INTRODUCTION

Research and investigation into the use of electrostatic techniques to monitor the condition of a jet engine or gas turbine gas path commenced in America in the early 1970s. The American work demonstrated the potential of the technique, but appeared to cease in about 1979.

Stewart Hughes Limited saw the potential of the technique but recognised the need for a basic understanding of the fundamental principles of the technique. An extensive programme of research and latterly development work has been undertaken over the past few years. A basic understanding and knowledge base of the physical mechanisms has been developed and is being used to exploit the full potential of the technique.

The basic premise is that distresses produce electrostatically charged particles. The principle of the technique is to monitor electrostatically charged debris present in the engine. The exhaust gas has a normal level of electrostatic charge which gives the background signal. The signal will change when increased amounts of electrostatically charged debris are present in the gas. This may be due to various reasons:

(i) 'Debris-producing' faults in the gas path, such as blade rubs, combustor burns etc
(ii) High levels of carbon being formed in the combustion chambers and being shed
(iii) Wear of abradable seals or coatings
(iv) Ingested material

The increase in electrostatic activity is monitored using suitable sensors strategically placed in the gas path.

This paper describes the research work which was necessary to provide an understanding of the mechanisms involved. This forms the basis of the technique which is described with examples of application to various engines.

2.0 RESEARCH WORK

A good understanding of the fundamental principles is the key to this technique, so that its maximum potential is achievable. The work programme started purely as research. This has continued throughout to support the development work, so that problems can be addressed and understood.

The research work has been carried out in three distinct phases.

2.1 Initial research

The initial aim of the research work was to build confidence in the principles of the technique. Several fundamental questions had to be addressed to establish the overall feasibility of using such a technique.

The first fact to establish was that metallic debris carried electrostatic charge and to investigate the importance of various parameters in the electrostatic charging of metal powders.

This work was carried out on a small experimental rig, shown in Figure 1. This rig is used by the Wolfson Electrostatics Unit of the University of Southampton, UK, for fundamental investigations of insulating material powder charging. Two different powder feed systems were used during the course of the

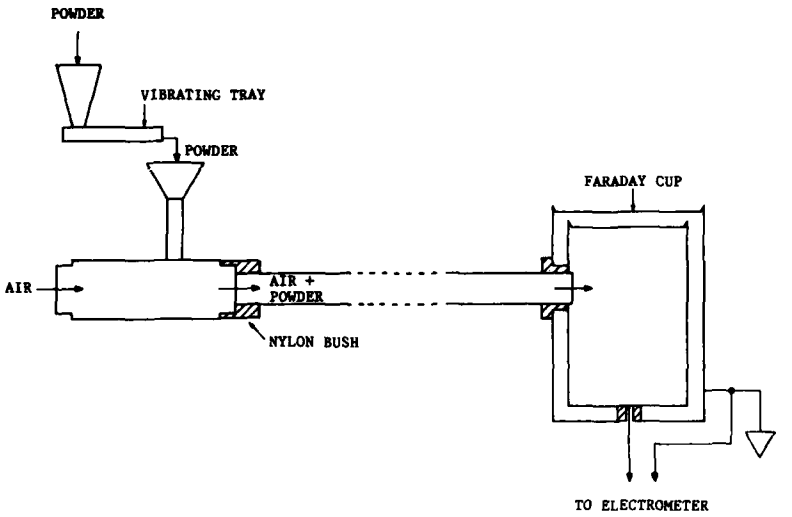

FIGURE 1 : Small tube powder flow rig

work. Various parameters thought to be important were investigated using this rig. These included, tube length, tube diameter, powder type and particle size, bends, obstacles. The Faraday cup measures the electrostatic charge on the powder collected in it.

Several different powders were used in the experiments, including aluminium, stainless steel 316, Nimonic 80, Inconel and Amdry 995 (coating powder). Various particle sizes were also used.

The important conclusions from this work were:

(i) The charging of metal debris is a real effect and the charges involved are measurable, repeatable, and of a similar order to those acquired by non-conducting materials.

(ii) Several parameters were identified as having a significant effect on the charge on the debris. These include debris velocity, tube geometry, collisions, material type and debris size.

Figure 2 shows the results of a simple dimensional analysis undertaken on the data acquired from this experimental rig. The data collapses to a curve. The absicissa being the ratio of tube length to diameter (L/D) and the ordinate function of charge, flowrate, time and tube diameter. This correlation demonstrates the consistency of the results. Consideration of a typical jet engine gas path indicates that the L/D values will not approach the large values used in the experimental work, and will more typically be in the steep slope area at the start of the curve.

(iii) The results showed good agreement with American work, with similar trends evident, although the American work was carried out on much larger rigs.

2.2 Scaling effects and sensors

Once a basic knowledge of the principles and some confidence in the concept had been established the work was transferred to a larger experimental rig. The aim of this was:

(i) To start to establish scaling effects

(ii) To enable investigations of sensor and signal conditioning characteristics and requirements to commence.

A schematic of the experimental rig is shown in Figure 3. The scale parameters of the large to small rigs were approximately:

Tube cross-sectional area	115:1
Air velocity	2:1

The charge in the debris was again established using a Faraday cup, and for the bulk of the tests various sensors were mounted in the tube to investigate the signal characteristics (Section 2.2.2)

2.2.1 *Scaling effects*

The programme of work investigated the same parameters as covered on the small tube rig, and used the same powder types. The important results were:

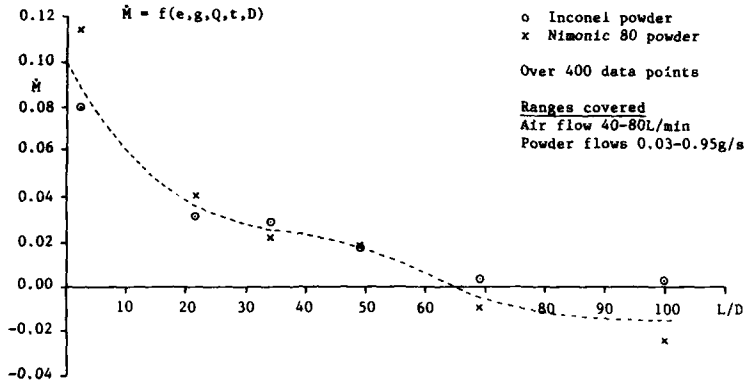

FIGURE 2 : Non-dimensionalised test data

(i) The magnitude of charge on the debris was greater than in the small tube rig.

(ii) The increase of velocity produced an increase of specific charge (charge/mass ratio) for each debris type. This correlates with the trend established in the small tube rig where the air velocity could be varied.

(iii) The variation in specific charge for the different material types and particle sizes followed the same trends as those shown previously.

(iv) The non-dimensional analysis produced a consistent set of results, which tied up with the small rig tests, showing that the effects could be scaled.

2.2.2 *Preliminary sensor assessment*

For the bulk of the above tests sensors were positioned in the tube so that the signals produced by the charged debris could be correlated with the charge measured in the Faraday cup, and the sensor performance assessed. The sensor output was conditioned to produce a voltage proportional to rate of change of charge. This work was crucial to providing a suitable means of detecting the debris outside the laboratory situation. Several sensor configurations were tested, including a full ring and rod type sensors. The most successful configuration was a ring sensor, and the capability of this was enhanced by separating the full ring into segments. The overall conclusions showed that:

(i) All of the sensors were sensitive to charged powder passing by them.

(ii) The full ring gave the best signal to noise performance, with additional, positional information being provided when the sensor was segmented.

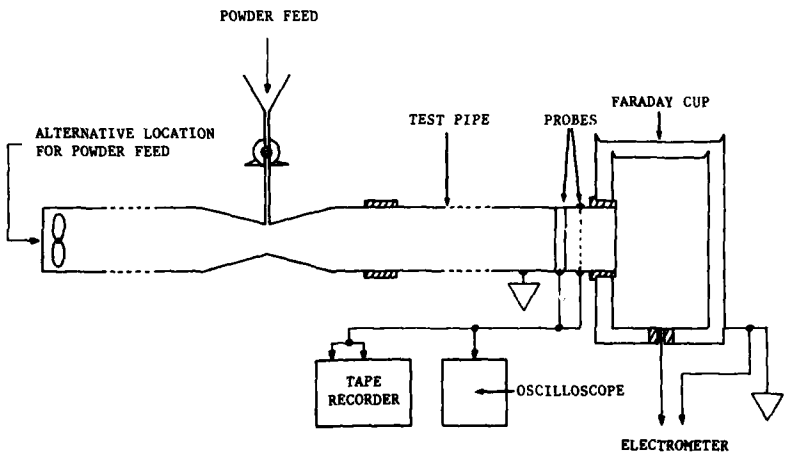

FIGURE 3 : Schematic of large tube rig

(iii) The amplitude of the measured signal varied with the same parameters shown to be important in the preliminary work.

(iv) Various parameters affected the sensor performance, including its physical size and electrical properties.

The work also showed that the signal characteristics varied with different sensor designs.

In order to maximise the use of information about the debris from the signal characteristics a sensor design had to be identified so that assessment and understanding of signals had a common base. Additionally work had to be carried out to translate the design information into sensors which could be fitted on engines.

The sensor and signal conditioning electronics development work is outlined in Section 4.

2.3 Further experimental tests

2.3.1 *General work*

The objectives of this work were to improve the understanding of the physics of the mechanisms and to relate this to the signals which are likely to be produced by a distress in the engine. All the experimental work was carried out using ring sensors to monitor the signals. In some cases the Faraday cup was also used to collect the debris to corroborate the probe results. The output signal from the electronics is in volts. This is directly related to the rate of change of charge, dQ/dt measured by the sensor.

In previous experimental work various parameters were identified as being important in the charging mechanism.

These were:

(i) Material type
(ii) Particle size
(iii) Distance travelled by the debris
(iv) Obstacles
(v) Velocity

The effect of these parameters has been assessed on the sensor signal as well as:

(vi) Variation in tube/duct cross-section
(vii) Foreign object type materials

(a) The techniques for injecting the debris into the rig have all produced charged debris. It appears to be the macro effects, such as momentum change, material type etc which are important.

(b) The material type and particle size and shape play an important role in the signal characteristics. Fine debris tends to travel with the airstream in a cloud, and larger flakes and particles become more dispersed because of the aerodynamic effects on the individual particles. The shape of the particles affects the dispersion pattern and signal characteristic.

(c) Insulating type materials tend to produce slightly higher amplitude signals than the metal debris. There does not appear to be a consistent pattern of, for example, negative first signals from insulating materials and positive leading edge signals from metal debris.

(d) Contact between the debris and various obstacles appears to produce a transfer of charge. Other parameters which affect the charge are also active in the engine, so that the debris is likely to retain its charge during its passage through the engine.

(e) An increase in the duct cross-sectional area affects the signal amplitude, because more axial dispersion of the debris is possible and the amplitude is proportional to $1/d^2$ where d is the distance between the debris and the sensor. This can be overcome by suitable sensor design and positioning.

2.3.2 *Single particle investigations*

Previous work indicated that the signal produced by various debris types was affected by the dispersion pattern of the particles and therefore by the shape and size of the particles within the debris cloud.

The following work was undertaken to explore this variation in a controlled way, first by using single particles of various shapes and surface areas, and then by examining the signal from clouds of the single particles. The effects on the signal of the surface area, shape, etc can thus be separated from effects due to particle/particle interaction.

This was carried out in tandem with computer modelling of the sensor performance and signal. During the single particle experimental work it became evident that direct measurements of the charge, rather that rate of change of charge was a more satisfactory and sensitive technique. The bulk of the modelling work was concentrated on this approach and was compared with the experimental results.

Various shapes of single particle were produced from a standard piece of lead shot. These therefore had approximately the same volume but different surface areas. In addition three other sizes of spherical lead shot were used to provide debris of the same shape but with different volumes and surface areas.

A test duct (150 mm dia) was produced with full ring sensors at four axial locations. The debris was precharged before being introduced into the test tube using gravity feed. The radial position of the debris was carefully controlled at introduction to the tube, and was monitored after passage through the tube so that its radial distance from the sensors was known.

This work showed that the size of the charge on single particles of debris is related to the surface area. Therefore in a distress which produces debris of varying sizes, the larger pieces will carry a larger charge. The larger pieces are likely to travel slower than the small pieces, therefore within a cloud of particles the largest charge may occur at the rear. The larger particles are also more likely to impact with the turbomachinery.

The variation in shape of the debris does not affect the signal characteristic because the sensor senses the equipotential lines set up by the charge on the debris. Any variation in these due to the shape is very local to the debris and is therefore undetected.

From these results it may be inferred that the characteristic signatures produced in previous work were due to the different dispersion patterns of the particles of debris within the cloud.

This work also corroborated the results from the sensor modelling, showing the effect of velocity on the pulse signal, and the variation in the charge signal caused by the distance of the debris from the probe.

2.3.3 *Multiple particle investigations*

This formed a logical extension to the single particle work where the signal characteristics produced by single pieces of debris were investigated using controlled experiments. The work was undertaken to explore the way the signal was affected by clouds of debris.

One shape of debris was used, a spherical piece of lead shot corresponding to debris type 1 of the single particle work.

Each piece of debris was precharged to the same level by applying a voltage across each vacuum dropper pipe.

Pieces of debris were introduced into the tube at various radial locations from the same horizontal plane, and with various vertical separation distances. For each test the signals from particles for each dropper position were monitored separately and then simultaneously.

Particle to particle collisions were not simulated in these experiments. Any interaction between the separate charges and equipotential lines of the particles will be indicated by these tests.

The multiple particle work showed that the signal produced by a cloud of debris is the addition of the signals from each particle, up to the particle concentration tested. The signal characteristic is therefore dependent on the dispersion and size of the particles within the cloud.

2.3.4 *Origin of charge*

Previous experimental work has shown that various mechanisms affect the charge on the metallic debris.

However the work does not indicate whether the debris is charged by the action of the distress or in subsequent passage through the engine. It is also not evident whether any of the mechanisms are dominant and therefore alter any previous charge on the debris.

Some work has been undertaken to investigate the charging mechanisms in a controlled way. The single particle approach was used to try to separate individual charging effects into component blocks. When each of the mechanisms has been considered it should be possible to reconstruct the blocks to give a picture of a realistic distress.

Effects of impact:

When two dissimilar metals are brought into contact, the energy levels of the electrons in the two metals will not in general be the same. Consequently electrons will flow from the metal with the higher energy levels (ie smaller work function ϕ) to that with the lower energy levels. Once the energy levels are equal an equilibrium will be established and no further flow will occur. The flow of electrons results in a potential difference at the junction of the two metals, this is known as the contact potential.

The net negative charge in the one metal and the corresponding positive charge in the other will be confined to a very narrow surface layer at points of microscopic contact between the two metals. Since an equilibrium has now been established the charges will remain in place when the metals are separated.

The time constant of the electron flow involved in this process is very small, hence it should be possible for it to occur during a collision between two metals. To test this possibility steel ball

bearings and lead shot were deflected off metal targets and the charge on the projectile was measured before and after impact.

The projectiles were held suspended by a stainless steel vacuum pipe and then released by venting the pipe to atmospheric pressure. Both the vacuum pipe and the target could be earthed or precharged as required.

It was found that the charge before impact was largely determined by the precharge on the vacuum pipe. However there was still a small charge present on the projectile even if the pipe was earthed.

If the target was earthed the charge after impact was always the same for the same projectile regardless of the precharge applied to the vacuum pipe. The size and the polarity of this signal varied as different target metals were used. In addition the amplitude of this residual charge signal increased as larger projectiles of the same material were used. This was due to the increase in contact area. If the target was precharged the residual signal could be altered according to the precharge used.

These results support the theory that the contact potential will produce charged metallic debris and that this mechanism unlike thermionic emission will work at low temperatures.

Size of particles undergoing collisions with turbine blades:

The gas flow through a turbine is essentially streamline. Consequently collisions with gas molecules will ensure that small particles are carried along with the flow. However, this will not be the case for large particles because of their much greater inertia and they will tend to collide with the turbine blades. Simple kinetic theory calculations using typical gas turbine parameters suggest that the change from small to large particles tends to occur at around 10 um diameter. More detailed calculations by Tabakoff and Hamed [Reference 1] suggest that one third of 15 um diameter fly ash particles will collide with blades in the first nozzle but almost all collide with subsequent blade rows. This occurs because the particles just manage to get through the first nozzle but are then in an unfavourable position for getting through the next blade row. It seems likely that even particles smaller than 10 um diameter are likely to collide with turbine blades. The reason for this is that the particles, although small, are still much more massive than the gas molecules. Thus only if the particles are comparable in size to the gas molecules could one be confident that a reasonable proportion would travel through the turbine without collisions.

Effects of friction:

The effects of friction on charge generation and charge exchange during particle to particle collisions were investigated using the single particle approach in experimental rigs.

Charging due to friction and collisions is related to differences in work function between the materials and the microscopic surface areas in contact.

Charge redistribution occurs when two metallic objects collide. The charge is proportional to the diameter of the objects as surface charge density depends on the curvature.

2.3.5 *Blade rub simulation tests*

All of the previous items of research work helped to extend the knowledge base and understanding of the physics involved in the principle of the electrostatic monitoring technique.

The rub simulation tests in the laboratory provided an opportunity to use the knowledge to understand what occurs when a blade rubs, in terms of the likely production of charged debris, and also to assess how the charge on the debris could be modified during passage through the engine.

The principle aim of the rub simulation work was to discover whether charged debris is produced in a rubbing situation for a range of materials, which parameters affect the detectable charge, what mechanisms are involved and how applicable the findings are to a real engine.

Metallic rub situations produce charged debris easily detectable by the charge monitoring system. The important parameters which affect the measurable charge are:

(i) *Rub pressure:* greater rub pressure produces more debris resulting in a larger detectable charge. Charge per unit debris appears to remain approximately constant.

The measurable charge increases with velocity, essentially as a consequence of greater debris production.

(iii) *Time between rubs:* rubs occurring at a high frequency cause considerable heat generation, resulting in greater debris production and higher detectable charge.

If the temperature in a particular area increases steadily over a period of time, the type of debris produced may change affecting the charge measured. The local heating weakens the materials and greater amounts of debris are produced due to the wear mechanisms.

(iv) *Materials:* the sign and magnitude of the charge on the debris will depend on the materials concerned. Predicting the results theoretically is difficult, but simple laboratory tests on material combinations could give a reliable estimate of what may happen in an engine.

These parameters all appear to affect the charge in a way that would favour the production of highly charged debris in an engine blade rub. If a detailed knowledge of the charge for a given blade rub was required some simple tests with the correct materials would allow a reasonable estimate of the real case to be made.

2.4 Current research work

Research work now centres around the use of a small gas turbine. The work involves investigation of various effects and signal characteristics, without doing seeded fault trials. This is backed up, where necessary, with laboratory testing and computer modelling work.

The engine is also a prime testing and development rig for sensors.

2.4.1 *Impacts on rotating machinery*

Previous experimental work showed that impacts can significantly alter the charge carried by the debris. Other work suggests that the bulk of debris particles are likely to impact with rotating machinery.

Tests have been made on the engine to investigate this effect using various materials.

From the results the behaviour of the materials can be broadly split into two classes, by their conducting properties. Metallic powders which are good conductors behave more consistantly than non-metallic materials, which are generally insulators. Some overlap does occur.

All the metallic materials tested showed an increase in charge after impact with the turbine, with consistency being shown in the polarity of the signals. This corresponds with the work functions of the materials used.

The non-metallic materials tested produced less consistent results, and gave both positive and negative signals. However broadly speaking the results follow the trend predicted by considering the work function.

In summary, all the materials tested, except two, became more detectable after impacting with the turbine.

2.4.2 *Contamination of the gas path by liquid*

The gas flow could potentially have two liquids present in it:

(i) Water. This is unlikely to affect the hot end.
(ii) Oil contamination may occur if seals fail.

FIGURE 4 : Ring probes mounted in exhaust cone

Some work has been carried out to establish whether oil is detectable using this technique. The results indicate that this should be possible.

This information can be used to enhance the understanding of data from engine tests, and to aid the signal analysis.

To date the results have been used in two ways:

(i) To enhance and provide explanations of engine data.

(ii) With an investigation into debris producing faults within a jet engine, to assess how the effects may affect the charge on debris produced by various faults as it passes through the engine.

The theoretical assessment of engine faults using the experimental data showed good corroboration with engine test data.

3.0 ENGINE TESTING

The research work provided confidence in the principles of the technique, but the acid test of any potential condition monitoring system is whether it works in an engine, and whether the engine operating environment affects the technique to make it inoperable. To date the technique has been tested on several different engines, in different environments.

3.1 Seeded fault trial

During the first two year programme of the research work the unexpected bonus of a piggy-back ride on a Viper engine test was offered by Rolls Royce plc and MOD. This provided a prime opportunity to test the technique as a known fault was seeded into the engine after a datum test.

Based on the experimental work SHL designed and built electrostatic sensors to fit into the jet pipe (Figure 4). These were mounted in the engine, together with four other types of equipment, to try to detect the fault.

3.1.1 *Datum test*

The engine was first run in standard form to give a 'datum' record for the four detection methods, there being a single shot of 'debris' injected into the air intake. This was primarily to assess typical signal levels on the Stewart Hughes electrostatic probes, caused by metallic debris in the gas stream, as the equipment had not previously been tested in a real engine. The debris injected into the engine was Inconel powder, the same as that used in the SHL experimental rigs.

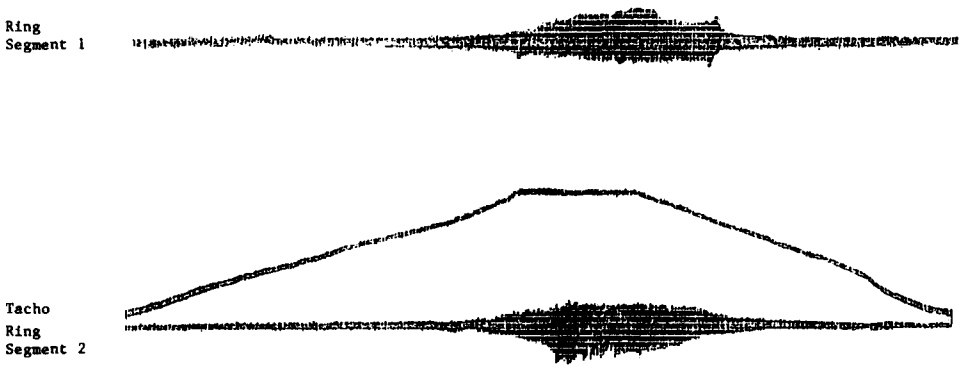

FIGURE 5 : Viper test data run

The background signal level (Figure 5) was about 40mV pk-pk at idle. As the engine accelerated the signal level increased gradually to about 85% speed and then increased more rapidly to about 200mV at 104% speed. The signal was approximately the same level on all four segments.

Figure 6 shows the signal produced by the ingested debris on two of the segments. It is clearly distinguishable above the background level and gave the first indication that the sensors could monitor electrostatically charged debris in the engine. It was particularly encouraging because the injected powder had travelled right through the engine and in particular the combustion chamber, and still carried a significant electrostatic charge.

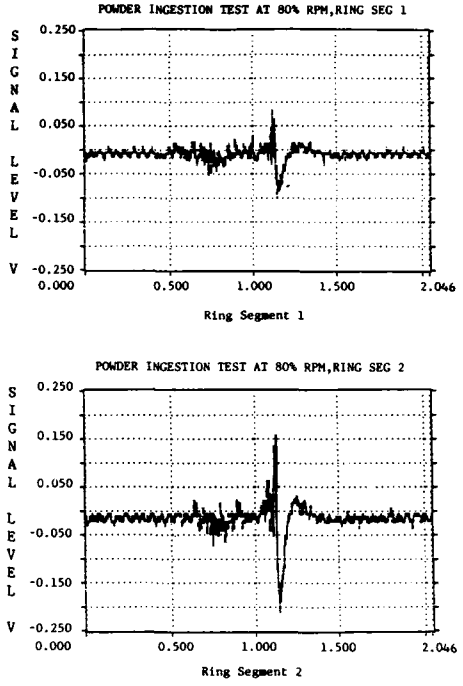

FIGURE 6 : Debris ingestion signal

3.1.2 *Blade rub test*

The engine was stripped and rebuilt with a faulty blade in the fourth stage compressor rotor. The tang root of the blade was partially cut through to try to simulate the effects of cracking. It was hoped that the blade was sufficiently 'faulty' to cause it to lean and produce a tip rub at some stage of the engine acceleration. The root was not completely cut through as this could cause loss of the blade from the disc.

The test programme consisted of slow acceleration and deceleration cycles.

After the test the engine was stripped to determine whether the blade had rubbed and to assess the amount of damage.

The signal produced on two of the segments is shown in Figure 7.

The signal level at engine idle was approximately 60mV.

As the engine was accelerated this level increased gradually reaching about 120mV at 85% speed, and 160mV at 93% speed. As the engine accelerated further the level increased and at about 97% rpm the signal was seen suddenly to approximately double in amplitude. As speed was increased to 104%, the signal amplitude increased to about 1 volt. This level fluctuated slightly while the engine remained at 104% rpm, decreased a small amount as the decel regime commenced and then reduced sharply at about 96% speed, gradually reducing to a background level similar to the accel case at 90% rpm. This pattern repeated when second and third accel/decel cycles were carried out although the maximum peak to peak amplitude was slightly less than for the first accel/decel.

It should be noted that:

The general signal level on the blade rub test is higher throughout the cycle, eg at 40% rpm it is 60mV on the blade rub test compared to 40mV on the datum test, and at 93% rpm is 160mV pk-pk on the rub test compared to 120mV pk-pk during the datum run. However the rate of change of signal level between these two speeds on both the datum and rub tests is about the same, being a factor of 3 on the datum test and 2.7 on the rub test.

It can be seen that the rate of change of signal level between about 97% and 104% speed on the rub test is much larger than on the datum test.

Engine Speed %	25%	40%	85%	93%	104%
Datum Test					
Signal level mV	30	40	70	120	200
(Signal at speed) / (Signal at 40% rpm)	-	1	1.75	3.0	5.0
Rub Test					
Signal level mV	40	60	120	160	1000
(Signal at speed) / (Signal at 40% rpm)	-	1	2	2.67	16.7

The engine was stripped to determine whether the blade had rubbed, Figures 8 and 9 show the blade and a half-casing. The touch mark on the half-casing was mirrored on the other half of the casing.

3.1.3 *Summary*

The Viper engine compressor blade rub test provided the prime opportunity to validate and confirm the results from the two year research programme.

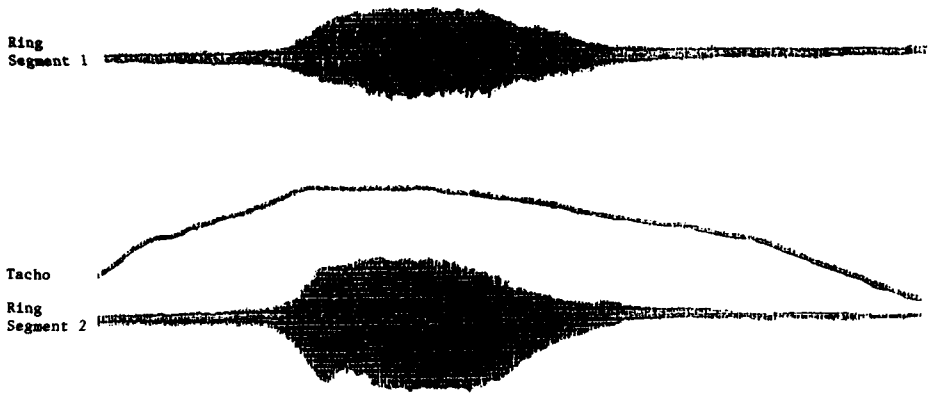

FIGURE 7 : Viper test with seeded blade rub - ring probe signals

1 The test showed conclusively the potential of the technique as a gas path distress monitor, with the added bonus that it was the only one of four real-time monitoring techniques which detected the rub.

2 Signal analysis showed that various parameters including amplitude of the signal changed when the blade rub occurred.

3 Comparison of experimental rig results and engine test data shows good corroboration.

4 The design and development work on the sensors in the experimental rig formed the capability to manufacture rugged sensors in a short time which required only minimum modifications to the engine casing.

5 Areas of improvement were identified for the sensors and signal conditioning.

3.2 Other engine tests

The technique has been tested on various engine installations, including Marine Tyne and Spey, a helicopter engine and a combustor development rig. None of these engine tests included seeded fault trials although methods of checking the functionality of the equipment were incorporated into each test.

Each of the tests provided information about various different aspects of the technique, for example, in the Marine engine application sensors were positioned in the large rectangular uptake. Tests were carried out in the test house, to assess the functionality of the sensors in such a large duct, and to identify and characterise the engine background signal. The system has since been tested on a Tyne installed in a ship to classify the environment to be experienced by the sensors and electronics, in terms of both the ambient conditions and the electrical and interference effects.

4.0 HARDWARE DEVELOPMENT

This is a crucial area to address because of the environmental and reliability requirements that equipment has to meet.

4.1 Sensors

Initial testing was carried out in the laboratory to assess various sensor configurations and the performance characteristics of the sensors.

This then had to be extended to make the sensors suitable for an engine environment.

The multi-segment ring (patented) gave the best results in the laboratory and this configuration was used in the Viper engine test. The sensor stood up well to the engine test and proved to be rugged and reliable, although various areas for improvement were identified. This configuration of sensor, with improved materials, fixings and signal leadout connections has been used in the Marine engine trials.

In the development of sensors several factors have to be considered:

(i) They may have to be non-intrusive.
(ii) The materials should be suitable for the environment.
(iii) They should be easy to fit or retrofit with minimum modifications.
(iv) The sensitivity should enable coverage of the whole duct.

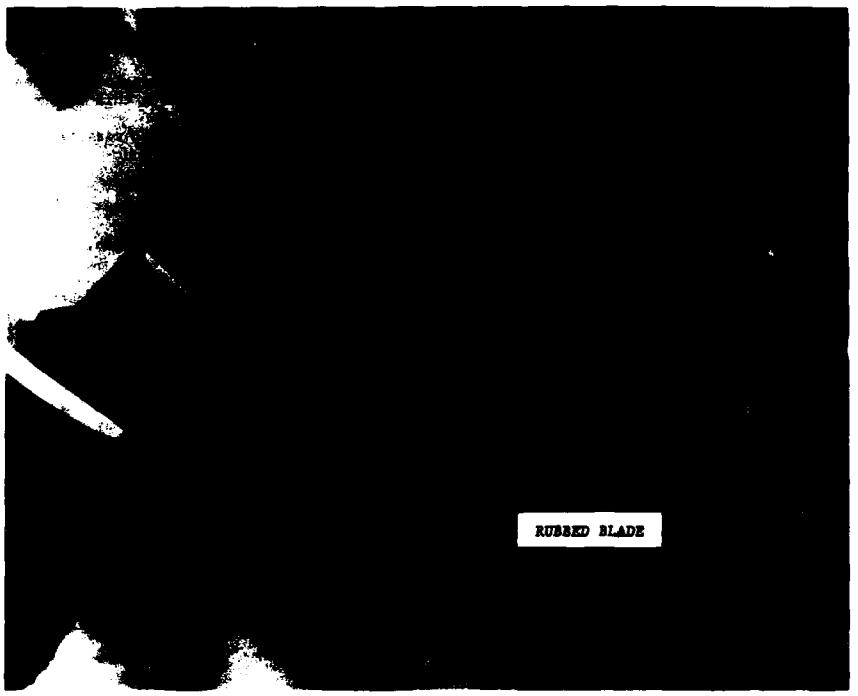

FIGURE 8 : 4th stage compressor rotor blades showing rubbed blade

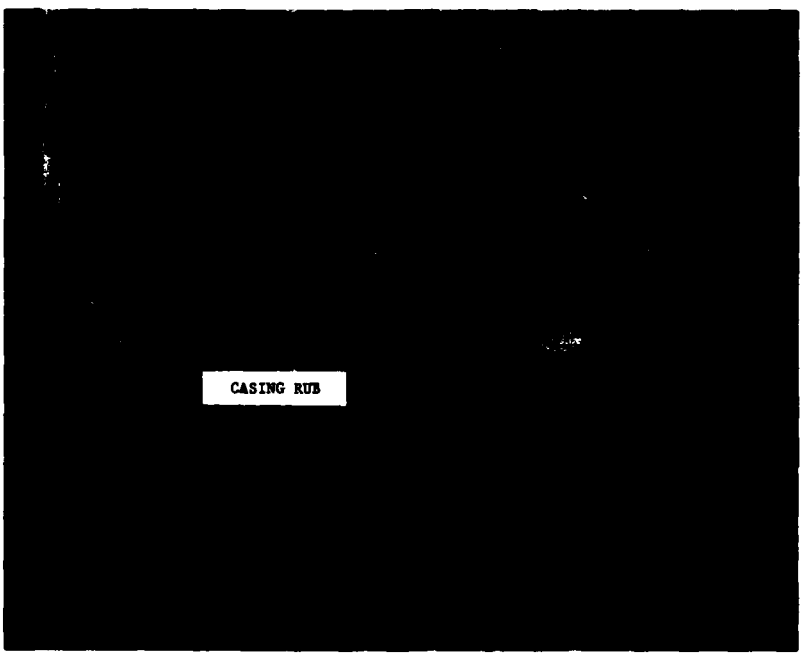

FIGURE 9 : Compressor half casing showing rub

The sensor development has been an active part of the work for the past two years, with varying degrees of success and failure. The Palouste is now used for sensor development and testing, and comparison is made with the existing sensors to enable assessment.

The signal conditioning technique used in the early research work and engine tests basically measured rate of change of charge, with the capability of inferring total charge from this measurement.

However, a more satisfactory and sensitive technique, which is now used, is to measure the charge directly. (Patents applied for).

4.3 Current system

The system is tailored to the application in terms of hardware installation, and analysis requirements.

There are currently two types of sensor configuration available for the engine application:

(i) Multi-segment 'ring' which is mounted in the exhaust duct or tail pipe, with each segment in the same axial plane. Several of these 'rings' may be used in the duct to provide additional information.

(ii) Individual 'button' type sensors (patents pending) which are used in discrete mounting points in the engine, using instrumentation type bosses, or other existing ports which may be available in the engine.

The signal conditioning may be mounted directly on the back of the sensor if the environment is suitable, or a short distance away.

The signal analysis has the primary aim of identifying the signal change from the background level and to discriminate between the possible causes identified in Section 1.0.

With suitable sensor positioning it is currently feasible to discriminate the faults further.

Further details can be obtained from Stewart Hughes Limited, Southampton UK.

5.0 OTHER APPLICATIONS - INGESTED DEBRIS MONITORING

The potential of the use of the electrostatic technique to monitor gas path faults in gas turbine/jet engines has been demonstrated on a variety of engines. This has been achieved by monitoring the exhaust gas. The use of the technique to monitor debris and foreign objects ingested into the intake of the engine is a potential application, which is currently being developed (patents pending). This could have several uses:

(i) Indication that the engine has ingested a foreign object, to initiate a visual inspection.

(ii) Indication of operating situations most likely to cause FOD, by correlating the detector system signal with operating condition recording.

(iii) Indication that the engine is ingesting significant quantities of sand or salt, so that overall condition and engine performance is monitored more closely.

5.1 Current work

The development work incorporates two test programmes.

A small gas turbine test engine is being used for the development work, to optimise the system configuration and signal processing requirements and to define the capability of the system.

Aircraft trials are also being undertaken to prove the system in the real environment.

5.2 Hardware

Sensors are positioned in the intake of the engine, and also ideally in the engine. The sensor configuration for the intake is a ring, which may be a single complete ring or segmented. The materials are suitable for the application and intake environment.

The associated signal conditioning may be mounted directly on the back of the sensor or a short distance away.

Figure 10 shows the schematic of a total system.

6.0 FUTURE WORK AND OBJECTIVES

(i) **Gas path debris monitoring**

It is anticipated that it should be possible to identify the fault to module level.

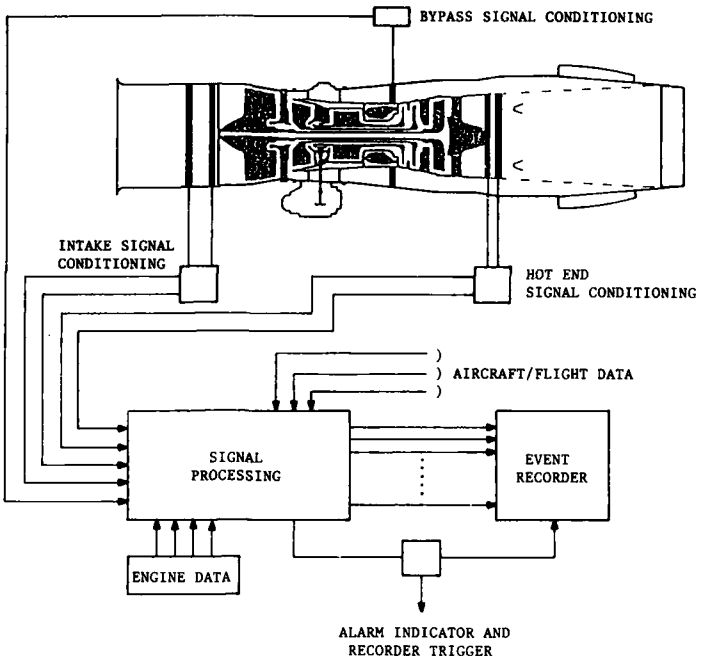

FIGURE 10 : General layout of FOD detector

The work being carried out involves seeded fault trials on a small gas turbine, accruing of engine test data from a variety of engines, hardware and software development. This will all be coupled with backup research work to ensure that the technique is used to its maximum potential.

(ii) **Integrated hot and cold end monitoring**

This offers many advantages for various applications, including possibly identification of where the ingested debris exits the engine.

(iii) **Integration of debris monitoring with other monitoring techniques**

A systematic approach to designing a condition monitoring system is based around corroboration of data from various monitoring techniques. This approach improves the discrimination of faults, reduces false alarm rates and enables long term prediction to be carried out.

7.0 REFERENCES

[1] W Tabakoff, A Hamed : The Dynamics of Suspended Solid Particles in a Two Stage Gas Turbine. Transactions of the ASME Journal of Turbomachinery Vol 108 October 1986.

ACKNOWLEDGEMENTS

The authors gratefully acknowledge the support for the Gas Path Debris programme received from the Procurement Executive, Ministry of Defence, and the very kind assistance of those involved in the preparation of this paper.

DISCUSSION

C. SPRUNG

Quelle est la sensibilité de votre système, c-à-d quelles sont les volumes ou masses minimales des débris que vous pouvez détecter?

Author's Reply:

It is difficult to give a straight answer but we measured particles down to a few μm. We detected also the small sand particles which were not eliminated by the helicopter engine filters.

G. WINTERFELD

Can you distinguish between the electrically charged soot particles from the combustion and the other debris particles?

Author's Reply:

The results show that an engine has a normal level of charge which gives the background signal. For most engines this varies with the operating regime. During tests when metallic debris was present in the gas path the signal changed significantly, indicating the presence of the metallic debris.

The baseline footprint for each engine can be established, which includes the effect of the charged soot and carbon particles. Deviations from the baseline footprint indicate the presence of other debris in the gasstream, or higher than normal levels of soot and carbon.

C. SCURA

1. Did you test your system with reheat in operation?

2. Is there any velocity limit of particles above which it is not possible to detect them?

Author's Reply:

1. NO, we have not tested the equipment on engines with reheat in operation. We are considering these kind of engines, but the sensors would be installed upstream of the reheat.

2. At the present the system has the capability of detecting particles in a jet engine or gasturbine. The velocity of the particles will be up to gas velocity.

D.E. GLENNY

1. How do your "integrated monitoring" distinguishes between ingested sand particles and other engine generated debris in the exhaust, especially in helicopters which may or may not be fitted with particles separation?

2. Can the monitoring system measure the erosion of compressor blades due to sand erosion, as the sand particles could be contaminated with metal particles?

Author's Reply:

1. To date the integrated monitoring has not been tested on an engine. However laboratory tests indicate that it should be possible to correlate the intake and the exhaust sensor signals. With knowledge of the engine operating condition the expected time lag between the sand entering and leaving the engine can be predicted. This information can be used to establish whether the signals monitored on the exhaust sensor are due to the ingested material or other engine generated debris.

2. As the sand is likely to be contaminated with metal particles it is likely that the nature of the signal monitored on the exhaust sensor will be different to that caused by sand alone. Hence it should be possible to monitor the blade erosion.

An Intelligent Sensor System for Equipment Health Monitoring of Ferromagnetic Wear Debris Concentration in Fluids

K.W. Chambers, M.C. Arneson, J.L. Montin and W. Dueck
Atomic Energy of Canada Ltd. Research Company
Whiteshell Nuclear Research Establishment
Pinawa, Manitoba, Canada ROE 1LO

C.A. Waggoner
Defence Research Establishment Pacific
CFB Esquimalt, FMO Victoria
B.C., Canada V0S 1B0

Summary

FERROSCAN^R is a device that has been developed for the Canadian Department of National Defence by Atomic Energy of Canada Limited (AECL) for monitoring the relative concentration of ferromagnetic wear debris in fluid systems and is produced by SENSYS, a business unit of AECL. FERROSCAN^R generates a wear profile in real time and uses it to detect the onset of an increase in the rate of wear of ferromagnetic components. This paper describes the background, development and operating principles of the sensor and presents some engineering test results.

1. Introduction

The normal wear of bearing materials releases metallic particles of wear debris into the lubricating systems of machines. A marked increase in the rate of change of the wear debris concentration is indicative of abnormal wear: it is accompanied by shifts to a larger mean particle size (1) and heralds the onset of component failure. A device capable of continually monitoring the concentration of ferromagnetic wear debris in real time warns of impending failure and, thus, enables remedial action to be taken before failure occurs.

2. Historical Background

The principle for measuring the concentration of ferromagnetic particles in fluids as described in this paper, was originally developed for determining the concentration of suspended ferromagnetic particulate material in the heat transport systems of CANDU power reactors (2). In such systems, suspended ferromagnetic material, principally magnetite, is of particular interest since it constitutes one of the chief means by which radionuclides are transported around the coolant circuit.

In the fall of 1981 this technology was recognized by C.A. Waggoner, a tribologist working for the Department of National Defence at the Defence Research Establishment Pacific, as a potential on-line device for determining the amount of ferromagnetic wear debris in lubricating oil systems. Consequently, a multi-phase research and development program funded by DND was begun to adapt the technology for use on the lubrication systems of gas turbine engines and helicopter gear boxes.

A five-phase development program from 1982 to 1987 proved the technology, demonstrated a prototype product and resulted in an agreement between DND and AECL to actively promote commercial exploitation of FERROSCAN^R.

3. Principles of Operation

FERROSCAN^R consists of a sensor coil, a trapping magnet and a microcontroller. The fluid sample stream passes through a cylindrical sensor coil which is the inductive component of an RF oscillator: when the ferromagnetic content within the active volume of the coil is changed, the inductance in the RF circuit changes also and this manifests itself as a change in oscillator frequency. For a simple series circuit consisting of an inductance, L, capacitance, C, and resistance, R, the resonance frequency is given by:

$$f = 1/2\pi\sqrt{LC} \qquad (1)$$

Thus, if the ferromagnetic content within the sensor coil is increased this results in an increase in the inductance, L, and the frequency of the oscillator will decrease.

To selectively collect ferromagnetic material, an electromagnet is built around the sensor coil. When the magnet is energized, ferromagnetic particles are collected over the coil windings and the oscillator frequency decreases until the trapping magnet is de-energized. The ratio obtained by dividing the resultant frequency change by the trapping interval is a linear function of the bulk concentration of ferromagnetic particulate material.

The operation of FERROSCAN^R is best described with the help of the frequency/time profile shown in figure 1. When the trapping magnet is energized, the oscillator frequency undergoes a step change from f(A) to f(B) due to inductive coupling between the sensor and magnet windings. As particles of ferromagnetic wear debris are trapped

against the inside of the sensor coil windings, the frequency decreases progressively from f(B) to f(E) due to a steady increase in inductance. When the magnet is de-energized, the trapped ferromagnetic material is released and the oscillator frequency returns to its initial value f(A)=f(B). The slope, s, of the frequency ramp measured within the trapping interval $\{t(C)-t(D)\}$ is given by

$$s = \{f(C)-f(D)\}/\{t(C)-t(D)\} \qquad (2)$$

and, as figure 2 shows, it is a linear function of the bulk concentration of suspended ferromagnetic particulate material. A natural limit exists to the amount of material that can be trapped as the trapping interval is continuously extended. This is the result of a reduction in the magnetic field gradient as ferromagnetic particles build-up across the pole gap and in the concommitant reduction in trapping efficiency (see section 5). Thus the oscillator frequency tends to a plateau value for very long trapping times and figure 3 demonstrates this behaviour. It is found, however, that the drop in frequency required to make precise measurements of $\{f(C)-f(D)\}$ is small enough that the variation of frequency with trapping interval over the range of interest can be considered linear. Thus, typical values of $\{f(C)-f(D)\}$ are a few tens of kilohertz and, as can be seen in figure 4, a linear approximation over this range is a good one.

FERROSCAN^R can be operated in several modes depending on application. The first mode involves measuring the frequency change for a fixed trapping interval. The advantage of this approach is that it provides a fixed cycle time and enables a single controller to monitor many sensors with ease. However, using a trapping interval of 10 seconds, non-linearity in response becomes significant at concentrations in excess of approximately 150 ppm (note figures 3,4).

In a second mode of operation, the trapping interval is measured for a fixed change in frequency, δf. Thus, the trap is energized until δf has been attained, then it is de-energized and the resulting trapping interval used to compute the slope, s. In this manner, the sensor always operates in its linear trapping range whether the ferromagnetic particulate concentration is low (long trapping interval) or high (short trapping interval).

The third and preferred mode of operation is a combination of the two above where the trapping period is variable between upper and lower limits and can adjust to changes in concentration. This combination enables FERROSCAN^R to respond satisfactorily over a large dynamic range covering very clean (long trapping times) and very dirty (short trapping times) systems.

4. Sensor Calibration

The test apparatus used for the majority of the FERROSCAN^R development work is represented in figure 5 and consists of a primary loop, A, simulating a lubrication system and a bypass loop, B. Heaters installed in the reservoir allow the oil to be maintained at temperatures up to 180°C with a precision of ±1°C.

Particle size fractions ranging in size from less than 5 μm to greater than 250 μm were prepared from iron powder by seiving. Known weights of these fractions were added to oil in the loop reservoir and circulated through the sensor to calibrate its response to changes in concentration. With the exception of high temperature experiments, DEXRON II was used as a representative oil: for high temperature work MIL 23699 was used. The action of the stirrer and circulating pumps helped to reduce, but could not eliminate, sedimentation. Consequently, the actual concentration of suspended iron particles was determined by the chemical analysis of oil samples withdrawn from the loop.

The major part of the FERROSCAN^R program prior to 1987 has been concerned with development and characterization of a sensor having a bore of 0.125 inches. This sensor operates as a full-flow device over a linear flow velocity range of 0.8 to 4.8 meters per second (7 to 40 mL per second) but at higher flow velocities is usually run in the bypass mode. Sample flow in the bypass mode is provided by either a small gear pump or a flow nozzle. A typical calibration plot for one of these sensors has already been given in figure 2.

5. FERROSCAN^R Sensor Response

5.1 Factors Related to Trapping Efficiency

The trapping efficiency, ε, of the sensor is defined by the expression

$$\varepsilon = 1 - c'/c \qquad (3)$$

where c, c' are the concentrations of suspended ferromagnetic particulate material upstream and downstream of the trapping magnet, respectively.

The four principle factors which determine trapping efficiency are the radial gradient of the magnetic field, particle size, linear flow velocity and viscosity. An approximate theoretical treatment indicates that trapping efficiency should vary inversely as the viscosity and linear flow velocity, directly as the radial component of the magnetic field strength and as the square of the particle radius and this is supported in general

by the data shown in figures 6, 7, 8 and 9. (Note that in figures 6,7 and 9 the trapping efficiency is expressed as response per unit concentration rather than as the dimensionless parameter ε).

The effect of viscosity on sensor response is shown in figure 6. Although the viscosity dependence is not strictly a reciprocal one, it does support the inverse relationship suggested by the foregoing model.

The variation of sensor response with linear flow velocity is shown in figure 7 and these data indicate the anticipated inverse dependence at flow velocities in excess of 1.7 m/s. At lower flow velocities, ε decreases: this is attributed to the fact that if the flow velocity is sufficiently low, viscous drag is not great enough to completely flush away the particles before the trapping magnet is re-energized.

In many instances, normal operating conditions for an engine or transmission are such that lubricant viscosity and flow velocity vary to a small enough extent that the resultant effect on sensor response is negligible.

Figure 8 shows the anticipated linear correlation between trapping efficiency and magnetic field strength (magnet current).

The data in figure 9 show sensor sensitivity increasing in a non-linear fashion with increasing particle size although not the square dependence suggested above.

The particle size behaviour gives rise to a positive feature for FERROSCAN^{R}. As the rate of wear increases the mean particle size of the resulting debris increases also. This behaviour sharpens the "knee" that is obtained in the wear profile (as the result of increasing sensitivity with increasing particle size) and, thus, makes the onset of abnormal wear easier to detect.

5.2 Factors Related to Oscillator Frequency

From electromagnetic theory, the inductance of a coil having cylindrical geometry can be expressed in terms of the magnetic permeability of the material within its core, μ, the number of turns per centimeter, n, and the core volume, V, as follows:

$$L = \mu n^2 V \qquad (4)$$

Substituting this expression for L into equation (1) and differentiating with respect to μ gives

$$\delta f/\delta \mu = f/2\mu \qquad (5)$$

The quantity $\delta f/\delta \mu$ can be regarded as the sensitivity of the sensor to changes in the ferromagnetic content of the material within the core of the sensor coil. Thus from equation (5), sensor sensitivity will, for a given value of μ (material within the core), be directly proportional to the frequency of the RF oscillator.

Oscillator frequency is affected by changes in dimensions of the sensor coil as a result of thermal expansion and by temperature-induced changes in the magnetic permeability of the material within the core of the sensor coil (see above).

Net thermal expansion/contraction is determined by the balance of heat dissipated by the magnet winding and by heat flow from the oil stream. Thus, if the temperature of the sensor coil increases its volume will increase and the oscillator frequency will decrease in accordance with equation (5) above: conversely, a decrease in temperature will result in an increase in oscillator frequency. It has been observed during the course of this work that the net effect of temperature-induced changes in magnetic permeability on oscillator frequency is in the same sense as that resulting from thermal expansion/contraction, namely, the frequency decreases with rising temperatures and increases with falling temperatures.

In the majority of applications thermally induced effects are small and involve errors of less than 5% in measured response. These effects can be readily compensated by monitoring the changes in oscillator base frequency and applying the correction to the observed sensor response.

6. Engineering Test Bed Results

6.1 Grain Auger Gearbox

Figure 10 shows the wear profile obtained using a single, 0.125 inch sensor and sample pump with a small, right angle drive gearbox having a rated torque of 59 inch.pounds (3.8%). It can be readily seen that initial increases in applied load resulted in a gradual increase in response, but, beginning at 24.5% applied torque, response increased dramatically and continued to increase until eventual destruction at 420 minutes. These trends were supported by chemical analysis of oil samples taken during the course of the run which demonstrate a one-to-one correspondence between wear debris content and sensor response.

6.2 Kiowa Helicopter Tail Rotor Gearbox

A similar experiment was carried out using a Kiowa tail rotor gearbox. During the course of this experiment, the rate of wear of the bearings and gears was deliberately increased by reducing torque on the input pinion race retainer nuts and culminated in removal of the bearing shim, thereby reducing clearance between the input and output pinions to zero. The sustained increase in wear rate which resulted from this action is shown clearly by the wear profile in figure 11. It was found necessary to terminate the run short of the target of 130 hours of continuous operation when vibration of the test stand became so pronounced it caused the speed and torque control relays to open and close inadvertently thus making control of the test stand impossible. The sensor response data were again supported by the chemical analysis of oil samples taken during the course of the run.

6.3 General Electric T-56 Gas Turbine Engine

A three-sensor FERROSCAN^{R} system was fabricated under contract to DREP and run on the lubrication systems of two General Electric T-56 engines which were undergoing tests for the Department of National Defence at the National Research Council, Ottawa. The sensors were used to monitor ferromagnetic wear debris on the engine feed line and on the engine and gearbox scavenge lines for a total of 30 runs, each run lasting approximately 1 hour. The sensors indicated very low concentrations of wear debris throughout the entire test period and these results were confirmed by the chemical analysis of samples withdrawn from the test loop. These experiments were important since they constituted the first long-term engineering test of the prototype system and suggested many software and hardware improvements.

In the three examples cited above, the sensors were operated and controlled by a dedicated computer. Output consisted of sensor response as a function of elapsed time and was presented as hard copy on a printer.

6.4 Natural Gas Pumping Station

A FERROSCAN^{R} system consisting of four 0.125 inch sensors has been operating successfully since the beginning of September 1987 on a gas pumping station: three sensors monitor wear debris produced by three bearings on the turbine/compressor using small, individual sampling pumps. The fourth sensor monitors the combined scavenge oil flow of the gas turbine engine which drives the turbine-compressor, using a flow nozzle to provide a sample stream for the sensor. To date, the concentration of ferromagnetic particulate material at all four sensor locations has remained at or near the detection limit (approximately 0.5 ppm) and these results have been confirmed by the analysis of samples withdrawn from the four sample loops.

6.5 Shipboard Installation

A three-sensor system using 0.125 inch sensors and pressure-driven sample flow has been operating successfully on a coastguard vessel since mid-October 1987 where it is being used to monitor the concentration of ferromagnetic wear debris in the propulsion engine and propeller shaft lubrication systems. The wear debris concentrations in these systems have tended to be higher than those encountered in the installations described in 6.3 and 6.4 above but have not, to date, indicated any significant changes in rate of wear.

6.6 Aerospace Uses of FERROSCAN^{R}

FERROSCAN^{R} systems are being readied for installation on selected military and civilian aircraft where they will be used to monitor ferromagnetic wear debris. These systems use a variety of sensors with different bores that can accept the entire lubricant flow: this is made necessary by the fact that lubricant scavenge flow in most aircraft can contain up to 80% air. As in the case of oil alone, these sensors also respond linearly to changes in the concentration of ferromagnetic wear debris in mixtures containing large proportions of air.

The installations described in 6.4, 6.5 and 6.6 are operated and controlled by small, rugged microcomputer which, in addition to producing continuous data readout approximately once a minute, can store store short term (5-minute peak values for 3.5 days), medium term (30-minute running averages for 32 days) and long term data (24-hour peak values for 34 months) for up to eight different sensors. These data are accessible through FERROFILE, a software utility which, in addition to downloading stored data, provides a means of displaying that data graphically for trend analysis.

7. Concluding Remarks

FERROSCAN^{R} is an intelligent, on-condition monitor system which generates a ferromagnetic wear debris profile in real time: it provides a means of detecting the onset of an increase in the rate of wear of ferromagnetic components and, consequently, of indicating when remedial action should be taken.

Current research and development is concerned with the evolution of more diverse and advanced sensors which, together with parallel developments in controller design, will promote the ability of FERROSCAN^{R} to satisfy the need for this technology in all sectors of industry.

Acknowledgement

The authors wish to thank P.T. Howe for his general encouragement and help in producing the figures.

References

1. Suh, N.P., "An Overview of the Delamination Theory of Wear", Wear, 44 (1), August 1977, pp. 1-16.

2. Arneson, M.C., Chambers, K.W., Smith, I.M., and Swiddle, J.E., "Probe for Determining the Concentration of Ferromagnetic Particulates in Water at High Temperature and Pressure", Power Industry Research, 1, March 1981, pp. 87-90.

Figure 1. **Oscillator frequency/time profile**

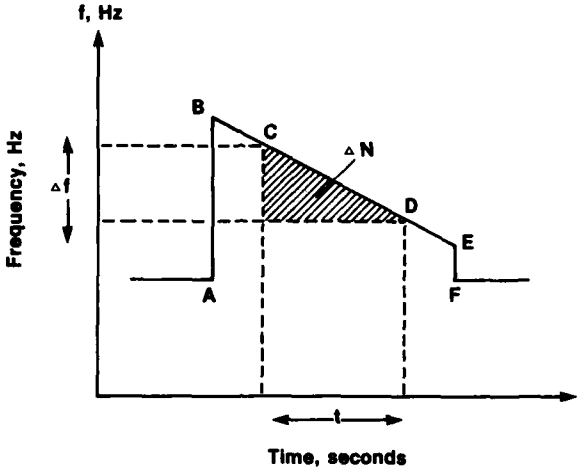

Figure 2. **Ferroscan: typical calibration plot**

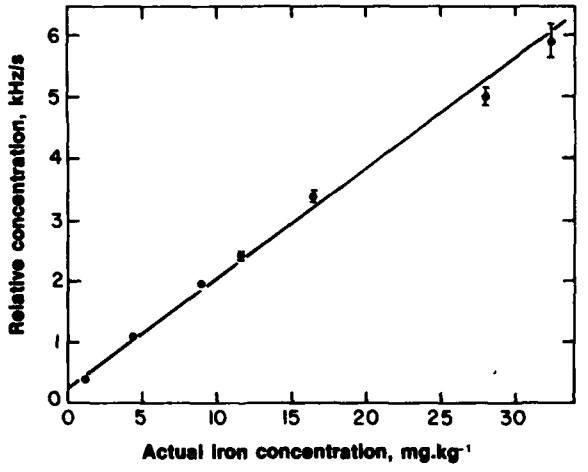

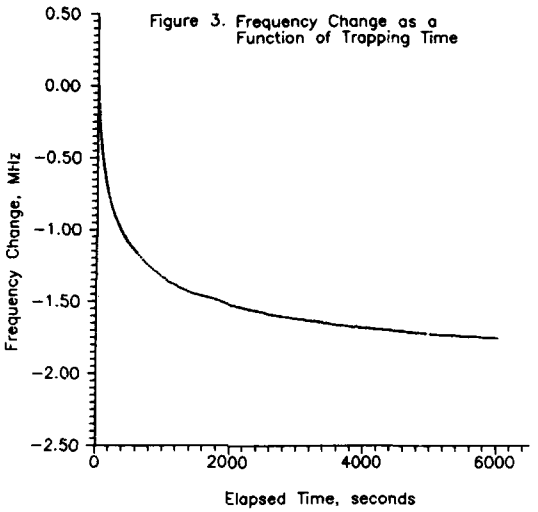

Figure 3. Frequency Change as a Function of Trapping Time

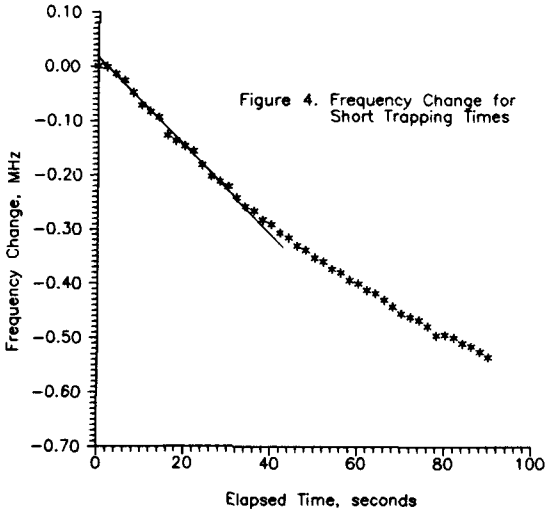

Figure 4. Frequency Change for Short Trapping Times

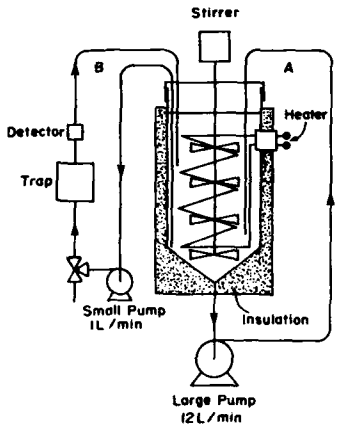

Figure 5 Test Loop

Figure 6. The Effect of Viscosity on Sensor Response

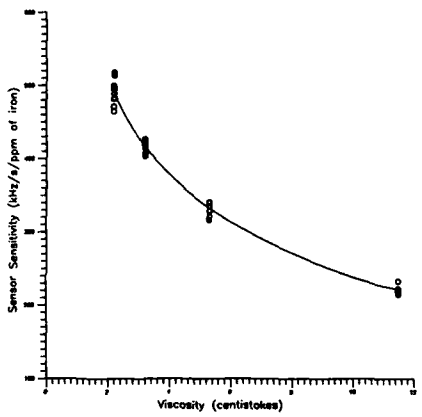

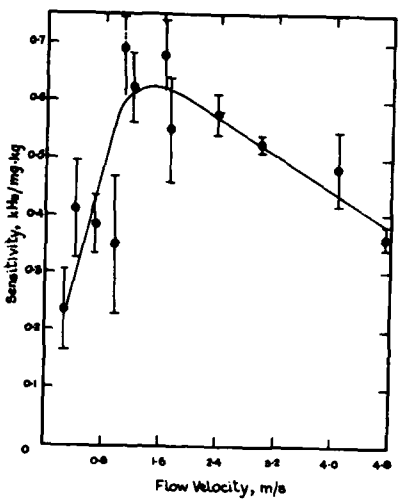

Figure 7. Sensor Response as a Function of Flow Rate

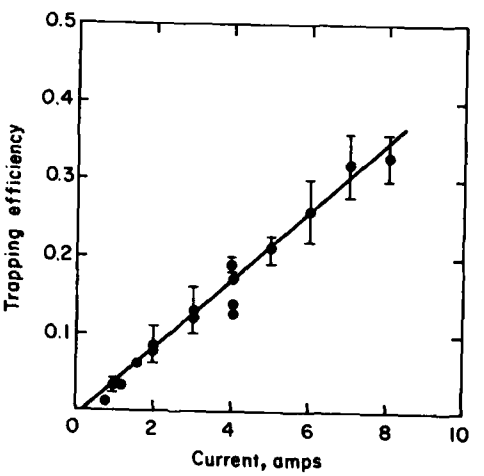

Figure 8. Trapping Efficiency as a Function of Magnet Current

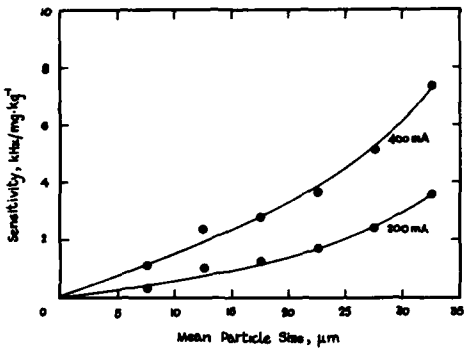

Figure 9. Sensor Response as a Function of Particle Size

Figure 10. Field test: grain auger gearbox

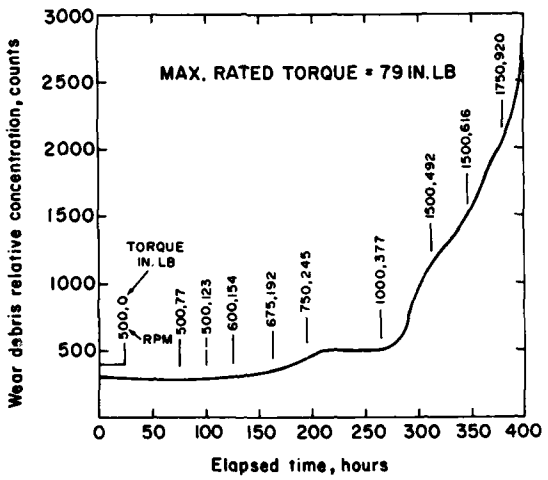

Figure 11. **Field test: Kiowa tail rotor gearbox**

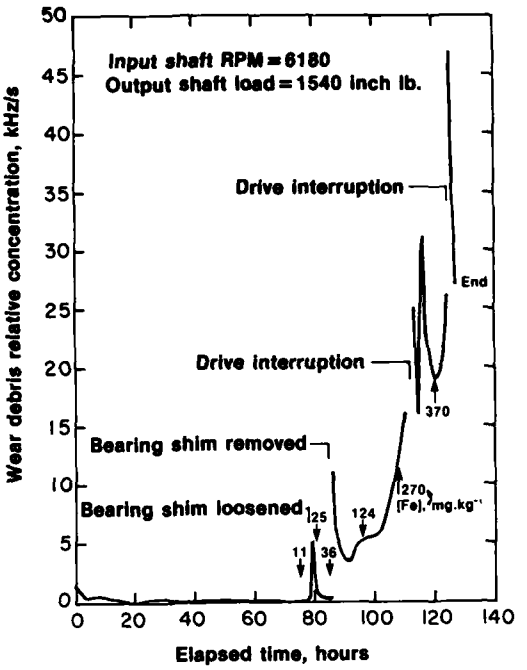

DISCUSSION

R. FEATHERSTONE

We heard this week that spectrographic oil analysis techniques (SOAP) are becoming less effective in identifying wear debris as lubricating oil filters are being selected ever finer, removing more particles of the debris. Is the sensitivity of your system adequate to pick up where the SOAP leaves off?

Author's Reply:

Ferroscan probes are installed in-line, immediately downstream of the wearing component and upstream of any filters so that an increase in rate of wear is detected as soon as it occurs.

With regard to the particle size range accessible to us, we have successfully monitored ferromagnetic wear debris concentrations in which the particle size varied from .04 μm to about 2000 μm.

In addition, the system responds linearly to changes in concentration of suspended ferromagnetic particulate material, for oil containing up to 90% air by volume.

G. TANNER

Is there any residual magnetism in the particles that cause the orifice to clog?

Author's Reply:

If there were sufficient residual magnetism left on the steel particles after being trapped by the sensor to cause them to remain fixed after the magnet had been engaged, this would be evident, because of the attendant decrease in probe sensitivity. We had not observed this. The probe remains sensitive after repeated analysis in such system.

COMPASS*: A Generalized Ground-Based Monitoring System

by

M J Provost

Performance Systems Specialist

Rolls-Royce plc

DERBY

DE2 8BJ

England

Summary

Condition monitoring has developed from simple hand recording and analysis of cockpit instrumentation to the use of electronic systems selecting and recording a multitude of measurements for transmission to ground-based computer systems, which store and analyse data from an entire fleet. COMPASS (COndition Monitoring and Performance Analysis Software System) is a ground-based computer system, currently being developed by Rolls-Royce plc for application on the Rolls-Royce RB211 and Tay and IAE (International Aero Engines) V2500 turbofans. After discussing the benefits of a monitoring system, this paper describes COMPASS, its sources of data and its analytical functions, including details of new techniques developed to improve the usefulness of the analysis that is done. The paper also shows how COMPASS is designed in two parts:

- Analytical functions specific to a given application.
- General host routines, providing all the "housekeeping" functions required in any monitoring system, including smoothing and trending, alert generation, fleet averaging, compression, data management and data plotting.

The use of the general host routines could be extended to cover any operation (civil or military, engine/airframe/APU, etc) which is to be monitored. The paper concludes by outlining the approach Rolls-Royce plc is adopting to enable the COMPASS host to be made available for widespread application.

List of Abbreviations

EGT	Exhaust Gas Temperature (V2500)
EPR	Exhaust Pressure Ratio: used as a thrust-setting parameter
N2	High Pressure shaft speed (V2500, Tay)
	Intermediate Pressure shaft speed (RB211)
TGT	Turbine Gas Temperature (RB211, Tay)
VIGV	Variable Inlet Guide Vanes (RB211)

* **COMPASS is a Registered Trademark of Rolls-Royce plc**

Introduction

Engine condition monitoring has developed over the last several decades from hand recording and analysis of cockpit instrumentation to the use of electronic on-board data gathering systems which select and record a multitude of engine and aircraft measurements for onward transmission to ground-based computer systems, which store and analyse data from an entire fleet. These ground-based computer systems have become more complex as the amount of data to be processed has increased, the data quality has improved, and user requirements for better diagnostic routines and user-friendliness have emerged; the aim is further reduction in cost of operation of the equipment being monitored.

COMPASS (COndition Monitoring and Performance Analysis Software System) is a ground-based engine condition monitoring computer system currently being developed by Rolls-Royce plc for initial application on the IAE (International Aero Engines) V2500 two-shaft turbofan (scheduled to enter service on the Airbus A320 in Spring 1989), the Rolls-Royce RB211-524G three-shaft turbofan (scheduled to enter service on the Boeing 747-400 in Spring 1989) and Tay two-shaft turbofan (in service on the Gulfstream IV and Fokker 100), and which will be available for use on future civil and military engines (and, retrospectively, on earlier versions of the RB211 and on RB183 turbofans), airframes and auxiliary power units. After summarising the benefits to be gained from monitoring, the paper describes COMPASS, its sources of data, and its analytical functions. It also describes the concept of COMPASS as a neutral host, ie a general system providing all the "housekeeping" functions (data input, output and storage, smoothing/trending, alerts and statistical calculations) required by any monitoring system. The approach Rolls-Royce plc is adopting for the use of COMPASS with other (non Rolls-Royce plc) diagnostic routines is also discussed.

The Benefits of a Monitoring System

The benefits of in-service monitoring are two-fold:

- Enhanced visibility of fleet condition.
- Reduced cost of operation.

Modern methods of data transmission mean that measurements taken in flight can be processed shortly after they are gathered by ground-based systems such as COMPASS, giving the operator visibility of the current state of engines, airframes, etc at that time, both in terms of performance (eg TGT/EGT margins at take-off) and mechanically (eg vibration).

Data recorded at take-off (either full power or derated) can be normalised so that temperature and shaft speed margins relative to red-line values can be estimated; these estimated margins can then be trended, enabling the operator to anticipate and thus avoid operational disruption caused by red-line exceedances. Monitoring the mechanical behaviour of the engine (eg vibration, oil pressure, temperature and consumption) as well as monitoring the results from module performance analysis routines produces information to detect incipient failures, enabling remedial action to be taken.

Information from a monitoring system can be used to:

- Quantify and understand the mechanisms of in-service deterioration.
- Define shop workscopes ahead of time.
- Schedule maintenance at times convenient to the operation and workshop capacity.
- Improve maintenance by providing more information on which to base decisions.
- Reduce ground running by making adjustments based on flight data.

The latter item produces savings directly by reducing manpower and fuel usage; however, savings from other items will depend on the ability of the operator to react to the information produced by the monitoring system. These potential savings arise from:

- Improved operational efficiency
    - Maintenance at operator's convenience

- Early warning of problems
- Matching of equipment to requirements

- Improved workshop utilisation
  - Planning of cost-effective work
  - Elimination of unnecessary work

- Improved fleet performance
  - More effective maintenance
  - Higher equipment standard from more effective rework
  - Better fuel consumption
  - Lower operating temperatures
  - Improved durability and reliability

Monitoring systems can therefore make an effective contribution towards a reliable and efficient operation.

What is COMPASS?

COMPASS is a ground-based engine health monitoring system with built-in flexibility to allow the user to select those functions he requires to maximise the benefits to his operation. These range between the extremes of simple trending of cockpit parameters (eg shaft speeds, TGT/EGT, fuel flow, vibration) and full module performance analysis plus mechanical analysis, with or without alert message generation. Input data to and output data from the analytical functions can be stored within the system and displayed on a terminal or printer. Depending on the user's operations, COMPASS can be configured to run either on-line on receipt of data or in batch mode. It is important to note that COMPASS is a system that reports by exception, only alerting the user when it is necessary; the user's attention is focused on exceptional events, rather than distracted by the process of searching through large quantities of normal output in order to discover the exceptional events manually.

The COMPASS/Aircraft interface is shown diagrammatically in Figure 1. Data from the electronic engine control unit and/or other engine parameter measurement devices is gathered by the aircraft condition monitoring system, which also takes in flight data, aircraft data and other engine data available on the aircraft data busses. The output from the aircraft condition monitoring system is then transferred, by some means which is operator dependent, into the operator's computer system, within which COMPASS is installed.

COMPASS can be considered to consist of four modules:

- An Analysis Module, where all calculations for the performance and mechanical functions take place.
- A Trend Module, where data input to and output from the analysis module can be processed through a smoothing/trending routine to produce alert messages if changes outside predetermined limits (in terms of levels, steps and rates of change) are detected.
- A Plot Module, which enables all information within the COMPASS data bases to be displayed on a screen and/or printer in trend, tabular, bar-chart or X - Y plot format.
- A Utility Module, which handles items such as system maintenance, generation of statistical data, data compression and data validation.

Sources of Data for COMPASS

Data for COMPASS is generated from four main areas:

- On-wing data
- Ground data
- Test-cell data
- Maintenance action data

The above data is received by the COMPASS system via an appropriate operator/COMPASS interface using a SIRF (Standard Input Record Format); individual data items are allocated defined positions in the SIRF, which ensures compatibility between COMPASS and the outside world.

On-wing data is provided by the aircraft condition monitoring system on board the aircraft. The exact format, content and criteria for generation of the output is agreed between the engine supplier, the airframe supplier and the operator. Outputs typically produced today are in the form of reports, such as:

(1) Engine Cruise Report

(2) Engine plus Aircraft Cruise Report

(3) Take-off Report

(4) Ground-run Report

(5) Engine Start Report

(6) Engine Advisory and On-request Reports

(7) Engine Divergence Report

Typically, COMPASS analytical functions will carry out analysis of data received via the SIRF from Reports (1) to (5) above; data from the other reports is stored on the COMPASS Engine History Data Store.

Ground data covers such items as oil uplift, and enters COMPASS via the SIRF.

Test-cell data also enters COMPASS via the SIRF. In order to avoid customised engine models (used as part of the analytical functions), the data needs to be corrected to standard conditions prior to input to COMPASS. Analysed test-cell data can be used as start points for the in-flight trend plots.

Maintenance action data typically includes date, time, aircraft identification, engine number, engine hours and/or cycles, engine installation position and recorded maintenance actions (expressed as coded words); all this data enters COMPASS via the SIRF. Maintenance actions which affect performance and mechanical behaviour can be identified, and used to reinitialise the smoothing/trending routines on parameters affected.

COMPASS Analytical Functions

Depending on the instrumentation available on the engine and the data-gathering system on the aircraft in which the engine is installed, the functions described below are all available in COMPASS. Some functions are, of course, available either within existing monitoring systems or as separate stand-alone programs; one of the advantages of COMPASS is that all functions are integrated into one system, making it easier to combine and correlate output from different analysis functions.

Module Performance Analysis and Sensor Bias Determination

This is the main performance analysis function; data recorded from on-wing or test-cell running of an engine is compared with that expected from a model of the engine at the observed power level and flight/test-cell conditions; the differences from expectations are used to estimate the efficiency and capacity changes of the turbomachinery making up the engine, as well as resolving any sensor bias which may be present.

This function uses Optimal Estimation techniques (Kalman Filtering); however, the Kalman Filter has one inherent problem in that measurement differences appropriate to known subsets of component changes and/or sensor biasses tend to be analysed as a combination of all possible changes and biasses. This can be confusing when the user is trying to decide on remedial action. Rolls-Royce plc has developed a proprietary addition to the basic Kalman Filter which overcomes the above mentioned characteristics, and focuses attention on the significant items. Two examples for a two-shaft turbofan are illustrated in Figures 2 and 3.

The upper portion of Figure 2 depicts the results from the basic Kalman Filter analysing a set of measurement differences consistent with a half percent reduction in both the high pressure compressor and high pressure turbine efficiencies, showing the assigning of these differences as being due to changes in all the possible component changes and sensor biases. The lower portion of Figure 2 shows the results from the proprietary addition; it is seen that the output corresponds to the changes used to generate the measurement differences. Figure 3 shows the results from a similar exercise, in which a set of measurement differences consistent with a half percent reduction in high pressure turbine efficiency and a half percent high pressure compressor exit temperature bias have been analysed.

Overall Performance

In this routine, gas path parameters (eg TGT/EGT, fuel flow, shaft speeds) are compared to the engine model, and deviations monitored.

Parameter SLOATL/Margin Calculations

This function estimates the margins at take-off for TGT/EGT and shaft speeds for an engine that is operated at full power. Additionally, the function estimates the SLOATL (Sea Level Outside Air Temperature Limit), which is the sea level ambient temperature at which the engine would have zero temperature or speed margin when operated at full power.

Thrust and EPR Derates

Percentage derated take-off thrust can be calculated from data gathered at take-off conditions. Delta EPR (from full rating) at take-off and at three climb altitudes can be input into COMPASS and accumulated in grouped frequency tables of up to seven ranges for take-off and five ranges for climb. All this data can be used to monitor engine usage.

Simulation

In this function, the engine model built into COMPASS can be used in the predictive mode to give expectations of performance parameters both with and without user-defined component changes; this function is useful for "what-if" studies.

N2/EPR Tramline Monitor (RB211 only)

In this function, the operation of the VIGV controller is monitored by comparing N2 and EPR values, taken during engine acceleration to take-off power, against N2 vs EPR "tramlines" (limits).

Vibration

Tracked shaft speed and broad band vibration readings are normalised and trended.

Fan Trim Balance

In this routine, vibration, phase angle and speed data from the fan, gathered at take-off and cruise, can be analysed on user request to provide balance weight and position information for fan trim balancing without a dedicated ground run. This function is also applicable to test-cell operations if relevant data is available.

Engine Start

This function analyses data taken during engine start; TGT/EGT is normalised at selected high-pressure shaft speeds, as a function of starter duct pressure and oil temperature, and compared to the expected TGT/EGT. Deviations from expectations are then monitored.

Flight Profile

Shaft speeds recorded during various flight phases are input into COMPASS for subsequent statistical analysis and engine usage evaluation.

Oil Pressure/Temperature

Both parameters are normalised as functions of high-pressure shaft speed and trended.

No 4 Bearing Pressure (V2500 only)

This scavenge bearing pressure is normalised and monitored.

Oil Consumption

In this function, oil consumption is either calculated from oil tank levels recorded during taxi (taking into account oil temperature, burner pressure and high pressure shaft speed) or calculated from manually-entered oil uplift figures.

Nacelle and Pylon Temperature Analysis

In these functions, the nacelle or pylon temperature is recorded and compared with a model of the appropriate temperature; deviations are monitored, to indicate the presence of air or gas leaks within the nacelle or pylon.

Oil Analysis (SOAP)

Information from SOAP (Spectrometric Oil Analysis Program) can be submitted to COMPASS; wear particle generation rate can then be calculated, making appropriate allowances for dilution due to the addition of oil during routine servicing.

Magnetic Chip Detector Data

In this function, qualitative comments are submitted to COMPASS based on chip detector inspection. If a debris tester is used to provide a quantitative assessment of the material found on the chip detector plugs, the function will calculate debris accumulation rate for trending purposes.

COMPASS Smoothing/Trending and Alert Functions

As stated earlier, COMPASS is designed to report by exception; this philosophy demands sophisticated routines for assessing the significance of changes and trends in the input data and the results from the analytical functions described earlier. The two functions that do this are the Smoothing/Trending function and the Alert Function, which are described in this section.

In choosing a smoothing/trending routine, a set of basic requirements were laid down:

- The routine must use the current data point and estimates from the immediately previous point only, ie it must be recursive.
- It must have a small computational overhead, since many items (both input to and output from the analytical functions described earlier) can potentially be processed.
- It must produce useful output from a limited amount of data.
- It must cope correctly with unequally spaced data, since it is highly likely that data points will arrive with varying time periods or cycle numbers between them.
- Ideally, the routine should estimate trend (ie rate of change) directly.

Of the available methods, only Optimal Estimation satisfies all the requirements; more traditional methods, such as Exponential Smoothing, only satisfy the first three criteria. The routine produces best estimates of the true level and trend (rate of change) of the parameter being monitored; the response of the algorithm can be "tuned" to achieve the required balance between sensitivity to genuine changes and over-response to noise in the raw parameter values. In essence, the Smoothing/Trending routine quantifies the "character" of the time series in terms of level and trend, as well as giving assessments of possible outliers or sudden changes in the series. Given a direct estimate of rate of change, prediction of events (over the short term) becomes possible.

Comprehensive alert facilities are available in the Alert Function to warn the user when parameters have moved outside limits. Two levels of alert (denoted "yellow" and "red") are provided for both maximum and minimum values of any parameter being monitored. In addition to such "absolute" alerts, a similar system for "relative" alerts is provided; in the case of "relative" alerts, the parameter is compared with an initial value generated at the start of the series, and alerts generated when the difference from the initial value exceeds defined limits. By applying the Alert Function to the output (level, trend and difference between actual and predicted parameter value) from the Smoothing/Trending function, sophisticated alerting of the user to significant events is provided.

An important point to note is that all aspects of the smoothing/trending "tuning" and alert level settings are entirely under user control, and can be set up to meet user requirements without reprogramming.

Another feature of interest in COMPASS is a combination of the Module Performance Analysis and Sensor Bias function with the Smoothing/Trending function; output from the Smoothing/Trending function applied to the gas path measurement differences from expectation can be used as input to the Module Performance Analysis and Sensor Bias function, giving estimates of true level, trend and sudden changes in both component changes and sensor biasses. This approach uses less computer space than smoothing/trending of each component change and sensor bias series individually.

COMPASS Software Architecture

COMPASS has been designed to run on a variety of computer systems, and provide a flexible environment within which the analytical functions and utilities may be run. COMPASS has been designed to run on computers which support:

- 32 bit INTEGER and REAL numbers.
- Approximately 600K region size.
- FORTRAN 77 compiler.
- FORTRAN direct access input/output, if supplied filing system is used.

These requirements imply that a mainframe or super mini is the most suitable host computer for COMPASS.

The architecture of COMPASS is shown schematically in Figure 4. It is seen that the system to operate COMPASS consists of three basic elements:

- Operator environment software, which provides the environment within which COMPASS operates. It has to supply COMPASS with data and commands defining the processes to be carried out, and accept from COMPASS the outputs from these processes. Because of the vast range of possible computer hardware environments and operating practices, it is necessary for the operator to provide the software to perform these functions.
- COMPASS software, containing the COMPASS analytical functions and utilities.
- Interfaces, providing the linkage between COMPASS software and the operator environment software. These would normally be written by the operator according to specifications supplied; however, if the COMPASS filing system is used, the associated interfaces are supplied as well.

Aspects of COMPASS Software

This consists of a number of modules, the invocation and subsequent behaviour of which is controlled by commands submitted by the user. Among the modules provided are the following:

- Analysis Module. The Analysis Module is responsible for sorting input data on the Engine History Data Store and also for performing the analysis functions described previously, and storing the results of the analysis on the Engine History Data Store. The functions to be performed are selected by an array of switches in the incoming data. The module is normally invoked automatically whenever data is passed to it; however, reprocessing of previously stored data is possible on user request. The module also performs any reprocessing that is necessary due to data being submitted out of sequence ("back dating") for analytical functions where the order of data is important (eg Smoothing/Trending).

- Plotting module. The Plotting Module is the principal means by which the user obtains visibility of COMPASS input and output; it enables data which has been recorded on the Engine History Data Store to be presented in a variety of user-defined formats.

  Four basic types of display are available:

  - Tables. Tabular display of parameters chosen from a specified Engine History Data Record and its immediate relatives.

  - Barcharts. Barchart display of the same data as available for Tables.

  - Trend Plots. Tabular and semi-graphical display of parameters chosen from a specified range of Engine History Data Records against a time dependent parameter (eg time since installation, cycles).

  - X - Y Plots. Semi-graphical cross-plot of one or more parameters against a single X parameter.

  With the aid of a library of plot definitions stored within the COMPASS filing system, the analyst may use the Plotting Module to inspect the data stored on the Engine History Data Store to assist with maintenance planning, fault diagnosis, fleet statistics etc.

- Alert Processing Module. This module allows Alert Reports generated by the Analysis Module and stored on the Alert Report Data Store to be selectively accessed, displayed either in full or summary form, deleted or acknowledged (ie flagged as having been noted and actioned). Remaining unacknowledged Alert Reports can also be identified.

- Compression Module. The purpose of this module is to reduce historical data to a series of meaningful statistics, enabling the old data to be deleted in order to make space for new data. The compressed data is stored back on the Engine History Data Store as Compressed Data Records, and is available for subsequent examination using the Plotting Module.

- Maiden Point Module. This module performs similar statistical calculations to the Compression Module for the first few individual Engine History Data Records related to (re)installation of an engine. This creates a Maiden Point Record in the Engine History Data Store which may subsequently be displayed using the Plotting Module for comparison purposes.

- Fleet Averaging Module. This module allows various statistics to be calculated across a user-defined fleet. Fleet Average Data Records are created on the Engine History Data Store for subsequent examination using the Plotting Module.

Concept of Neutral Host

The above section shows that COMPASS is modular in design, and essentially consists of two distinct classes of routines:

- A set of application-dependent analysis routines specific to a given engine (say).
- A set of application-independent routines providing general calculation facilities, eg:
  - Smoothing/Trending.
  - Alert generation and processing.
  - Compression.
  - Maiden Point generation.
  - Fleet Averaging.
  - Data Management.
  - Data plotting and display.

In this context, it should be noted that the creation of the application-independent routines represents 75%-85% of the total task of creating a monitoring system.

This leads to the concept of a Neutral Host, within which application-dependent routines reside, providing all the general facilities required to turn a set of analysis routines into a fully-fledged monitoring system, as illustrated in Figure 5. A useful analogy is a hotel; private rooms are provided for each occupant with access to general services (restaurants, bars, swimming pools, etc) that are not duplicated in each room.

It is therefore possible for any OEM (Original Equipment Manufacturer) to implant his own specific analysis routines within the host, with only minor changes to the SIRF to cope with particular specialised measurements. In this way, COMPASS can be extended from being an engine monitoring system to a total equipment monitoring system, providing the operator with a common tool for engine, airframe, auxiliary power unit (APU) and environmental control system (ECS) monitoring. Taking the idea a stage further, COMPASS can be configured to monitor civil, military, industrial and marine gas turbines, or indeed any other operation requiring data analysis, smoothing/trending of data, alert generation and data storage and display.

Proposal For Licensing COMPASS

If the generality of application of COMPASS described in the previous section is to be exploited to the full, OEMs will require:

- commercial confidentiality to protect their proprietary data and analytical functions
- professional software support for the COMPASS host
- user satisfaction with the whole system

To meet these requirements, Rolls-Royce plc has licensed COMPASS to a third-party software house (Systems Designers plc); this ensures:

- professionalism of software creation and support
- independence from OEM suppliers, leading to the required level of confidentiality

Benefits to the OEMs include

- concentration of software effort on equipment analysis
- reduced cost of creation of monitoring systems

Benefits to the users include

- a single method of operation for all equipment being monitored
- host improvements are available for all equipment being monitored
- reduced implementation and support costs
- better software support from a dedicated software house

All parties benefit from the avoidance of re-invention of the general functions each time a monitoring system is created, with all the cost savings that this implies.

Under the above licensing arrangements, COMPASS could have numerous users, be installed in various computer environments, monitoring different equipment supplied by a variety of OEMs using a variety of diagnostic routines. The user would receive in-service support which would recognise all these aspects and ensure problems indicated by COMPASS are correctly resolved; in addition, the support would be tailored to suit the needs of individual users and OEMs. The software house would establish the necessary communications with users and OEMs, cross-refer problems where relevant, carry out COMPASS modifications where necessary to benefit the user/OEM community, and maintain COMPASS documentation.

Conclusions

COMPASS is a state-of-the-art ground based condition monitoring system containing all the necessary software to store and analyse data for an entire fleet. Several new features in the Module Performance Analysis and Smoothing/Trending functions have been incorporated to improve the quality and usefulness of the analysis, and to enable COMPASS to report by exception; this relieves the user from the task of manually reviewing a multitude of plots to determine significant events. It is designed to be highly flexible in operation, with standardised interfaces such that any equipment manufacturer can, through third party licensing arrangements, implant specific diagnostic routines. COMPASS can provide one system for both equipment manufacturers and users, not only in the field of civil aviation but also in military, industrial and marine gas turbines; indeed the system is applicable to any industrial or transport operation which requires data to be analysed, smoothed and trended, with alerts generated and output displayed as appropriate.

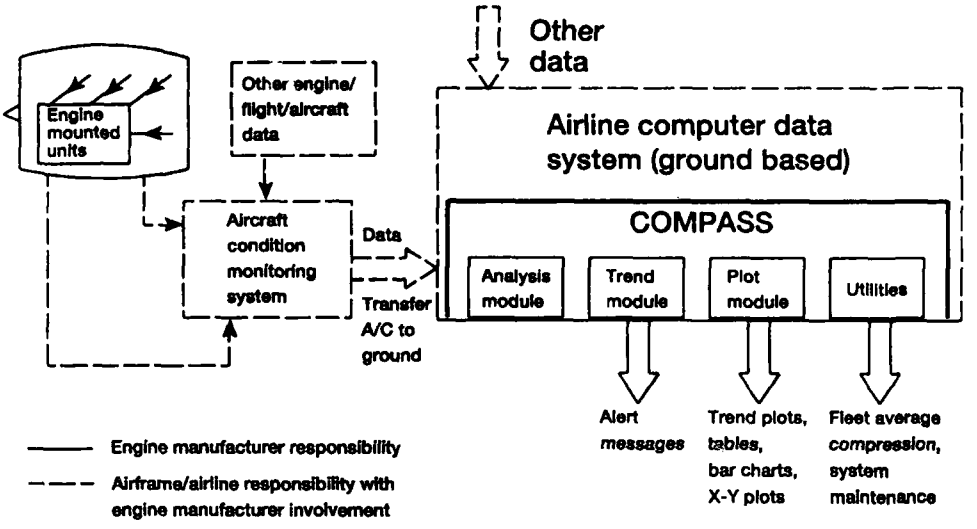

Figure 1 COMPASS-Aircraft Interface

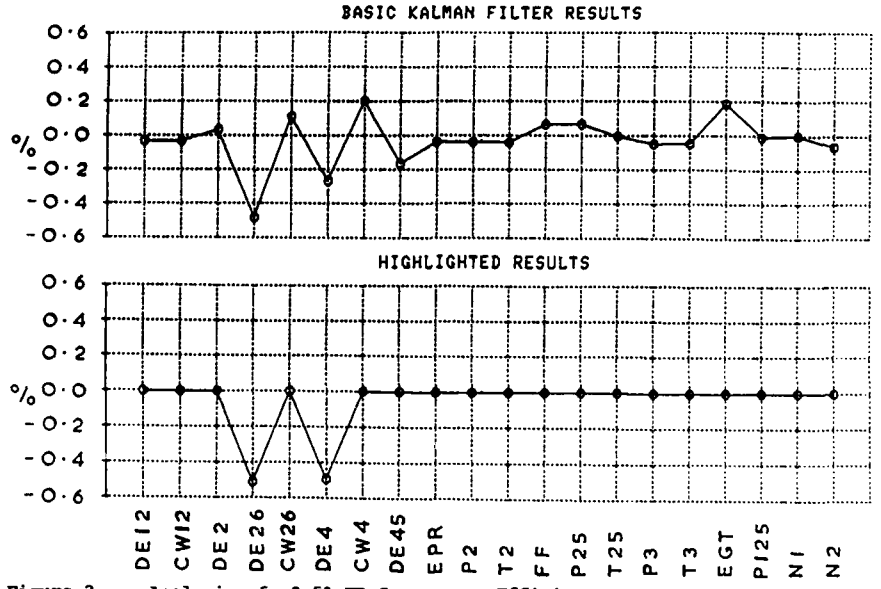

Figure 2 Analysis of -0.5% HP Compressor Efficiency and -0.5% HP Turbine Efficiency

Key

DE12: Fan Tip efficiency change
CW12: Fan Tip capacity change
DE2 : Fan Root/Booster efficiency change
DE26: HP Compressor efficiency change
CW26: HP Compressor capacity change
DE4 : HP Turbine efficiency change
CW4 : HP Turbine capacity change
DE45: LP Turbine efficiency change
EPR : Exhaust Pressure Ratio bias
P2 : Inlet total pressure bias
T2 : Inlet total temperature bias
FF : Fuel flow bias
P25 : HPC inlet total pressure bias
T25 : HPC inlet total temperature bias
P3 : HPC exit total pressure bias
T3 : HPC exit total temperature bias
EGT : Exhaust Gas Temperature bias
P125: Fan Tip exit total pressure bias
N1 : Low Pressure shaft speed bias
N2 : High Pressure shaft speed bias

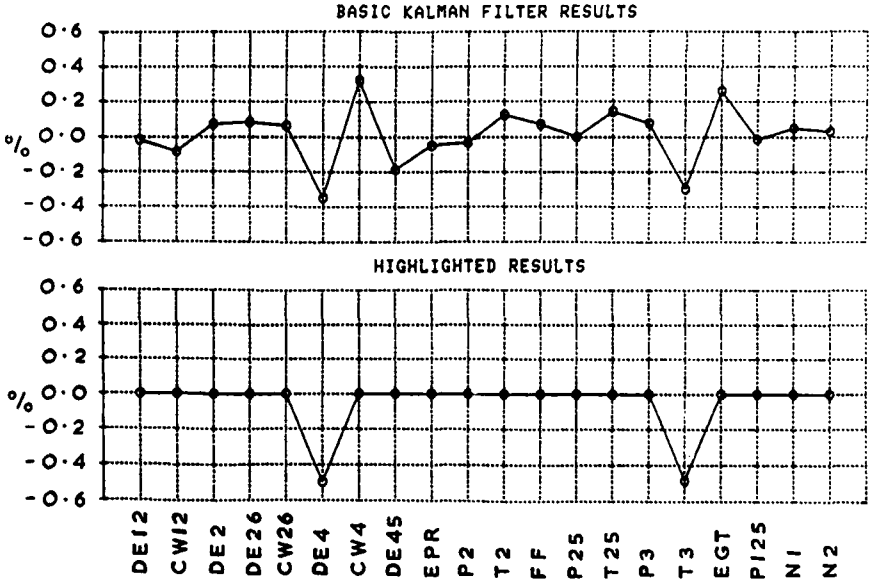

Figure 3 Analysis of -0.5% HP Turbine Efficiency and -0.5% HP Compressor Exit Total Temperature Bias

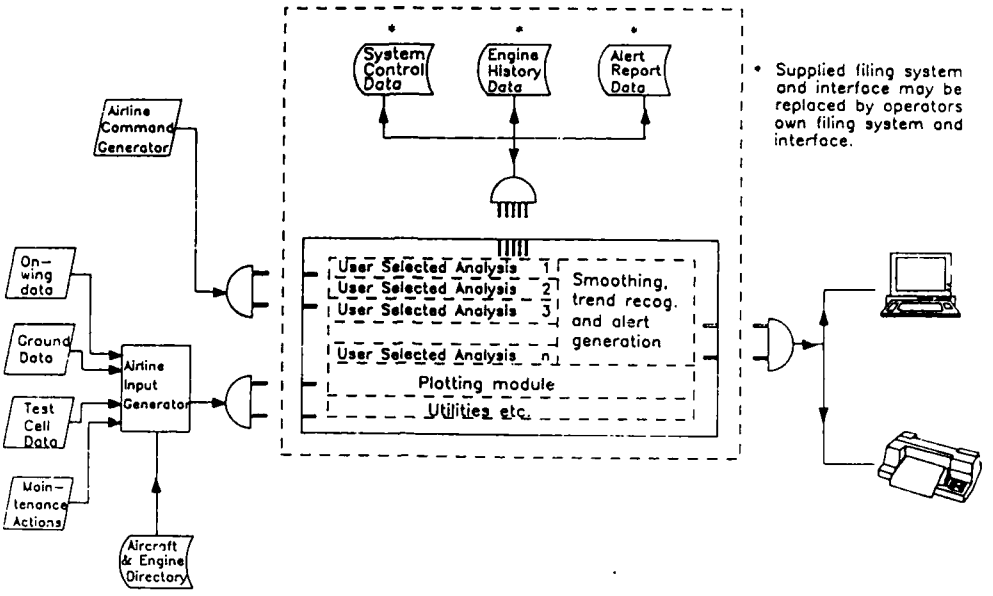

Figure 4 COMPASS System Architecture

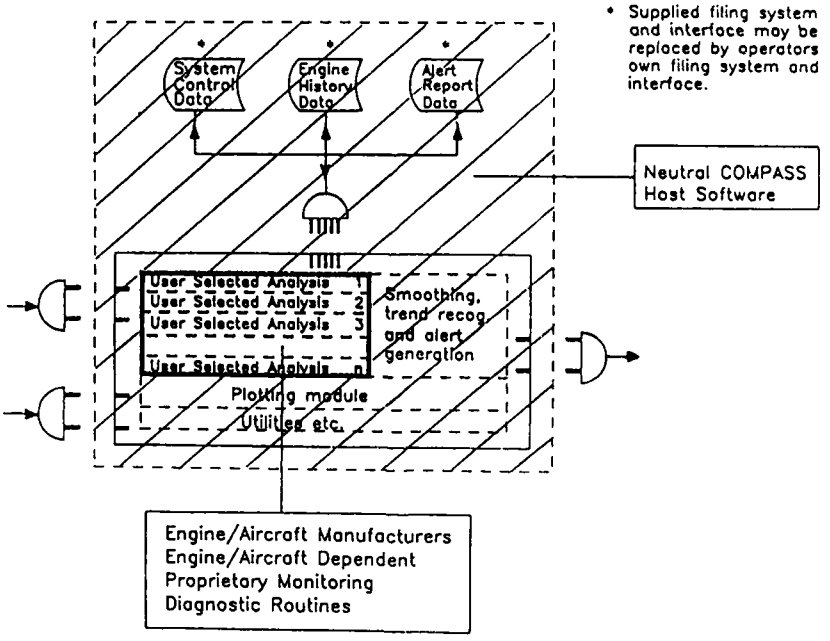

Figure 5 COMPASS Neutral Host Concept

DISCUSSION

D. DOEL

Has the COMPASS Kalman Filter Concentrator been applied to data corrupted by noise?

Author's Reply:

It was not possible in the time allocated to cover the extensive testing of the Kalman Filter and "Concentrator" that has been done. Single and multiple component changes and/or sensor biasses have been analyzed, both with and without random noise applied to the measurements. These results, together with the results from the analysis of actual engine data, indicate that the Kalman Filter and "Concentrator" behaves as well as or better than other methods or engine analysis.Apparent diagnostics "failures" can occur when, due to the structure of the analysis problem, gas-path measurement differences can combine to produce spurious evidence of different component changes and/or sensor biasses to the ones expected. It should be noted that any engine analysis method will fail in this situation: the only way to avoid this is to further distinguish individual component changes and sensor biasses from each other.

F. AZEVEDO

Is COMPASS available for RB211-524-B4 model?

Author's Reply:

It is intended that COMPASS will be made available for all marks of RB211 by appropriate additions, modifications and/or data changes to the analytical functions for the RB211-524G. The exact list of monitoring functions available will depend on the instrumentation fitted: airlines should discuss the full capabilities for the RB211 marks they operate with ROLLS-ROYCE plc.

42-14

REPORT DOCUMENTATION PAGE			
1. Recipient's Reference	**2. Originator's Reference**	**3. Further Reference**	**4. Security Classification of Document**
	AGARD-CP-448	ISBN 92-835-0481-X	UNCLASSIFIED

5. Originator	Advisory Group for Aerospace Research and Development North Atlantic Treaty Organization 7 rue Ancelle, 92200 Neuilly sur Seine, France
6. Title	ENGINE CONDITION MONITORING – TECHNOLOGY AND EXPERIENCE
7. Presented at	the Propulsion and Energetics Panel 71st Symposium, held in Quebec City, Canada, 30 May—3 June 1988.

8. Author(s)/Editor(s)	**9. Date**
Various	October 1988
10. Author's/Editor's Address	**11. Pages**
Various	494

12. Distribution Statement	This document is distributed in accordance with AGARD policies and regulations, which are outlined on the Outside Back Covers of all AGARD publications.

13. Keywords/Descriptors

Engines
Monitors
Mechanical efficiency
Military operations
Diagnosis
Wear

14. Abstract

The Conference Proceedings contain 40 papers presented at the Propulsion and Energetics Panel 71st Symposium, on Engine Condition Monitoring – Technology and Experience, which was held 30 May—3 June 1988 in Quebec City, Canada.

The Symposium was arranged in the following sessions: Miltary Operations (11); Civil Experience (5); Manufacturer's Perspective (6); Turboprops and Turboshafts (3); Systems (6); Diagnostic Methods (5); and Advanced Technologies (4). Questions and answers of the discussions follow each paper.

The aim of the Symposium was to provide a forum for military and civilian users of engines, for manufacturing engineers and for research scientists to discuss the considerable experience with engine condition monitoring accumulated in recent years.

AGARD Conference Proceedings No.448 Advisory Group for Aerospace Research and Development, NATO ENGINE CONDITION MONITORING – TECHNOLOGY AND EXPERIENCE Published October 1988 494 pages The Conference Proceedings contain 40 papers presented at the Propulsion and Energetics Panel 71st Symposium, on Engine Condition Monitoring – Technology and Experience, which was held 30 May–3 June 1988 in Quebec City, Canada. The Symposium was arranged in the following sessions: Miltary Operations (11); Civil Experience (5); P.T.O	AGARD-CP-448 Engines Monitors Mechanical efficiency Military operations Diagnosis Wear	AGARD Conference Proceedings No.448 Advisory Group for Aerospace Research and Development, NATO ENGINE CONDITION MONITORING – TECHNOLOGY AND EXPERIENCE Published October 1988 494 pages The Conference Proceedings contain 40 papers presented at the Propulsion and Energetics Panel 71st Symposium, on Engine Condition Monitoring – Technology and Experience, which was held 30 May–3 June 1988 in Quebec City, Canada. The Symposium was arranged in the following sessions: Miltary Operations (11); Civil Experience (5); P.T.O	AGARD-CP-448 Engines Monitors Mechanical efficiency Military operations Diagnosis Wear
AGARD Conference Proceedings No.448 Advisory Group for Aerospace Research and Development, NATO ENGINE CONDITION MONITORING – TECHNOLOGY AND EXPERIENCE Published October 1988 494 pages The Conference Proceedings contain 40 papers presented at the Propulsion and Energetics Panel 71st Symposium, on Engine Condition Monitoring – Technology and Experience, which was held 30 May–3 June 1988 in Quebec City, Canada. The Symposium was arranged in the following sessions: Miltary Operations (11); Civil Experience (5); P.T.O	AGARD-CP-448 Engines Monitors Mechanical efficiency Military operations Diagnosis Wear	AGARD Conference Proceedings No.448 Advisory Group for Aerospace Research and Development, NATO ENGINE CONDITION MONITORING – TECHNOLOGY AND EXPERIENCE Published October 1988 494 pages The Conference Proceedings contain 40 papers presented at the Propulsion and Energetics Panel 71st Symposium, on Engine Condition Monitoring – Technology and Experience, which was held 30 May–3 June 1988 in Quebec City, Canada. The Symposium was arranged in the following sessions: Miltary Operations (11); Civil Experience (5); P.T.O	AGARD-CP-448 Engines Monitors Mechanical efficiency Miiitary operations Diagnosis Wear

Manufacturer's Perspective (6); Turboprops and Turboshafts (3); Systems (6); Diagnostic Methods (5); and Advanced Technologies (4). Questions and answers of the discussions follow each paper. The aim of the Symposium was to provide a forum for military and civilian users of engines, for manufacturing engineers and for research scientists to discuss the considerable experience with engine condition monitoring accumulated in recent years. ISBN 92-835-0481-X	Manufacturer's Perspective (6); Turboprops and Turboshafts (3); Systems (6); Diagnostic Methods (5); and Advanced Technologies (4). Questions and answers of the discussions follow each paper. The aim of the Symposium was to provide a forum for military and civilian users of engines, for manufacturing engineers and for research scientists to discuss the considerable experience with engine condition monitoring accumulated in recent years. ISBN 92-835-0481-X
Manufacturer's Perspective (6); Turboprops and Turboshafts (3); Systems (6); Diagnostic Methods (5); and Advanced Technologies (4). Questions and answers of the discussions follow each paper. The aim of the Symposium was to provide a forum for military and civilian users of engines, for manufacturing engineers and for research scientists to discuss the considerable experience with engine condition monitoring accumulated in recent years. ISBN 92-835-0481-X	Manufacturer's Perspective (6); Turboprops and Turboshafts (3); Systems (6); Diagnostic Methods (5); and Advanced Technologies (4). Questions and answers of the discussions follow each paper. The aim of the Symposium was to provide a forum for military and civilian users of engines, for manufacturing engineers and for research scientists to discuss the considerable experience with engine condition monitoring accumulated in recent years. ISBN 92-835-0481-X

AGARD
NATO OTAN
7 rue Ancelle · 92200 NEUILLY-SUR-SEINE
FRANCE
Telephone (1)47.38.57.00 · Telex 610 176

DISTRIBUTION OF UNCLASSIFIED AGARD PUBLICATIONS

AGARD does NOT hold stocks of AGARD publications at the above address for general distribution. Initial distribution of AGARD publications is made to AGARD Member Nations through the following National Distribution Centres. Further copies are sometimes available from these Centres, but if not may be purchased in Microfiche or Photocopy form from the Purchase Agencies listed below.

NATIONAL DISTRIBUTION CENTRES

BELGIUM
Coordonnateur AGARD – VSL
Etat-Major de la Force Aérienne
Quartier Reine Elisabeth
Rue d'Evere, 1140 Bruxelles

CANADA
Director Scientific Information Services
Dept of National Defence
Ottawa, Ontario K1A 0K2

DENMARK
Danish Defence Research Board
Ved I
2100

FRANCE
O.N.E
29 A
9232

GERMAN
Fachi
Physi
Karls
D-75

GREECE
Helle
Aircr
Depa
Holar

ICELAND
Direc
c/o Fl
Reyja

ITALY
Aeronautica Militare
Ufficio del Delegato Nazionale all'AGARD
3 Piazzale Adenauer
00144 Roma/EUR

LUXEMBOURG
See Belgium

NETHERLANDS
Netherlands Delegation to AGARD
National Aerospace Laboratory, NLR
P.O. Box 126
2600 AC Delft

NORWAY
Norwegian Defence Research Establishment
Attn: Biblioteket
P.O. Box 25

UNITED STATES
National Aeronautics and Space Administration (NASA)
Langley Research Center
M/S 180
Hampton, Virginia 23665

THE UNITED STATES NATIONAL DISTRIBUTION CENTRE (NASA) DOES NOT HOLD STOCKS OF AGARD PUBLICATIONS, AND APPLICATIONS FOR COPIES SHOULD BE MADE DIRECT TO THE NATIONAL TECHNICAL INFORMATION SERVICE (NTIS) AT THE ADDRESS BELOW.

PURCHASE AGENCIES

National Technical
Information Service (NTIS)
5285 Port Royal Road
Springfield
Virginia 22161, USA

ESA/Information Retrieval Service
European Space Agency
10, rue Mario Nikis
75015 Paris, France

The British Library
Document Supply Division
Boston Spa, Wetherby
West Yorkshire LS23 7BQ
England

Requests for microfiche or photocopies of AGARD documents should include the AGARD serial number, title, author or editor, and publication date. Requests to NTIS should include the NASA accession report number. Full bibliographical references and abstracts of AGARD publications are given in the following journals:

Scientific and Technical Aerospace Reports (STAR)
published by NASA Scientific and Technical
Information Branch
NASA Headquarters (NIT-40)
Washington D.C. 20546, USA

Government Reports Announcements (GRA)
published by the National Technical
Information Services, Springfield
Virginia 22161, USA

Printed by Specialised Printing Services Limited
40 Chigwell Lane, Loughton, Essex IG10 3TZ

ISBN 92-835-0481-X